THE BULK MODULUS, SHEAR MODULUS, AND POISSON'S RATIO OF ISOTROPIC ICE TESTED IN CREEP

By

KIMBER B. P. OSIOWY

A Thesis
Presented to the University of Manitoba
in Partial Fulfillment of the
Requirements for the Degree of
Master of Science in Civil Engineering

Winnipeg, Manitoba

August, 1989

ISBN 0-315-54795-2

THE BULK MODULUS, SHEAR MODULUS, AND POISSON'S RATIO OF ISOTROPIC ICE TESTED IN CREEP

BY

KIMBER B.P. OSIOWY

A thesis submitted to the Faculty of Graduate Studies of the University of Manitoba in partial fulfillment of the requirements of the degree of

MASTER OF SCIENCE

ABSTRACT

The objective of the experimental program described in this thesis was to determine the bulk modulus, shear modulus, and Poisson's ratio of a freshwater, granular ice with an average porosity of 1.2%. The study was initiated as a result of boundary value problems encountered in the analysis of the work of Kjartanson (1986) on pressuremeter creep testing in laboratory ice.

All testing was carried out in triaxial cells at a temperature of -2.0°C on ice made using the same techniques as Kjartanson used. Six isotropic compression tests and five quick-step isotropic compression tests were run to determine the bulk modulus. Six single stage, constant-mean-normal-stress triaxial shear tests and one multi-step test were run to determine the shear modulus and Poisson's ratio of Kjartanson's ice. Mean stresses ranged from 1.0 to 2.5 Mpa during the test program. The deviator stress in the single stage shear tests was 0.8 Mpa.

The elastic bulk modulus of the ice was determined to be 1.02 Gpa. This decreased to an effective (time-dependent) value during creep that was dependent upon bulk (hydrostatic) stress. The elastic shear modulus for ice of average density was 0.18 Gpa. During creep the effective shear modulus was dependent

on axial strain and independent of mean stress, deviator stress, and density. Dilation caused by micro-cracking at the instant of deviator stress application resulted in values of Poisson's ratio greater than 0.5 for low mean stresses. At high mean stresses, the confining pressure reduced the dilatory effect. During creep, when subject to deviator stress, the specimens exhibited very little volume change, and the time-dependent Poisson's ratio was 0.5.

ACKNOWLEDGEMENTS

This study was carried out under the supervision of Dr. D.H. Shields, Department of Civil Engineering, University of Manitoba. The author wishes to express his sincere gratitude to Dr. Shields for suggesting this topic of research, and for his guidance, encouragement, and support throughout the investigation.

The author also wishes to thank Mr. B. Graham, Dr. D. Burn and Dr. L. Domaschuk who, as members of the author's thesis examining committee, provided useful ideas and constructive criticism. The advice of Dr. J. Graham was also appreciated in the writing of this thesis.

Special thanks are due to Mr. Rob Kenyon for his much appreciated guidance in the laboratory phase of this study and for his overall excellent advice. Thanks are also due to Messrs. M. Green, P. Lach, B. Lingnau, J. Oswell, and N. Piamsalee for their assistance in the laboratory.

The author would like to acknowledge the financial support of the National Science and Engineering Research Council and the Civil Engineering Department.

Finally, and most importantly, the author wishes to thank his family and friends for their encouragement and support during the past two years.

TABLE OF CONTENTS

List of Figures

List of Tables

List of Photographic Plates

CHAPTER ONE

INTRODUCTION

Engineering in Arctic and Sub-Arctic conditions is an area of growing importance in Canada. Construction in these regions is often associated with the search for energy resources, and requires a knowledge of the engineering properties of ice and frozen soil. Many structures are founded on ice, and others, such as spray-ice islands, are actually built of ice.

This thesis is part of a larger project the purpose of which is to formulate creep models for ice tested with the pressuremeter. The use of the pressuremeter for in situ testing avoids the problems associated with obtaining and transporting samples, and tests the frozen soil or ice in its natural environment, under the prevailing stresses. The use of the pressuremeter allows the engineer to analyze the test data on site and to decide immediately if he or she has sufficient data for design. Sinha (1987) has stated the need for more volumetric strain data for ice. The author believes that this study addresses that need and furthers our knowledge of the engineering properties of ice.

The present study is an extension of the work of Kjartanson (1986) on pressuremeter creep testing in laboratory ice. In the analysis of Kjartanson's test results, it was found that a knowledge of the volume change properties of his ice was required. In response to this need, the present triaxial test program was conceived to determine the bulk modulus, shear modulus, and Poisson's ratio of Kjartanson's ice.

The triaxial tests were carried out in a cold room at -2.0 °C and the mean stress employed varied from 1.0 to 2.5 Mpa. The deviator stress was 0.8 Mpa for all tests. Each test was divided into two phases; the first phase was isotropic consolidation of the ice specimen to determine the bulk modulus. The second phase was started after volumetric deformation of the specimen had effectively ceased, and was a constant mean normal stress shear test. The results of the second test phase were used to determine the shear modulus and Poisson's ratio of the ice specimen.

There is some data in the literature on the elastic values of bulk modulus, shear modulus and Poisson's ratio for ice, but virtually none on the manner in which these properties change with time during creep. Previously published studies have not examined the volume change properties of ice in creep.

CHAPTER 2

THEORY

2.1 Introduction

The purpose of the present study was to determine by triaxial testing the bulk modulus, shear modulus, and Poisson's ratio of the polycrystalline[1] ice used by Kjartanson in his pressuremeter test program. This chapter reviews the theory of the above mentioned material properties, and discusses in more detail the background of the present triaxial test program.

[1] The term *polycrystalline ice* refers to a mass of ice made up of many crystals, or grains. Ice grains usually have a maximum size of ≈10mm. *Isotropic Ice* refers to ice in which the properties are the same in all directions. The term *granular ice* refers to polycrystalline ice in which the crystals have a randomly-oriented granular shape, often hexagonal. *Columnar ice* refers to polycrystalline ice in which the grains are elongated along the axis of growth. *Saline ice* may be frozen sea water or laboratory-made saltwater ice.

2.1.1 Background to the Triaxial Testing Program

The purpose of the triaxial testing program was to determine the bulk modulus, shear modulus, and Poisson's ratio of polycrystalline ice. The need for this information arose out of the work of Kjartanson on pressuremeter creep testing in laboratory ice. (See Kjartanson et al (1988) for a description of the parameters of his test program). In his study Kjartanson compared his experimental results to the predictions given by a strain-hardening formulation of simple power law creep theory, and to the results given by a modified second-order fluid model. In formulating these models, Kjartanson made certain assumptions. One assumption was that the ice he used (laboratory-grown, pure granular ice) was incompressible. That is, he assumed that Poisson's ratio was 0.5. A second assumption he made was that the pressure was zero at the wall of the steel confining tank in which the test took place. The outside diameter of the pressuremeter was 70 mm and the diameter of the steel tank was 1.0 m. As Kjartanson et al had doubt as to the validity of these assumptions they were examined further.

Frank (1988) analyzed the case of the pressuremeter test in a confined tank of finite external radius in an effort to determine the pressure at the tank wall. He used Norton's power law and assumed the ice to be compressible. In order to determine the degree of compressibility of the ice which Kjartanson used in his study, the bulk modulus, shear modulus, and Poisson's ratio were required. As Kjartanson's tests were creep tests it was important to have a knowledge of these properties as they changed with time. A search of the literature proved that very little work had been done on these mechanical properties of ice (whether saline or freshwater), especially concerning the change in these properties with time. Indeed most studies on the mechanical properties of ice have been carried out in uniaxial compression, while in most engineering applications ice undergoes multiaxial stress. For these reasons it was decided that a test program was necessary to determine the mechanical properties of the ice which Kjartanson used, and how they changed with time.

2.1.2 <u>The Triaxial Test Program</u>

Constant mean normal stress triaxial creep tests were used to determine the volume change properties of the ice. Stress controlled (lever arm deadweight) triaxial cells were used to load a cylindrical ice specimen first in isotropic compression and then in shear. The shear phase of the test was begun only after volumetric deformations in isotropic stress had effectively ceased (that is, reached a volumetric strain rate of 1.5×10^{-5} hr^{-1}). A deviator stress of 0.8 MPa was applied to the specimen during the shear phase of the test. Mean stresses applied to the specimen were in the same range as those used by Kjartanson (1.0 to 2.5 MPa). All testing was carried out at -2.0°C in a refrigerated cold room.

Six isotropic compression tests, six constant mean normal stress shear tests, and one multi-step constant mean normal stress shear test were performed at mean normal stresses of 1.0, 1.5, 2.0, and 2.5 MPa. Note that while all test specimens were subjected to both isotropic compression and shearing forces as stated above, not all of the specimen test data was utilized. For example, only the isotropic compression data of Tests 1 and 2 were deemed of sufficient quality to be utilized in the present study. Table 2.1 summarizes the history of each specimen tested for the present study. Data from certain tests (T1S, T2S, T3IC, T3S, and T7IC) were not utilized because of equipment problems.

The following nomenclature was used when referring to individual tests - TnIC, TnS, TnUC, or TnMS. The "T" indicates "Test", while the "n" refers to the specimen number. "IC" refers to the isotropic consolidation tests, "S" refers to the shear tests (constant mean normal stress shear tests), "UC" refers to the uniaxial compression test, and "MS" refers to the multi-step shear test. See Chapter 3 for a detailed description of test equipment and procedures.

The bulk modulus K was determined from the isotropic compression phase of the test, and the shear modulus G and Poisson's ratio μ determined from the shear phase of the test. It was assumed that volumetric deformation of the specimen during the shear phase was due only to the applied deviator stress. This assumption was based on the separation of the stress system into mean normal and deviatoric components and that the ice was isotropic. The creep behaviour under hydrostatic stress was studied by means of isotropic compression tests, while the creep behaviour under deviatoric stress was studied using triaxial compression tests. In the triaxial compression tests the mean normal stress was kept constant at all times so that all strains were the result of changes in deviatoric stress only. This approach has been successfully used by Domaschuk (1969) to evaluate the static shear modulus of unfrozen soil.

2.2 Bulk Modulus of Polycrystalline Ice

The bulk modulus, K, of a material is a measure of the amount of volumetric strain which that material undergoes due to a given bulk, or hydrostatic, stress. There is a paucity of data in the literature on the bulk modulus of ice, and Sinha (1987) points to the need for volumetric strain data. What relevant information that was found is summarized below in terms of theory, previous work, and controlling variables.

2.2.1 Bulk Modulus - Theory

The bulk modulus K may be expressed as

$$K = \frac{\delta \sigma}{\delta \varepsilon_v} \tag{2.1}$$

where σ = Bulk or hydrostatic stress

ε_v = Volumetric strain due to a change in σ

For an elastic isotropic material the bulk modulus may also be expressed as a function of other material constants as

$$K = \frac{E}{3(1-2\mu)} \tag{2.2}$$

where E = Young's modulus

μ = Poisson's ratio.

There are a number of variables which control the mechanical properties of ice. Those which affect the bulk modulus of pure granular ice (such as the ice made using Kjartanson's method - see Section 3.3.1) include pressure (stress level), temperature, grain size, density, and hydrostatic stress application rate. All of these are discussed in subsequent sections. Gold (1977) states that ice can be assumed to respond elastically to stress when the period of application is less than 100 s for stress less than 1 MPa. For the perfectly elastic case, using equation (2.2), a value for bulk modulus of 10.3 GPa can be calculated for granular freshwater ice. This was obtained using a perfectly elastic Young's modulus of 9.3 GPa (Sinha, 1977), and 0.35 for poisson's ratio (Murat and Lainey, 1982), both determined by static testing. Mellor (1979) gives a value of about 9.0 GPa for the bulk modulus of pure polycrystalline ice at temperatures significantly below zero. Ice experiences visco-plastic deformation, or creep, even at low stress levels. Therefore most compression tests on ice do not determine the true bulk modulus but rather the effective (time dependent) bulk modulus, Ke. The term Ke will be used in this thesis when referring to the bulk modulus of the ice as determined by the present study.

2.2.2 Bulk Modulus - Previous Work

It would seem reasonable to expect ice to reach equilibrium some time after it was compressed hydrostatically. That is, it may be expected that the volumetric strain rate would eventually reach zero under a constant hydrostatic stress. The volumetric strain rate of a specimen would not be expected to be globally constant or monotonically increasing because this implies that the specimen would eventually disappear. Unfortunately there is no data in the literature to confirm or refute this hypothesis. It has been shown (Hobbs, 1974) that when ice is subjected to slow isothermal compression up to high pressures, phase changes occur in accordance with the P-V-T phase diagram (see Figure 2.1), and high density polymorphs may be formed. At these very high hydrostatic pressures ($\approx$3000 MPa) volume strains can be very large (see Figure 2.2).

2.2.3 Bulk Modulus - Controlling Variables

It has been established that ice at high homologous temperatures (that is near the melting point), will compress as hydrostatic pressure increases. Figure 2.2 confirms this. However, because of the visco-plastic nature of ice, it continues to deform volumetrically after a pressure has been applied and is held constant. The attenuation of volumetric deformation with time is not known. It is not known, for example, if the time to attenuation for granular ice increases or decreases for an increase in hydrostatic pressure. It is important to know how the volumetric deformation attenuates because effective bulk modulus is a direct function of volumetric strain.

Temperature has a well documented effect on the deformation of ice under load (see, for example, Traettberg, Gold, and Frederking (1975), Duval and Ashby (1983), and Jacka (1984)). In general, the response of ice to axial stress becomes more ductile as the temperature increases. This may not be the case for bulk stress since Mellor (1984) speculates that a small volume of water present in the ice lattice should not have much effect on the bulk modulus of ice because K for water is not much lower than K for ice. At -2°C, there is still unfrozen water at the triple points between grains (Sinha, 1989). Note that the temperature control in the present study was precise and accurate - the specimen temperature was maintained at -2.0°C ± 0.1°C.

A further variable affecting volumetric strain may be the lowering of the melting point due to pressure. The highest hydrostatic pressure applied in the present study was 2.5 MPa. At this pressure the melting point of ice is lowered to -0.2°C (Hobbs, 1974). It is believed that at -10°C and atmospheric pressure all water is frozen in pure ice (Hobbs, 1974). Note that Weertman (1963) states that in a polycrystalline ice specimen unfavourably orientated crystals are subjected to stresses appreciably greater than average, and the stress concentration factor is of the order of 2 or 3 (Barnes, Tabor, and Walker, 1971). Therefore, the melting point may have been lowered to -0.6°C at certain grain boundaries in the present study.

The effect of grain size in uniaxial and confined compression and tension tests has been studied (see, for example, Jacka and Maccagnan (1984), Cole (1985), Cole (1987), and DuVal (1981)). There is no data in the literature on the effect of grain size on volumetric strain. It is generally agreed that ice grains undergo recrystallization during uniaxial compression. Jacka (1984) concludes,

> ice crystal size has little or no effect on the miminum flow rate of isotropic polycrystalline ice. It may however affect the primary or transient flow rate, and thus the time to reach minimum strain rate.

This effect may extend to volumetric deformation. Note that in the present study, initial grain size was constant at 1.2 mm.

Mellor (1979) presents evidence that the bulk modulus of snow and ice is dependent upon the density or porosity of the ice (see figure 2.3). He states that if the ice is under pressure for a sufficiently long period of time the pore volume tends to adjust according to the gas laws.

A final variable influencing effective bulk modulus is hydrostatic stress application rate. Mellor (1979) concludes that overall compressibility is not much different for high rate and low rate compression, at high stresses. The effect of hydrostatic stress application rate at low stresses such as in the present study is not known.

2.3 Shear Modulus of Polycrystalline Ice

The shear modulus, G, of a material is a mechanical property that relates the amount of shear strain a material undergoes to the shear stress acting on the material. Shear modulus has been determined for polycrystalline ice, but usually by dynamic methods such as sonic testing. Static methods of measuring shear modulus require measurement of volume change, or of lateral strain as well as axial strain. Some authors have measured the lateral strain of ice under uniaxial compression, and the shear modulus may be determined from their results. Shear modulus is discussed below in terms of theory, previous work, and controlling variables.

2.3.1 Shear Modulus - Theory

Shear modulus may be expressed as

$$G = \frac{S_{oct}}{\gamma_{oct}} \tag{2.3}$$

where S_{oct} = Octahedral shear stress
γ_{oct} = Octahedral shear strain

Equation 2.3 may also be expressed as

$$G = \frac{(\sigma 1 - \sigma 3)}{2 \times (\varepsilon 1 - \varepsilon 3)} \tag{2.3a}$$

where

$\sigma 1$ = Axial stress
$\sigma 3$ = Hydrostatic stress
$\varepsilon s = 2 \times (\varepsilon 1 - \varepsilon 3) \times 3^{-1}$ = Shear strain (2.3b)
$\varepsilon 1$ = Axial strain
$\varepsilon 3$ = Radial strain (for a cylindrical sample)
$\varepsilon 3 = (\varepsilon v - \varepsilon 1)/ 2$ (2.3c)

Strains are considered positive in compression. For an elastic material, the shear modulus may also be expressed as a function of other material constants as

$$G = \frac{E}{2\ (1 + \mu)} \tag{2.4}$$

The behaviour of granular non-saline ice in shear is controlled by a number of factors, including stress application rate, stress level, stress difference (deviator stress), temperature, density, and grain size. For the perfectly elastic case, using equation (2.4), a representative value of 3.5 GPa can be calculated for the shear modulus of polycrystalline ice at -10°C. This was obtained using a perfectly elastic value of Young's modulus of 9.3 GPa (Sinha, 1977), and 0.35 for Poisson's ratio (Murat and Lainey, 1982), both determined by static testing.

Since the present study involved time-dependent, non-elastic deformation, the term effective shear modulus, Ge, will be used in this thesis to denote the quantity represented by equation 2.3 for plastic deformation.

2.3.2 Shear Modulus - Previous Work

There is some data in the literature regarding the shear modulus of ice determined by dynamic methods. In a survey of the elastic constants of sea ice, Weeks and Assur (1967) report values of shear modulus varying from 0.6 to 3.0 GPa determined by seismic field methods. Gold (1966), in a survey of the elastic constants of freshwater ice determined by sonic methods, reports values of shear modulus ranging from 3.27 to 3.66 GPa. As the speed of the seismic or sonic wave causes loading times of much less than 1 second, these G values may be viewed as purely elastic constants.

Sinha (1986a, 1986b) measured the axial and lateral strain of sea-ice specimens subjected to uniaxial compression. Thin sections of the ice revealed a columnar-grained structure, which causes anisotropic behaviour under load. Figure 2.4a shows results from Sinha (1986b) for a strain rate of 10^{-7} s^{-1}, which is in the range of minimum creep rates attained in the present study. Figure 2.4b illustrates the results of a similar test conducted at a strain rate of $10^{-4}s^{-1}$, these results approach the behaviour the specimens exhibited at the instant of loading during the present test program.

2.3.3 Shear Modulus - Controlling Variables

The rate at which the load is applied to a specimen in a creep test can have an effect on the long term behaviour of the specimen. Mellor (1979) states that a relatively high stress applied instantaneously can damage a specimen prematurely. Microcracks that occur as a result of a stress rate that is too high will enhance the creep of the specimen (Sinha 1988). It is important therefore to consider the stress application rate when designing a test program because it will have an effect on the temporal characteristics of the effective shear modulus.

Stress level may also have an effect on the properties of the effective shear modulus-time curve. In general, the higher the deviator stress acting on a specimen the faster it will deform (see, for example, Jacka (1984)). There is no data in the literature on the manner in which the effective shear modulus changes with time, at any stress level.

There has been a moderate amount of work on the effect of confining pressure during compression testing of ice (Jones 1982, Hausler 1981, Nawwar, Nadreau, and Wang, 1983). Jones found that confining pressure increased the strength of ice up to a limit of ≈40 MPa, after which the effect was reversed. Nawwar et al found that strength increased rapidly up to confining pressures of 1 MPa, after which the effect was linear up to the maximum confining pressure applied of 2.8 MPa. Note that strength is not the same as shear modulus, or stiffness. Jones' test data indicates that for a strain-rate of 5.5×10^{-3} s^{-1} the slope of the stress-strain curve in the elastic range does not seem to change as confining pressure varies from 0 to 85 Mpa. This indicates that the axial stiffness (Young's modulus) does not change with confining pressure at high strain rates. If it is accepted that axial stiffness and shear stiffness are related, then it may be postulated that confining pressure will have little effect on shear modulus.

Temperature has a well-documented effect on the strain rate of ice in uniaxial compression (Mellor and Testa 1969). See Figure 2.5. This effect is especially significant near the melting point of ice. When testing at near-melting point temperatures, a small change in temperature may cause an appreciable change in strain rate. Just how this strain rate dependence on temperature affects G is not clear.

The effect of pressure melting has already been discussed in the previous section on bulk modulus (Section 2.2.3). As was the case with effective bulk modulus, the effect of unfrozen water on the effective shear modulus is not known. Note that for the present study, the maximum stress applied during the shear phase of the test was 3.13 MPa (confining stress plus deviator stress at a mean stress of 2.5 Mpa). If a stress concentration factor of 3 is assumed, the melting point would be lowered to -0.7°C at certain grain boundaries.

In considering the effect of density or porosity on the effective shear modulus of granular ice, the key question is how does the porosity affect the axial and radial straining? Traetteberg et al (1975) show in Figure 2.6 that Young's modulus for polycrystalline ice increases fairly strongly with density. This would imply that axial strains increase with porosity, but the effect on radial strain is not known.

It is difficult to draw any conclusions from the literature about the effect of grain size on shear modulus. Cole (1987) has shown that at high strain rates (10^{-4} to 10^{-3} s^{-1}) the strength of polycrystalline ice decreases with increasing grain size. This can be seen in Figure 2.7. However, as discussed previously, the strength of ice may not be a reliable indicator of stiffness. The exact effect of grain size on shear modulus is not addressed in the literature.

2.4 Poisson's Ratio of Polycrystalline Ice

The Poisson's ratio of a material is equal to the lateral strain divided by the axial strain that the material experiences under an axial load. Poisson's ratio has been determined for polycrystalline ice both by dynamic and by static methods. Poisson's ratio is discussed here in terms of theory, previous work, and controlling variables.

2.4.1 Poisson's Ratio - Theory

Poisson's ratio may be expressed as

$$\mu = -\varepsilon 3/\varepsilon 1 \qquad (2.5)$$

where $\varepsilon 3$ = lateral strain

$\varepsilon 1$ = axial strain

Note that strains are positive in compression. Poisson's ratio in freshwater granular ice is controlled by a number of variables, including density, grain size, temperature, stress state, and stress application rate. The term Poisson's ratio is usually reserved for cases of purely elastic loading. In cases where plastic deformation occurs, the use of the term "strain ratio" is suggested by Sinha (1986a). It is denoted by μe, indicating the time dependent nature of this quantity. Another term, μi, is used to denote the instantaneous strain ratio. The difference between these two terms is that μe is the ratio of the <u>total</u> radial strain to the <u>total</u> axial strain whereas μi is the ratio of the radial to axial strains occurring over a specific (usually short) period of time. The term strain ratio will be used in the present study to indicate that equation 2.5 is being used for a specimen that has undergone plastic deformation.

2.4.2 Poisson's Ratio - Previous Work

As stated previously, Poisson's ratio has been determined by both dynamic and static methods. Weeks and Assur (1967) in a survey of seismic field determinations of the elastic moduli of sea ice present values of Poisson's ratio ranging from 0.28 to 0.38. Gold (1966) lists values of Poisson's ratio ranging from 0.31 to 0.36 for freshwater ice. These values were determined sonically, and represent the pure elastic case, as do the seismic data. A value of 0.30 is accepted as representing the elastic case for freshwater ice, and 0.50 the plastic case (Sinha, 1986a).

Published studies of Poisson's ratio using static methods are few, but include Gold (1958), Murat and Lainey (1982), and Sinha (1986a, 1986b). Gold tested freshwater ice, while Murat and Lainey and Sinha tested columnar saline ice. Gold reported static tests performed on multigrained ice stressed at the rate of 200 kPa s^{-1} for a temperature ranging from 0°C to -40°C. Poisson's ratio values of from 0.30 to 0.54 were reported. Murat and Lainey assessed the change in instantaneous strain ratio with stress rate for temperatures of from -5°C to -40°C. Sea ice beams were loaded in flexure, and longitudinal and transverse strains measured. They found that μ_e decreased with increasing stress rate down to near the value determined by sonic methods, as shown in Figure 2.8. Sinha (1986a) measured the axial and lateral strains for rectangular sea ice specimens subjected to uniaxial compression. He applied high strain rates (10^{-4} to 10^{-3} s^{-1}) and found that μ_e increased monotonically during the loading period. Final values immediately after unloading were ≈0.8. He states that these values of μ_e which are significantly higher than 0.5 (the theoretical limit for incompressible flow) were due to dilation caused by cracking. Sinha (1986b) also tested columnar iceberg ice in constant strain rate uniaxial compression at -10°C. He measured axial and lateral strain on rectangular specimens. Strain rates varied from 10^{-7} to 10^{-4} s^{-1}. Figure 2.4a shows the results of a test carried out at 10^{-7} s^{-1}. Mellor (1983) and Sinha (1986a) both state that the effective strain ratio should increase from ≈ 0.3 to an upper limit of ≈ 0.5 as the material response becomes more ductile.

2.4.3 Poisson's Ratio - Controlling Variables

The effect of density or porosity on the axial and lateral strain of a specimen is discussed in Section 2.3.3. Mellor (1983) states that μ for freshwater ice does not vary much with density. Schwarz (1977) quotes a study by Bush and Goldschmidt (1970) which indicated that μ for other materials varied by less than 10% as porosity varied by up to 30%. Previous work on Poisson's ratio (see Section 2.4.2) has not dealt with density in a systematic manner. Therefore it is not known how μ_e will change as density changes.

As with density effects, there has been no systematic study of the effect of grain size on Poisson's ratio in polycrystalline ice. Sinha's studies on Poisson's ratio (1986a, 1986b), used two different types of columnar ice with two different grain sizes (1 mm and 8.5 mm diameter, varying length). At a strain rate of 3×10^{-4} s^{-1}, and a temperature of -10^oC, the ice with 1 mm grains had $\mu \approx 0.37$ at failure. At a strain rate of 1×10^{-4} s^{-1}, and a temperature of -10^oC, the ice with 8.5 mm grains also had $\mu \approx 0.37$ at failure. Failure is defined here as the peak of the stress-strain curve. The author does not believe that the comparison of these two tests is sufficient reason to claim that μ is not affected by grain size. The ice tested by Murat and Lainey (1982) was columnar-grained, with grain sizes perpendicular to the direction of growth equal to 1 mm. Their results are shown in Figure 2.8.

Murat and Lainey (1982) determined effective strain ratio at -40°C, -30°C, -20°C, and -5°C, as shown in Figure 2.8. Their results indicate an increase in effective strain ratio with increasing temperature. The results of Gold (1958) are in agreement with this observation.

The stress state of ice will also affect the effective strain ratio. Confining pressure will subdue internal cracking which causes dilation (Mellor 1983). (Dilation is responsible for an increase in effective strain ratio (Sinha, 1986b)). Therefore the lateral strain will be reduced and Poisson's ratio will be reduced as compared to an unconfined specimen.

There is some confusion in the literature regarding the effect of stress application rate (or strain rate) on the strain ratio of ice. Murat and Lainey (1982) concluded that the effective

strain ratio decreased with increasing stress application rate, as shown in Figure 2.8. Sinha (1986a, 1986b) found for varying strain rates that the effective strain ratio increased with time. Sinha found that samples tested at higher strain rates had higher limiting strain ratios, due to greater cracking activity. It is difficult to compare the results of Sinha to those of Murat and Lainey because of the different test methods employed, and because Murat and Lainey do not show the variation of effective strain ratio with time.

In summary, this chapter has reviewed the theory, previous work, and controlling variables of the bulk modulus, shear modulus, and Poisson's ratio of polycrystalline ice. These mechanical properties are directly influenced by the pressure (stress level), temperature, grain size, density, and strain rate of the ice. The majority of the previous work on the bulk modulus, shear modulus, and Poisson's ratio of polycrystalline ice has been directed towards the determination of elastic properties, often by dynamic methods. Very few of the previous studies have concentrated upon the time-dependent, visco-plastic nature of deformation in ice, especially as regards the change in mechanical properties with time.

Table 2.1

Summary of Specimen Histories

Specimen Number	Isotropic Compression	Shear	Mean Stress (Mpa)
1	X (T1IC)	-	2.5
2	X (T2IC)	-	2.0
3	-	-	2.5
4	X (T4IC)	X (T4S)	1.0
5	X (T5IC)	X (T5S)	1.5
6	X (T6IC)	X (T6S)	2.0
7	-	X (T7S)	2.5
8	-	X (T8S)	Unconfined Compression
9	X (T9IC)	X (T9S) (T9MS)	2.5 2.5

"X" indicates that the data from that test was used in the present study, with the test name in brackets.

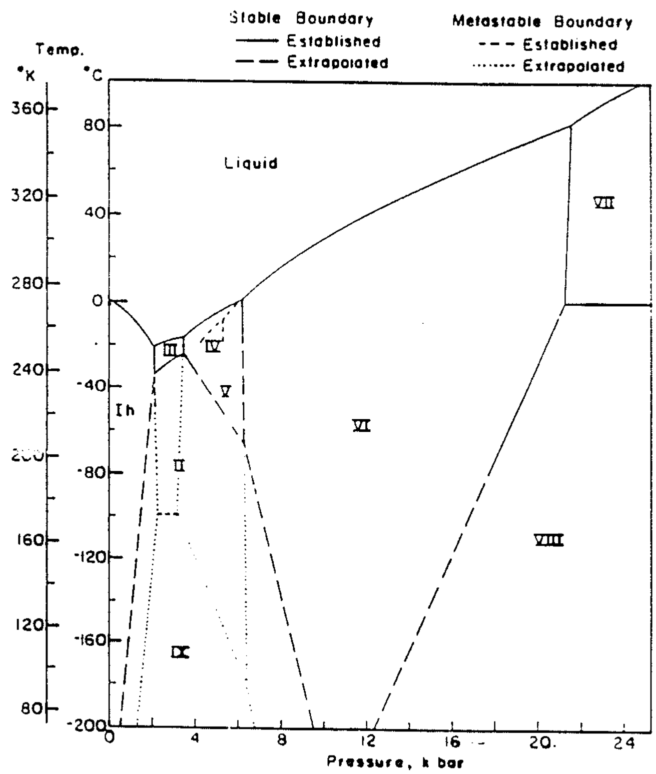

Figure 2.1 Phase diagram for ice (Mellor, 1979)

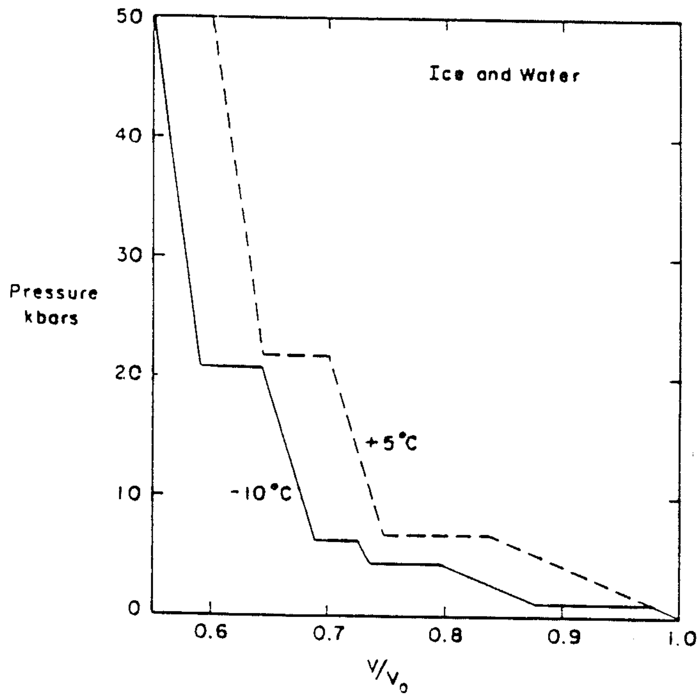

Figure 2.2 Volumetric stress/strain characteristics for isothermal compression of ice at -10°C and water at +5° (Mellor, 1979)

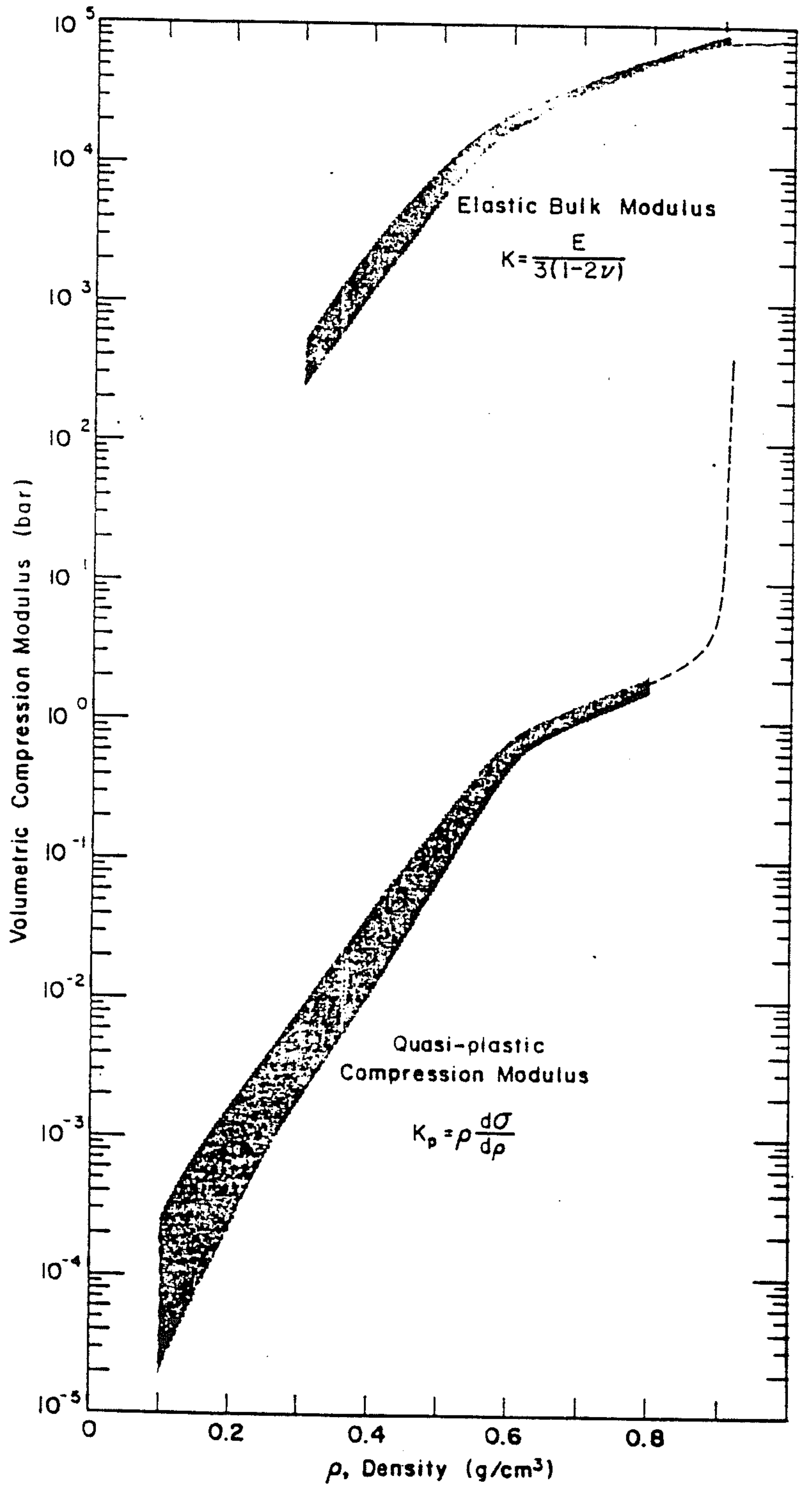

Figure 2.3 Volumetric compression moduli plotted against bulk density for snow and ice (Mellor, 1979)

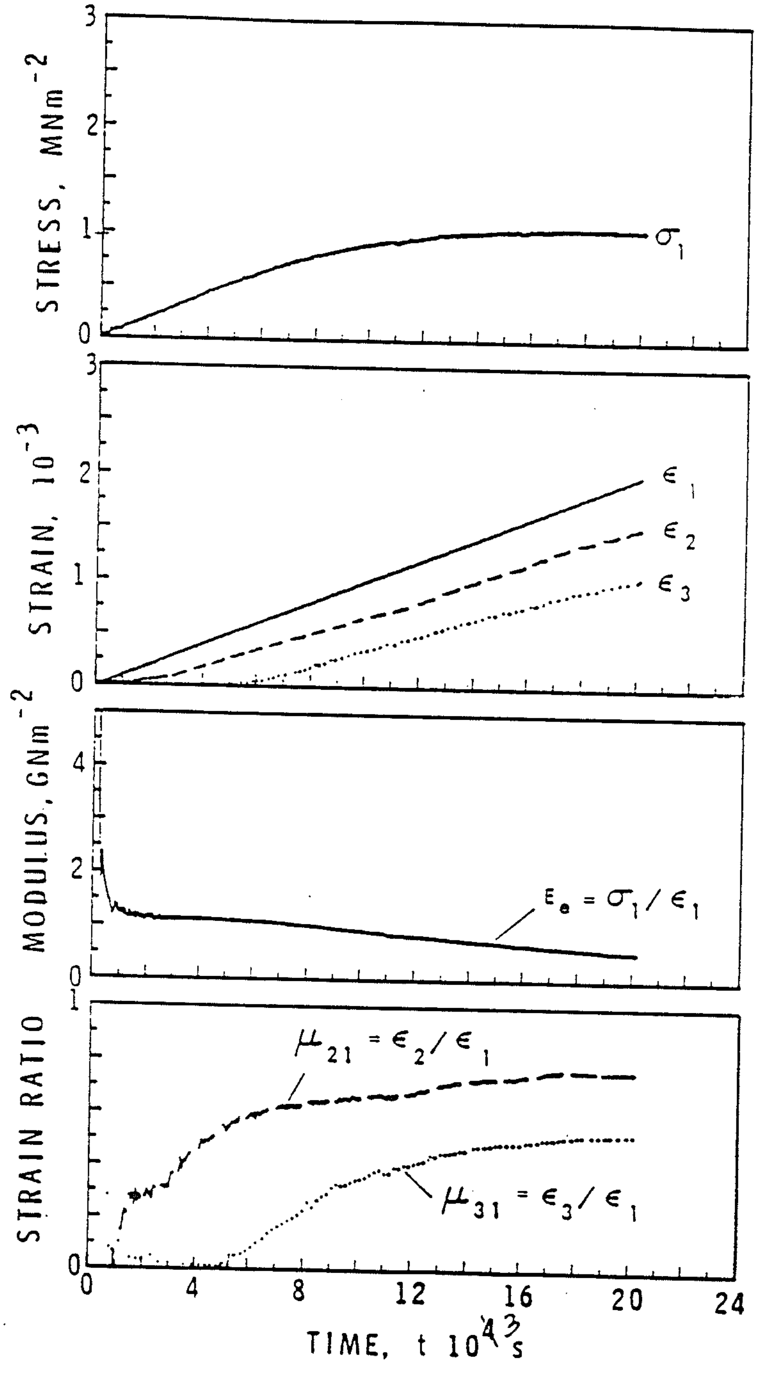

Figure 2.4a Stress, strain, effective modulus and strain ratio histories of columnar ice at -10°C at strain rate of 1×10^{-7} s^{-1} (Sinha, 1986b)

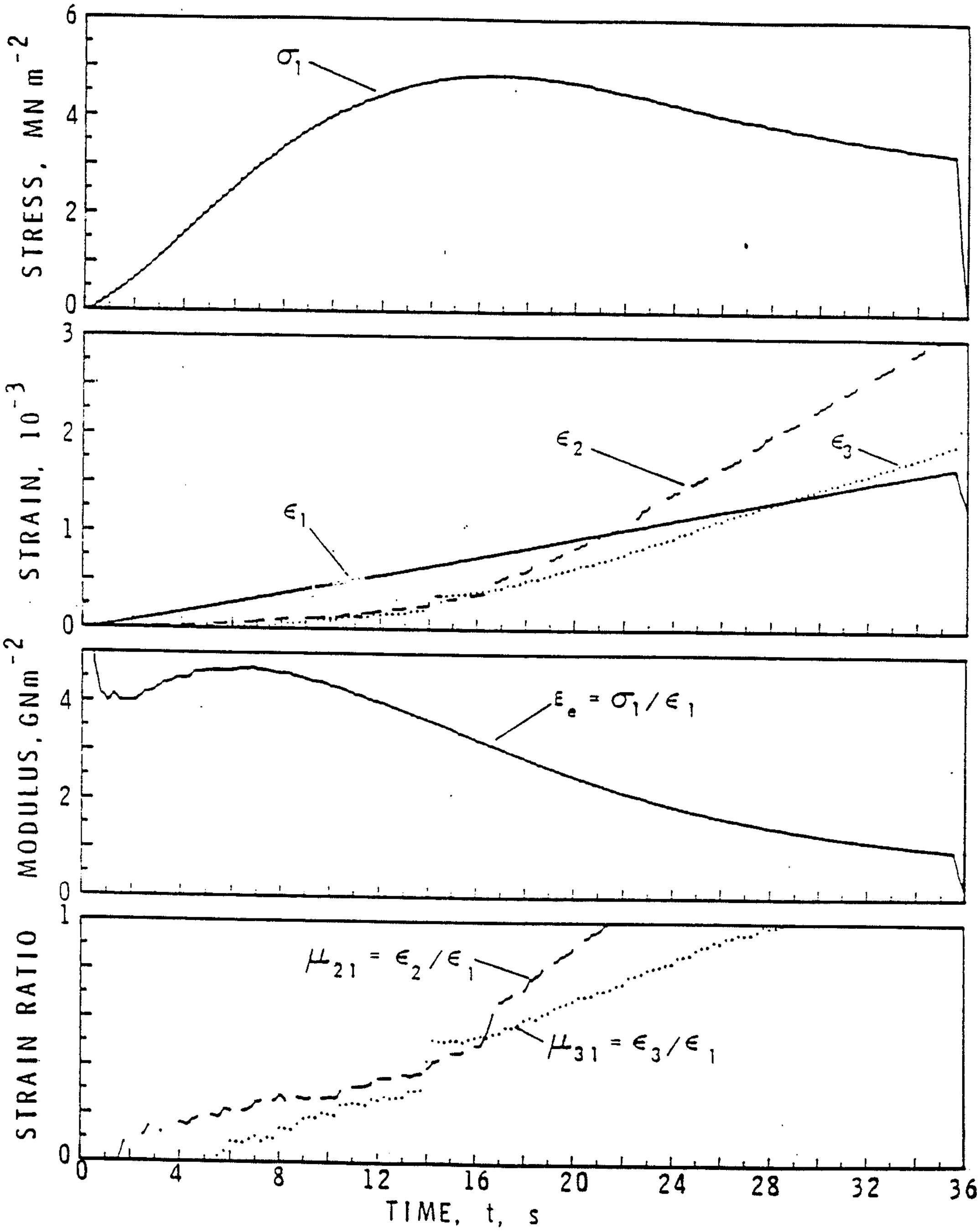

Figure 2.4b Stress, strain, effective modulus and strain ratio histories of columnar ice at -10°C at strain rate of 1×10^{-4} s^{-1} (Sinha, 1986b)

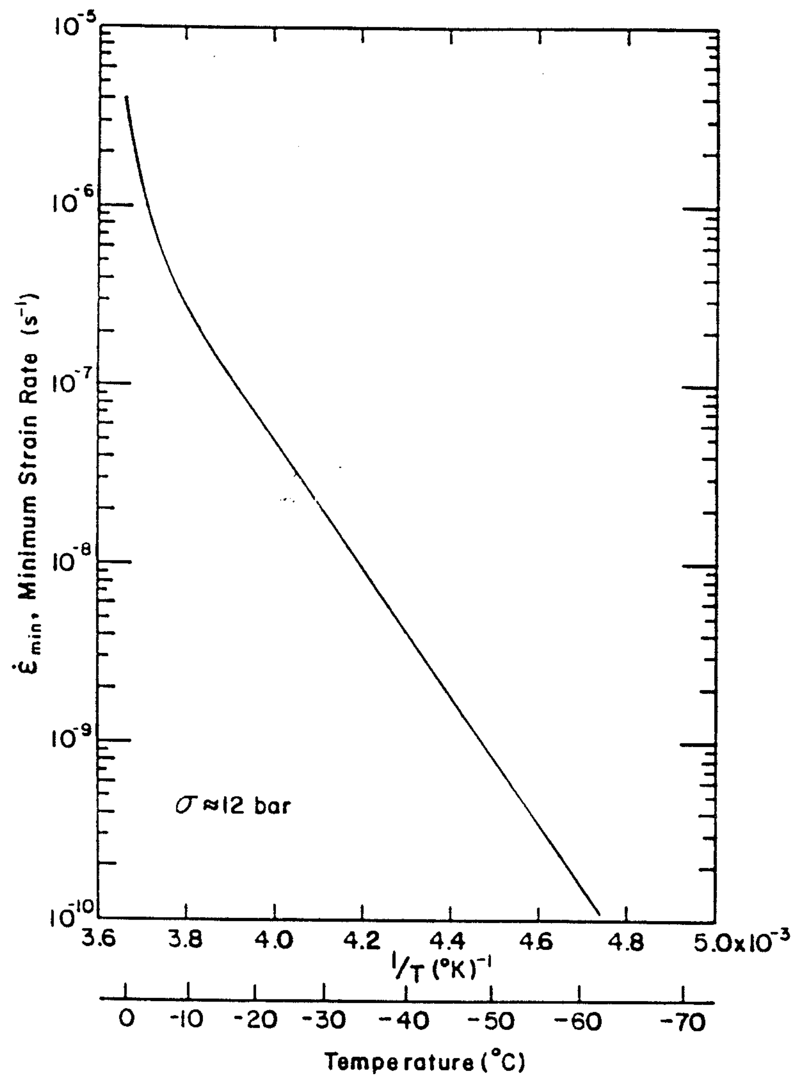

Figure 2.5 Empirical relation between minimum strain rate and temperature for high-stress creep (Mellor and Testa, 1969)

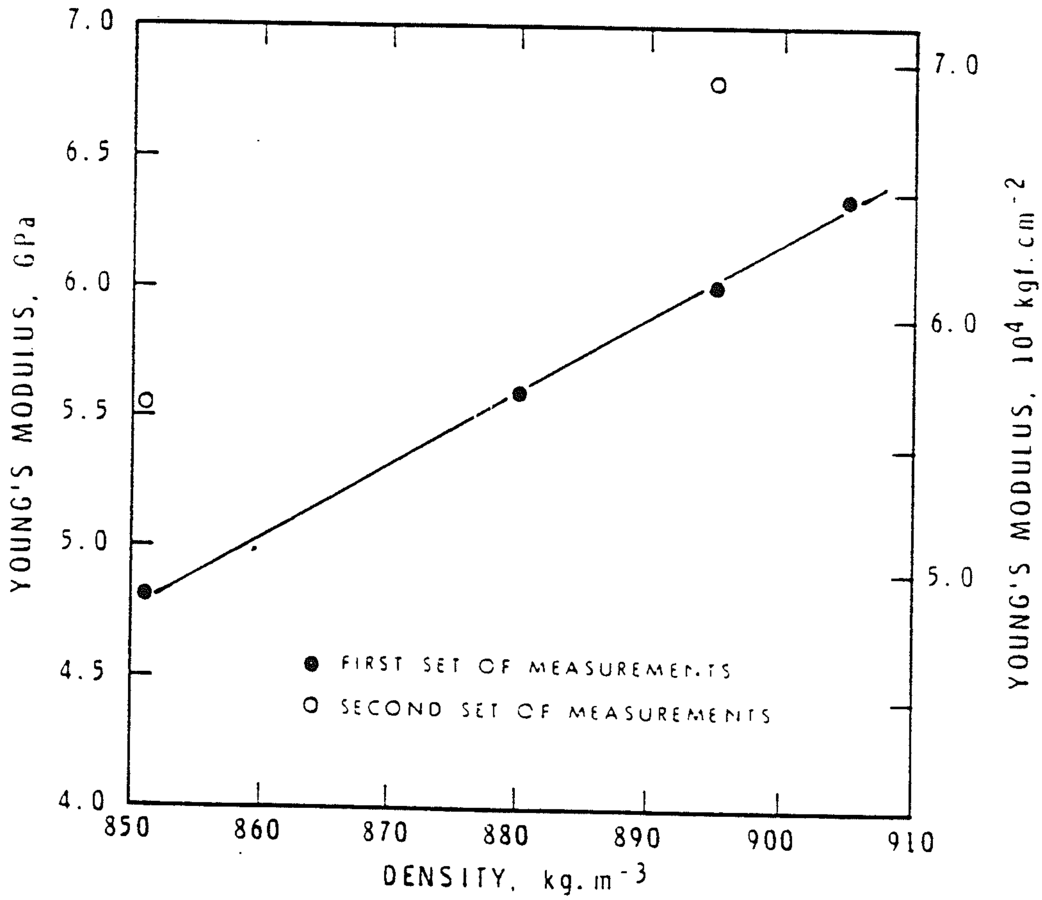

Figure 2.6 Dependence of Young's modulus on density of freshwater ice (Traetteberg, 1975)

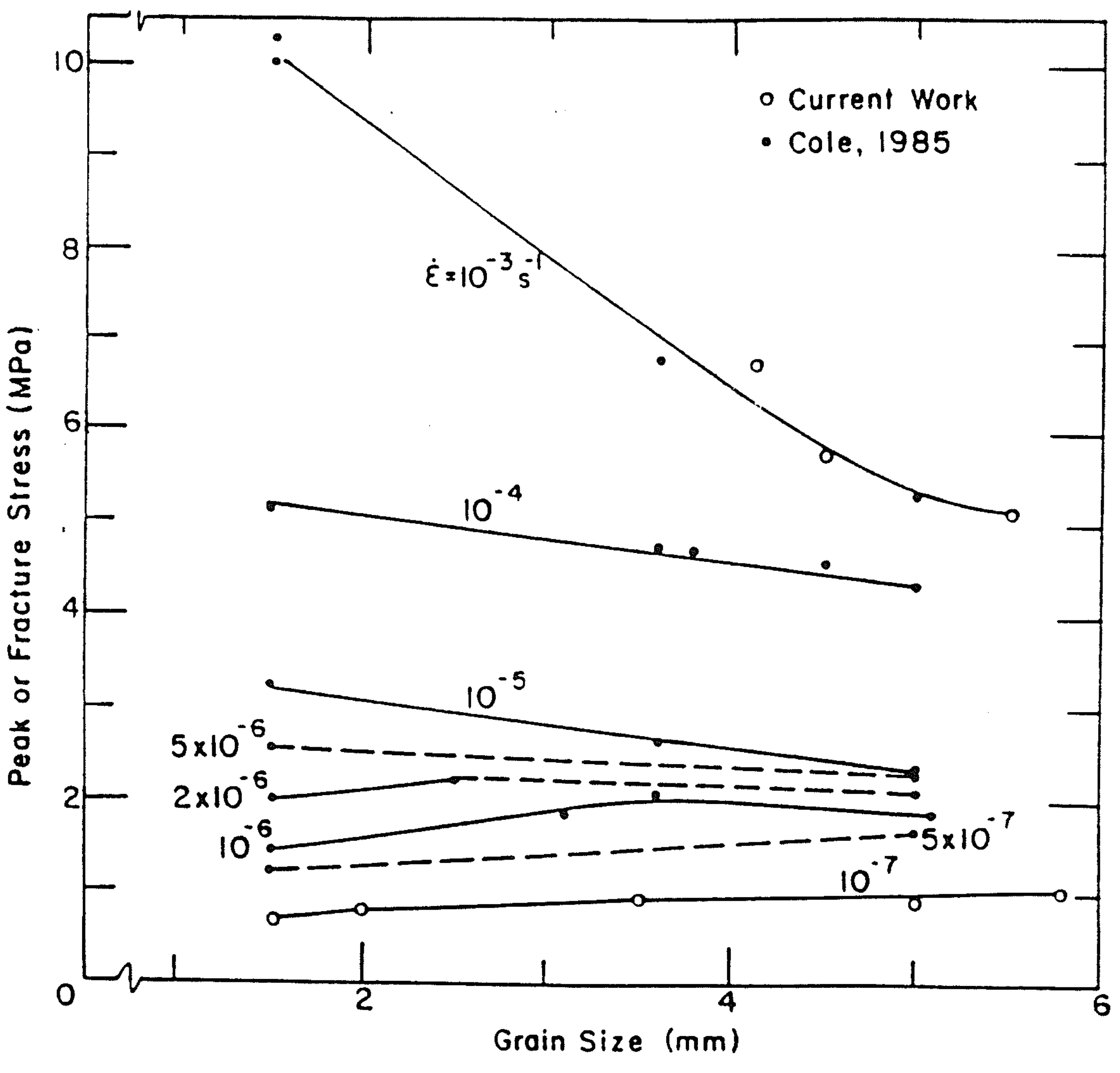

Figure 2.7 Peak stress vs. grain size for freshwater ice at -5°C (Cole, 1987)

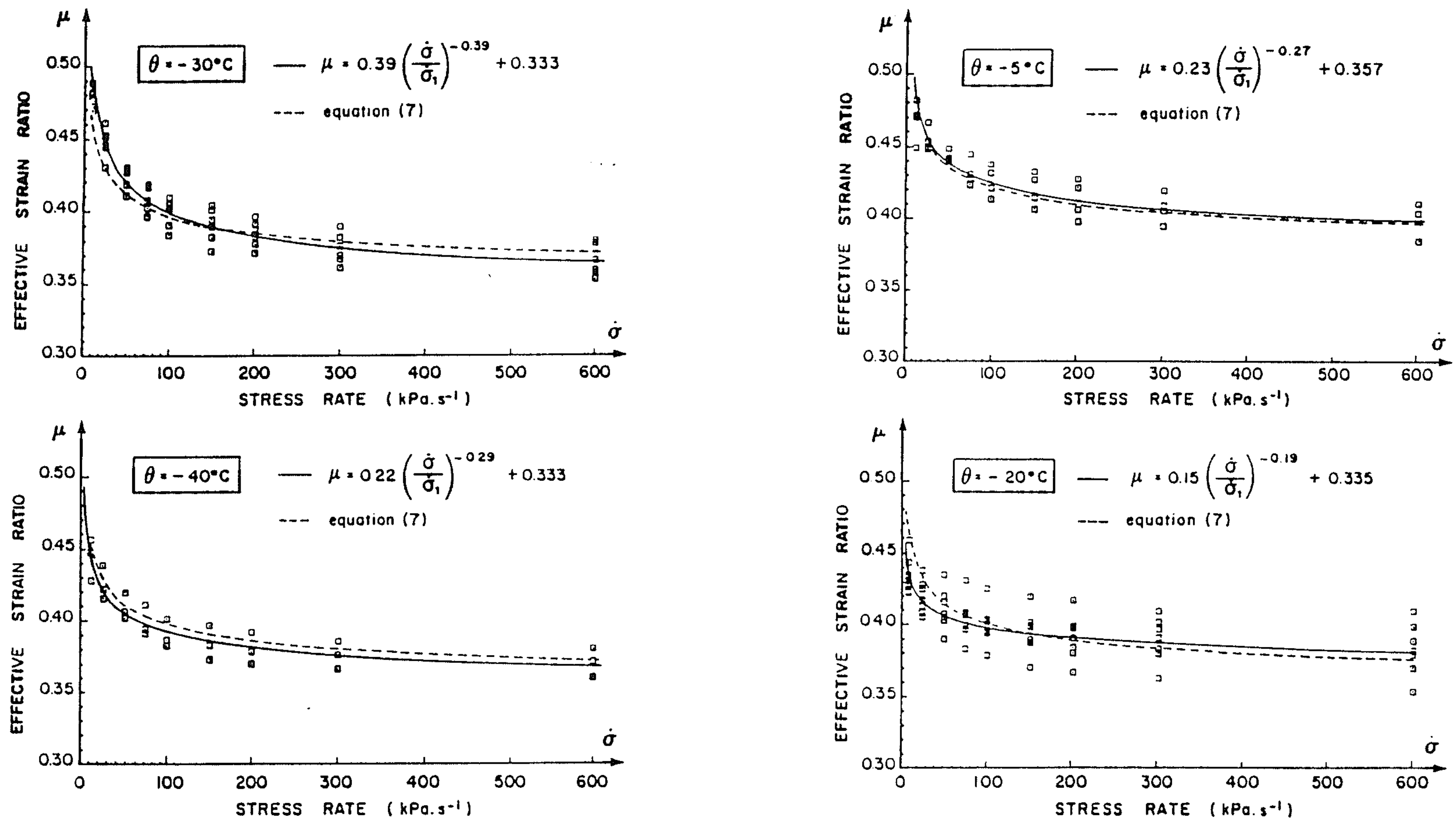

Figure 2.8 Variation of effective strain ratio with stress rate for various temperatures for columnar ice (Murat and Lainey, 1982)

CHAPTER THREE

TEST EQUIPMENT AND PROCEDURES

3.1 INTRODUCTION

This chapter examines the equipment that was used to make and test the polycrystalline ice specimens. The procedure followed for each test is also reviewed.

3.2 TEST EQUIPMENT

Refer to Figure 3.1 for the layout of the testing system.

3.2.1 Triaxial Cells

The triaxial cell (Figure 3.2) was the heart of the triaxial ice testing apparatus. The cell was based on a National Research Council of Canada design and was of a double-walled aluminum construction. Copper tubing was wound around the outside of the inner cylinder. The tubing was connected to a temperature bath which pumped constant temperature coolant through the tubing at a steady rate thereby cooling the antifreeze in the triaxial cell. Each cell, of which two were used in the test program, had a built-in thermistor in the inner chamber to monitor the sample temperature. Figure 3.2 is a schematic of the triaxial cell. The ice specimen was placed in the inner cell and the remaining space in the inner cell was filled with anti-freeze. The inner cell was connected through a port in the cell base to the volume change burette as indicated in Figure 3.2. Volume changes in the inner cell were reflected by a change in the level of anti-freeze in the volume change burette. The level of the anti-freeze in the burette could change because of one or more of four phenomena. These were system compliance (including anti-freeze compression - see Figure 4.1), thermal expansion and contraction of the anti-freeze liquid (found to be 0.45 CC/ ^{o}C/ 1000 CC), ice specimen volume change, and intrusion of the piston into the inner cylinder. The thermal expansion and contraction of the ice itself was negligible in comparison to these four mechanisms.

3.2.2 Load Application

The cylindrical ice samples were subjected to two types of loading - axial and radial. The axial load was applied through a Farnell lever arm constant load frame. The radial load was applied to the sample through fluid pressure. Compressed nitrogen gas was fed directly to the anti-freeze fluid. The anti-freeze fluid surrounded the specimen and filled the space between the inner and outer cylinders. Note that by pressurizing the fluid in both the inner and outer chambers of the triaxial cell, the inner cylinder was not subjected to a differential pressure.

3.2.3 Temperature Control

There were three levels of temperature control in this testing program. First, the tubing coil on the outside wall of the inner cylinder was connected to a constant temperature Haake K Refrigerator Bath with a Haake F3 Controller. The fluid continuously circulating in the coil helped moderate any temperature fluctuation in the surrounding antifreeze. Secondly, the cell was placed in an insulated cabinet to further protect it from any temperature fluctuations in the cold room. Thirdly, the whole test system, excluding the electronics and the pressurized gas supply, was placed inside an environmentally controlled chamber, the cold room The combined effect of these controls was to keep temperature variations in the inner chamber to within ±0.1 degrees Celsius.

3.2.4 Instrumentaion

Each cell was equipped with 4 types of instrumentation, as described below.

Pressure Transducer - Dynisco pressure transducers effective in the 0-7 Mpa range were used. They were attached to the pressure feed line just before it entered the cell. The transducers were calibrated using a Lucas Barnet 8000 Series deadweight tester, and were accurate to within 15 kPa.

Thermistor - Each cell had a built-in thermistor in the inner chamber. The thermistors were calibrated using an ice-bath, a thermometer accurate to within ±0.01°C and a Haake Refrigerated Bath. The thermistor measured temperature accurately to within ±.01 degrees Celsius.

Axial Deformation LVDT - The change in sample height under load was measured by an HP 7DCDT-500 displacement transducer. These LVDT's were accurate to within ±0.013 cm and produced a steady signal free from interference. The axial LVDT's were calibrated using stainless steel gauge blocks.

Volume Change Device - Two methods of measuring the volume change of the sample were tried. The first method, which later proved unsatisfactory, employed an electronic volume change measurement device. A float located in a reservoir inside the device was attached to an HP 7DCDT-500 displacement transducer. The volume change device was calibrated using a GDS Controller which controlled volume changes to within 1 cubic millimeter. While the device performed well during a shear test at zero cell pressure, the device was not very sensitive to volume changes when it was pressurized. The problem may have been due to an asymmetrical float which caused the LVDT rod to tilt and the core to bind within the LVDT.

It was then decided to measure volume change with a simple burette system, as shown in Figure 3.1. Although this system necessitated manual readings, it was found to be accurate.

Note that the calibrations for the pressure transducer, the axial deformation LVDT, the thermistor, and the volume change device were carried out in cold room conditions at the test temperature of -2°C.

Power Supply - A 6-volt supply powered the instruments and fed the analog signals into the analog/ digital conversion card in the computer.

3.2.5 Data Acquisiton

A computer controlled data acquisition system was used to record the readings from the instruments (with the exception of the volume change burette). The heart of the A/D system consisted of an off-the-shelf computer board which served as multiplexer, analog-digital converter, and gain amplifier. The board was a Real Time Devices AD500 analog/digital conversion board. The data was stored on the computer's hard disk drive as it was read. A PC Generation IBM-compatible XT computer with a 30 megabyte hard drive was used in the data acquisition role.

3.2.6 Pressure Calibration

The sample volume change measuring system used in the test program was found to be compliant. Care was taken to minimize the amount of entrapped air in the system. Nevertheless, volume strain, as measured with the burette, and due only to the compression of the anti-freeze, expansion of the tubing and cell, and compression of entrained air, was approximately 0.26% at a pressure of 2.5 MPa. Due to the double-walled construction of the triaxial cell expansion of the inner cyclinder with pressure must have been negligible. The compliance calibrations gave repeatable results, suggesting that the measures to insure that no air bubbles were present in the cell at the time of testing were successful. Later test results, however, proved that entrapped air may have caused some variation in initial measured volumetric strain.

3.3 TEST PROCEDURE

The procedures which were followed to run a triaxial test are summarized here. The steps discussed include the production and freezing of the ice, coring of the specimens, sample preparation, sample testing, and post-test activities.

3.3.1 Production of Ice

It was important to follow the same procedure in making the ice for the present study as was used by Kjartanson (1986). This was accomplished using the same equipment as he used, and by adopting his procedure, summarized as follows:

1. The cold room in which the freezing barrel was situated was set to give an average temperature of 0 °C. The barrel in which the ice was produced was approximately one meter in diameter and one meter high, and is shown in Plate 3.1.
2. A water reservoir was filled with enough tap water to flood the sample (approximately 0.2 m^3). The water was chilled to the freezing point by pouring fine grained party ice into it.
3. Thermocouples were taped to a wooden rod which was then stuck into the barrel to monitor temperatures during and after the freezing of the specimen.
4. The freezing coils on the bottom of the barrel were covered with sand to prevent them being damaged by the core barrel during drilling. The freezing coils were hooked up to a condenser and assured that the ice froze from the bottom up. To prevent radial freezing, the sides of the barrel were insulated and the room was kept at 0°C during the freezing process.

5. The hose from the water reservoir was placed in the bottom of the tank and the tap controlling the flow was opened.

6. Immediately, two bags of fine grained party ice purchased from Arctic Ice Co. Ltd. of Winnipeg were poured into the tank and compacted 100 times with a specially constructed tamper. (The chemical properties of the tap water and the seed ice crystals are given in Table 3.1 from Kjartanson 1986).

7. Ice crystals were poured into the tank and compacted, bag by bag. Each bag formed a loose lift of ice crystals about 50 to 75 mm thick. Each lift of ice crystals was tamped 100 times with the special tamper. The pre-chilled water was allowed to flow into the tank at a steady rate, and was within 15 cm of the ice level at all times.

8. The level of the ice crystals was brought to within about 25 to 50 mm of the top of the tank. When the porewater had just flooded the top crystals, the tap was shut off and the hose removed.

9. The ice sample temperature and room temperature were monitored closely until the sample was completely frozen. The room temperature was maintained as close to 0°C as possible, so that neither significant freezing nor thawing occured on

the sample sides and top.

This method of making ice was modelled after that of Sego (1980). Samples produced in this way are reproducible and homogeneous as the ice density measurements presented in Chapter 4 indicate. Work by Thompson (1986) using thin sections showed a small variation in air content, however, going from top to bottom in the tank.

3.3.2 Coring

After the tank of ice was frozen (tank temperature was -2°C), core samples were extracted for testing. The core barrel used was of a modified CRREL design, with an outer diameter of 104 mm and inner diameter of 72 mm. The core barrel was turned with a hand-held power drill, and penetrated to the level of the sand at the bottom of the tank. The core barrel and drill are shown in Plate 3.2. After a core sample was extracted it was logged. The cores from a single borehole totalled approximately 65 cm in length and were usually broken into 4 sections. The appearance of the core was also recorded i.e. the size and amount of air bubbles and the structure of the ice. If the samples were not to be used immediately, they were wrapped in celophane and placed in a sealed plastic bag to prevent sublimation during storage. Some snow was added to the bag so that sublimation, if any, of the snow would occur first. The samples were stored in a freezer at -18 degrees Celsius. There was no visible evidence of sample disturbance during coring (no cracks visible). Any surface imperfections were removed during the lathing process.

3.3.3 Sample Preparation

The ice samples as extracted by the core barrel were not immediately suitable for triaxial testing because the ends were not perpendicular to the length and the diameter was not sufficiently constant. (Plate 3.3 shows a specimen during the machining process). To make a true cyclindrical triaxial specimen the ice samples were lathed to the proper dimensions by the following procedure.

1. The cold room was chilled to -5°C to ensure all metal parts were well beneath the freezing point.
2. The ice cores were brought into the cold room to bring them to cold room temperature. An ice-water mixture was prepared (the water was later used to freeze the sample onto the platens).
3. Both ends of a section of core barrel sample were cut to be perpendicular to the sample axis with a bandsaw.
4. A 6.35 cm diameter top platen was frozen onto one end of the unfinished sample. The platen had

been previously cooled to -18°C, and was in the cold room for about 10 minutes before it was used. The sample was frozen onto the platen by first covering the surface of the platen with ice water at 0 °C and then placing the sample directly on the platen immediately afterwards. The sample would freeze onto the platen, forming a strong and firm bond after a few seconds.

5. The platen was then placed in the chuck of the lathe and the sample was turned to a length of 140 mm (5.5 in.) and a diameter of 64 mm (2.5 in.).

6. The sample dimensions were then measured with calipers and the sample weighed to determine it's density.

7. The lower platen was attached to the other end of the sample using the same procedure as in 4.

8. The sample with both platens attached was placed on the base of the triaxial cell.

9. Silicone grease was applied to the vertical surface of the platens and the finished sample was covered with two rubber membranes, secured by a total of six O-Rings, to prevent infiltration by the anti-freeze and subsequent dissolving of the sample during testing. This combination of O-Rings, rubber membranes, and silicone grease was found to be effective.

3.3.4 Sample Testing

At this point in the test, the sample was on the base of the triaxial cell and was protected by two rubber membranes. Plate 3.4 shows the sample on the cell base.

3.3.4.1 Assembly of Triaxial Cell

The triaxial cell was assembled around the ice sample using the following procedure.

1. Attach the inner cylinder with its coolant coil to the base of the cell. When the inner cylinder is secure, turn on the temperature bath. Allow anti-freeze which has been cooled and de-aired for 6 hours to flood the inner cylinder from the bottom; stop when the anti-freeze is almost at the top.
2. Attach the top of the inner cylinder, allow anti-freeze to flow out of the bleed screw, and then replace the screw so that no air is trapped.
3. Attach the outer cylinder to the cell base, and then fix the top of the outer cylinder in place. When secure, open the lower valve again and allow anti-freeze to flood the annular space between the two cylinders.
4. When the cell is full, remove and quickly replace the two bleed nuts on the cell base

ensuring that no air is trapped.

5. Place the piston and fill the burette.

6. Allow the cell temperature to come to equilibrium at -2.0°C for at least six hours.

7. Apply a trial pressure of ≈70 kPa to check for leaks.

8. Attach LVDT, Thermistor, and pressure transducer to data acquisition system.

At this point the equipment was ready and a test could be started. Plate 3.5 shows the triaxial cell completely assembled in its insulated cabinet.

3.3.4.2 Isotropic Compression Test

The isotropic compression test was carried out to determine the effective bulk modulus, Ke, of the ice which Kjartanson used in his test program. Cell pressures used in the triaxial test program ranged from 0.8 to 2.5 Mpa. When the cell temperature was stabilized at -2.0°C, the desired pressure was applied by means of pressure-regulated compressed nitrogen gas. (Prior to application of the test pressure, however, a small pressure of approximately 70 kPa was applied to the cell to test for leaks). It took approximately 60 seconds for the test pressure to stabilize. Immediately after the cell pressure had stabilized, the burette level was recorded by eye, and the temperature and pressure were recorded by computer. During the first hours of a test, readings were taken approximately every 10 minutes. The frequency of readings decreased as the test progressed. The cell pressure was maintained constant until the volumetric deformation of the ice effectively ceased. Since the rate of volume change decreased asymptotically, it would have taken a very long time for the ice to stop deforming completely. Therefore, it was assumed, for practical purposes, that the ice had stopped deforming when the volumetric change decreased to a strain rate of $\approx 10^{-5}$ hr^{-1}. This assumption was based on the work of Rahman (1988) who performed similar tests on frozen sand. When this point in the test was reached, the shear test was begun.

3.3.4.3 Constant Mean Stress Shear Test

The constant mean stress shear test was carried out to determine the effective shear modulus, Ge, of the ice which Kjartanson used in his test program. The mean stress, σm, on the sample was determined as follows,

$$\sigma_m = (\sigma 1 + \sigma 2 + \sigma 3) / 3 \qquad (3.1)$$

where $\sigma 1$ = axial stress

$\sigma 2$, $\sigma 3$ = lateral stresses, at right angles to each other ($\sigma 2 = \sigma 3$ in the triaxial test).

When the sample had reached a volumetric strain rate of 1.5×10^{-5} hr^{-1} in the isotropic compression test, a deviator stress of 0.8 Mpa was applied to the sample.

At the same time, the cell pressure was reduced to compensate for the increased axial stress. Thus the mean stress on the sample was maintained constant. Mean stress levels used in the test program were 1.0, 1.5, 2.0, and 2.5 Mpa. These levels corresponded to the pressuremeter stresses used by Kjartanson in his program. A deviator stress of 0.8 Mpa was chosen because it was high enough so that the tests would not take an inordinate length of time, but low enough so that the visco-plastic nature of deformation in ice would be apparent. The deviator stress was not changed from test to test so that test results could be compared on an equal basis. The deviator stress was varied in the multi-step test.

The deviator stress was applied by placing the piston firmly on the top platen, locking the piston in place with the piston clamp screw, loading the required weights onto the lever arm, and then releasing the piston clamp screw. Thus the deviator stress was applied very quickly, just as the pressuremeter pressure was applied in Kjartanson's work. A reading of the burette and the electronic instruments was taken ≈ 3 seconds after application of the deviator stress. During the application of the deviator stress the data acquisition system was set to take readings at the maximum frequency of one reading every two seconds. Burette readings were taken every 10 minutes during the first hours of a test, and with decreasing frequency thereafter. The deviator stress of 0.8 Mpa was maintained until the sample had reached an axial strain of approximately 7%. The axial load and cell pressure were then released.

For the multi-step shear test, once the first step was completed (at an axial strain of ≈ 7 %), the cell pressure was lowered and the deviator stress was increased. In each of the second and subsequent steps, the deviator stress was increased by 0.4 Mpa, and the cell pressure accordingly lowered to maintain the mean stress at 2.5 Mpa. The deviator stress was applied incrementally - the cell pressure was lowered first and the required weights were then placed on the lever arm in order to increase the deviator stress by 0.4 Mpa above the previous level. The second and subsequent steps were run until axial strain for that step was ≈2%, and then the next load was applied. The lever arm on the load frame did not have enough travel to allow individual steps to reach a greater axial strain than 2%. A total of five steps were used for the multi-step test.

3.3.4.4 Post Test Activities

After the test had ended and the loads were released, the triaxial cell was disassembled and the rubber membranes removed from the sample. The condition of the sample and the position of the platens were recorded. Sample dimensions were measured, and the sample was weighed to determine it's density. The sample was then photographed and wrapped in cellophane and stored in an air-tight bag for later analysis.

TABLE 3.1

Chemical Properties of City of Winnipeg Tap Water and Arctic Ice Co. Ltd. Ice Crystals

Parameter	Tap Water(1) (mg/l)	Ice Crystals(2) (mg/l)
Fluoride	0.90	0.27
Total Hardness ($CaCO_3$)	83	8.46
pH	8.0	N.A.
Nitrate	<0.04	0.02
Chloride	2	2
Sulfate	<10	1
Calcium	22.5	5
Magnesium	6.2	0.54
Sodium	1.8	0.63
Potassium	1.4	N.A.
Iron	0.06	0.08
Manganese	0.01	0.02

N.A. - not available.

(1) data from "Water Quality Monitoring Report", 1984, City of Winnipeg Waterworks and Waste Disposal Department, Laboratory Services Branch.

- average values of 1984 given.

(2) data from Arctic Ice Co. Ltd.; report prepared by W.M. Ward Technical Services, Aug. 1982.

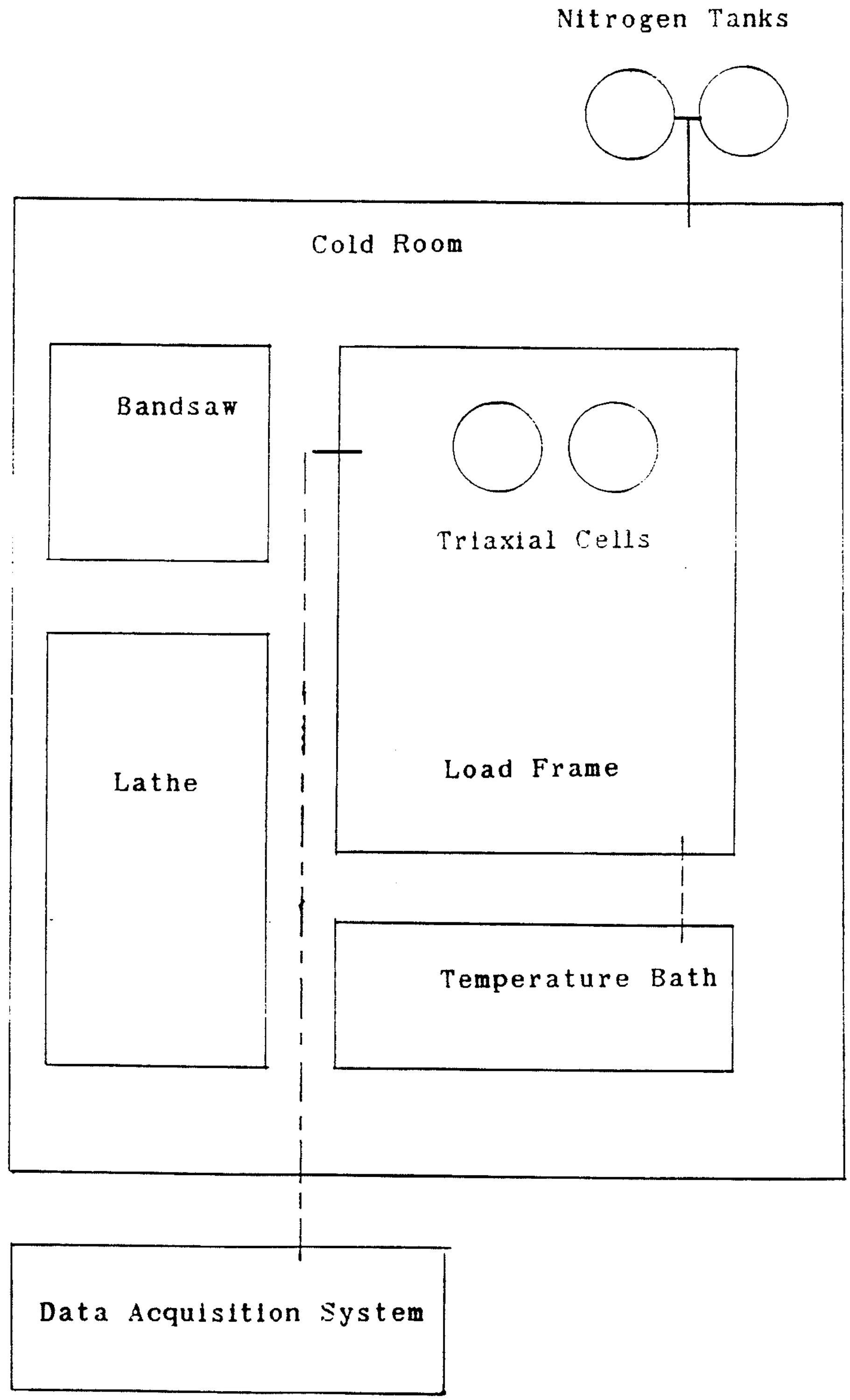

Figure 3.1 Test System Layout

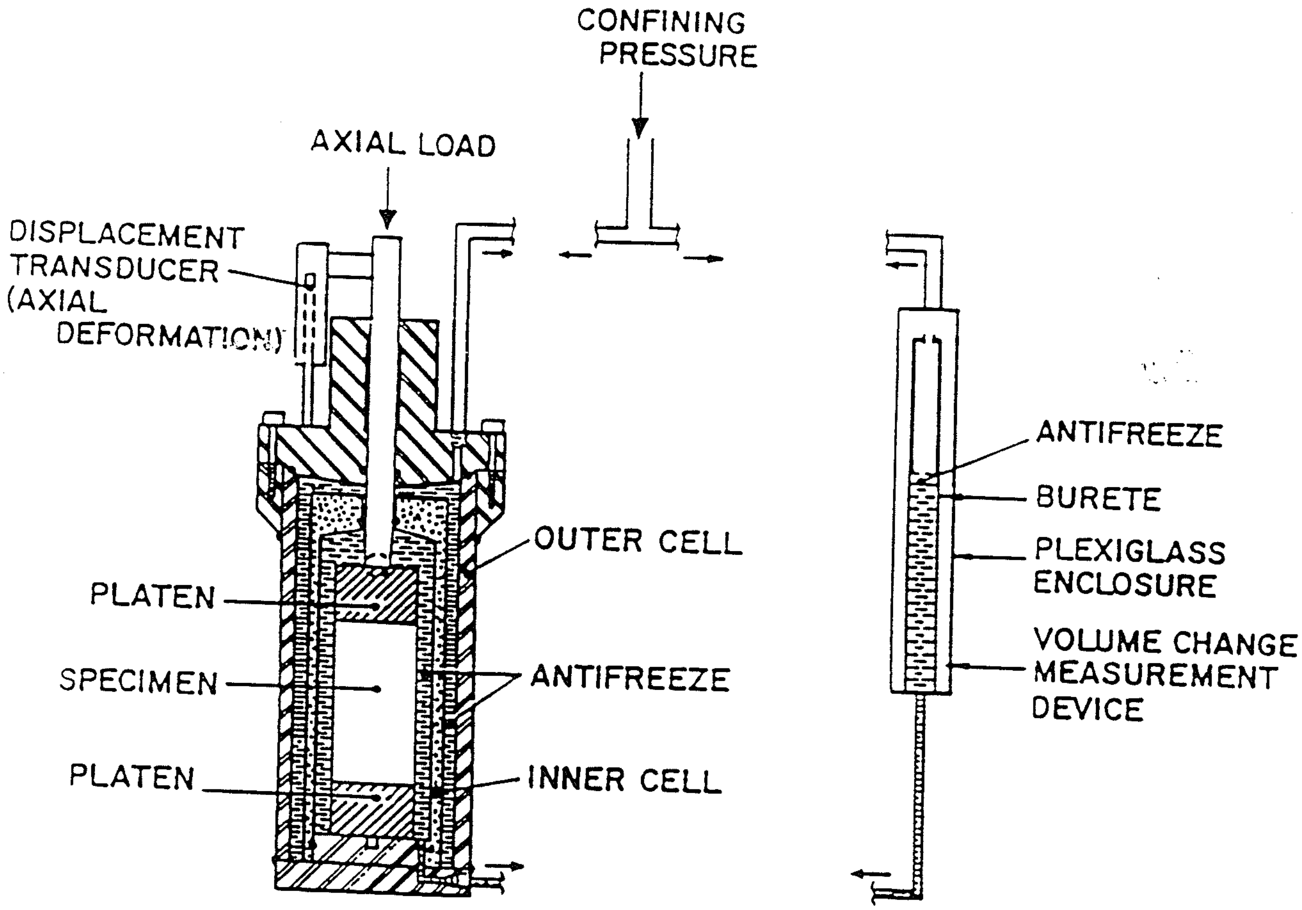

Figure 3.2 Cross section of triaxial cell and volume change device

Plate 3.1 Top of ice freezing barrel

Plate 3.2 Drill and core barrel

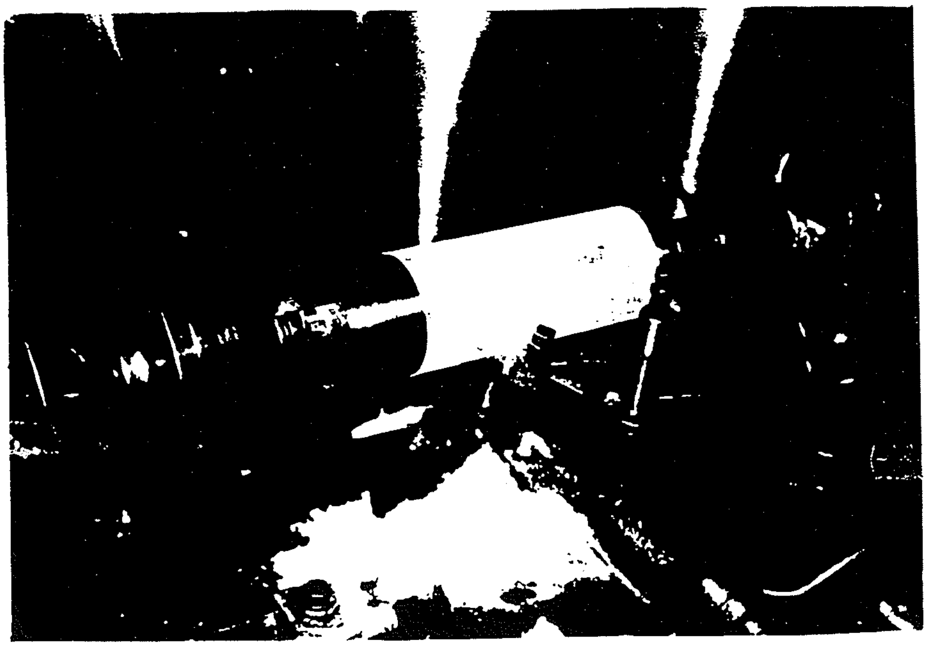

Plate 3.3 Ice specimen during lathing process

Plate 3.4 Ice specimen on triaxial cell base prior to testing (note protective rubber membrane)

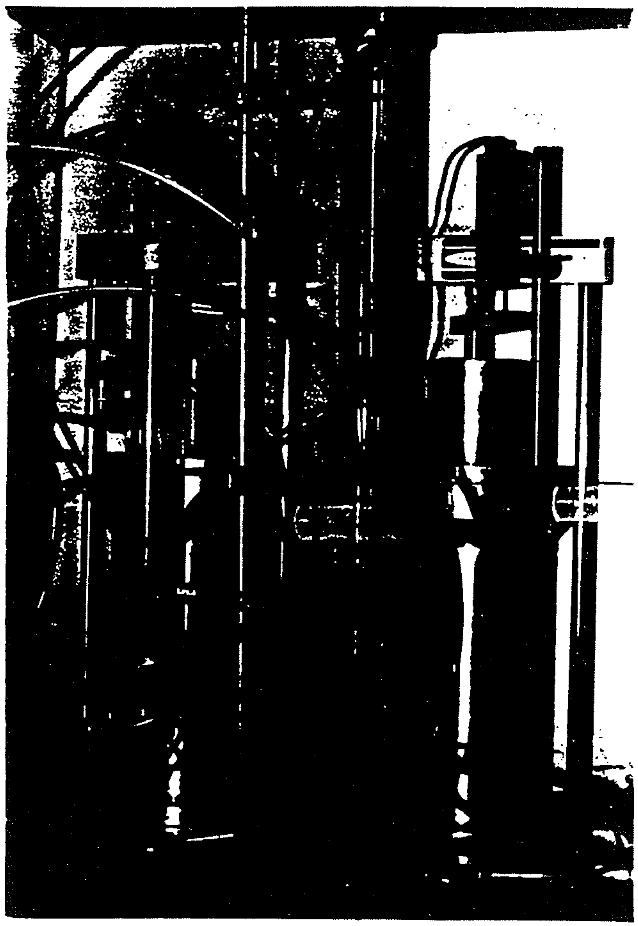

Plate 3.5 Fully assembled triaxial cells inside cabinet

CHAPTER FOUR

TEST RESULTS

4.1 INTRODUCTION

The results of the triaxial test program are presented here in terms of specimen strain and strain rate from the isotropic compression and the constant mean normal stress shear tests. In addition to this data, ice properties, test repeatability, and post-test inspection of specimens are discussed.

4.2 ICE PROPERTIES

The ice used by Kjartanson in his test program and in the present study had a slightly cloudy appearance due to entrapped air. The ice is described below in terms of appearance, density, and grain size.

4.2.1 Qualitative Description of Test Ice

The ice produced by Kjartanson's method (see Section 3.3) was not 100% free of air. During the flooding process, very small air bubbles (<0.5mm in diameter) attached themselves to the boundaries of the crushed ice used as seed ice. These small bubbles could be seen after the freezing process was complete as they formed a faint outline around the original seed crystals. The original seed crystals were between 6.5

and 13 mm in diameter. These very small bubbles were uniform in distribution throughout the ice. Occasionally, a bubble of air (up to 0.25 CC in volume) would become trapped between seed ice crystals during the flooding process and would remain after the barrel was frozen. These were random in nature, and could probably have been avoided if vibratory compaction techniques had been used, or if the ice/water mixture had been subjected to a vacuum.

4.2.2 Density of Test Ice

The density of each specimen is listed in Table 4.3. As may be seen in Table 4.3, the ice exhibited relatively uniform density characteristics. The average density of all test specimens was 0.906 g/cm^3 ± 0.007 g/cm^3. This corresponds to a porosity of 1.2% assuming the density of solid ice to be 0.917 g/cm^3. Note that the standard deviation of the densities is less than 1% of the average value. Also note that the samples were weighed after any surface pores were infilled.

4.2.3 Crystallography

A detailed crystallographic examination of Kjartanson's ice was carried out in 1987 by Thompson. His study determined that the average grain size of the ice was 1.35 mm, using the boundary-intercept method.

This conclusion was supported by a preliminary crystallographic examination of core samples by the author. The crystals in the ice were granular, and the c-axes of the crystals were randomly oriented in the horizontal plane. (Thompson, 1987). Examination by the author determined that the c-axes were also randomly oriented in the vertical plane. Refer to Thompson (1987) for a more detailed discussion of the crystallography of Kjartanson's ice.

4.2.4 Specimen Reproducibility

The process used in making test specimens for the present study is outlined in Section 3.3. The successful use of the lathe in forming the specimens ensured that dimensional tolerances were within close limits. Analysis of the specimen dimensions as measured by calipers gave the following results - average variation of specimen diameter along its lenth was 0.11%, while the average variation in specimen length was 0.14%. That is, specimen dimensions varied by approximately 1/1000. This is well within the standards for sample dimensions set by CRREL (1984).

4.3 EXPERIMENTAL RESULTS OF THE ISOTROPIC COMPRESSION TESTS

The ice specimens, formed according to the procedures outlined in Section 3.3, were first tested in isotropic compression. The purpose of the isotropic compression tests was to determine the bulk modulus of Kjartanson's ice. The results of these tests are presented below.

4.3.1 Volume Measuring Device Compliance

In order to determine the initial elastic compression of the ice specimen it was necessary to account for the compressibility of the anti-freeze liquid in the inner cell, the compression of any entrapped air, and the expansion of the equipment. The volumetric change of the anti-freeze system was subtracted from the total measured volume change, leaving the volumetric compression of the ice. Figure 4.1 shows the calibration curves of the volume measuring system. Above ≈0.7 MPa the curves had an average slope of 0.000492/MPa.

4.3.2 Isotropic Compression Test Results

A total of 6 single stage isotropic compression tests was performed for the present study. Test pressures varied from 1.0 to 2.5 MPa. The isotropic compression test program is summarized in Table 4.1. Individual tests are summarized in Figures 4.2 to 4.7. The results are presented in terms of volumetric strain, ignoring the initial elastic strain. That is, the first reading after the application of the cell pressure is treated as the zero point. The reason for this is discussed in section 4.2.3. Initial measured elastic compression for each test is shown in Table 4.2. The results of all isotropic compression tests are summarized in Figure 4.8. Volumetric strain rate data for each test are presented in Figures 4.9 to 4.14 for strain rates less than 0.01 %/hr, and is summarized for all isotropic compression tests in Figure 4.15. The strain rate curves indicate that all isotropic compression tests were terminated when the strain rate had slowed to $1.5 \times 10^{-5} hr^{-1}$.

The temperature during all tests was constant at $-2.0^{o}C$ $\pm 0.1^{o}C$. Figure 4.16 shows the temperaure during a typical test (Test T6IC). The pressure was also maintained constant during each test. Figure 4.17 shows the pressure during a typical test (Test T5IC).

In an effort to determine more accurately the initial elastic deformation that the ice specimen underwent as it was compressed volumetrically, several quick-step isotropic compression tests were performed. A quick-step test was set up in the same manner as a regular isotropic compression test. However, instead of applying the isotropic pressure for that test in one step and then measuring the volume change, the isotropic pressure was applied in four or five steps, and the volume change measured after each incremental pressure was applied. It took approximately 15 seconds to apply the incremental isotropic pressure and measure the volume change for each step. Therefore each quick-step test took approximately 75 seconds to complete. The main advantage of the quick-step isotropic compression test was that it eliminated the effects of any entrapped air in the system since the air would become entrained after a pressure of ≈ 0.7 Mpa was reached (Head, 1986). Individual quick-step tests are illustrated in Figures 4.18 to 4.22. QSIC1 and QSIC2 were performed on specimens T7 and T7A respectively, while QSIC3, QSIC4, and QSIC5 were the initial and repeat tests on the same specimen (specimen T9). Figure 4.23 summarizes all quick-step isotropic compression tests. The quick-step tests were used to determine the elastic bulk modulus.

4.3.3 Discussion of Isotropic Compression Test Results

The compliance calibration curves of the volume measuring device were applied to the volume changes measured at the instant of isotropic loading in order to calculate the elastic compression of the ice. The elastic compression of the specimens exhibited a large degree of variability, as Table 4.2 shows. It is postulated that varying amounts of trapped air caused the variation in measured initial elastic volume strain among tests. Note that 1 CC of air will cause an increase in apparent strain of 0.25%. Another possible cause of the variation in initial measured volume strain may be the pores in the ice structure. Although pores at the specimen surface were filled with drops of water, (to prevent the puncture of the protective membrane during pressure application) post-test inspection revealed that the membrane had occasionally been forced into pores in the ice. This would cause the fluid level in the burette to drop. This apparent volume change should not properly be included in the calculation of bulk modulus. Therefore an estimate of elastic bulk modulus based on the initial measured volumetric change in single stage tests may be incorrect. It was for this reason that the quick-step isotropic compression tests were performed.

It is worth noting in Figure 4.8 the apparent similarity of the volumetric creep curves. In general, the higher the isotropic stress, the faster the slope of the strain-time curve decreased. The tests were terminated when the volumetric strain rate was approximately 1.5×10^{-5} hr^{-1}. Table 4.1 gives the length of each test (i.e. the time required to reach a volumetric strain rate of 1.5×10^{-5} hr^{-1}). and Figure 4.24 illustrates how the length of each test decreased as mean stress increased. Figure 4.25 shows the decrease in final strain as consolidation pressure increased. As shown in Chapter 5, the effective bulk modulus versus time curve had become asymptotic by the time each isotropic compression test was terminated.

As shown in Figure 4.8, the creep curve of T9IC varies slightly from the other creep curves. Three successive quick-step isotropic compression tests (cycled tests) were performed on specimen T9 before the single stage isotropic compression test load was applied to the specimen. The reasons for the difference in behaviour are discussed in Section 6.2.

The quick-step isotropic compression tests experienced the same problem with apparent volumetric changes during the initial loading steps as did the single step tests. However, it is postulated that after the second step (1.0 Mpa) was reached, any trapped air bubbles went into solution (Head, 1986), and that any pores susceptible to membrane encroachment would have been entered. This hypothesis appears to be correct since the slope of the curve is constant above 1.0 Mpa. See Figure 4.16.

4.4 RESULTS OF CONSTANT MEAN STRESS SHEAR TESTS

Constant mean normal stress triaxial compression tests were performed in the present study to determine the effective shear modulus and the effective strain ratio of Kjartanson's ice. This type of test has been successfully used by Domaschuk (1969), Gill (1969), and Liu (1970) to evaluate the static shear modulus of unfrozen soil. Rahman (1988) used this test technique to determine the bulk modulus and shear modulus of frozen soil. For the present study, mean normal stresses of 1.0, 1.5, 2.0, and 2.5 Mpa were used. The deviator stress (the difference between axial and confining stresses) was always 0.8 Mpa for the single step tests. One multi-step test was performed at a mean normal stress of 2.5 Mpa, with the deviator stress increasing in steps.

4.4.1 Single Stage Test Results

A total of 6 constant mean stress shear tests was performed for the present study, all with a deviator stress of 0.8 Mpa. The results of these tests are presented in Figures 4.26 to 4.31 in terms of axial, radial, and shear strain. Summaries of all tests in terms of axial, radial, and shear strain are presented in Figures 4.32, 4.33, and 4.34 respectively. Axial strain rates are plotted in Figures 4.35 to 4.40 against time, and in Figures 4.41 to 4.46 against axial strain. Figure 4.47 summarizes the plots of axial strain rate against axial strain. Critical information for each test is presented in Table 4.4. Plots of specimen volumetric strain during shear are presented in Appendix A.

4.4.2 Multiple Stage Test Results

One multi-step constant mean stress shear test was performed for the present study. The test was performed on specimen T9 and five steps were used. The deviator stress on the sample was increased from 0.8 to

1.2 to 1.6 to 2.0 to 2.4 Mpa. As an indication of specimen behaviour under the increasing loads, the specimen took 62.5, 4.4, 1.3, 0.39, and 0.28 hours to reach 2% axial strain for steps one to five respectively. The results for T9MS are shown in Figure 4.48 in terms of axial, radial, and shear strain versus time. The results of each step are illustrated in Figures 4.49 to 4.53 in terms of axial, radial, and shear strain versus time. Figure 4.54 illustrates the axial strain rates for all five steps, while Figures 4.55 to 4.59 show the axial strain rates for each step individually.

4.4.3 Discussion of Results of Constant Mean Stress Shear Tests

Figure 4.32 shows some variation in the strain-time curves of the shear tests. The deviator stress was the same for each test (0.8 Mpa), but mean stress and specimen density varied from test to test. Four of the tests (T4S, T6S, T7S, and T8S) exhibit similar strain-time curves, while two tests (T5S and T9S) have less steep strain-time curves than the other four. The axial strain rate versus axial strain curves (Figures 4.41 to 4.46) show in general that the minimum strain rate occurs at approximately 1% axial strain, and is ≈ 0.03 %/hr. The decrease in axial strain rate which occurred in most samples at ≈ 6% axial strain was due to the increase in average radius of the ice specimen and the resultant decrease in effective stress on the specimen cross section.

With regards to the multi-step test, it is interesting to note the non-linear increase in strain rate as deviator stress increases, as indicated in Figure 4.54. A second interesting feature of the multi-step test is the slow response to an increase in deviator stress exhibited by the specimen during the fourth and fifth steps of the test. This is illustrated in Figures 4.58 and 4.59. In the first three steps (Figures 4.55 to 4.57), the specimen exhibited an immediate elastic response to an increase in deviator stress. This response was delayed in the final two steps.

Temperature and pressure control were very good during all shear tests. Refer to Figures 4.16 and 4.17 for an illustration of temperature and pressure variation with time.

4.5 TEST REPEATABILITY POST-TEST INSPECTION

In any test program it is important to establish that the tests are repeatable. Repeatability helps to prove that the test results are sound and that any conclusions drawn from those results are valid. Post-test inspection of specimens is important to determine the mode of failure.

4.5.1 Test Repeatability

Repeat tests were performed for the isotropic consolidation tests and for the shear tests. Tests T2IC and T6IC were both conducted at 2.0 Mpa, and are both illustrated in Figure 4.8. It may be seen that the strain paths for the tests are very similar, at no time differing by more than 0.1% volumetric strain.

Two constant mean normal stress shear tests (T7S and T9S) were run at the same mean stress of 2.5 Mpa (see Figure 4.32). Specimen T9S was much more compressible than specimen T7S, and showed more compressibility than the other tests. The apparent anomaly of Test T9S may not be unusual, however, if one considers the results of other researchers. For example, Mellor and Cole (1982) conducted unconfined compression tests on fine-grained isotropic ice at -5°C using both constant load and constant strain rate techniques. For two constant load tests (96CL and 117CL) conducted at the same deviator stress of 0.8 Mpa (as in the present study), the time to reach minimum axial strain rate was recorded. The minimum axial strain rate is usually reached at ≈ 1% strain (Mellor and Cole, 1983). For 96CL and 117CL the minimum strain rate was reached at 19 and 29 hours at axial strains of 1.01% and 1.02% respectively. For T7S and T9S 1% axial strain was reached at 16 and 22 hours respectively. On the basis of these observations the repeat tests in the present study showed greater similarity than those of Mellor and Cole (1982).

It may be concluded then that the specimens produced for the present study were reasonably reproducible, based on the measurement of specimen density and dimensional variations. It may also be concluded that both the isotropic compression and the constant mean stress shear tests were repeatable, on the basis of the strain-time data.

4.5.2 Post-Test Inspection of Specimens

After each test was completed, the triaxial cell was disassembled and the specimens were examined. In qualitative terms, the single stage specimens were usually slightly clearer after the test was completed than before it began. Larger bubbles were generally not evident. A slight barrelling of the specimen was sometimes observed. The surface of the specimen was generally slightly nuggetty, except that the surface of specimen T9, which underwent the multi-step shear test, was very nuggetty. Plates 4.1 and 4.2 show a typical single-step specimen upon completion of the shear test. (Specimen T4).

Table 4.1

Summary of Isotropic Compression Test Results

Test	Pressure (Mpa)	Volumetric Creep Strain at End of Test[1] (%)	Length of Test[2] (hr)
T1IC	2.5	0.67	154
T2IC	2.0	0.81	273
T4IC	1.0	0.91	312
T5IC	1.5	0.65	178
T6IC	2.0	0.81	236
T9IC	2.5	0.80	140

1 i.e. when volumetric strain rate reached 1.5×10^{-5} hr^{-1}

2 i.e. time required to reach volumetric strain rate noted above

TABLE 4.2

Summary of Initial Measured

Elastic Volumetric Strain

Test	Pressure (Mpa)	Initial Elastic Strain (%)
T1IC	2.5	0.46
T2IC	2.0	0.30
T4IC	1.0	0.46
T5IC	1.5	1.36
T6IC	2.0	1.17
T9IC	2.5	1.17

TABLE 4.3

Summary of Test Specimen Densities

Specimen	Density (g/cm^3)
K-1	0.902
K-2	0.896
K-3	0.900
T1	0.912
T2	0.909
T3	0.895
T3A	0.893
T3B	0.906
T4	0.915
T5	0.915
T6	0.907
T6A	0.908
T6C	0.906
T7	0.909
T7A	0.909
T8	0.907
T9	0.906

Average density = 0.906 g/cm^3

Sample Standard deviation = 0.007 g/cm^3

Average porosity = 1.2 %

TABLE 4.4

Summary of Constant Mean Stress Shear Test Results

Deviator Stress = 0.8 Mpa For All Tests

Test	Mean Stress (Mpa)	Length of Test (hr)	Strains at End of Test (%)		
			Axial	Radial	Shear
T9S	2.5	212	6.70	3.30	6.66
T7S	2.5	187	8.52	4.19	8.47
T6S	2.0	116	6.73	3.32	6.70
T5S	1.5	253	7.82	3.78	7.74
T4S	1.0	163	5.22	2.43	4.93
T8UC	-	189	8.50	4.24	8.49

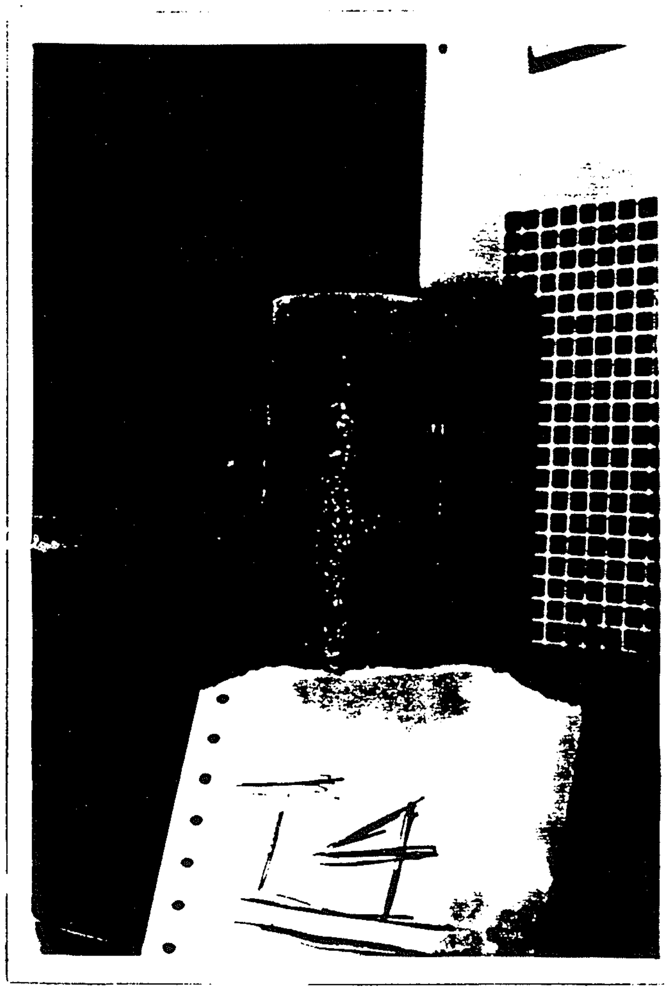

Plate 4.1 Specimen T4 after completion of shear test

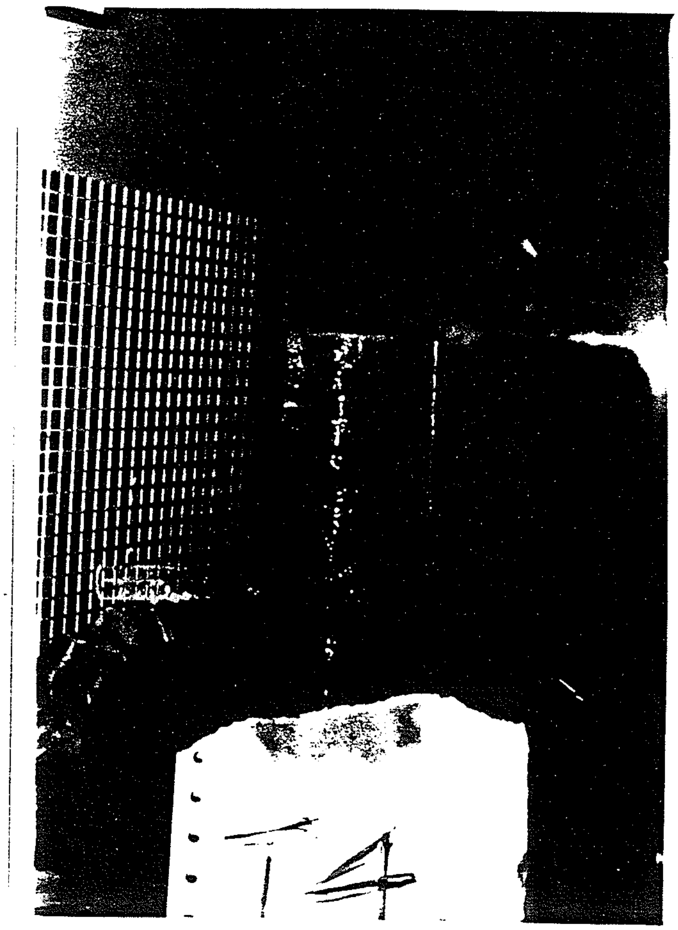

Plate 4.2 Specimen T4 after completion of shear test

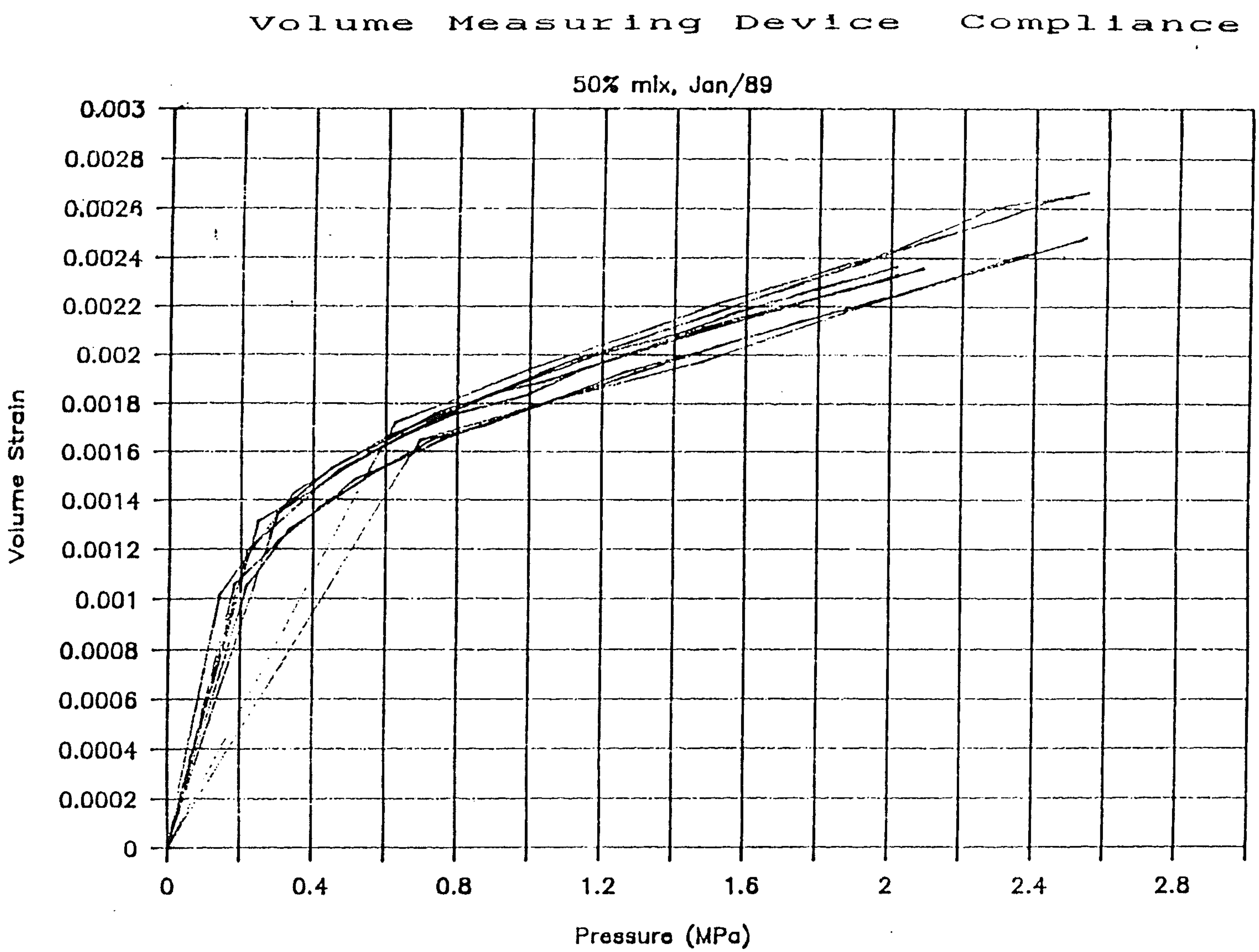

Figure 4.1 Volume measuring device compliance

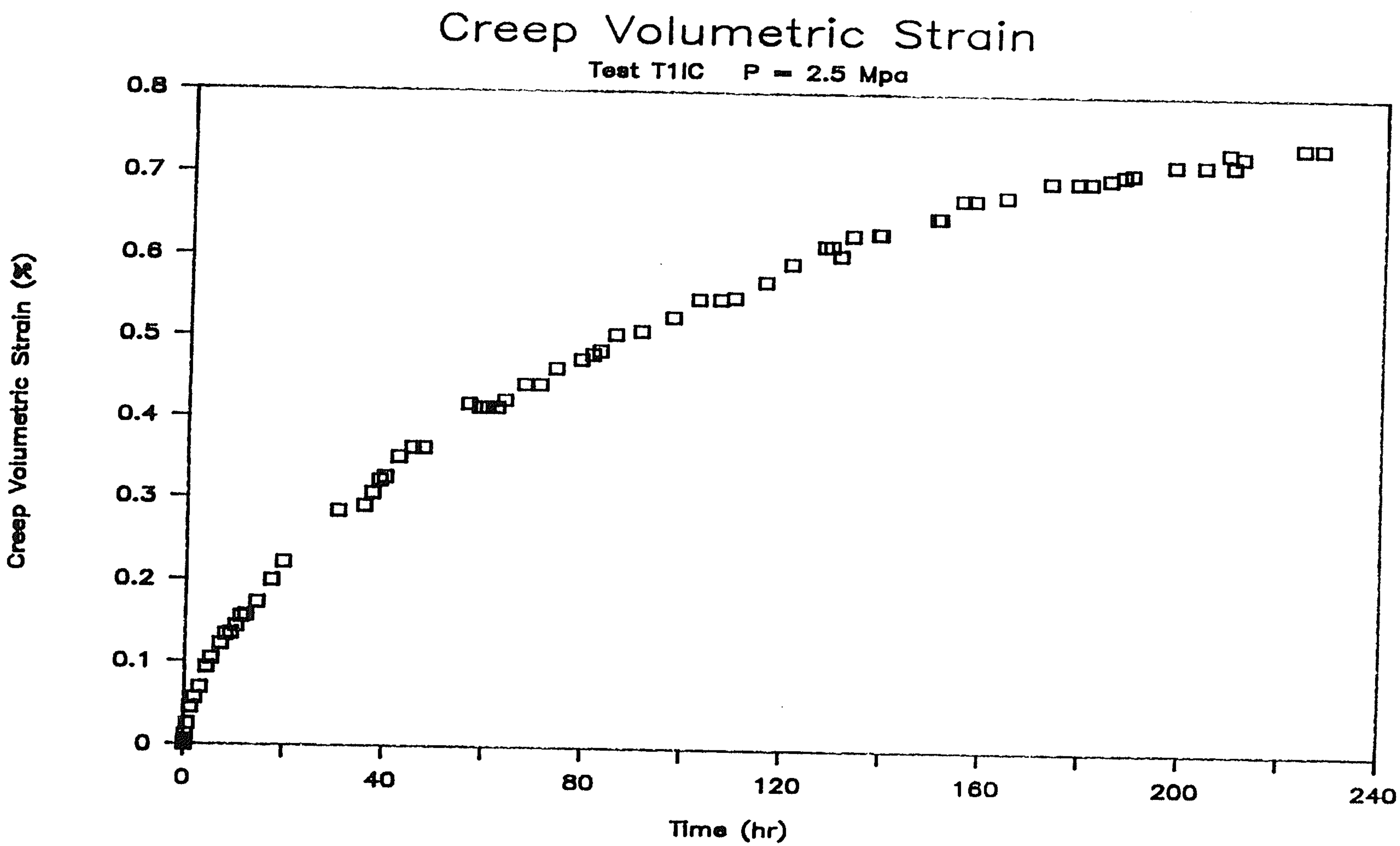

Figure 4.2 T1IC Creep volumetric strain

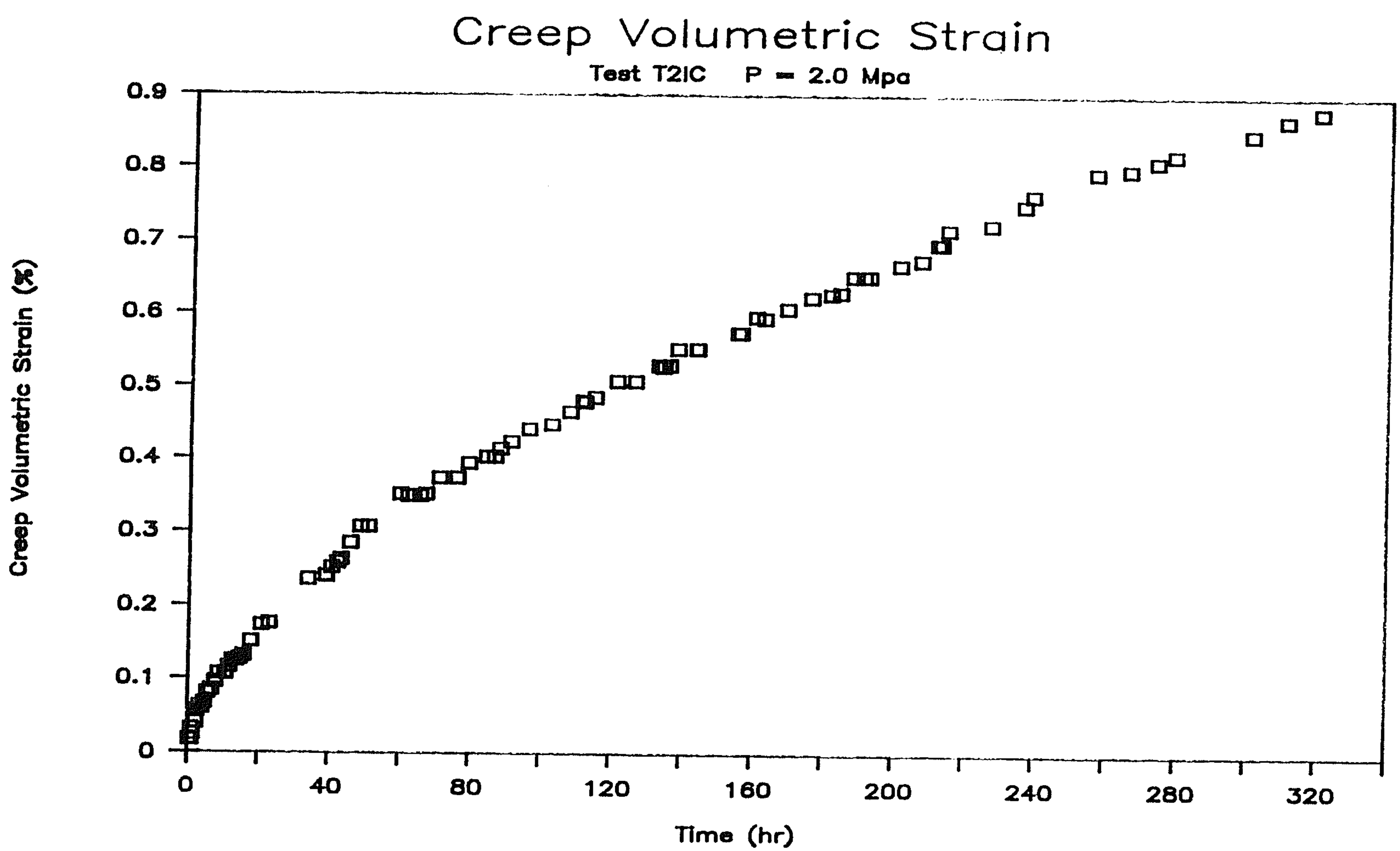

Figure 4.3 T2IC Creep volumetric strain

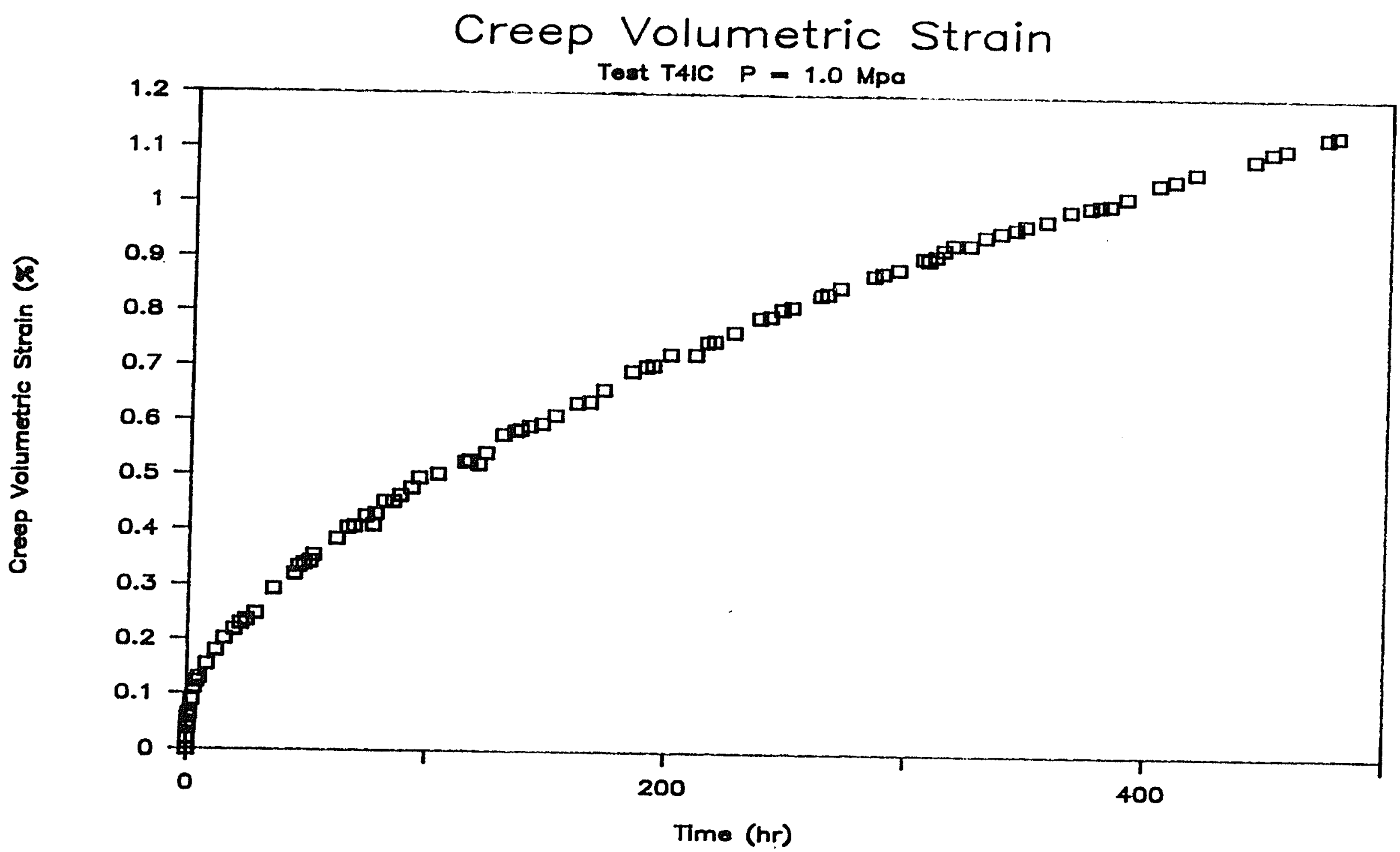

Figure 4.4 T4IC Creep volumetric strain

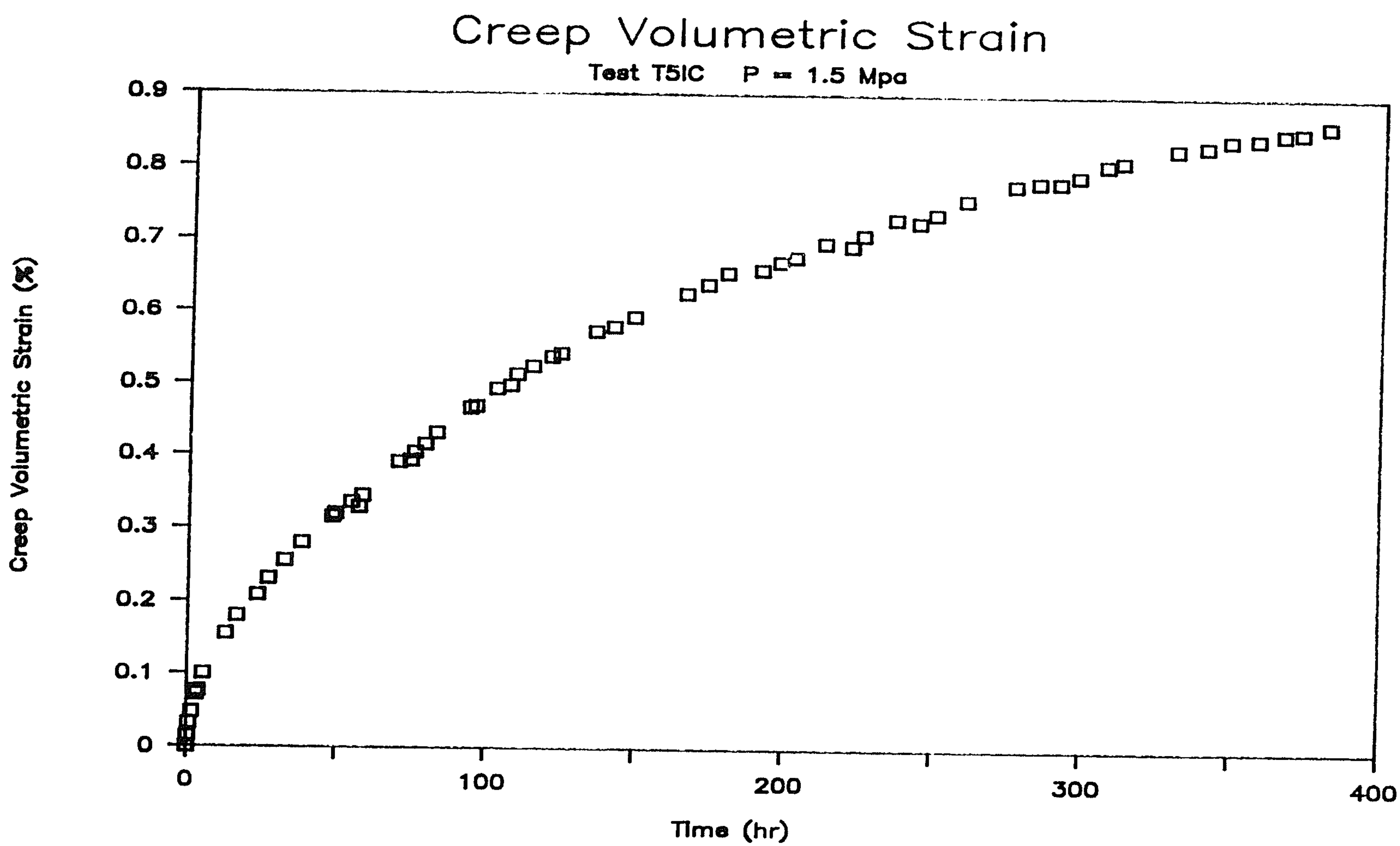

Figure 4.5 T5IC Creep volumetric strain

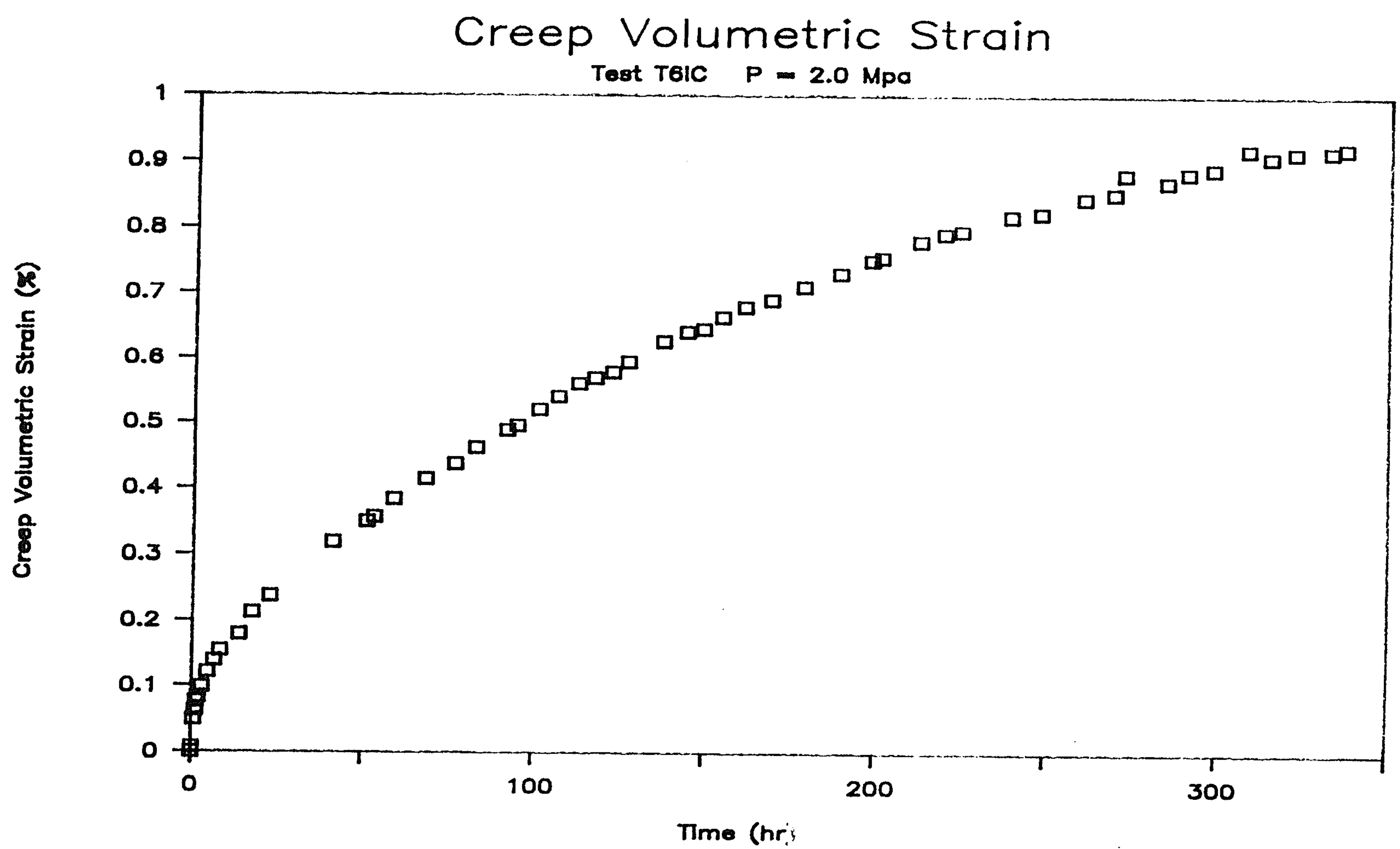

Figure 4.6 T6IC Creep volumetric strain

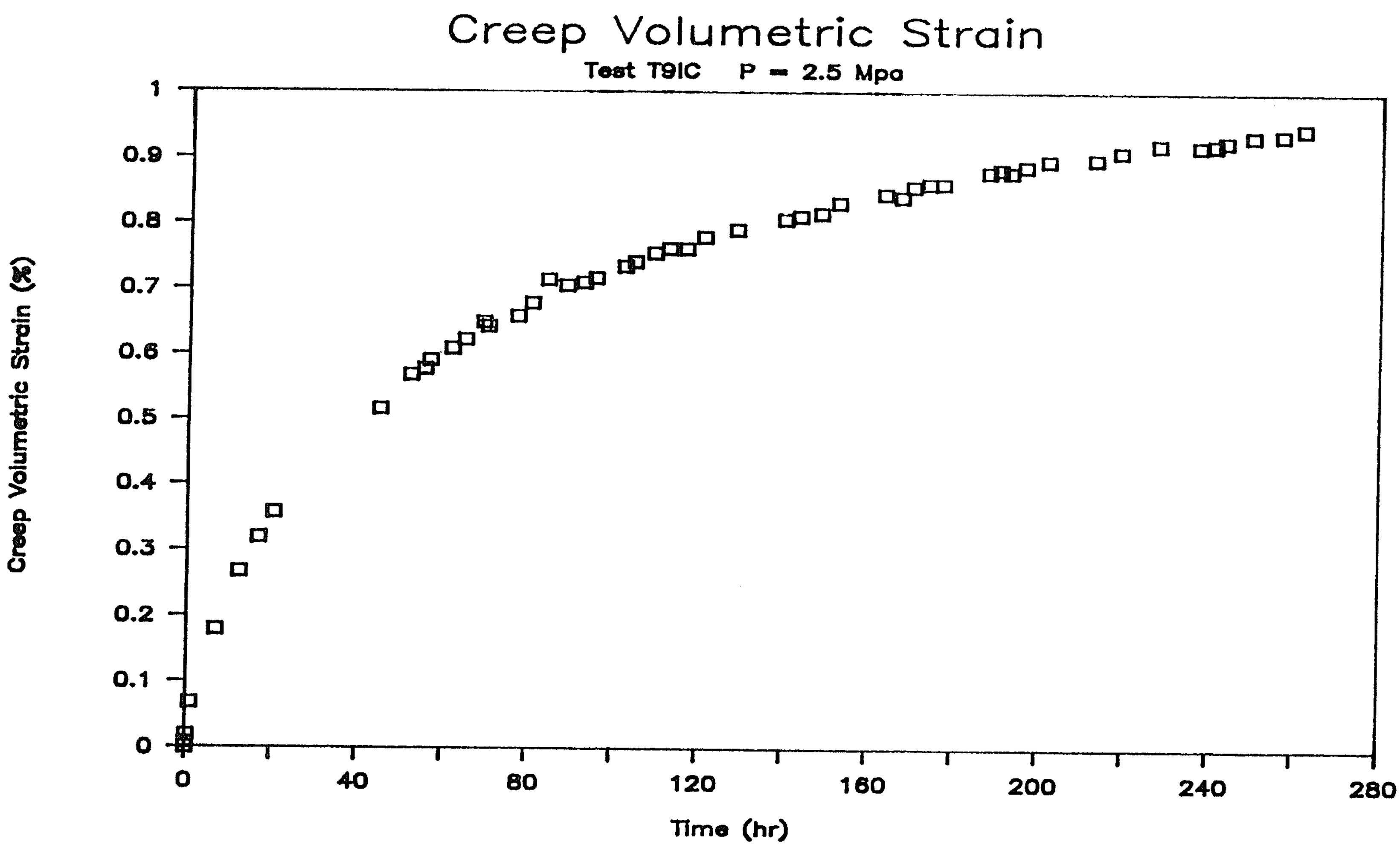

Figure 4.7 T9IC Creep volumetric strain

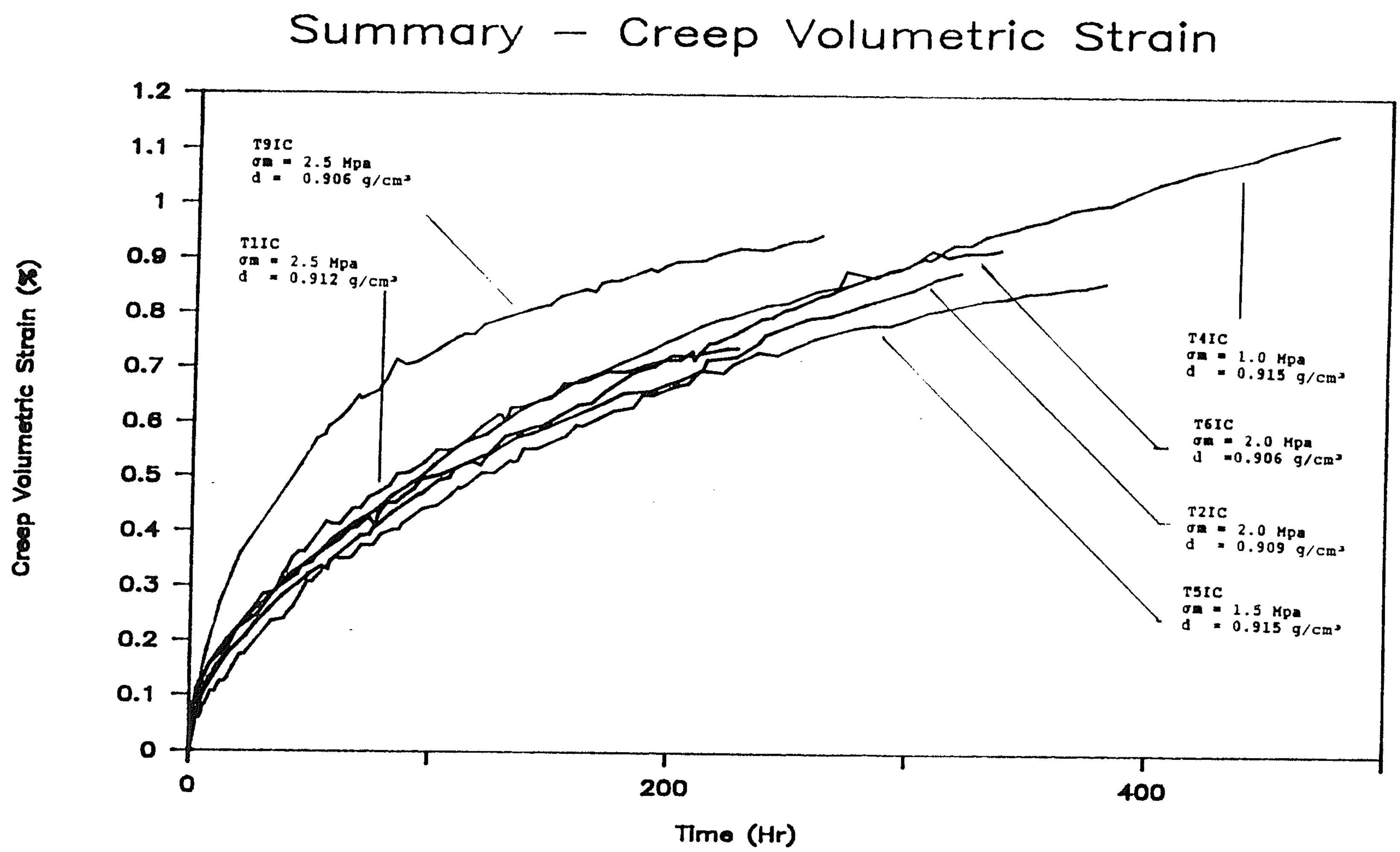

Figure 4.8 Summary of creep volumetric strains for isotropic compression tests

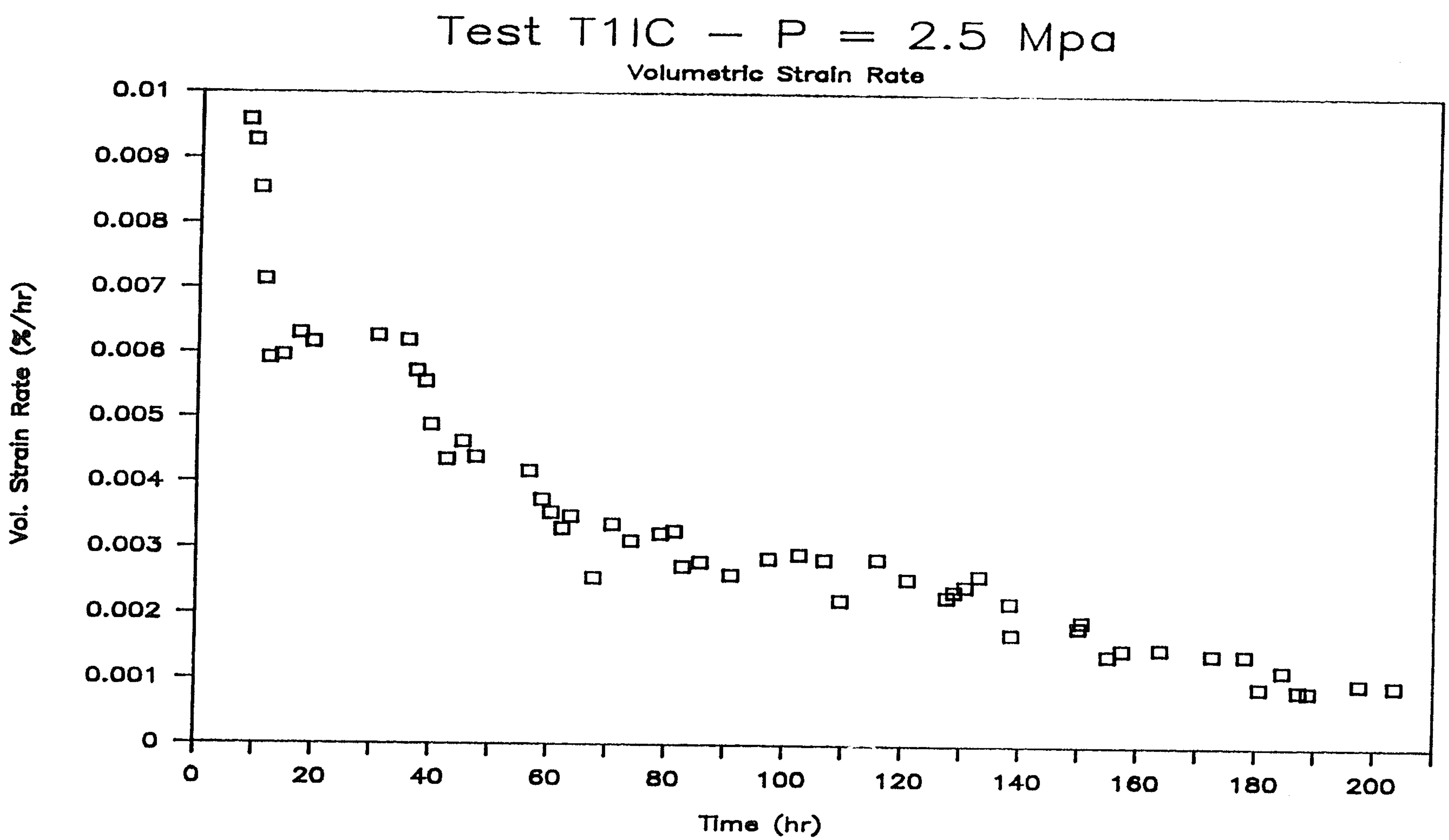

Figure 4.9 T1IC Volumetric strain rate

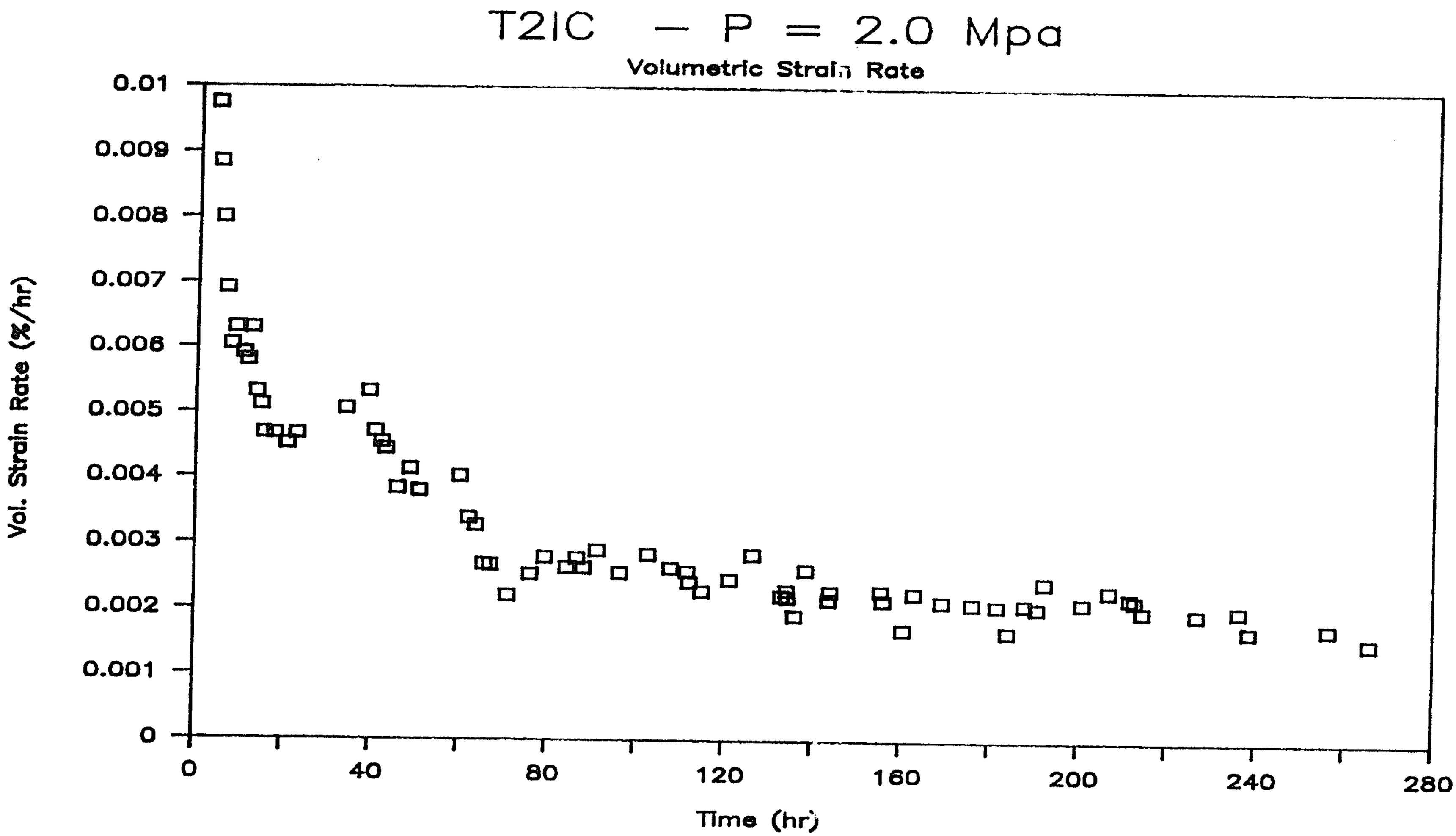

Figure 4.10 T2IC Volumetric strain rate

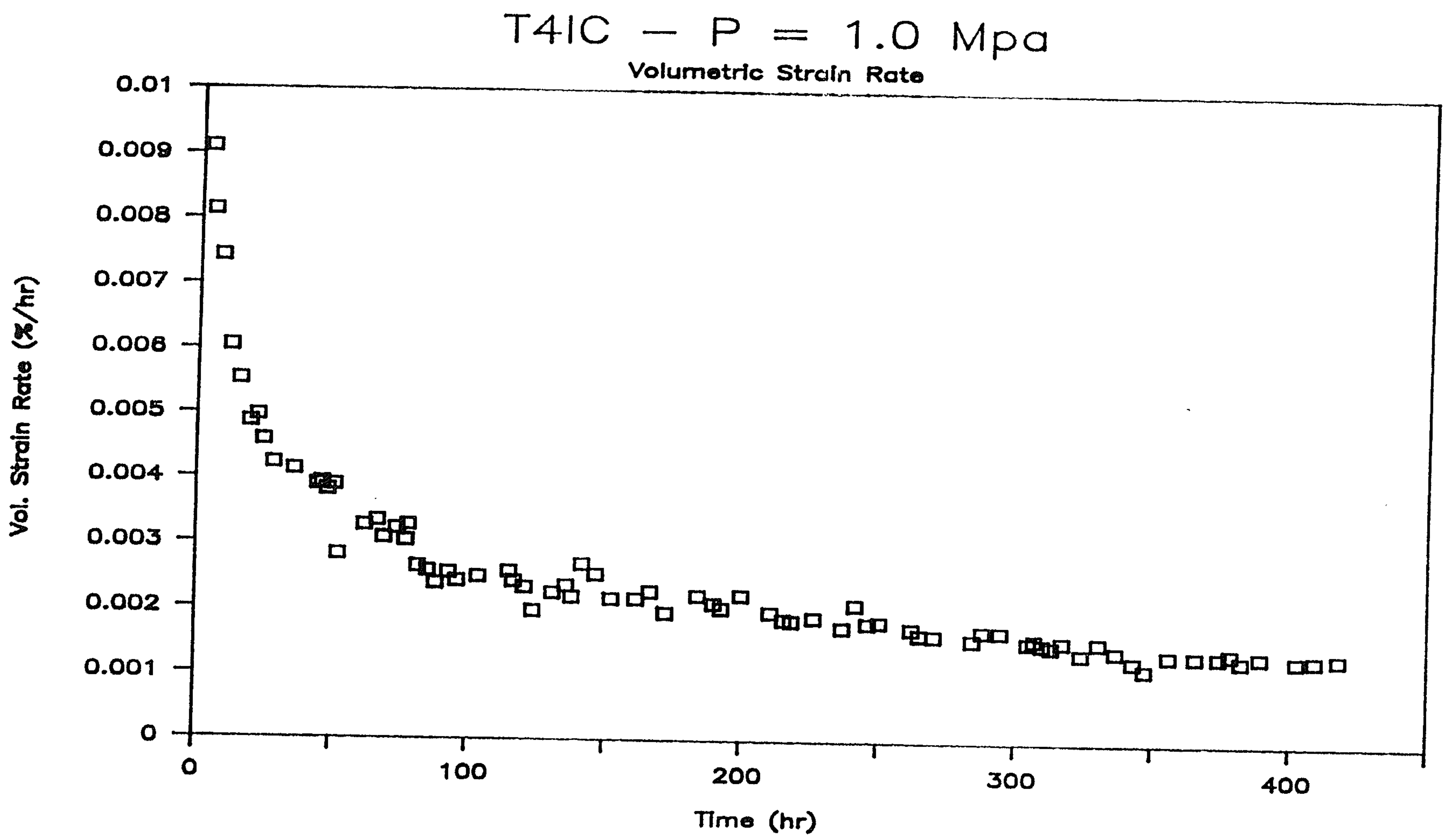

Figure 4.11 T4IC Volumetric strain rate

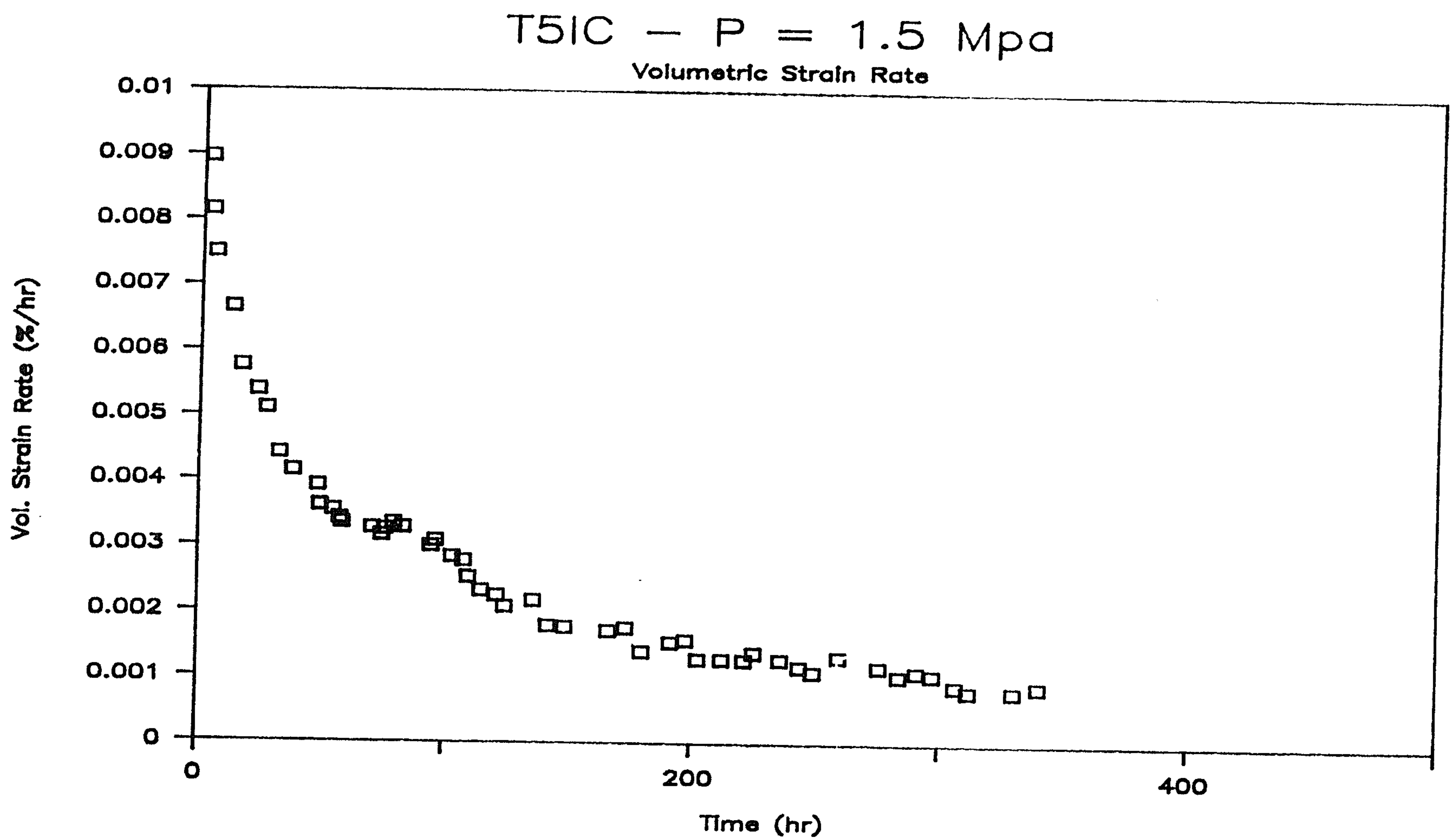

Figure 4.12 T5IC Volumetric strain rate

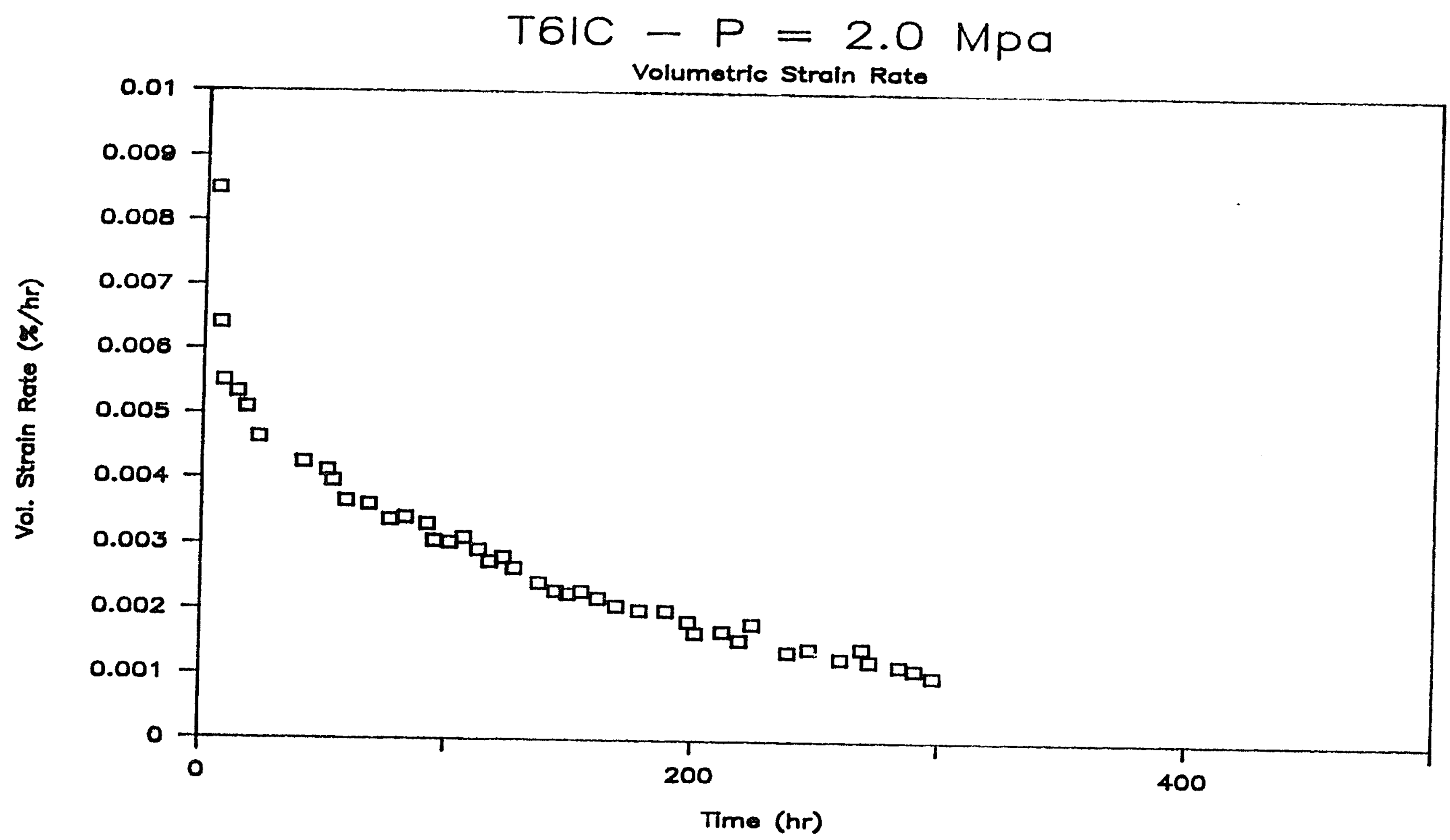

Figure 4.13 T6IC Volumetric strain rate

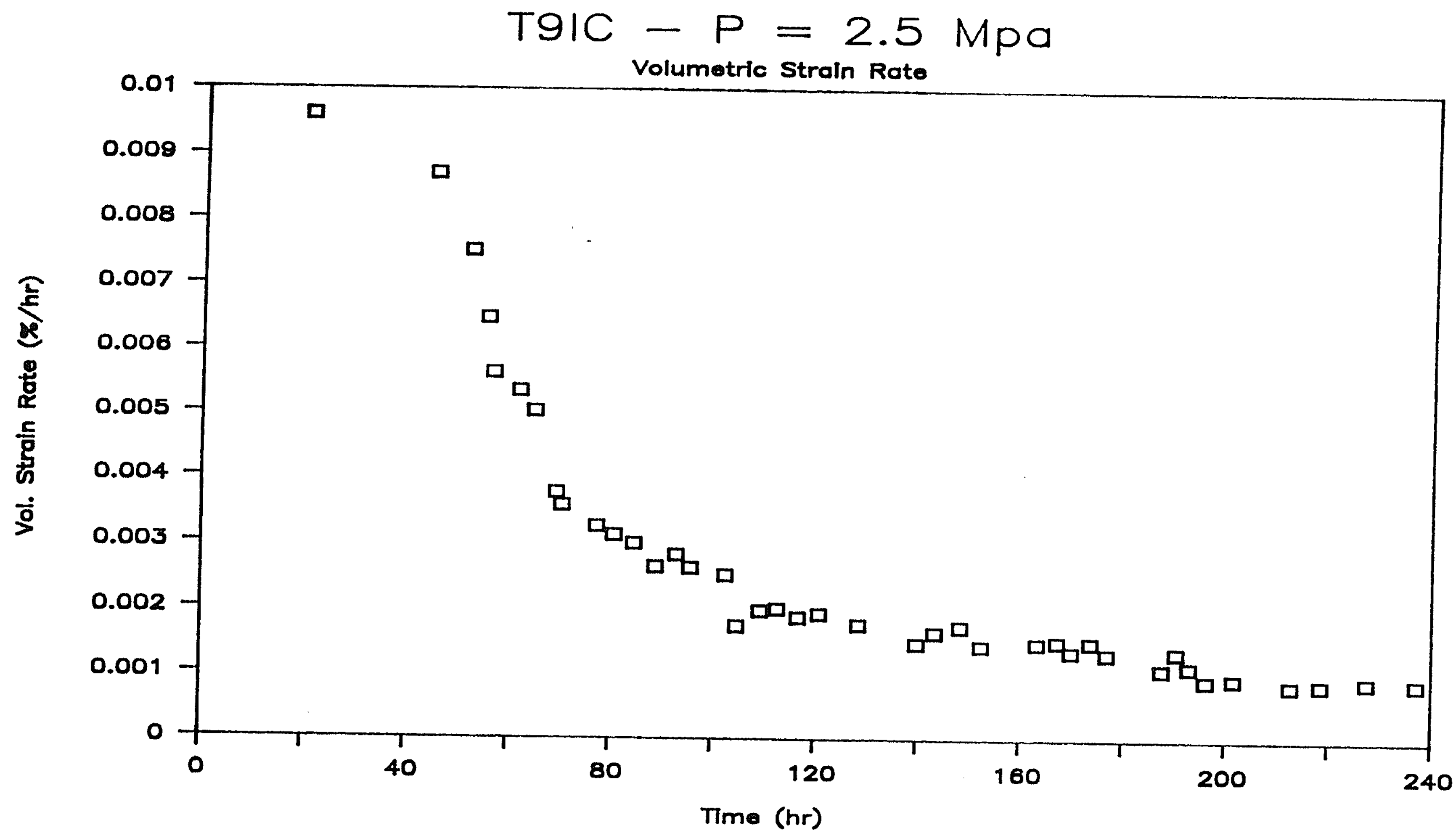

Figure 4.14 T9IC Volumetric strain rate

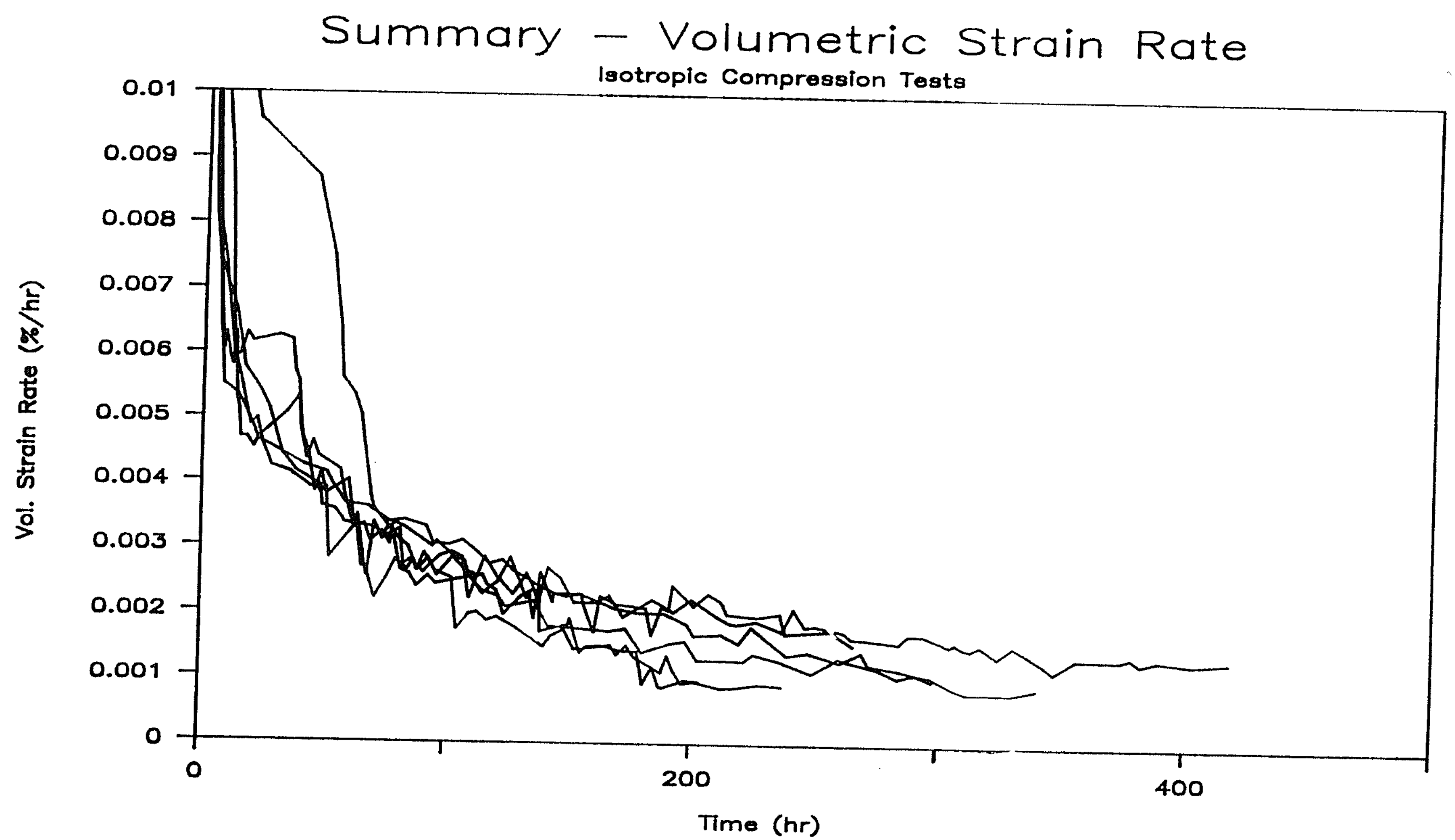

Figure 4.15 Summary of volumetric strain rates for isotropic compression tests

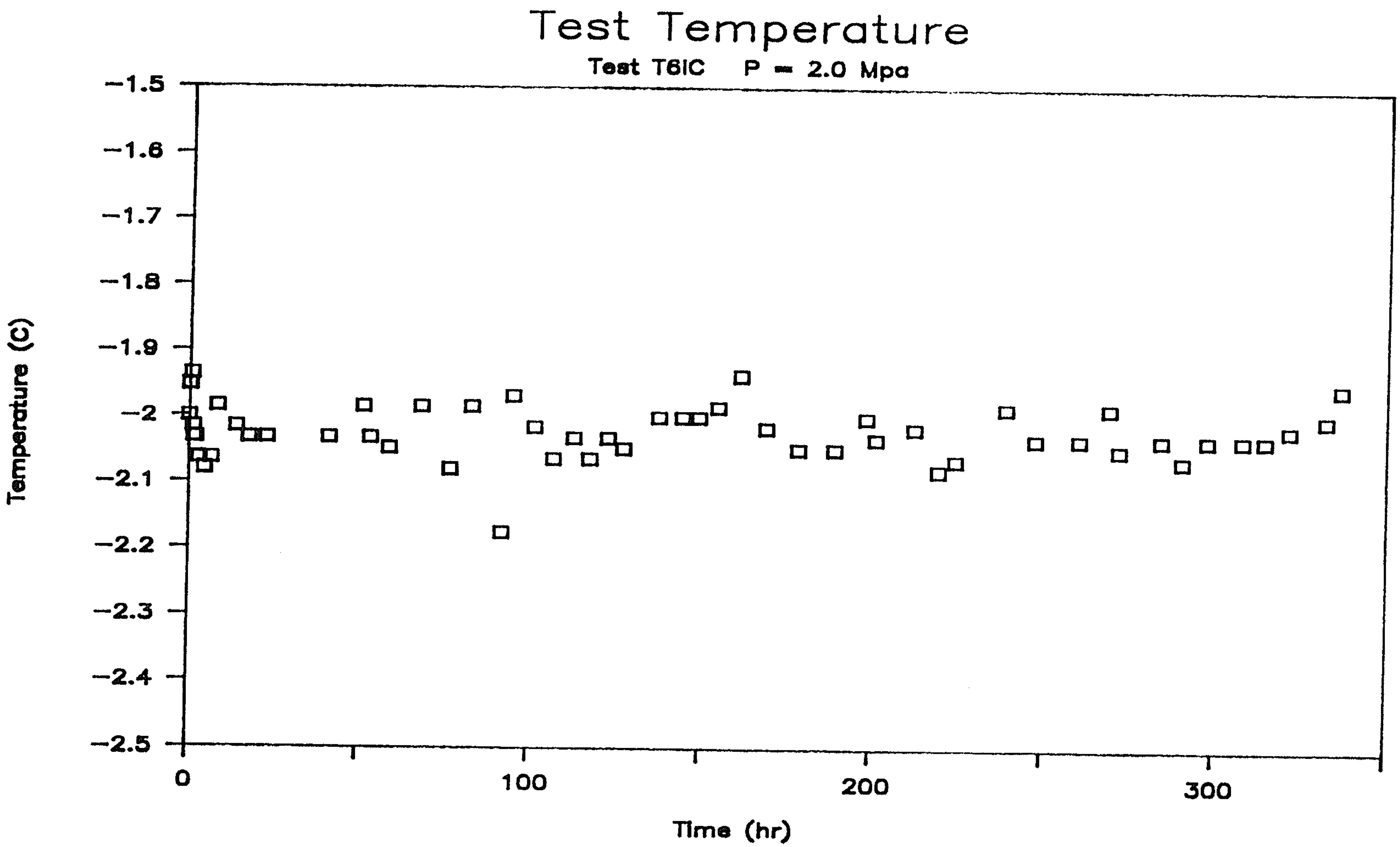

Figure 4.16 Specimen temperature during T6IC

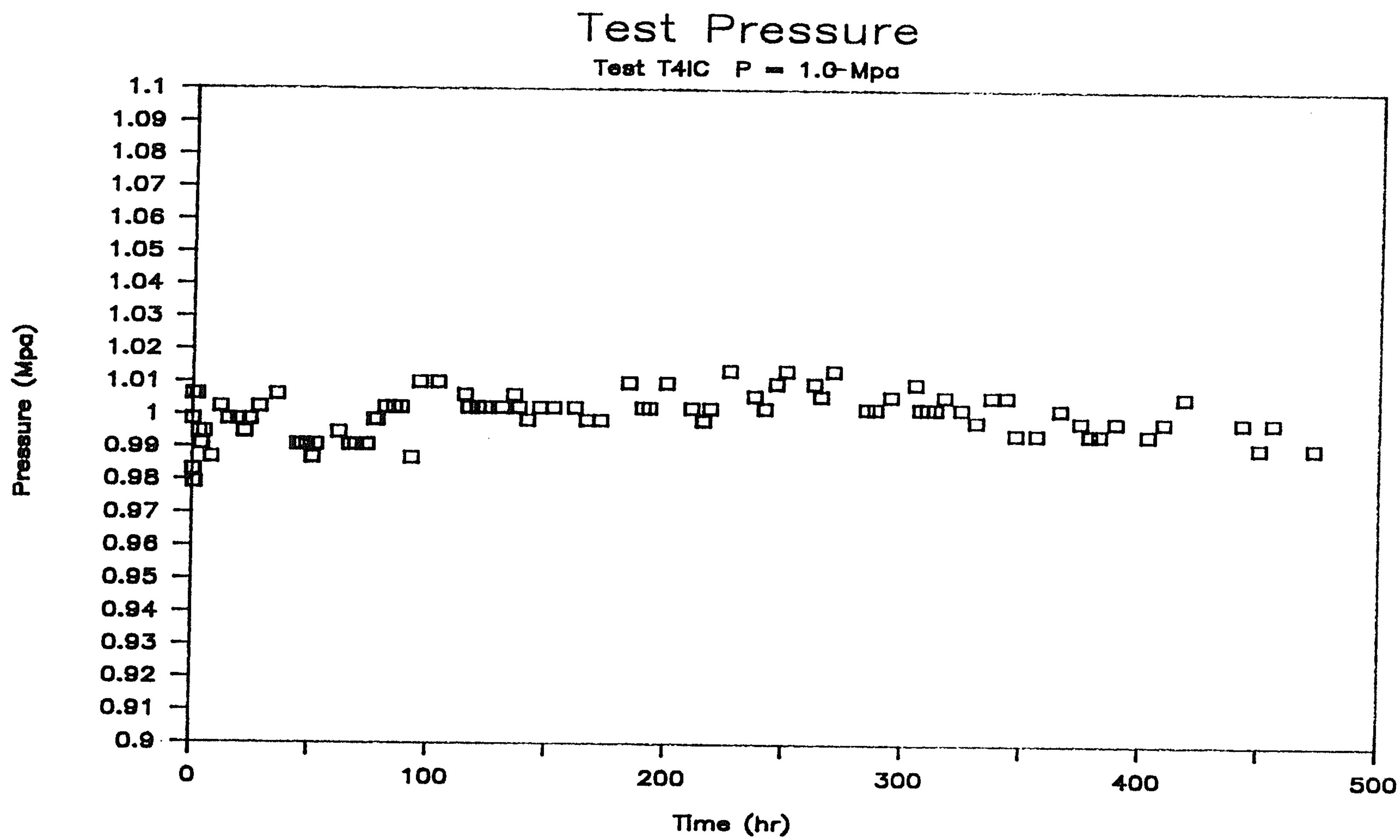

Figure 4.17 Cell pressure during T5IC

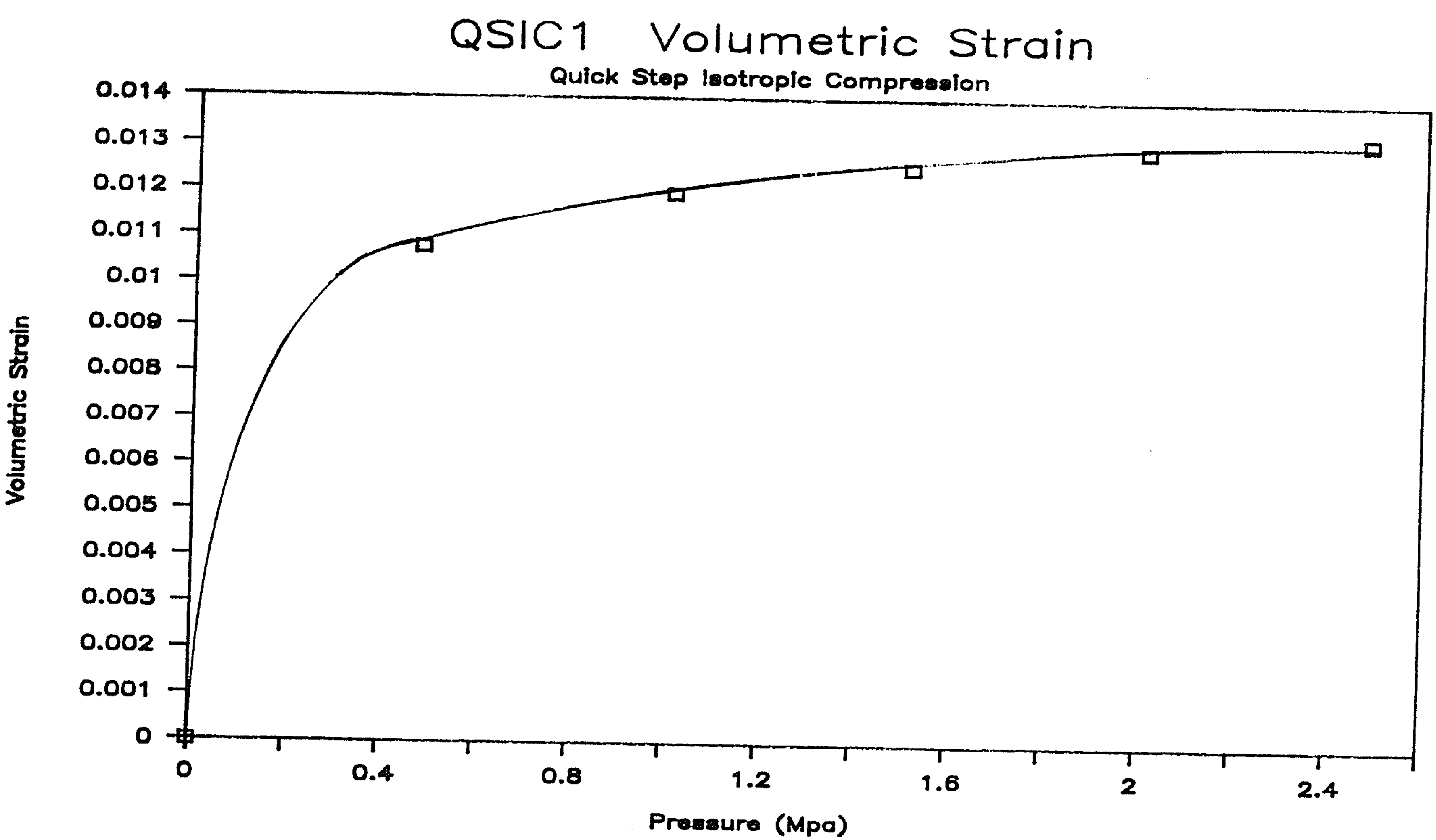

Figure 4.18 QSIC1 Volumetric strain

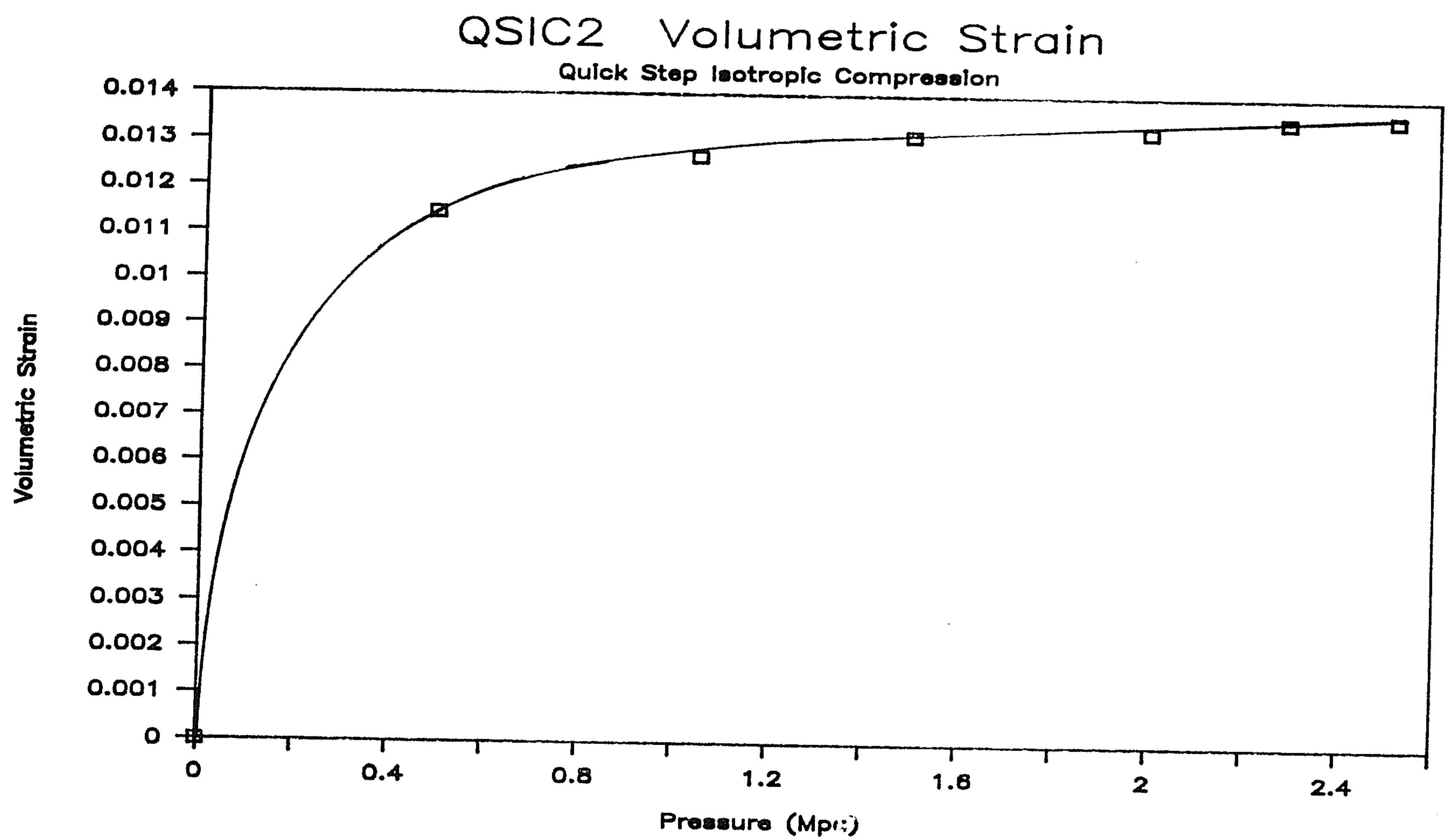

Figure 4.19 QSIC2 Volumetric strain

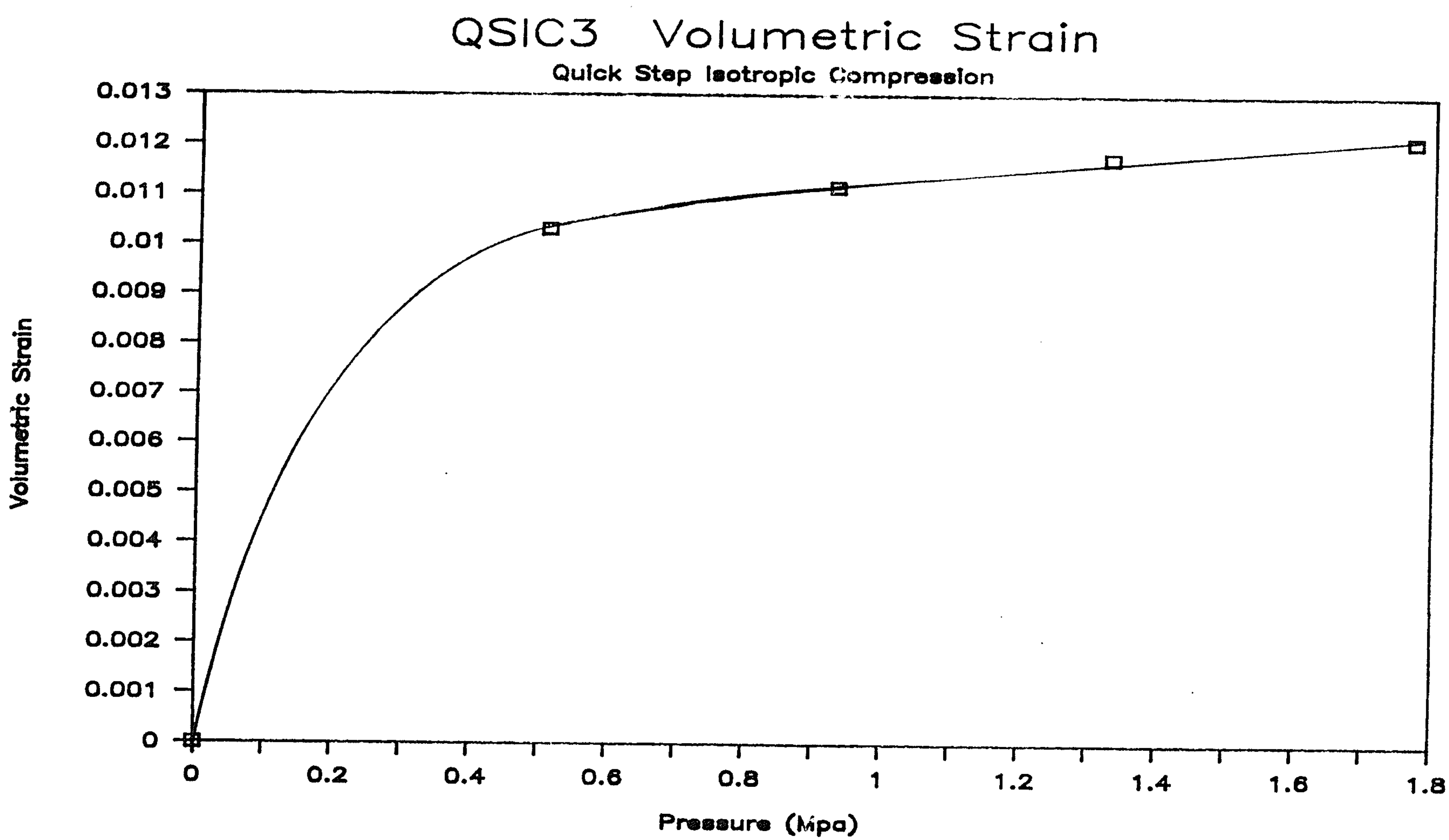

Figure 4.20 QSIC3 Volumetric strain

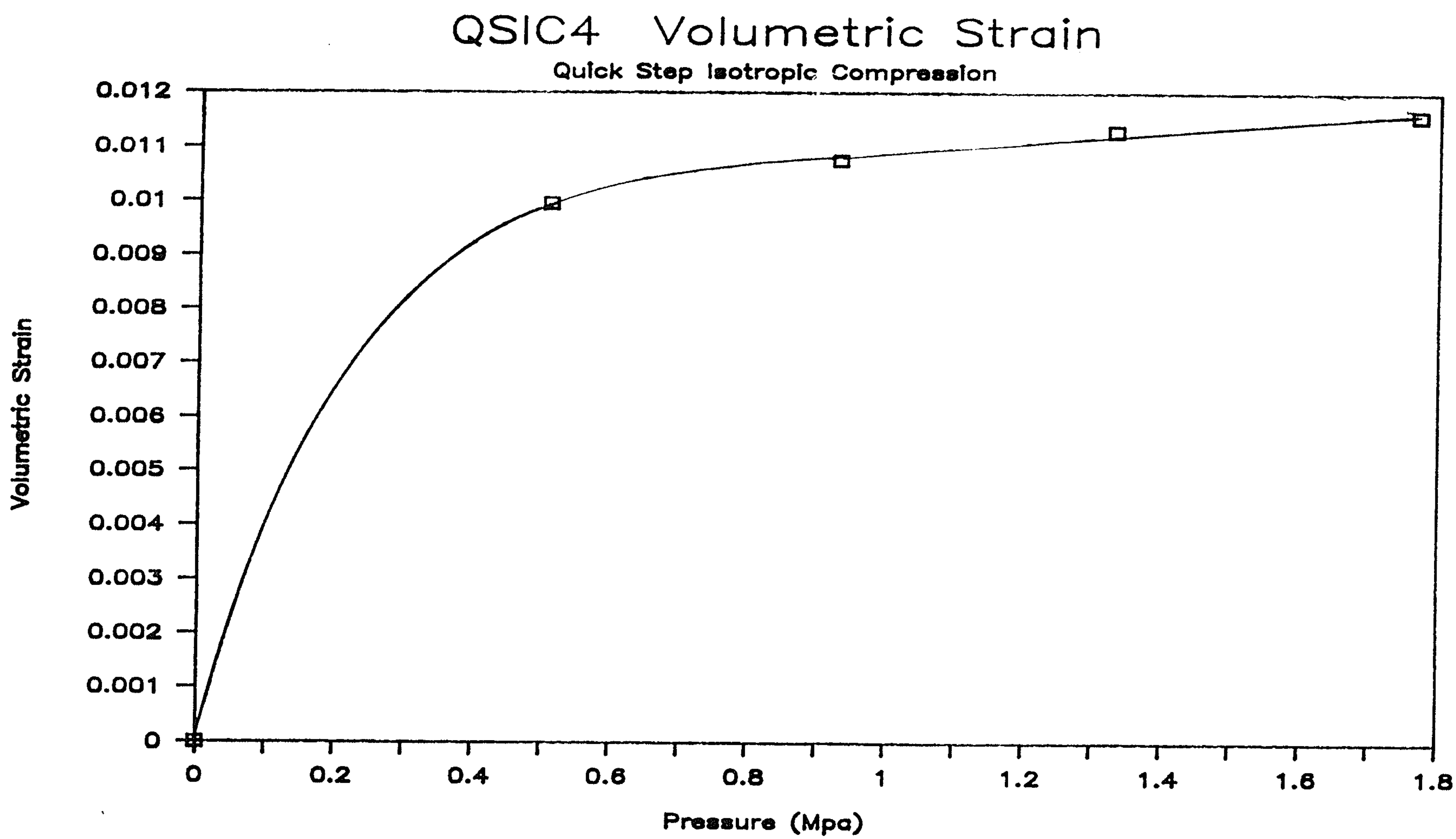

Figure 4.21 QSIC4 Volumetric strain

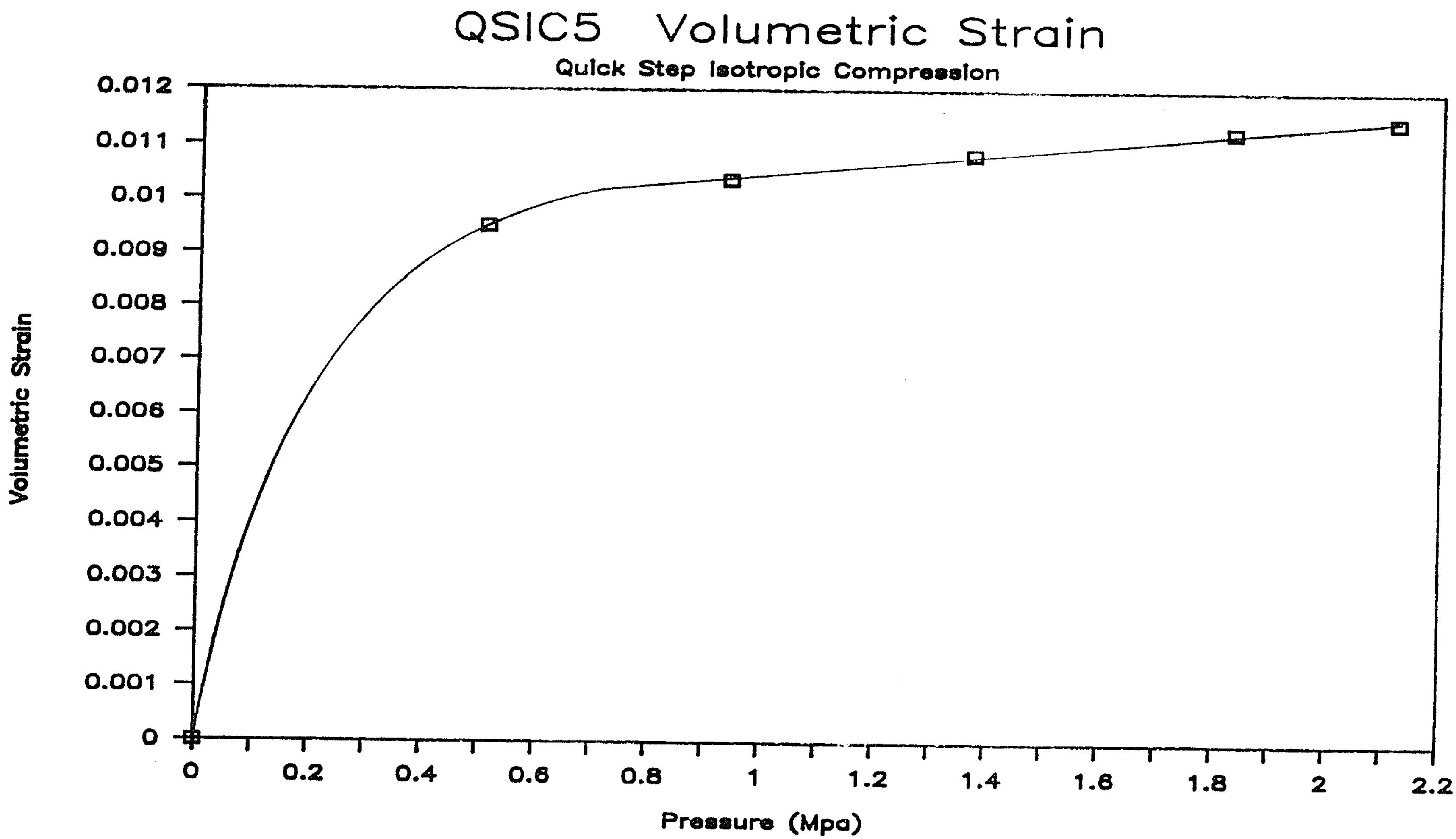

Figure 4.22 QSIC5 Volumetric strain

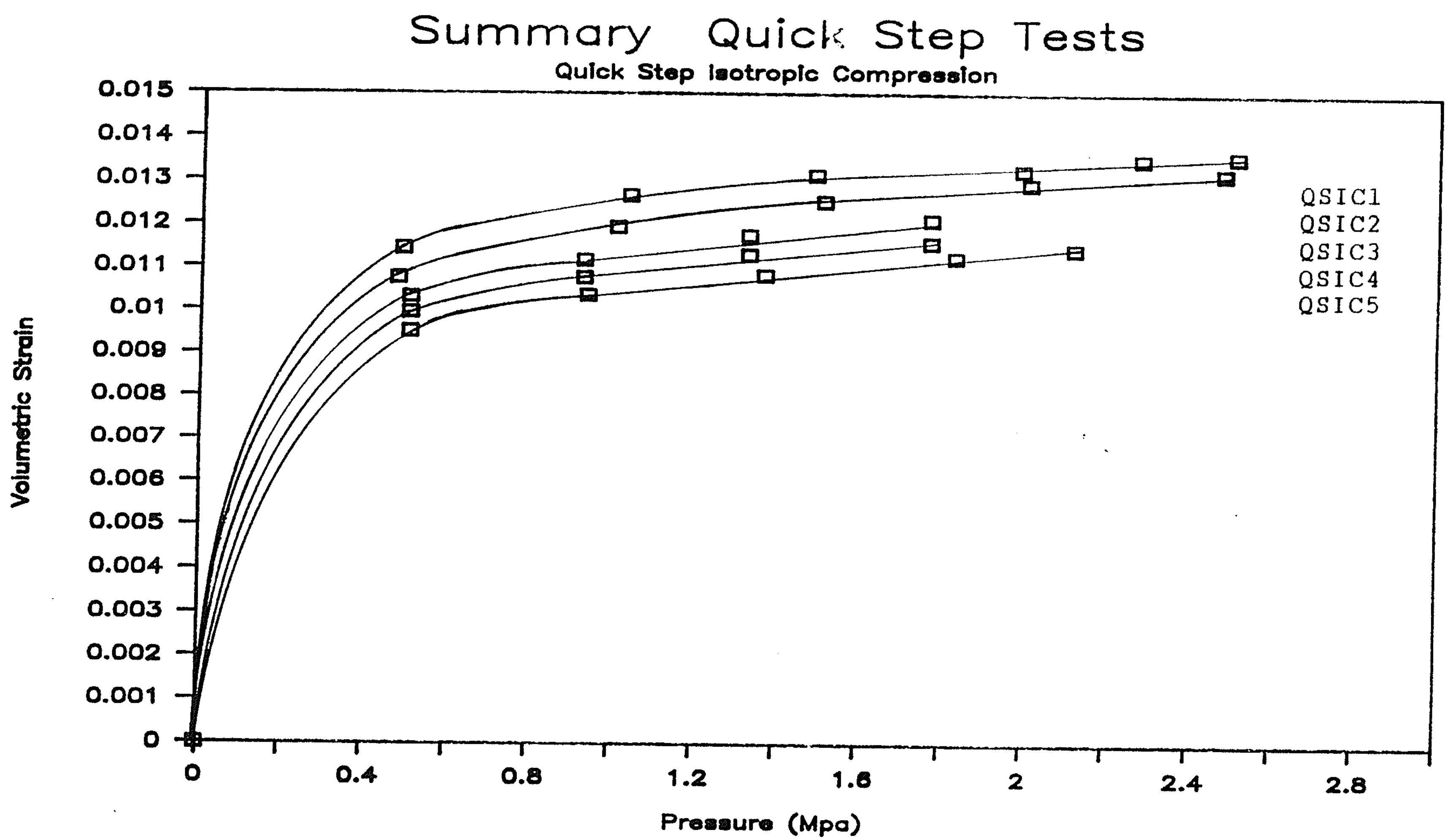

Figure 4.23 Summary of quick step isotropic compression tests

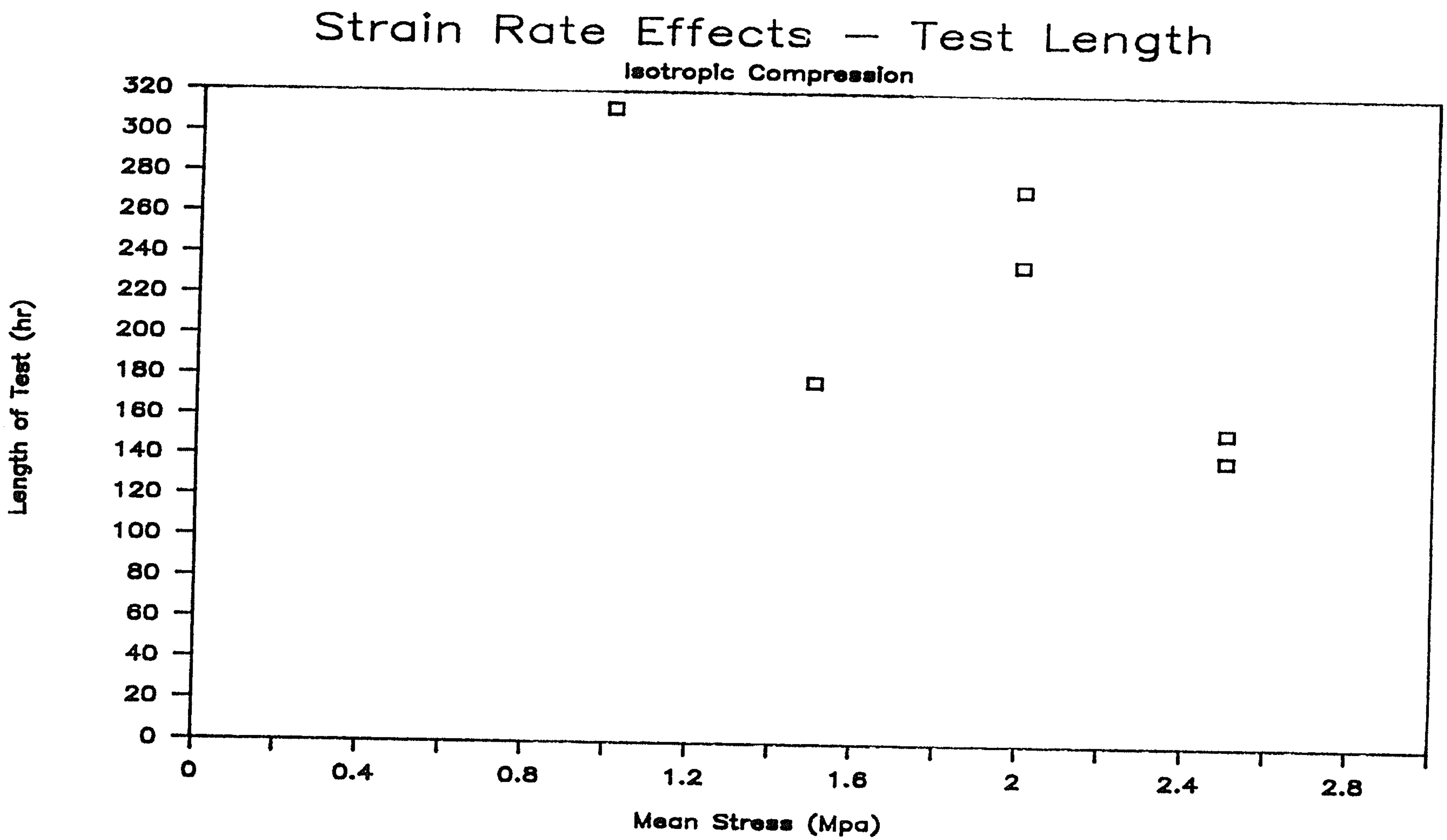

Figure 4.24 Effect of mean stress on test length

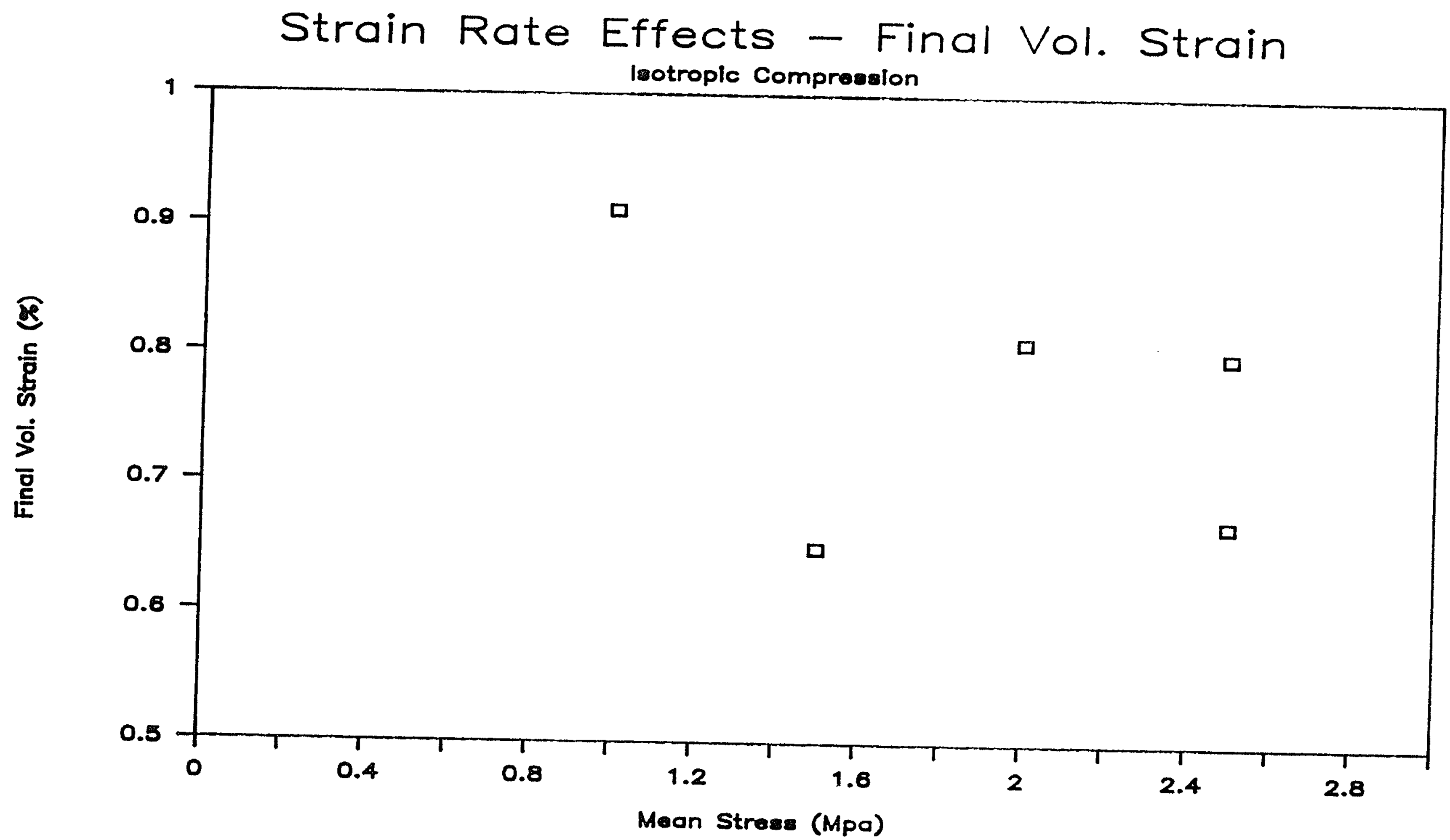

Figure 4.25 Effect of test pressure on final volumetric strain

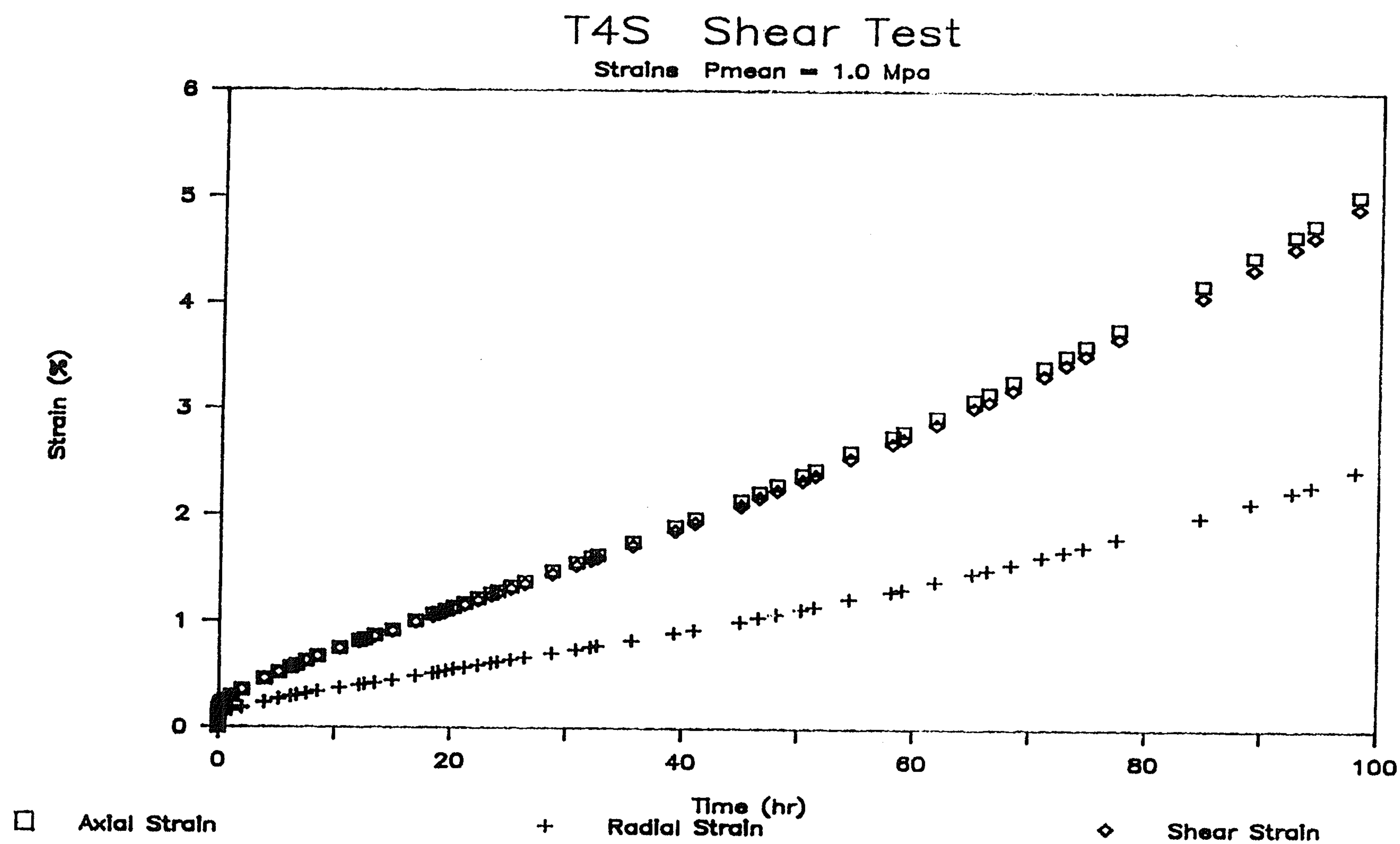

Figure 4.26 T4S Axial, radial and shear strain

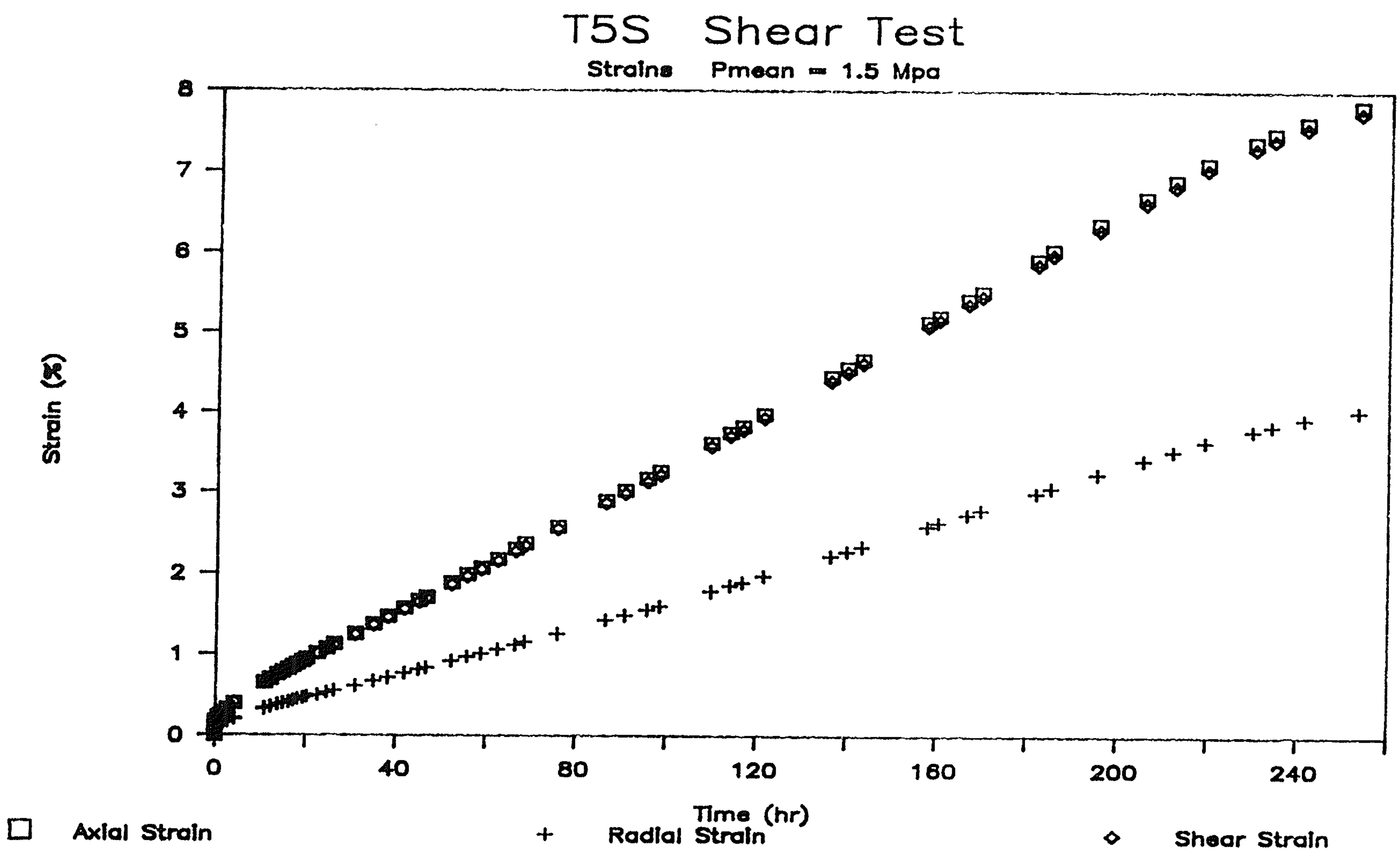

Figure 4.27 T5S Axial, radial and shear strain

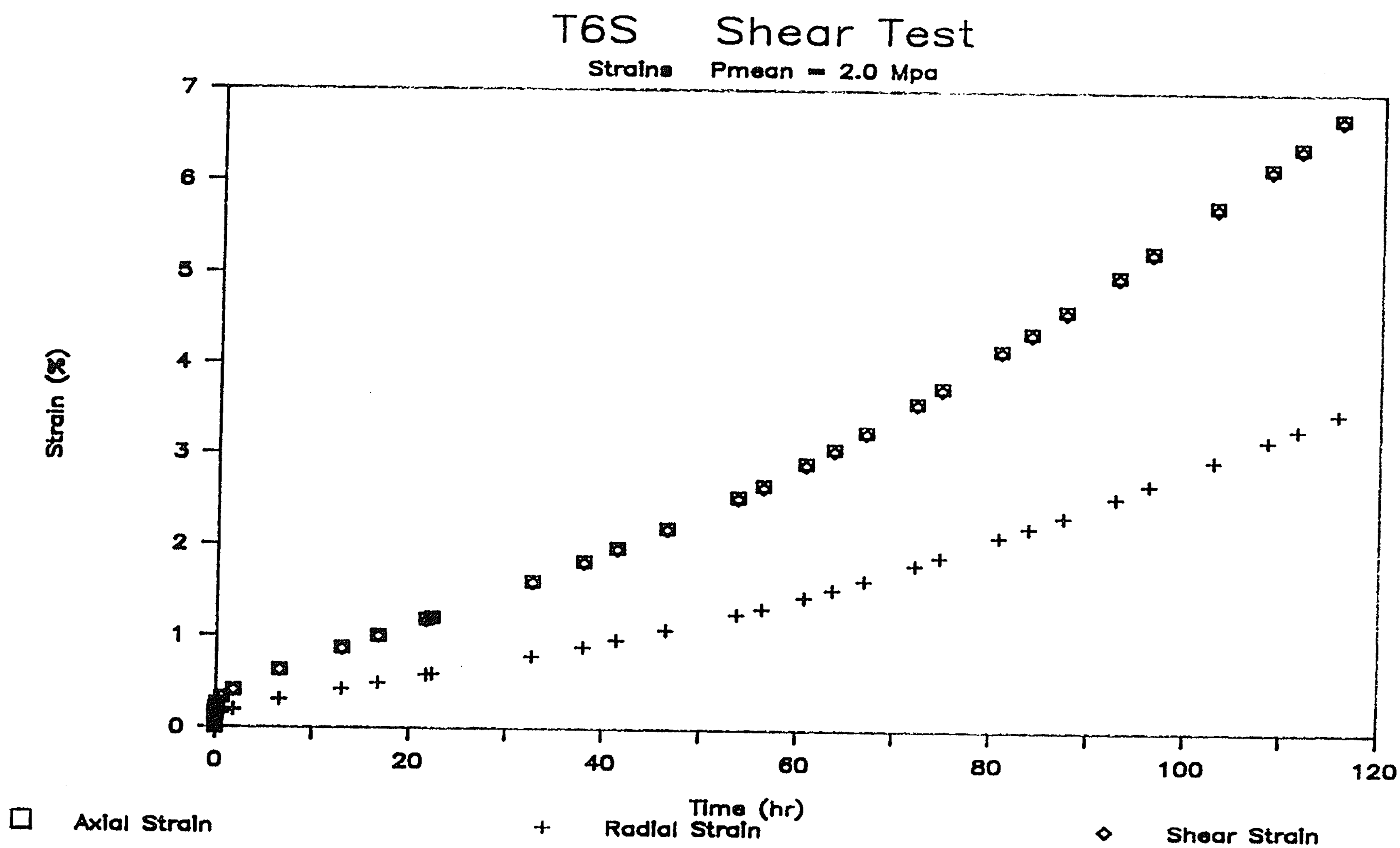

Figure 4.28 T6S Axial, radial and shear strain

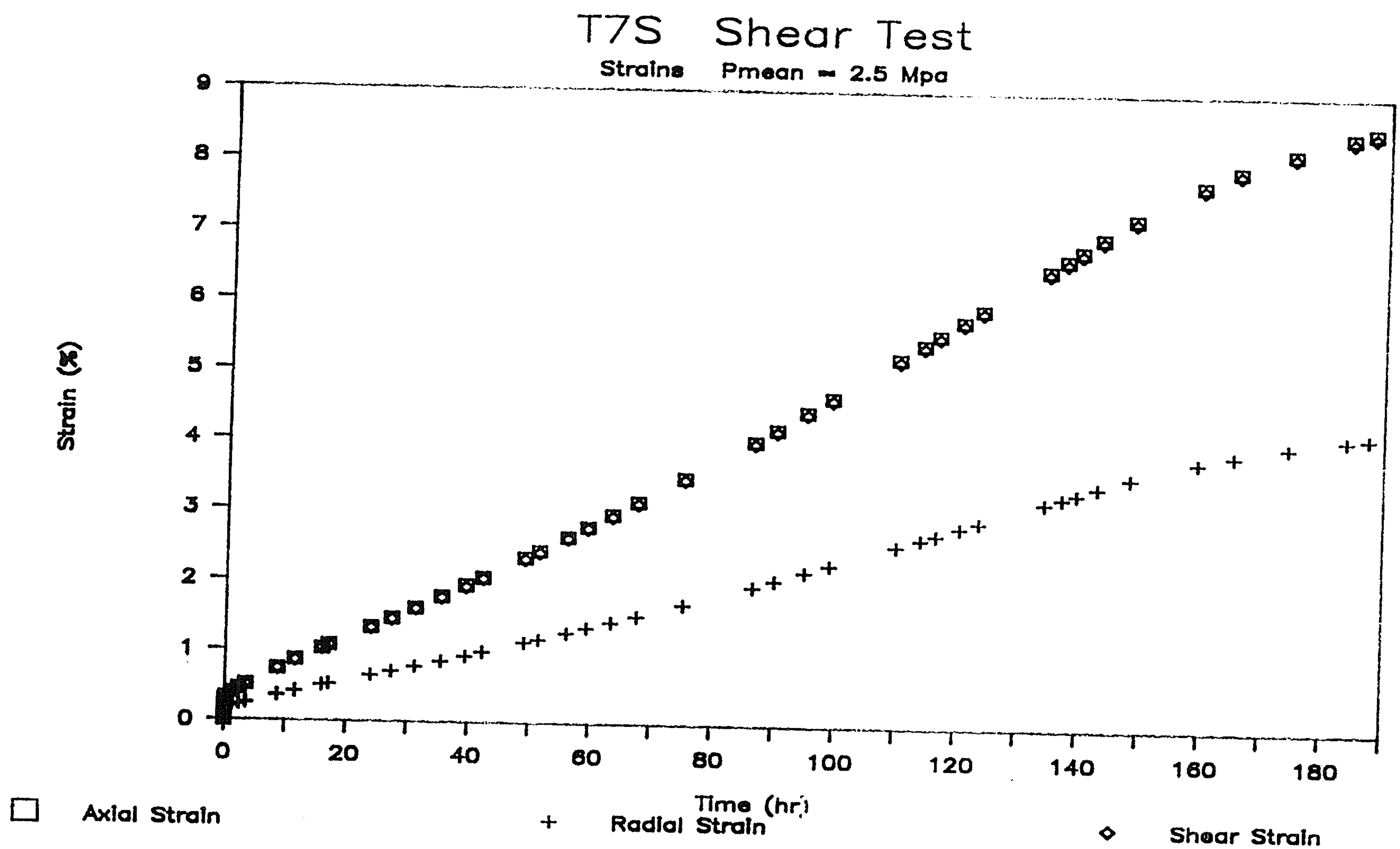

Figure 4.29 T7S Axial, radial and shear strain

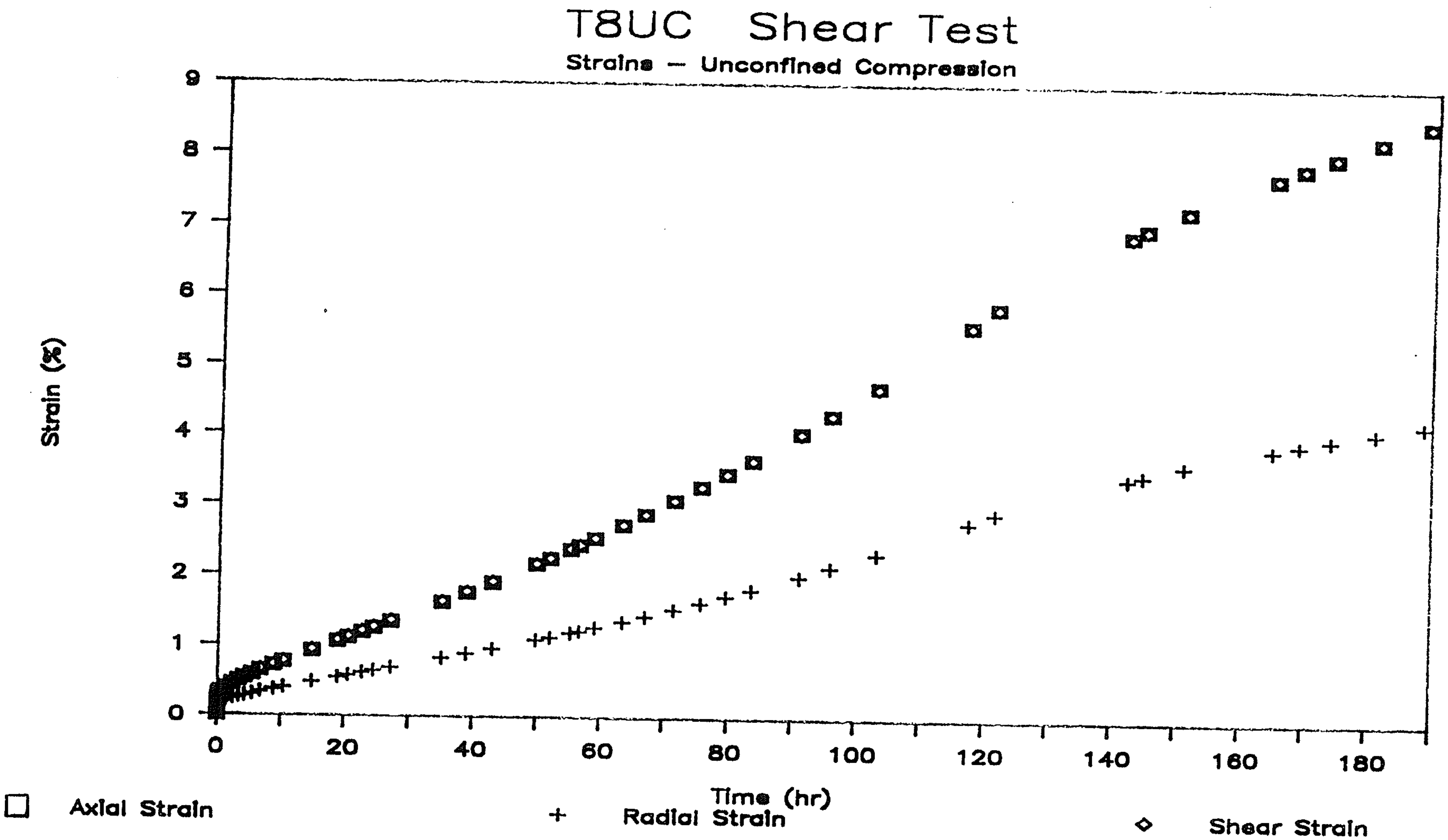

Figure 4.30 T8UC Axial, radial and shear strain

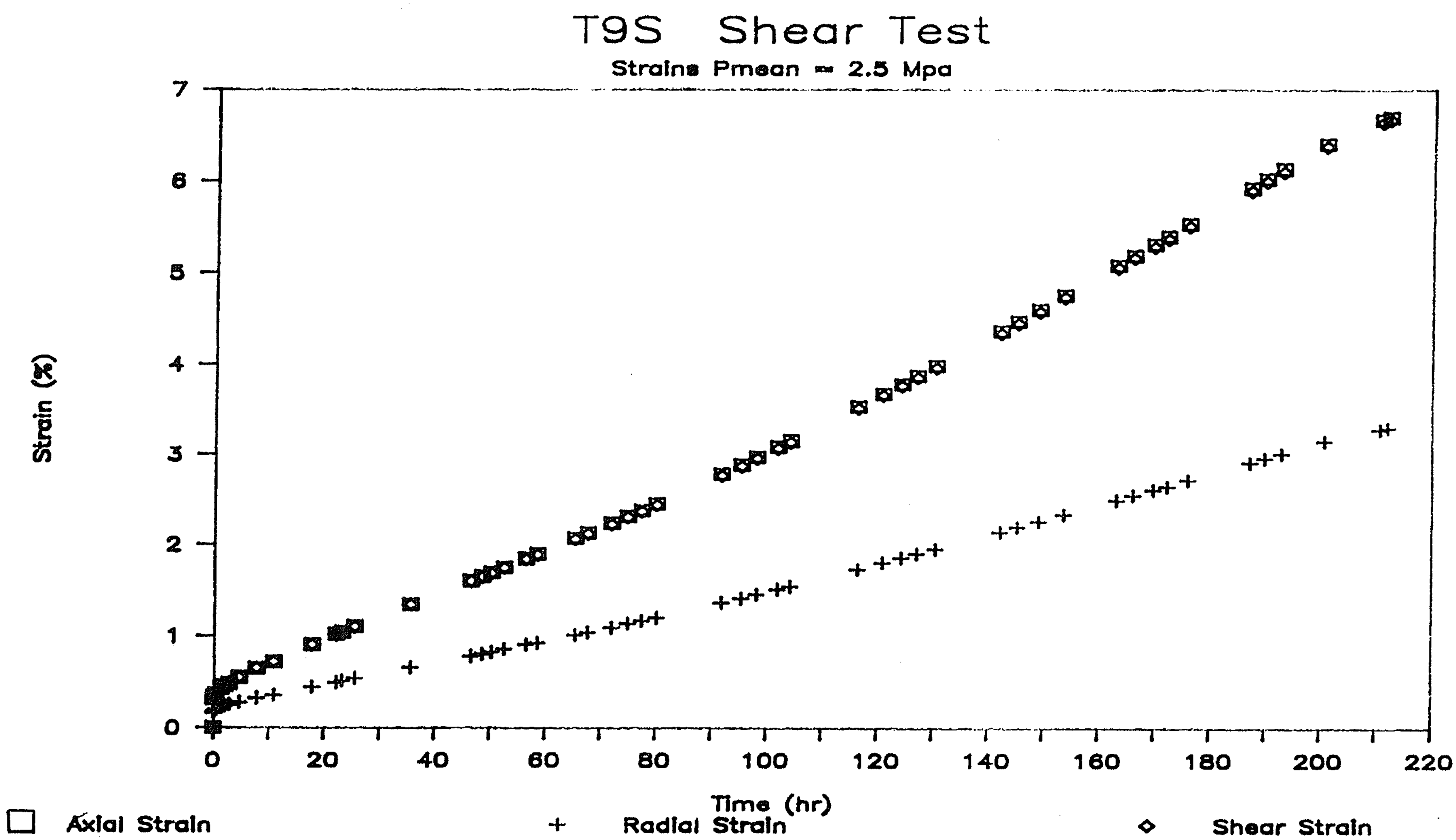

Figure 4.31 T9S Axial, radial and shear strain

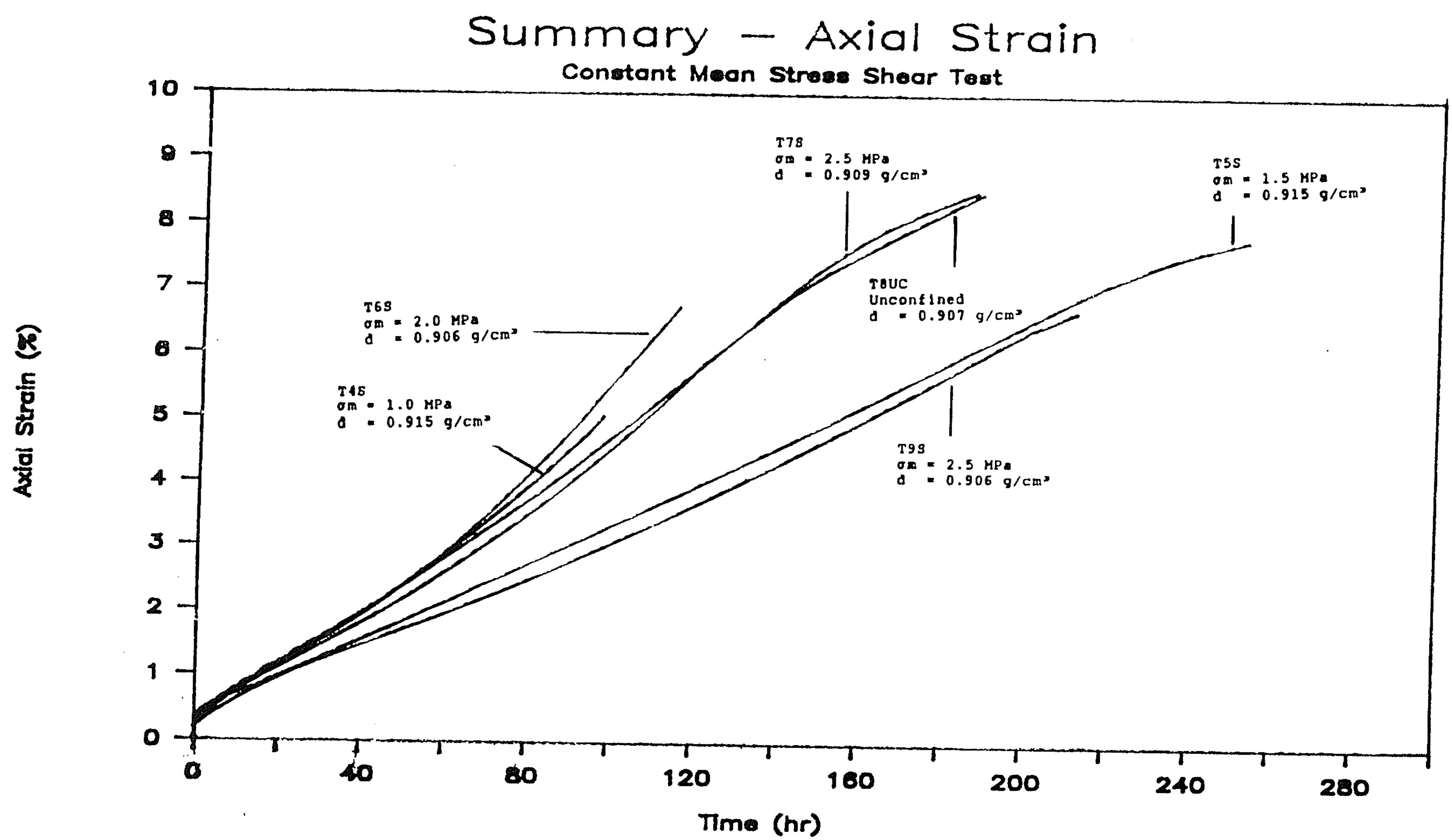

Figure 4.32 Summary of axial strains for shear tests

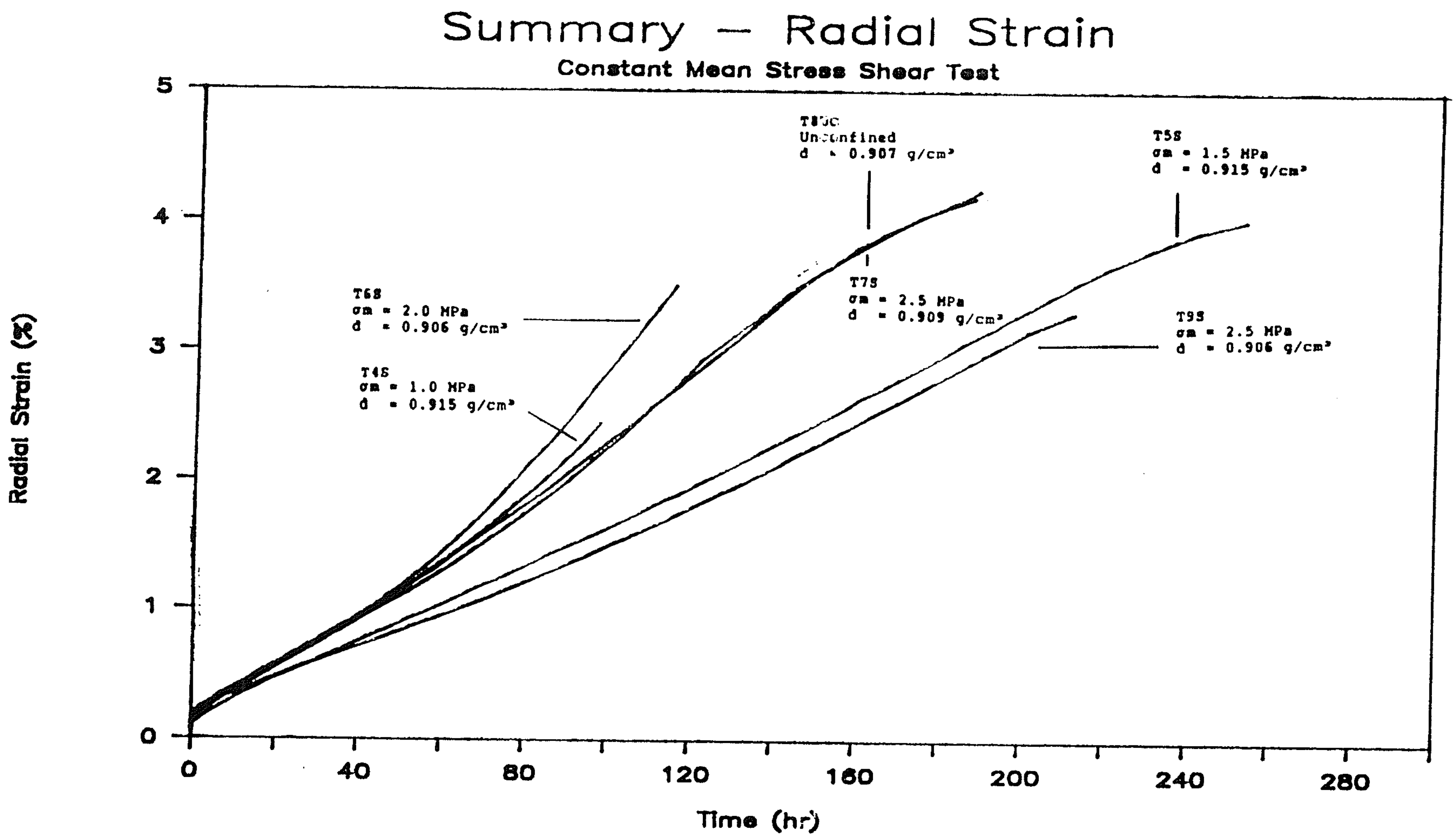

Figure 4.33 Summary of radial strains for shear tests

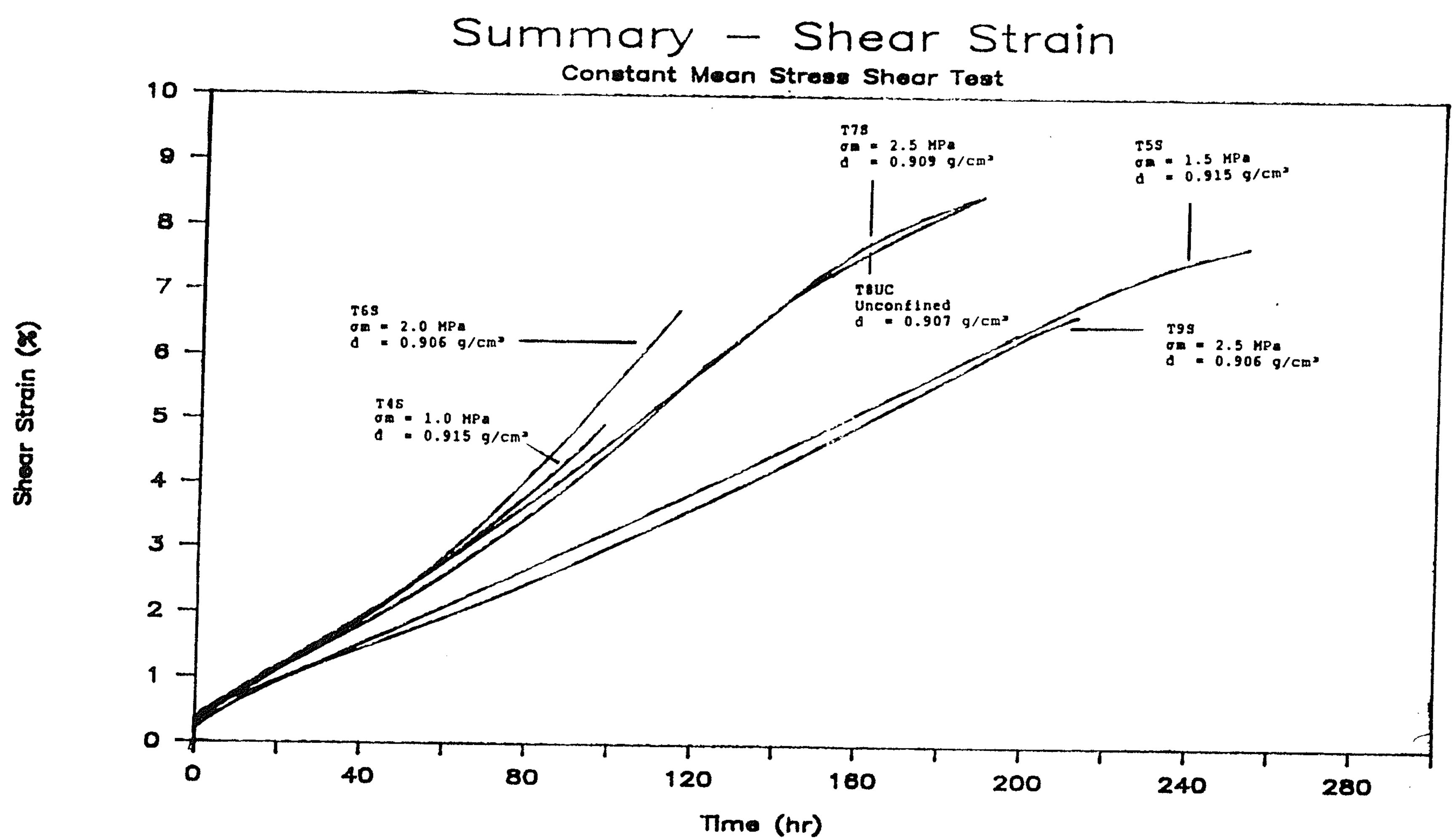

Figure 4.34 Summary of shear strains for shear tests

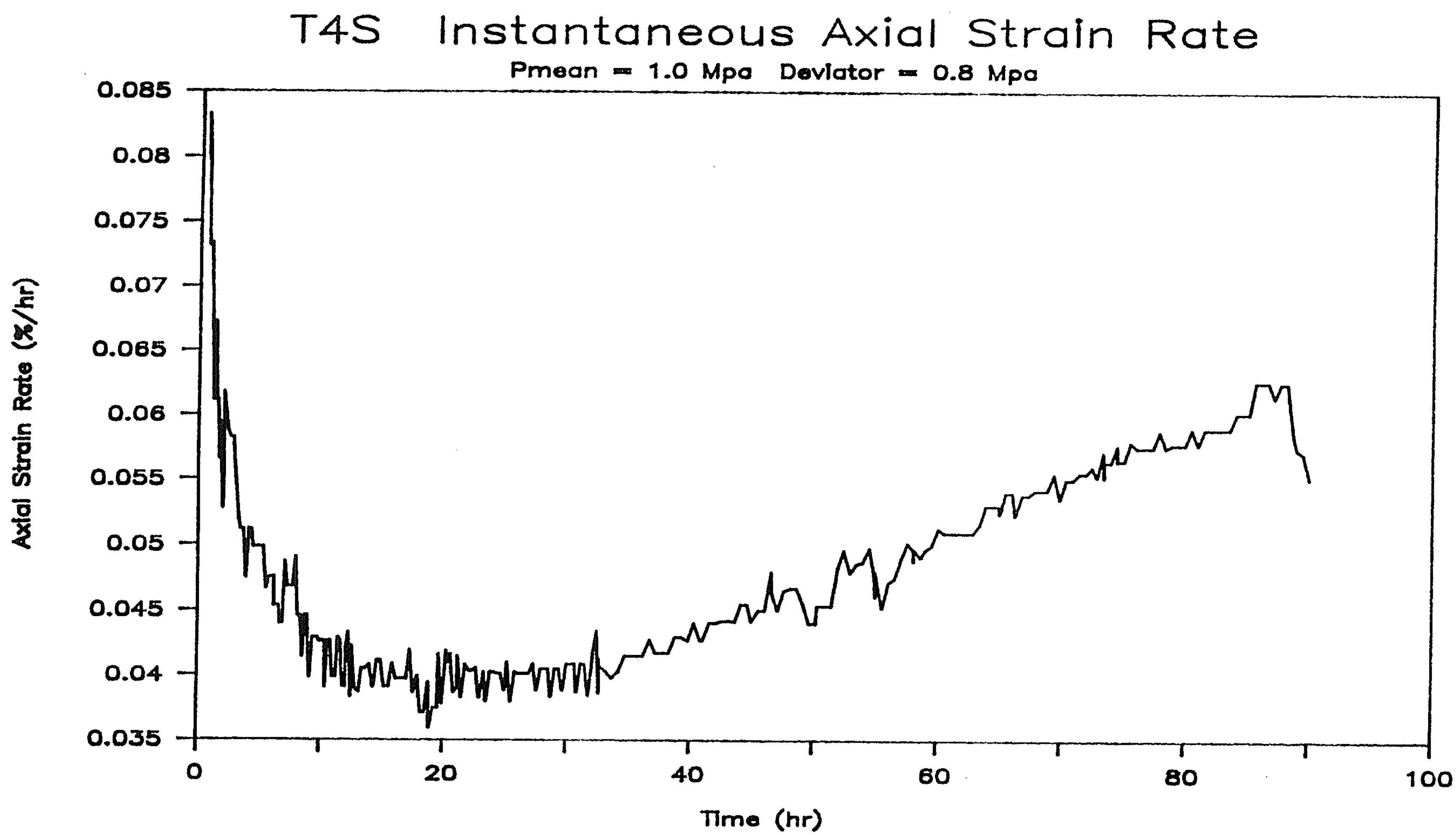

Figure 4.35 T4S Axial strain rate versus time

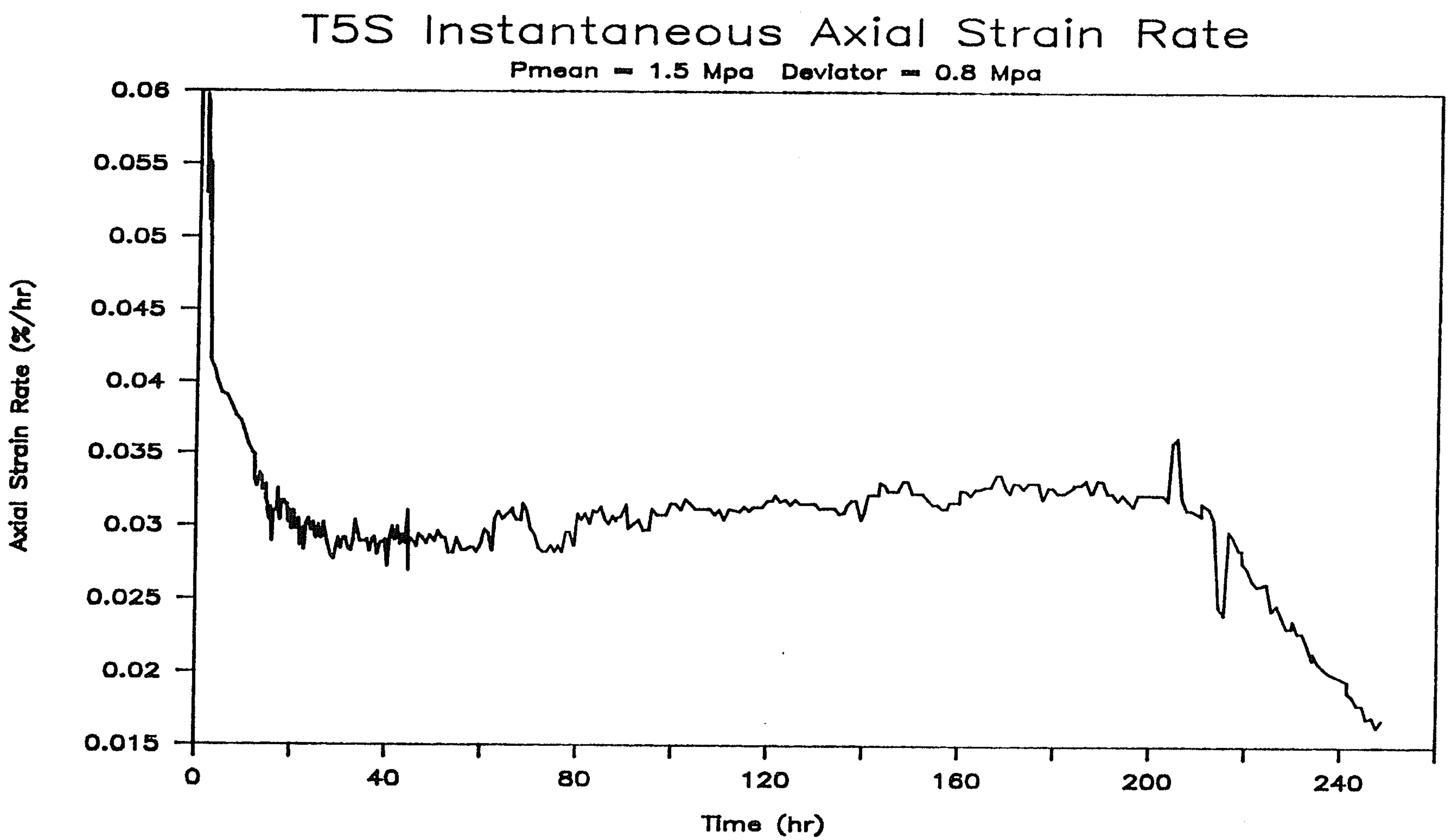

Figure 4.36 T5S Axial strain rate versus time

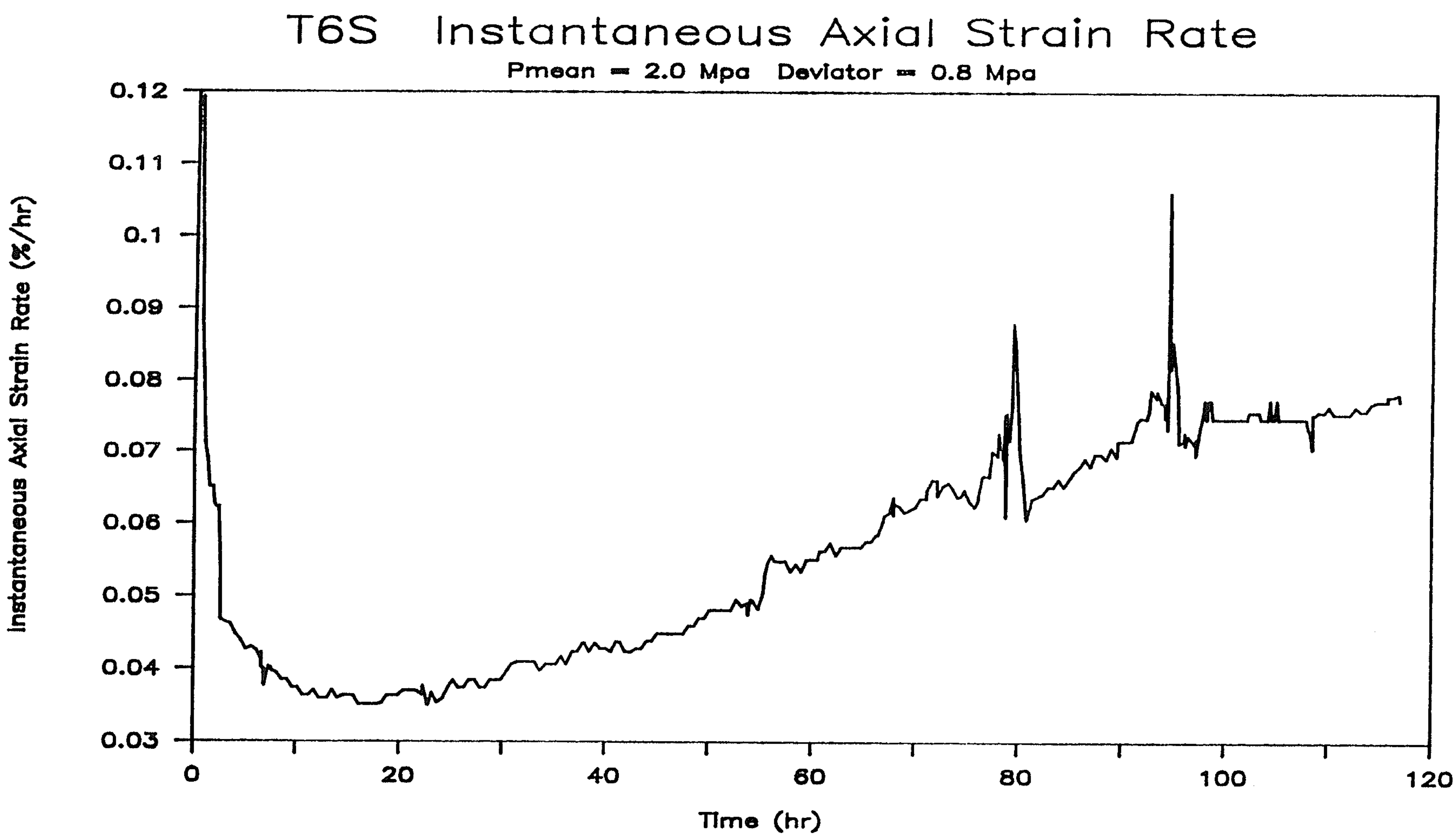

Figure 4.37 T6S Axial strain rate versus time

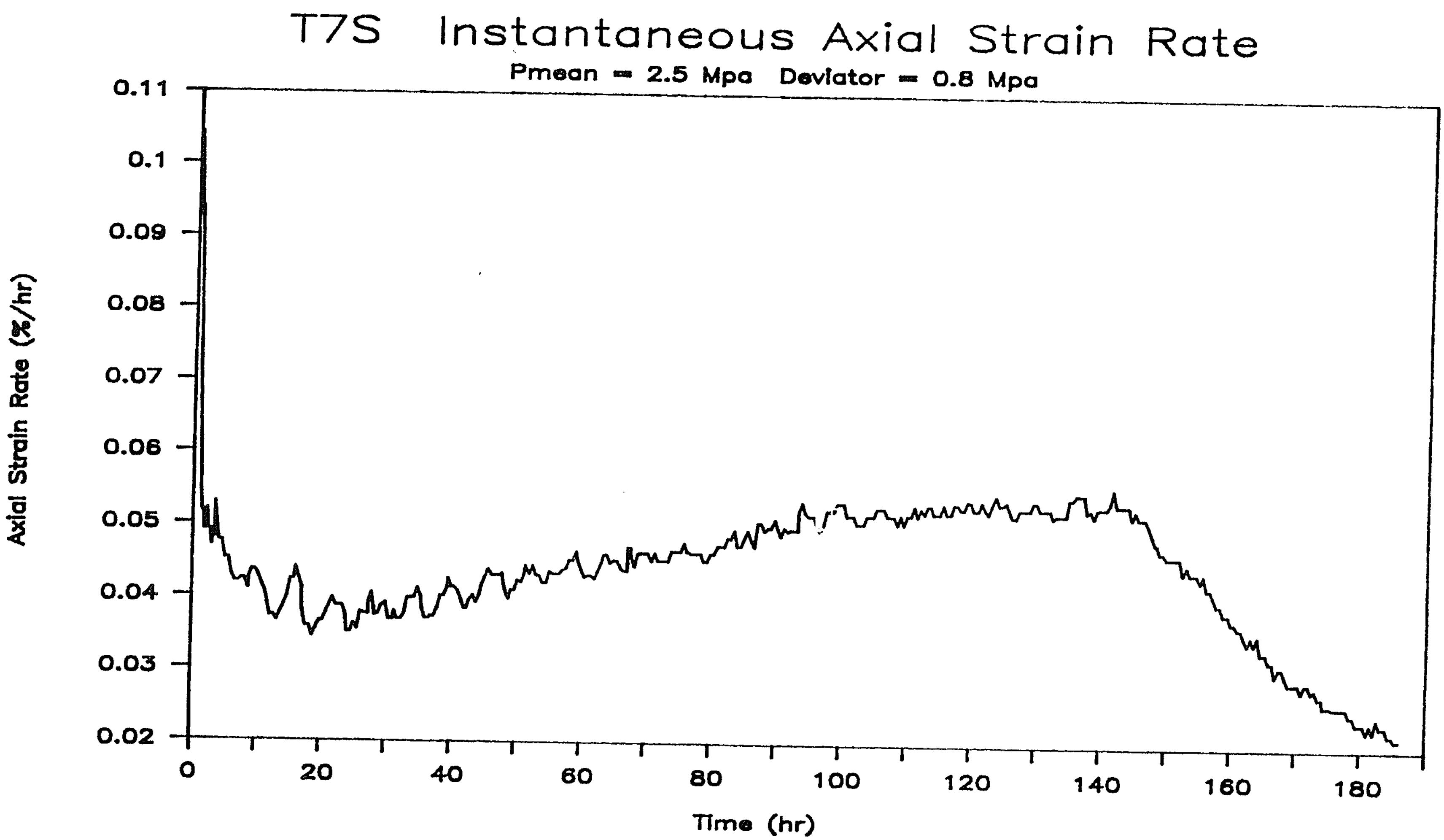

Figure 4.38 T7S Axial strain rate versus time

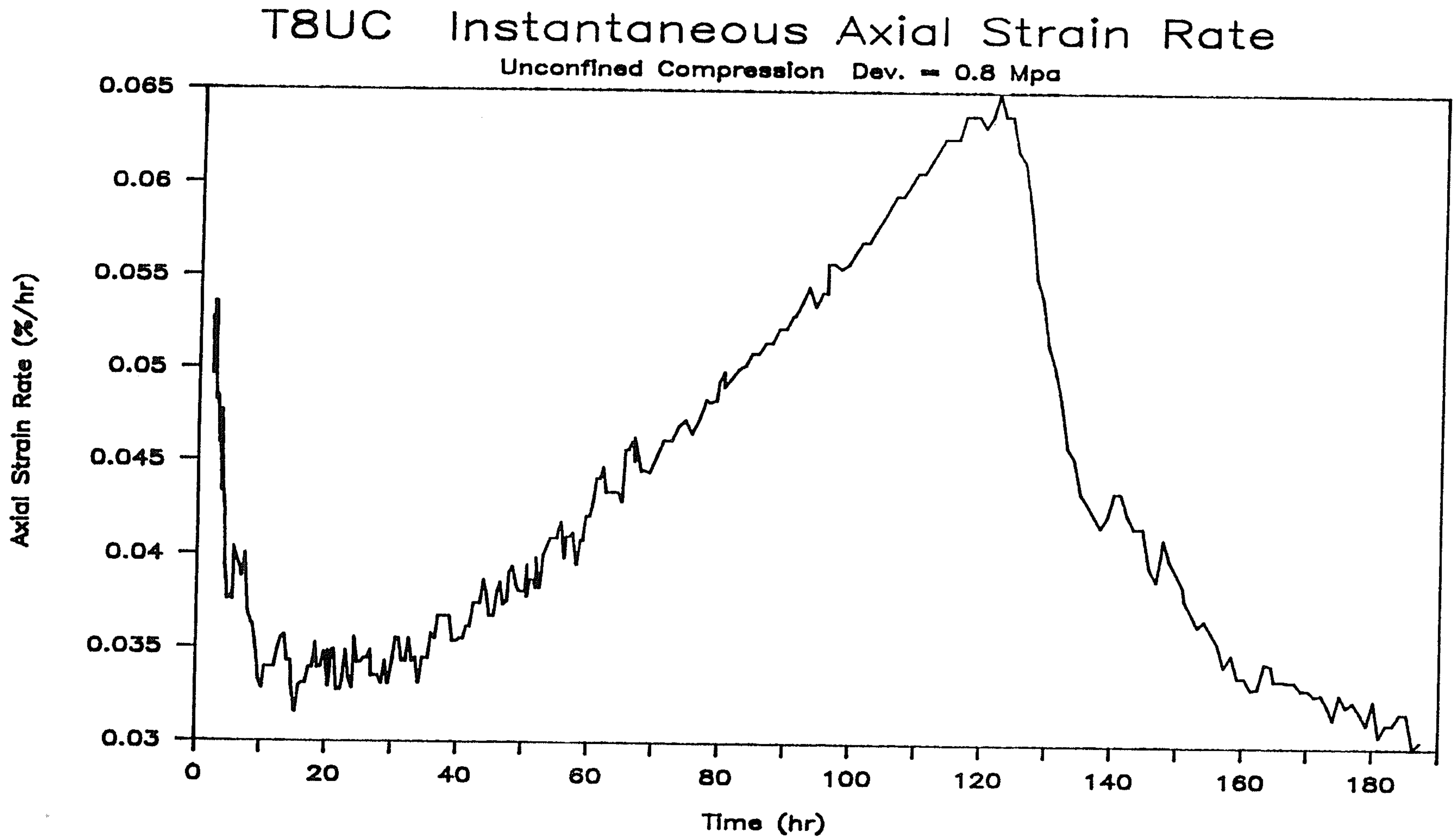

Figure 4.39 T8UC Axial strain rate versus time

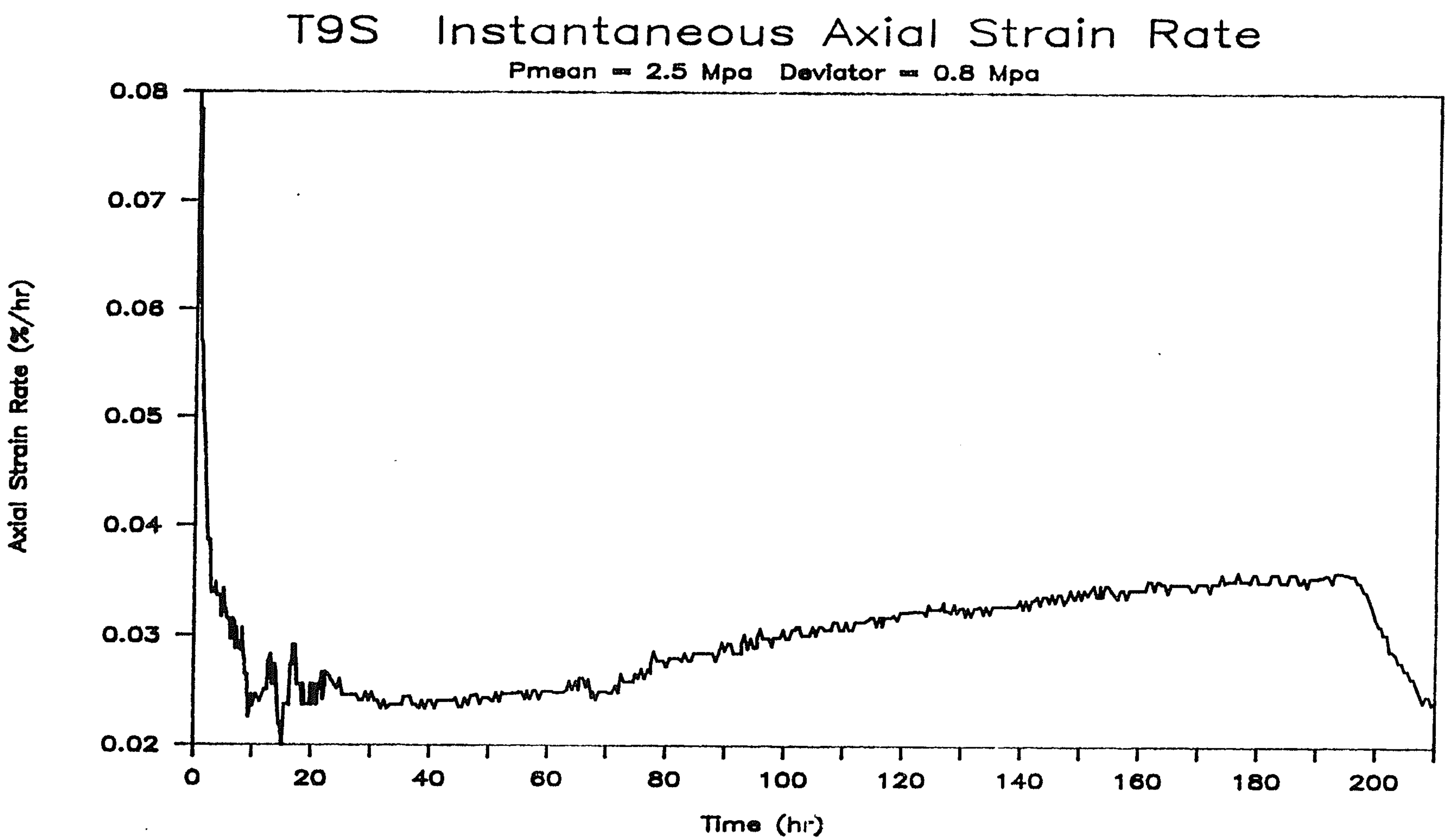

Figure 4.40 T9S Axial strain rate versus time

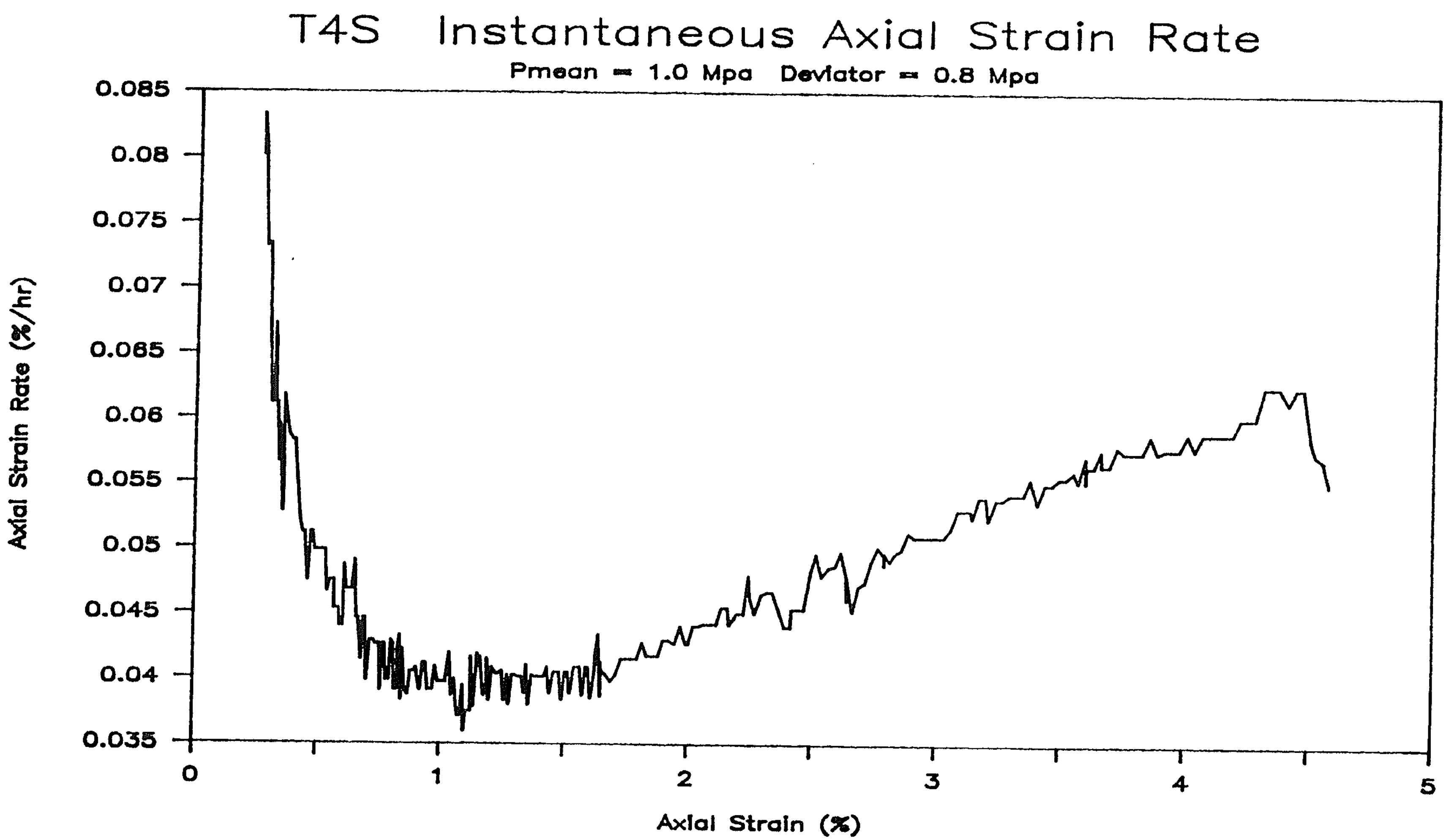

Figure 4.41 T4S Axial strain rate versus axial strain

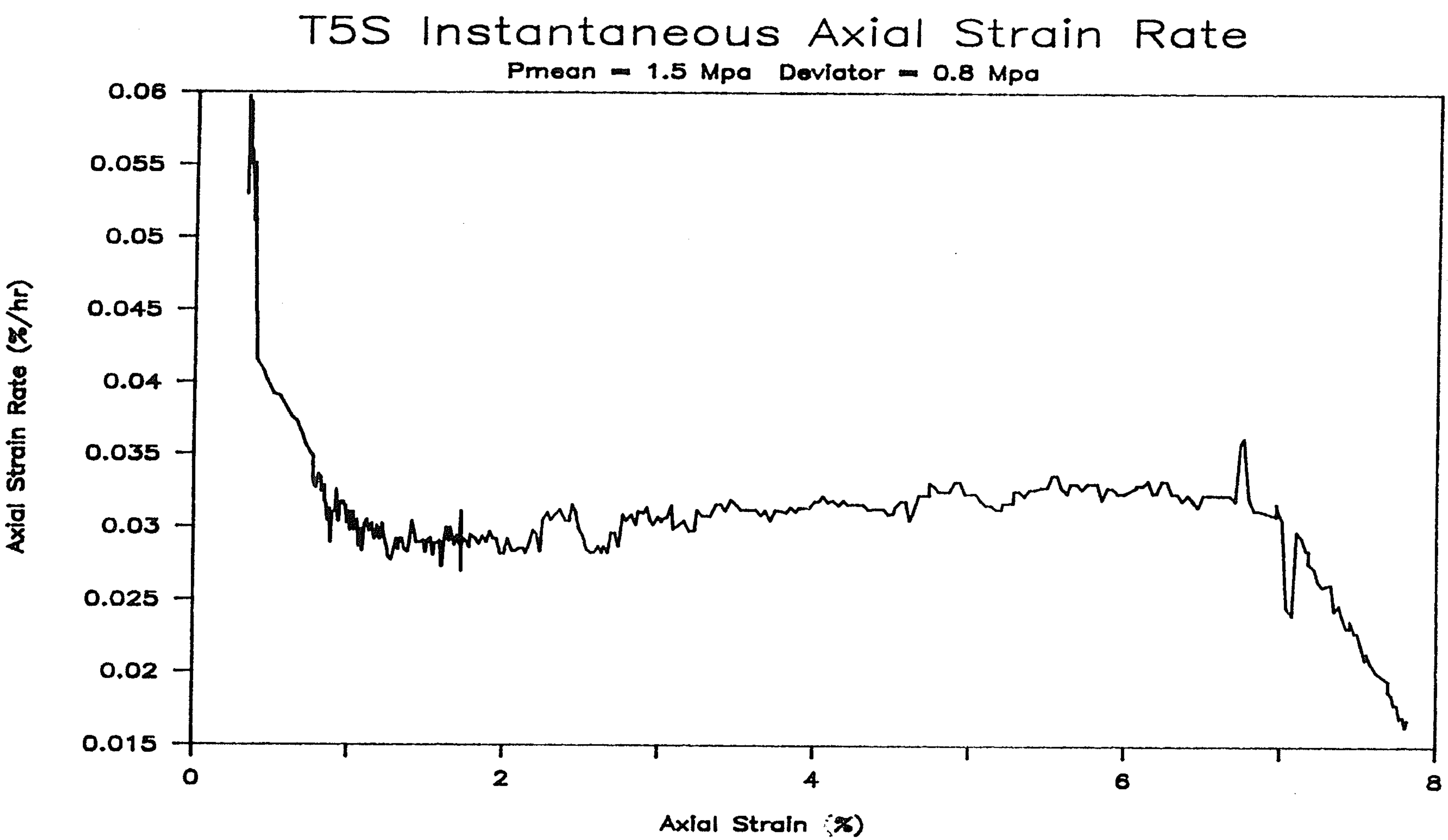

Figure 4.42 T5S Axial strain rate versus axial strain

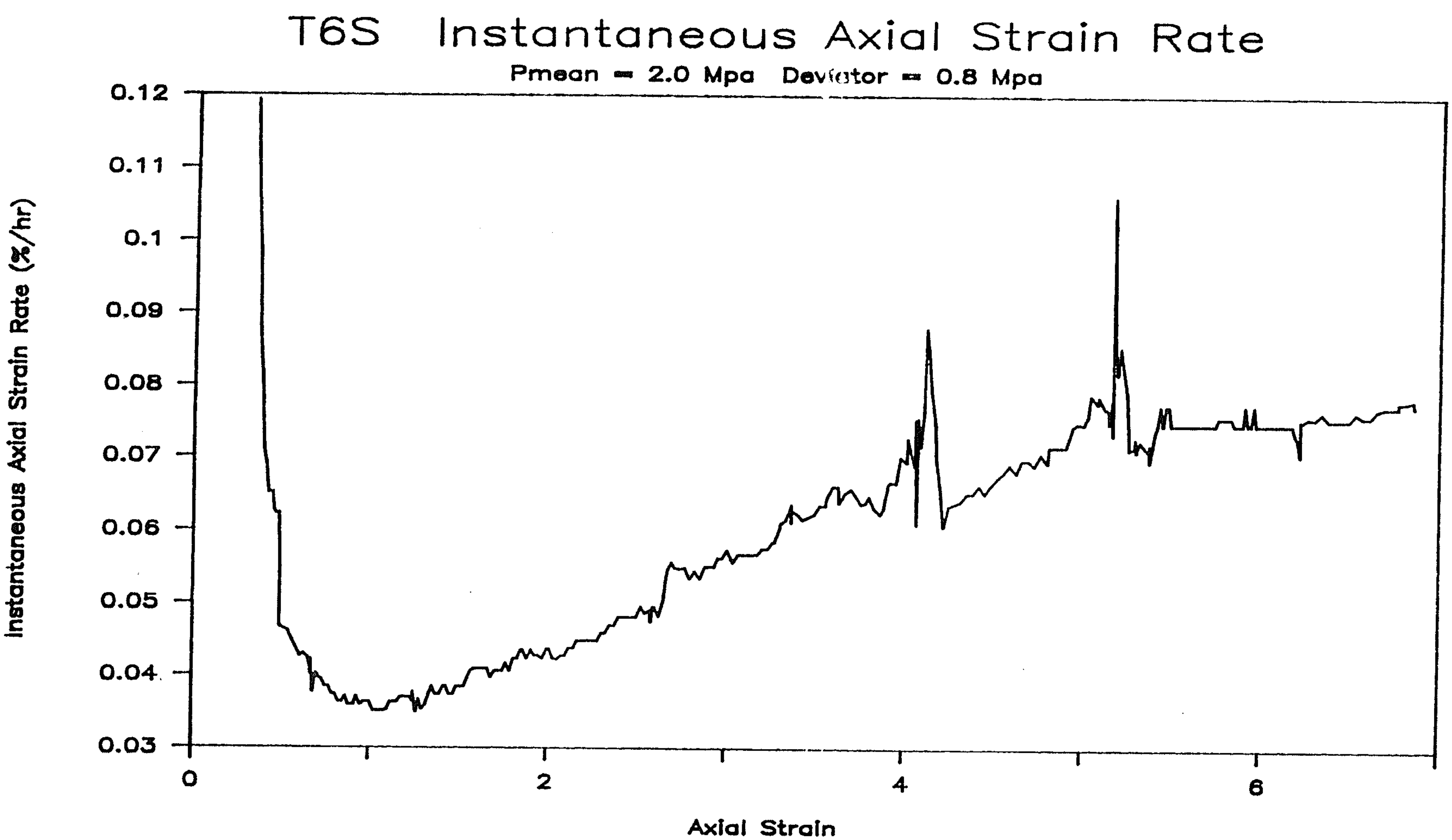

Figure 4.43 T6S Axial strain rate versus axial strain

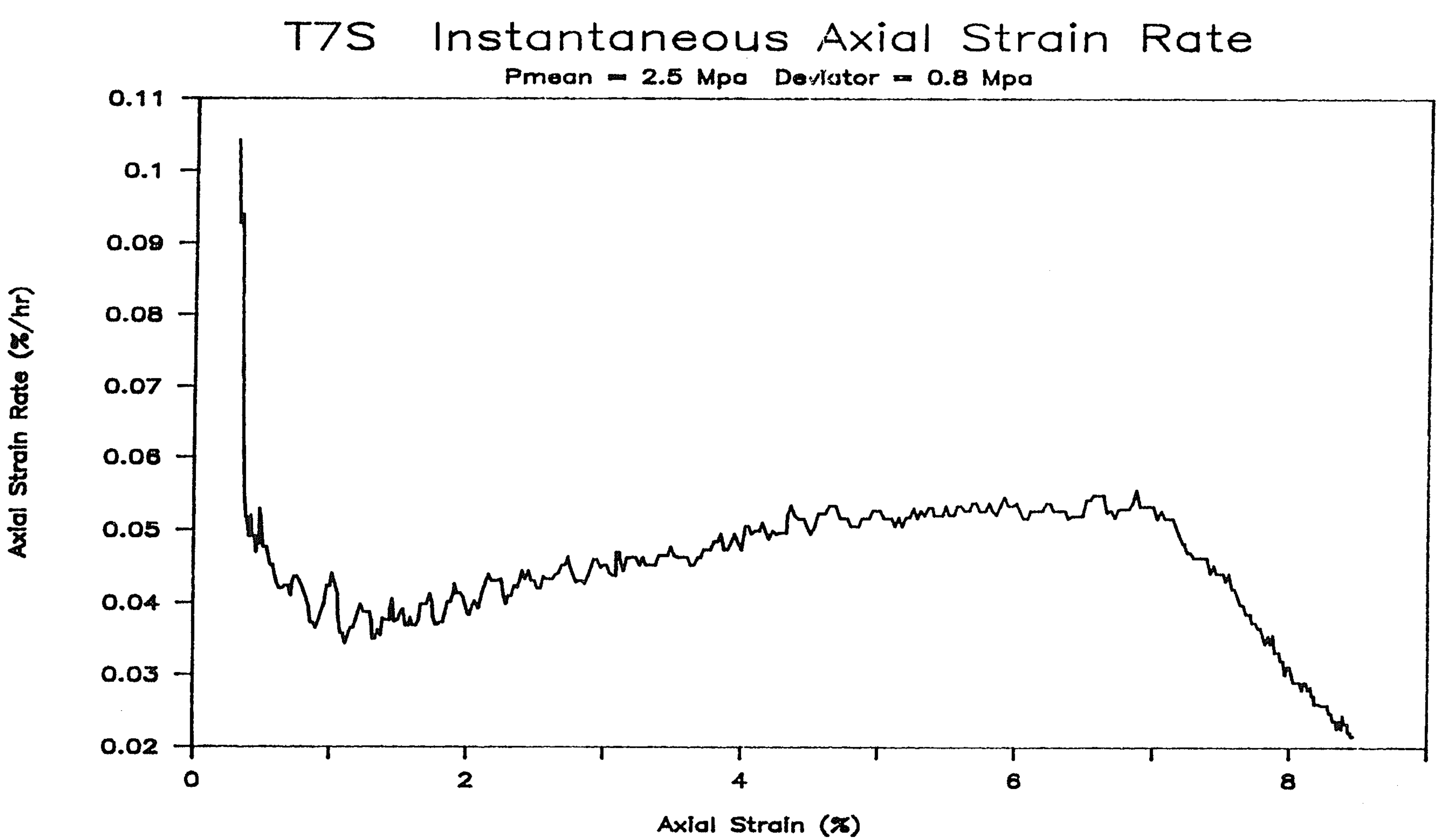

Figure 4.44 T7S Axial strain rate versus axial strain

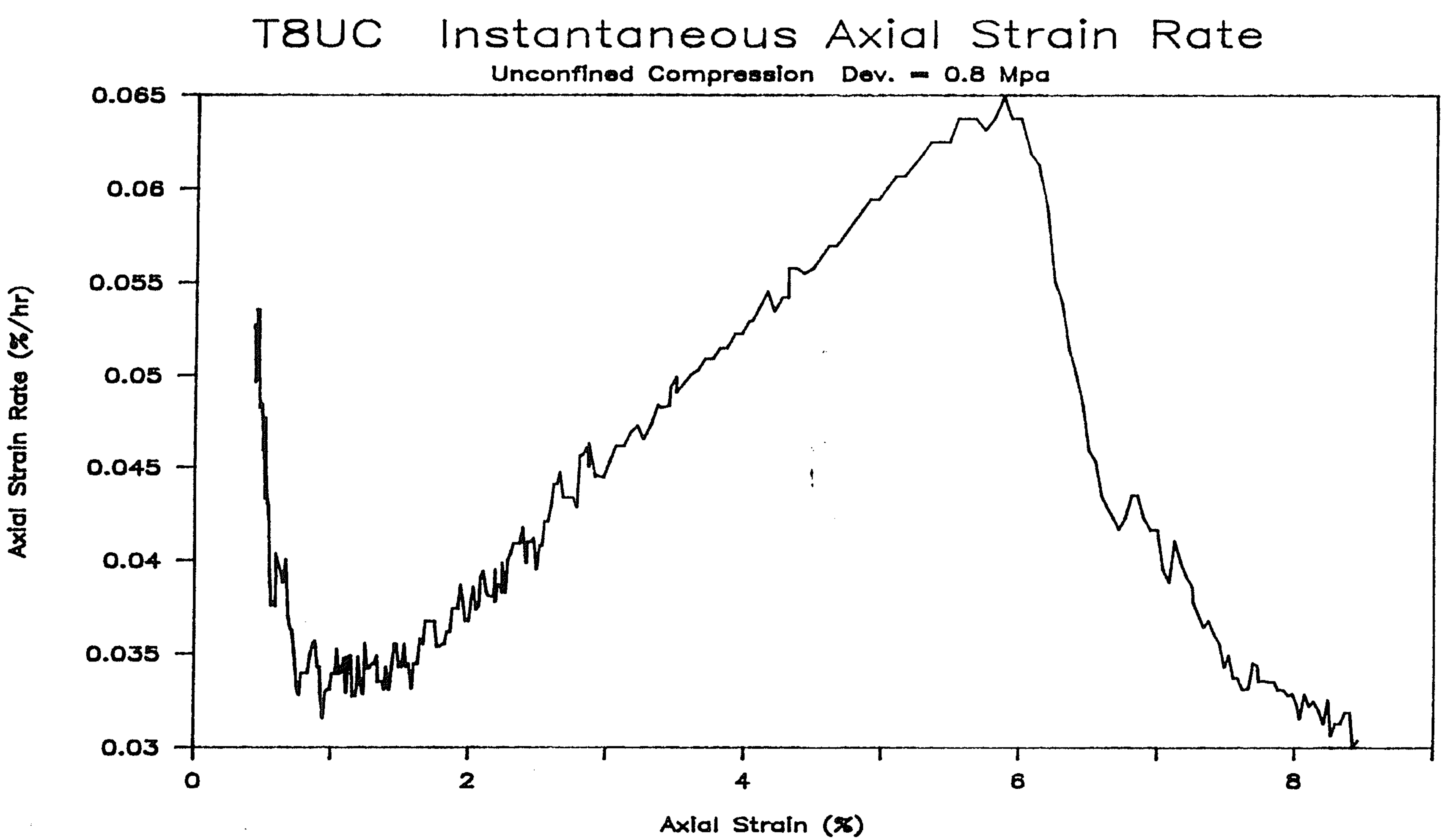

Figure 4.45 T8UC Axial strain rate versus axial strain

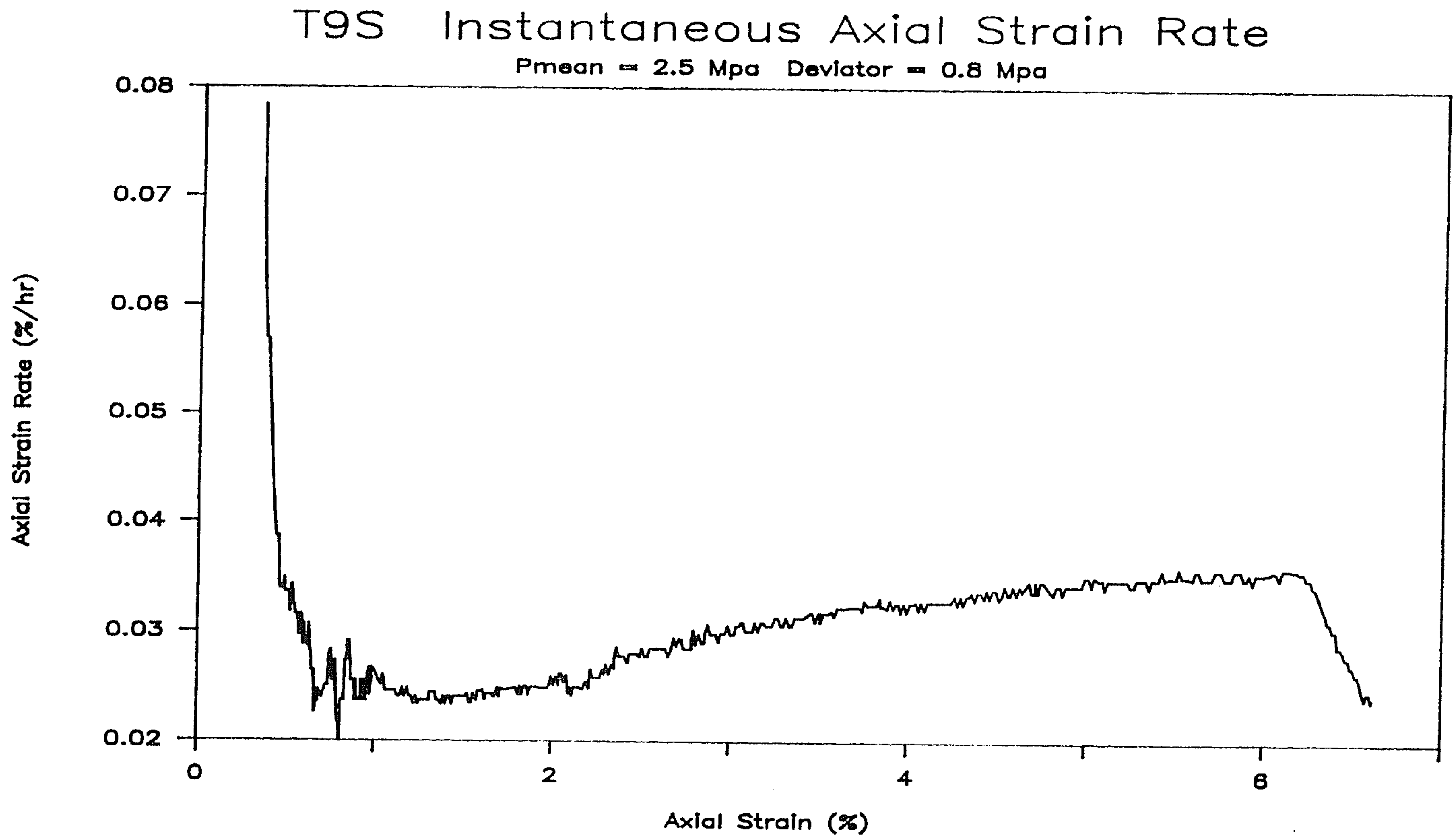

Figure 4.46 T9S Axial strain rate versus axial strain

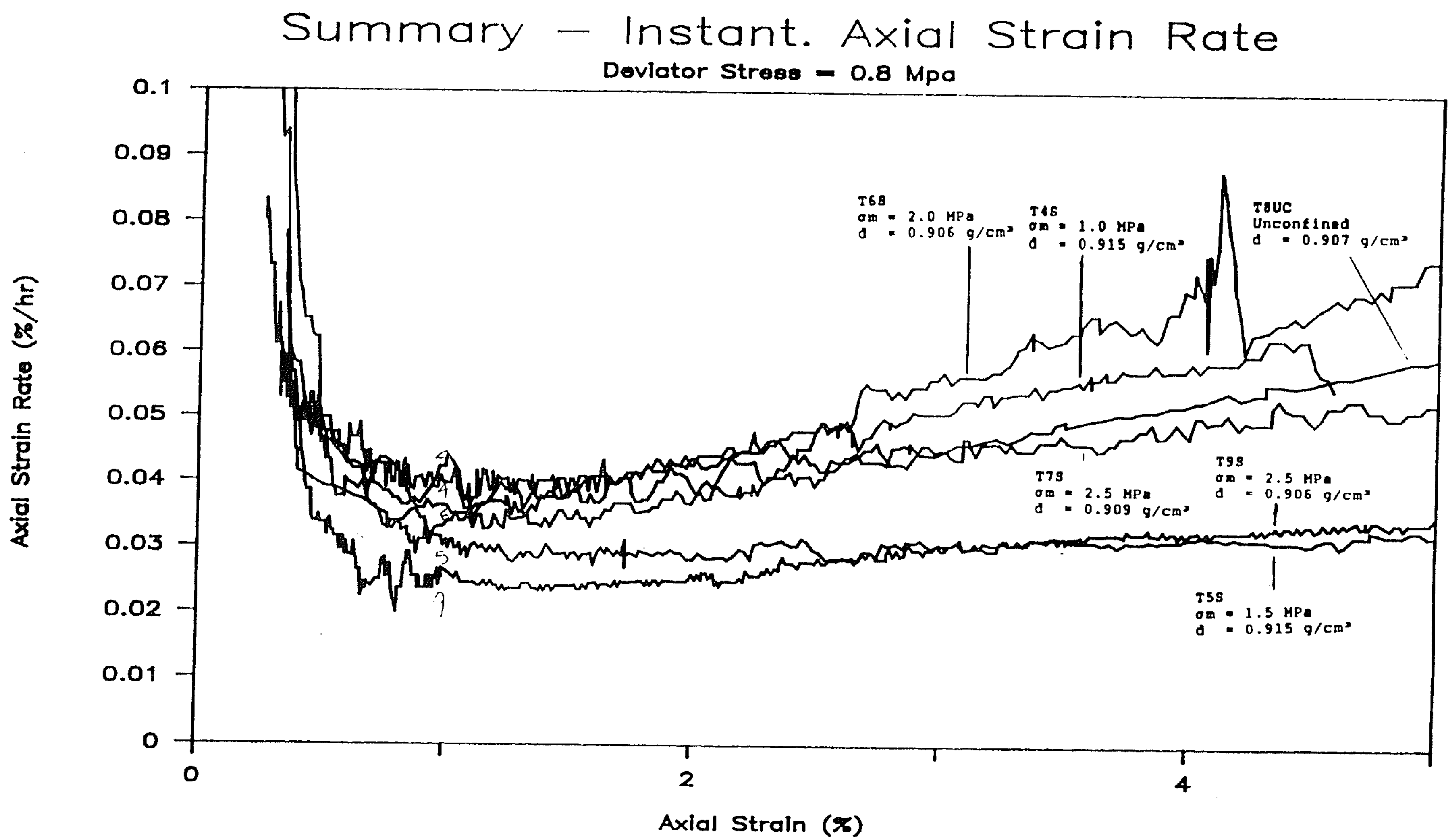

Figure 4.47 Summary of axial strain rate versus axial strain data for shear tests

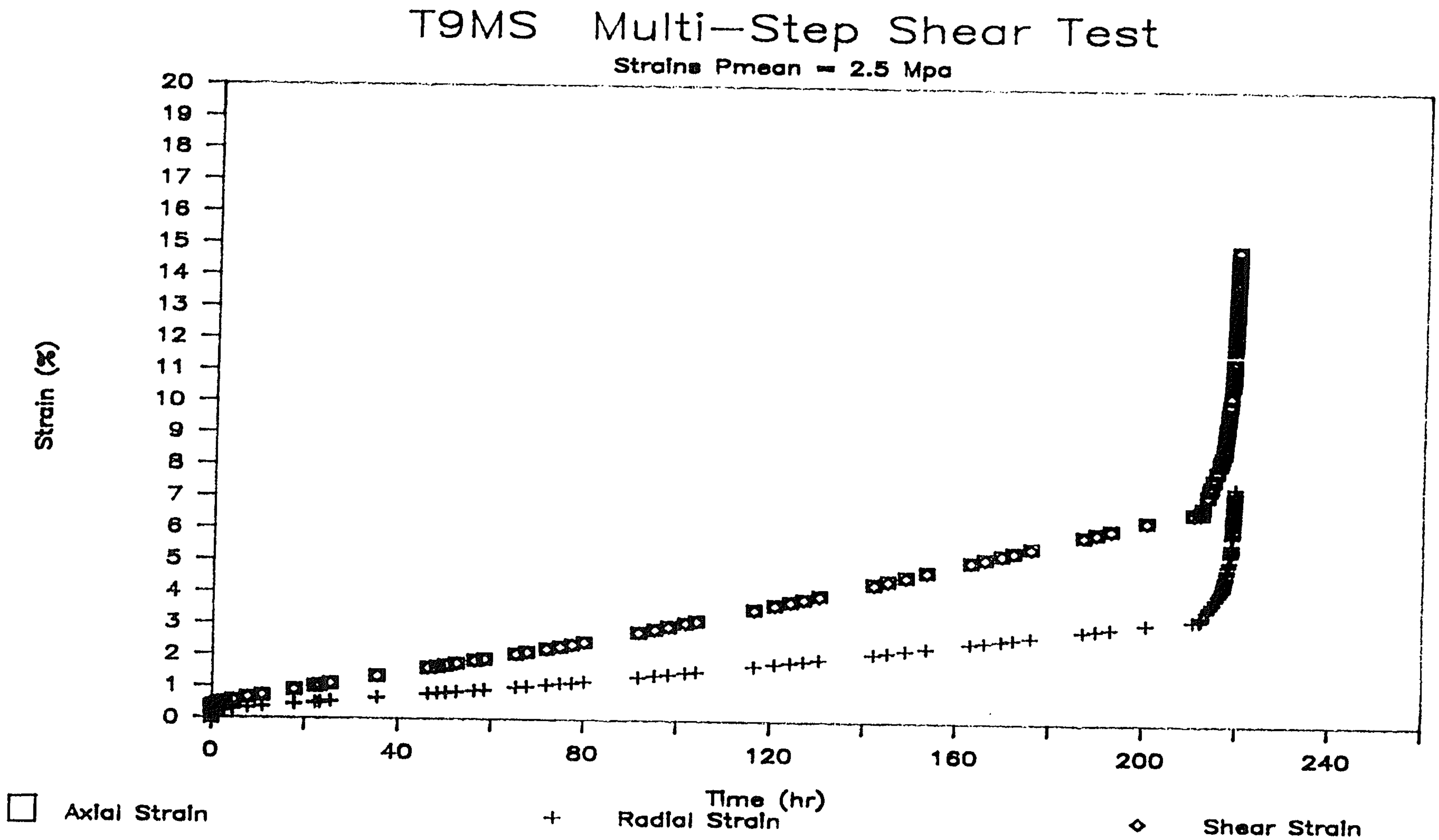

Figure 4.48 T9MS Axial, radial and shear strain

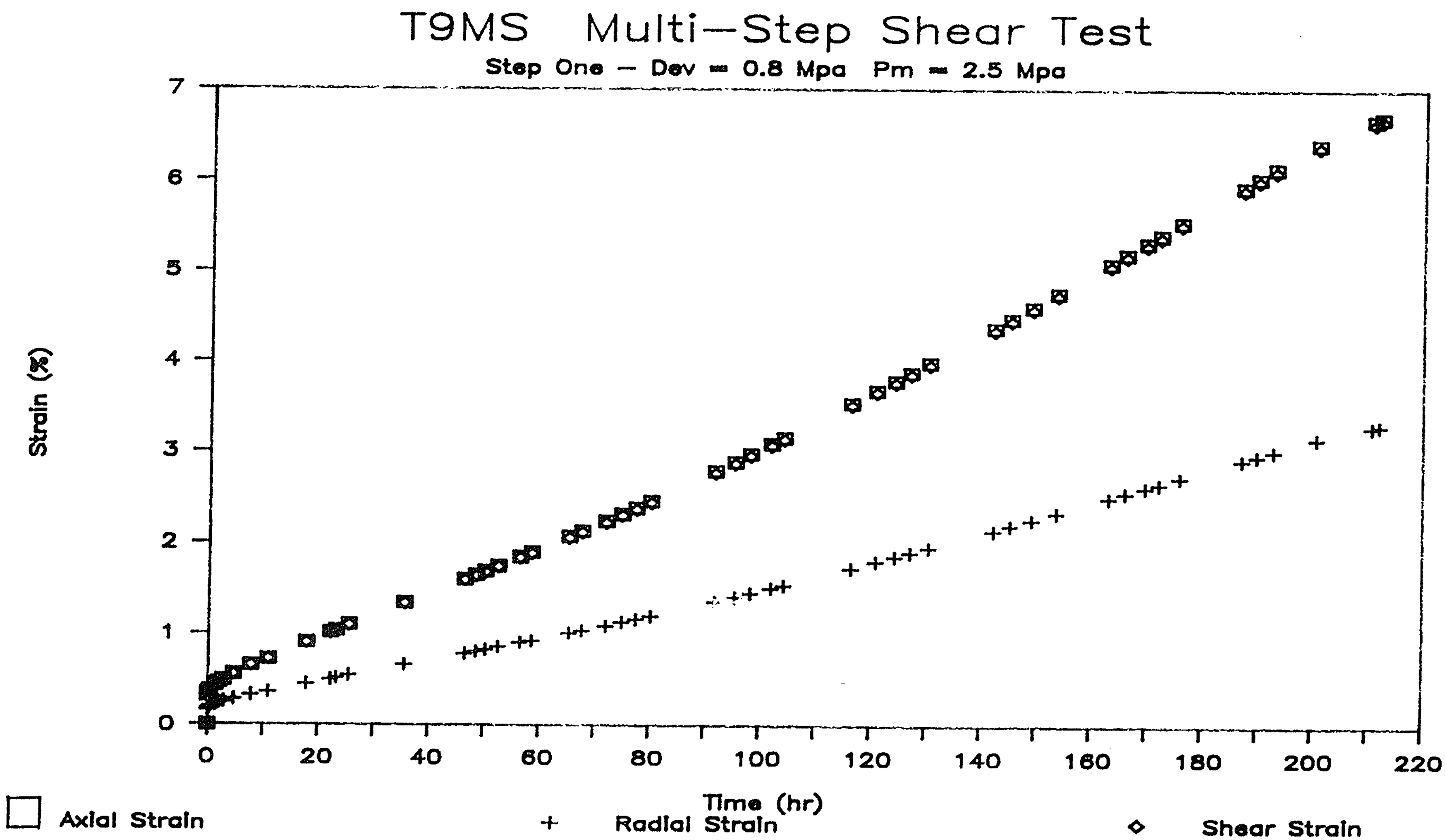

Figure 4.49 T9MS Step One Axial, radial and shear strain

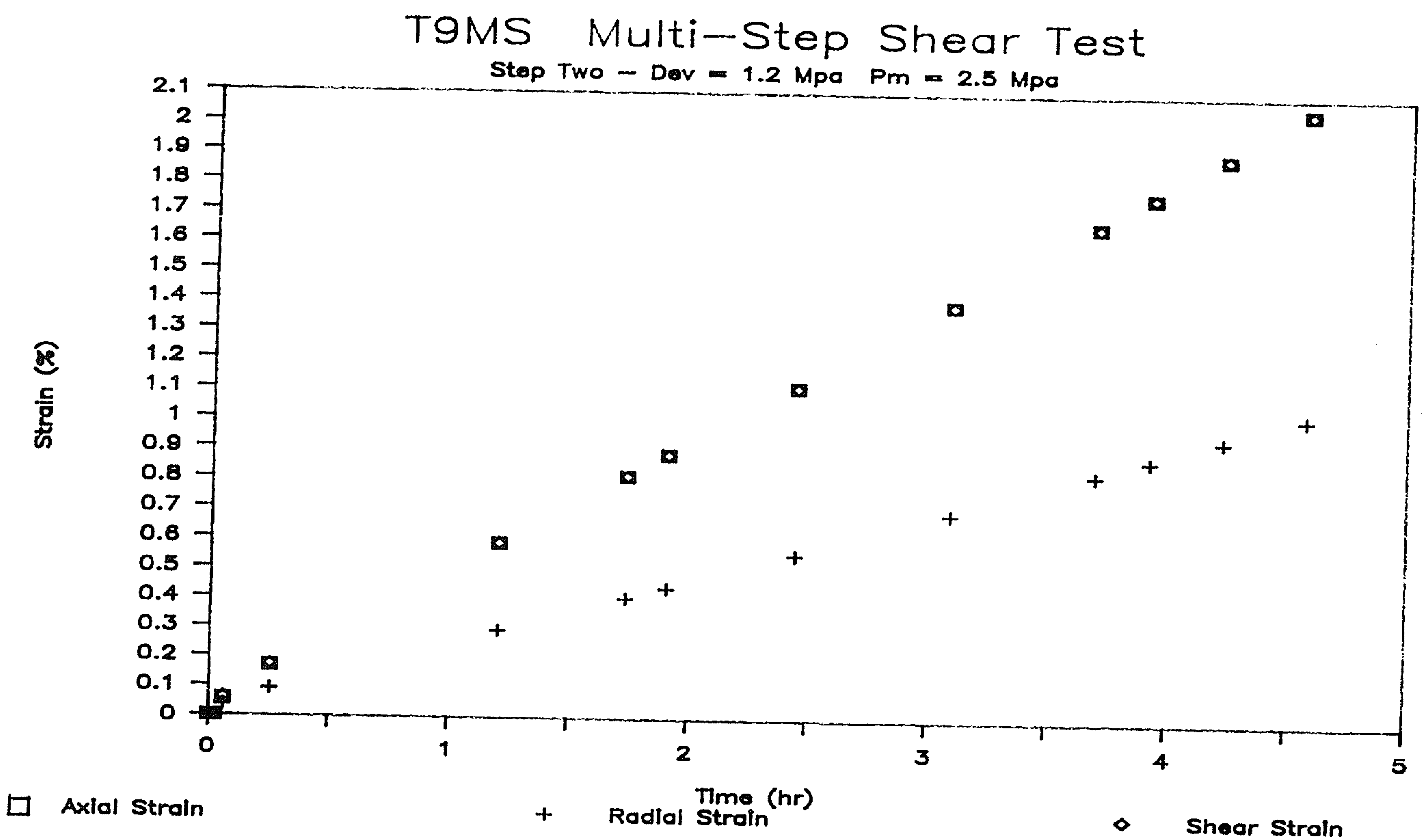

Figure 4.50 T9MS Step Two Axial, radial and shear strain

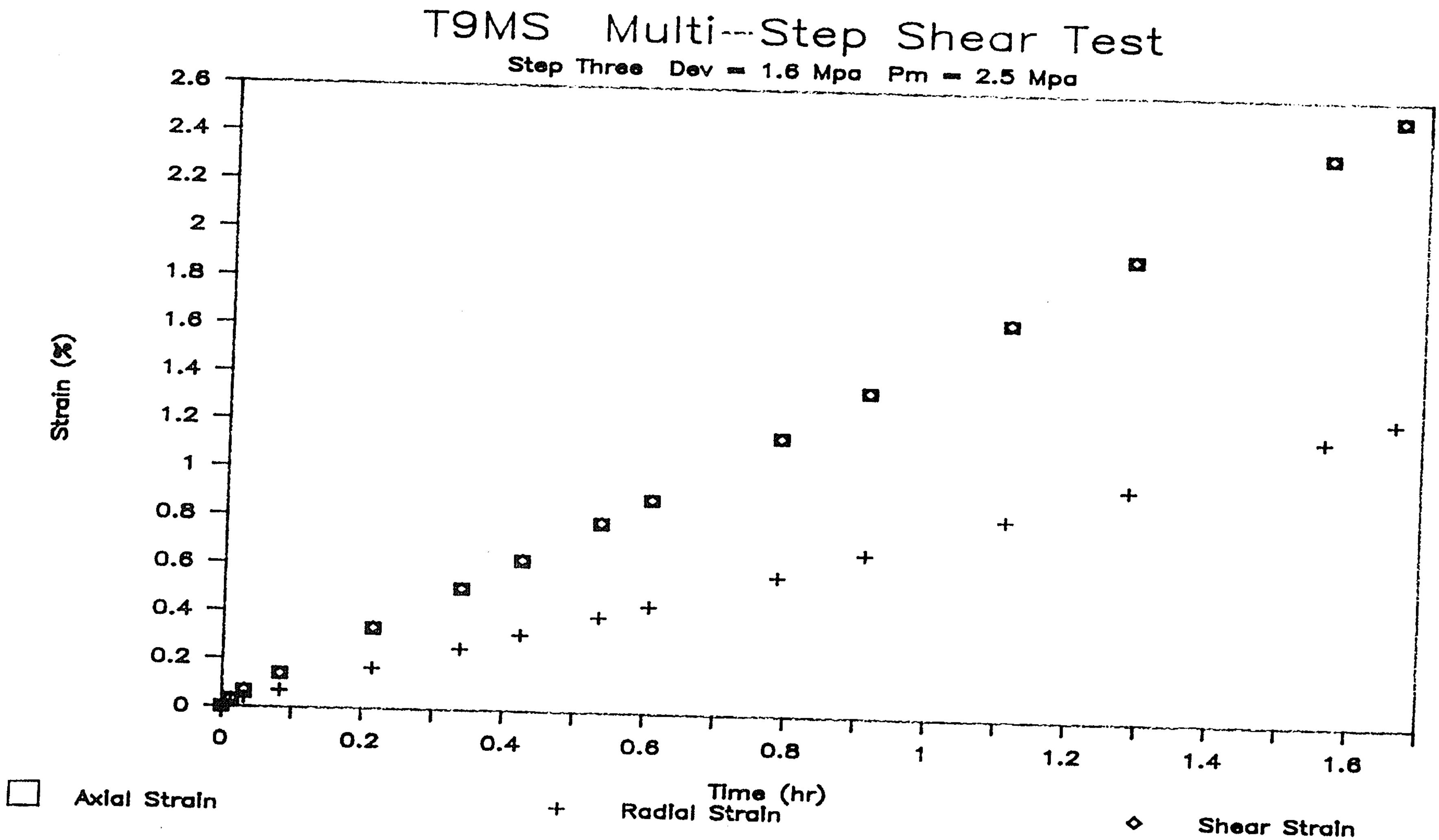

Figure 4.51 T9MS Step Three Axial, radial and shear strain

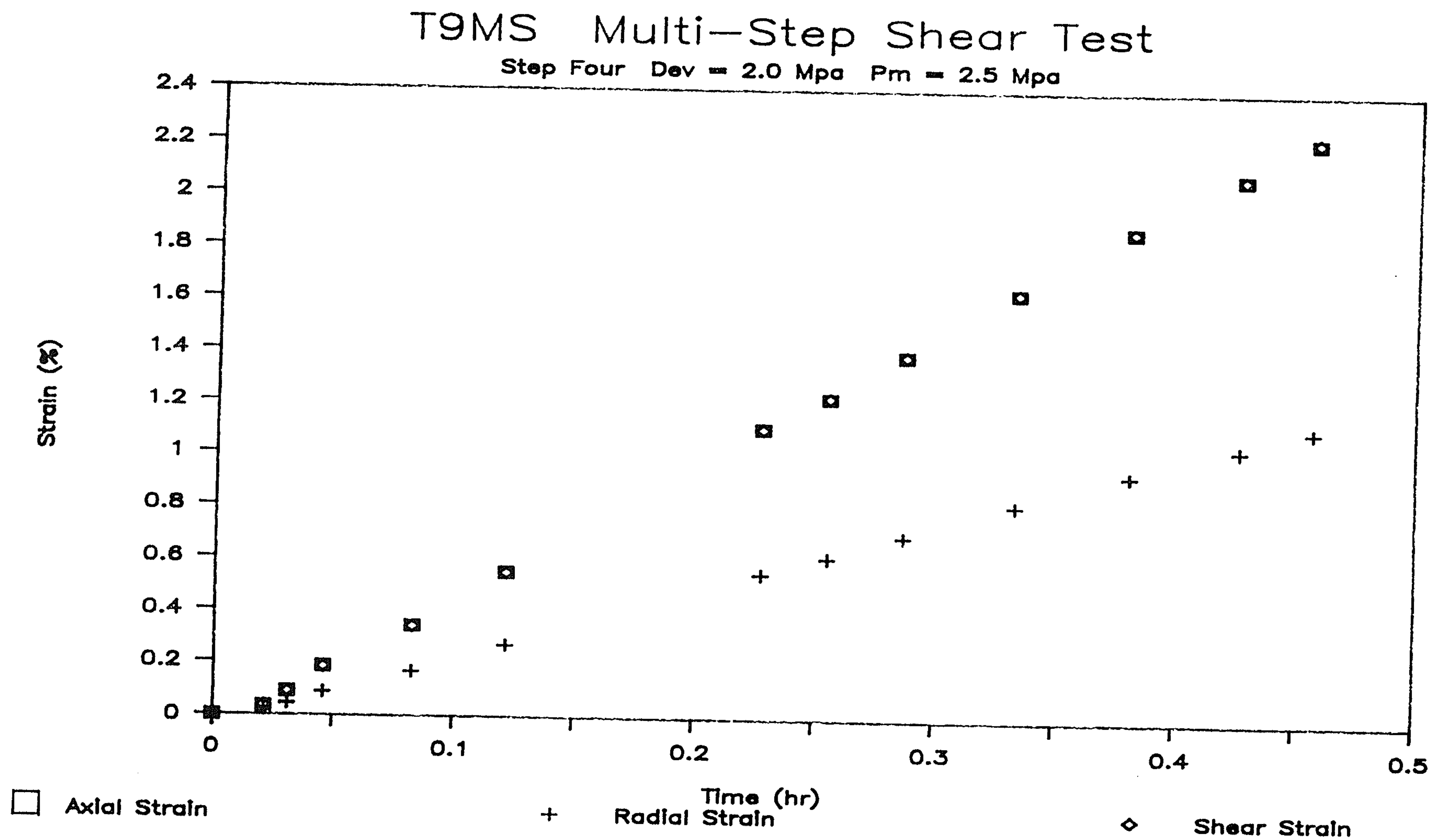

Figure 4.52 T9MS Step Four Axial, radial and shear strain

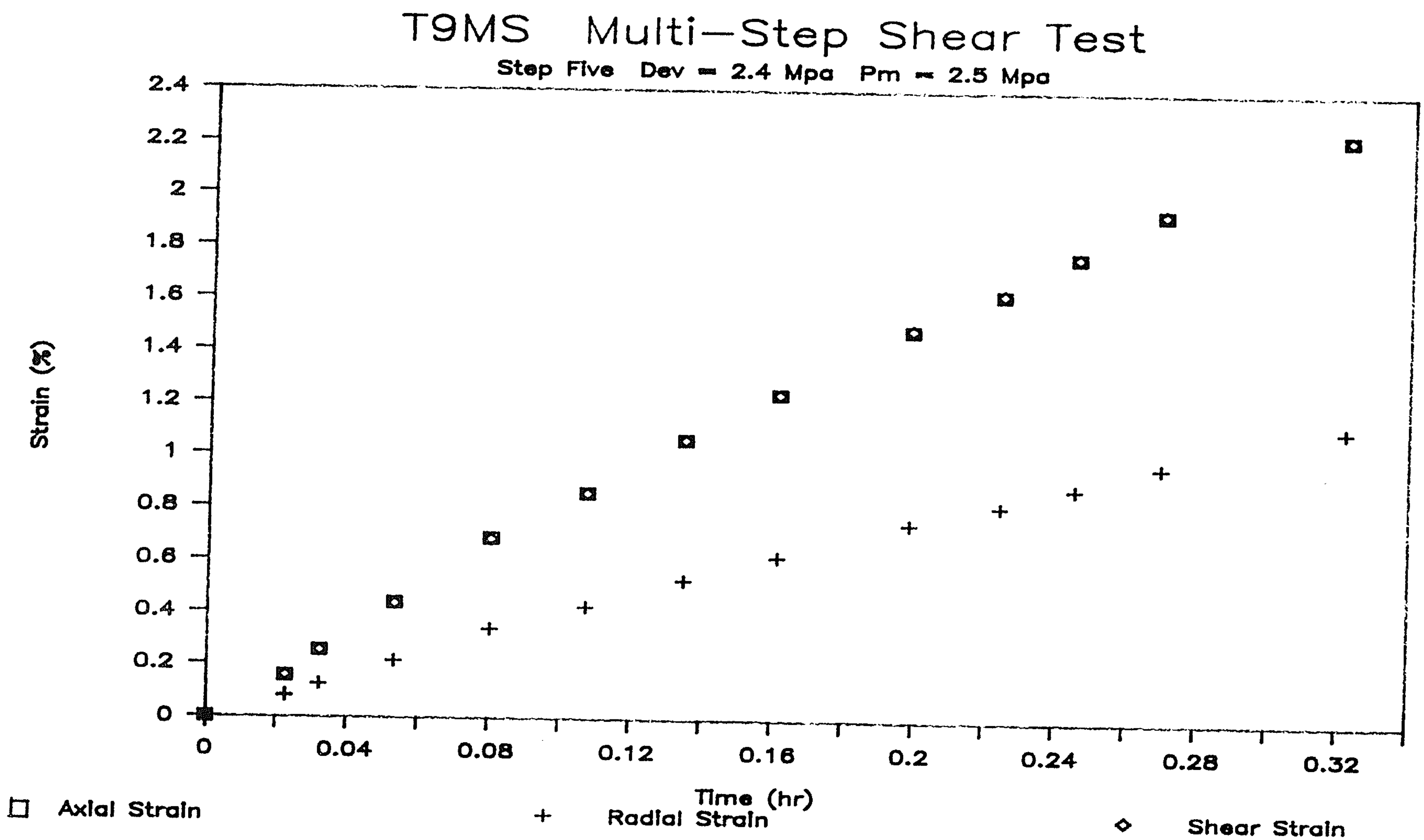

Figure 4.53 T9MS Step Five Axial, radial and shear strain

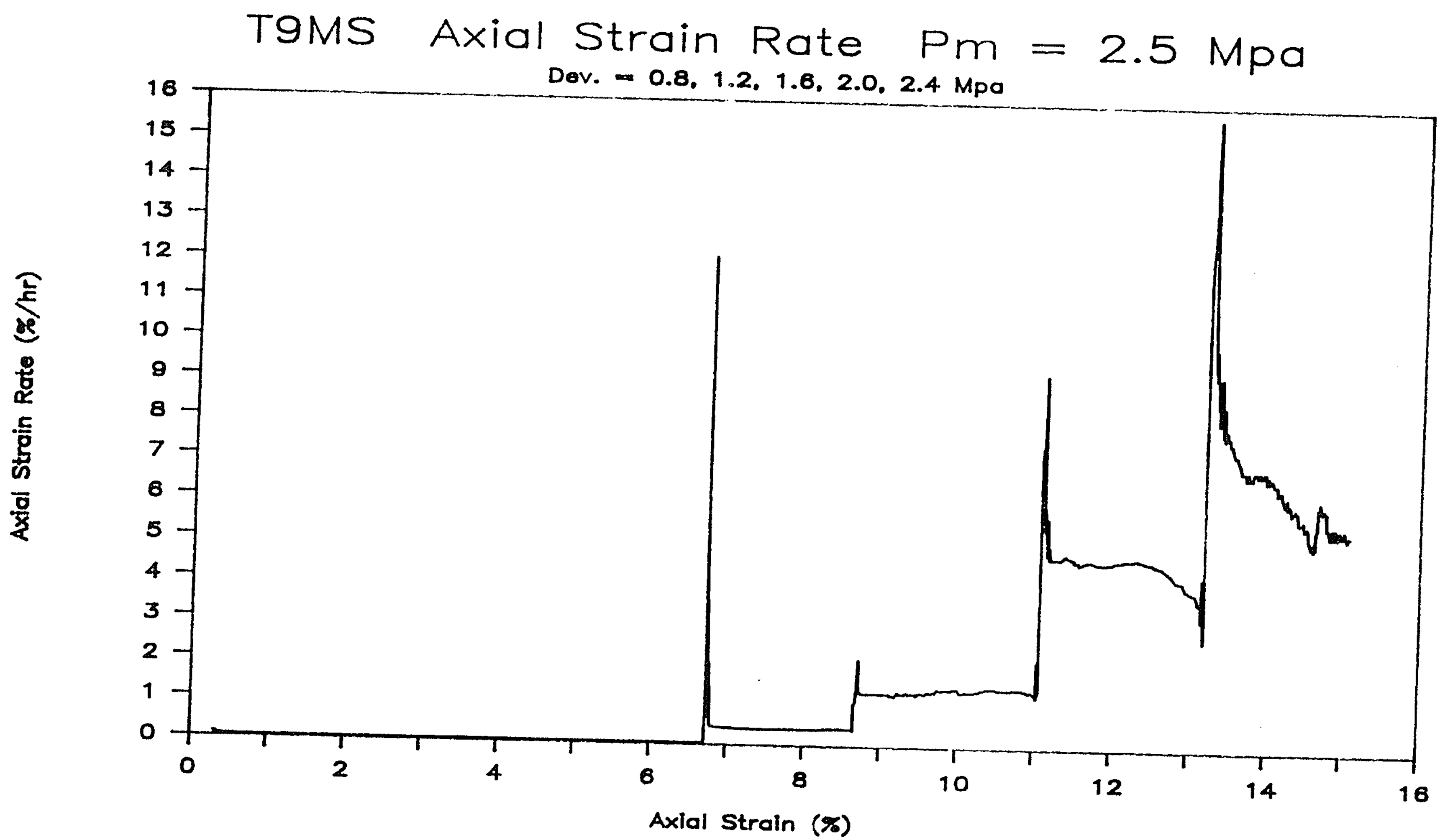

Figure 4.54 T9MS Axial strain rate

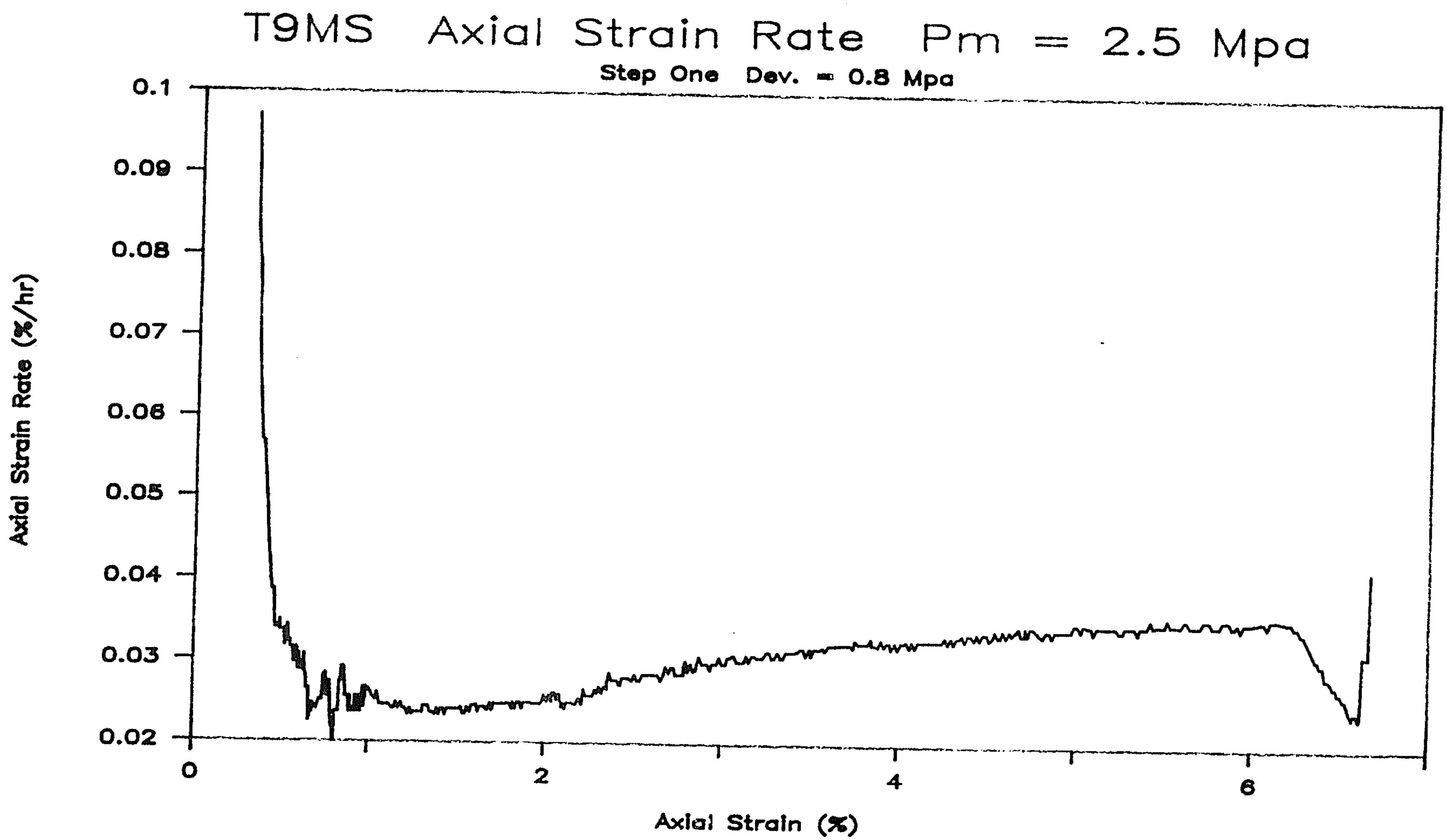

Figure 4.55 T9MS Step One Axial strain rate

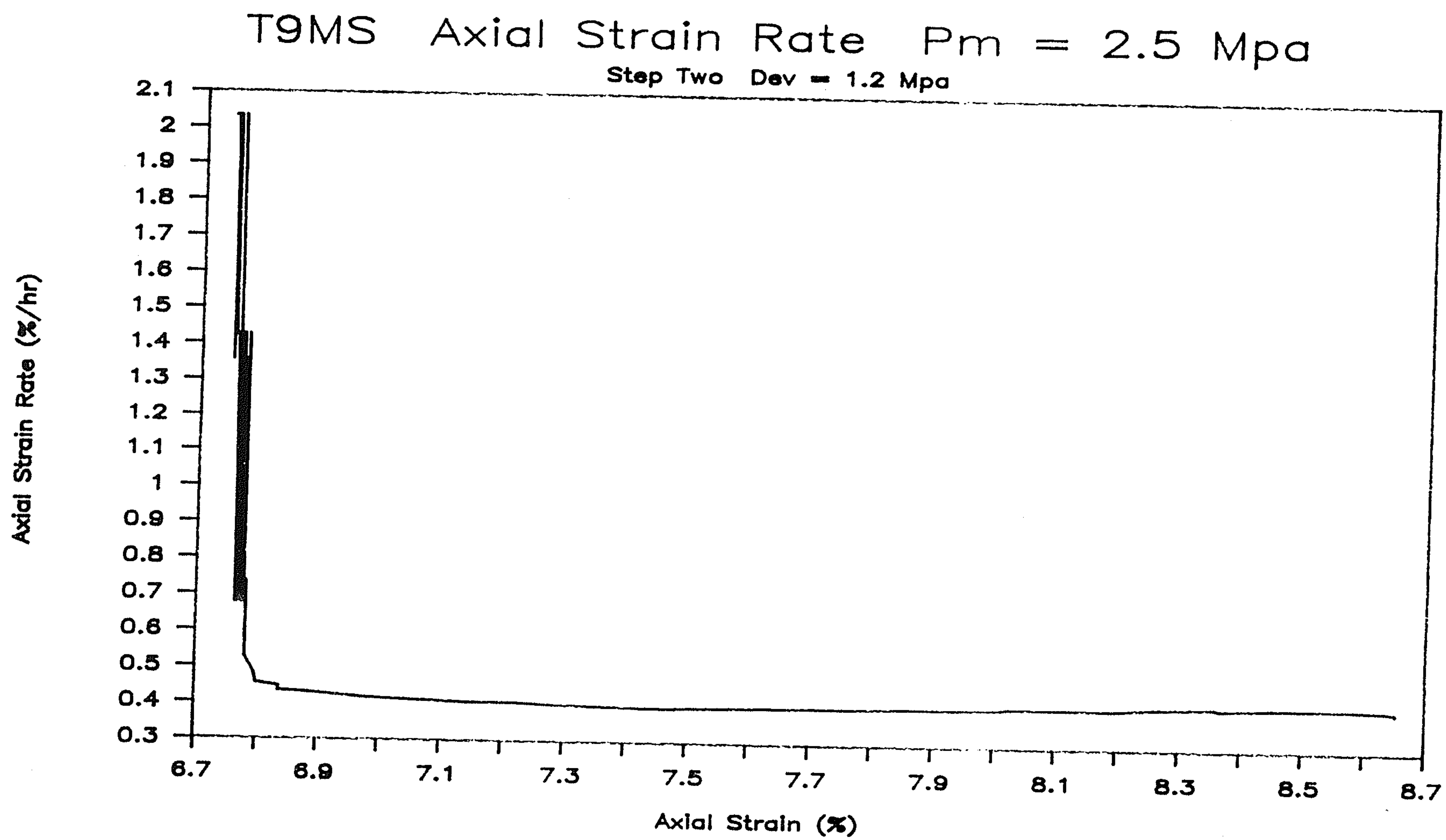

Figure 4.56 T9MS Step Two Axial strain rate

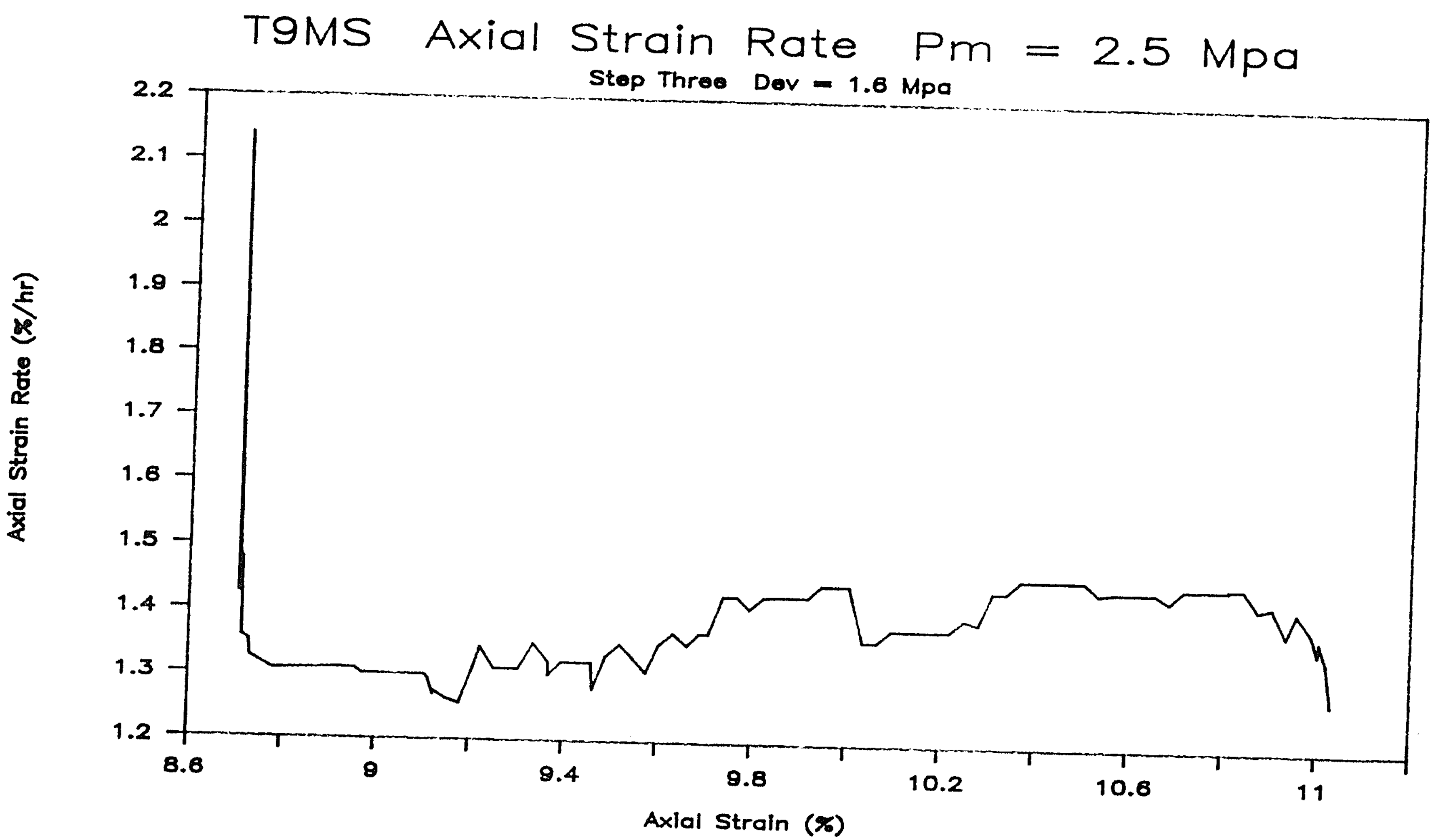

Figure 4.57 T9MS Step Three Axial strain rate

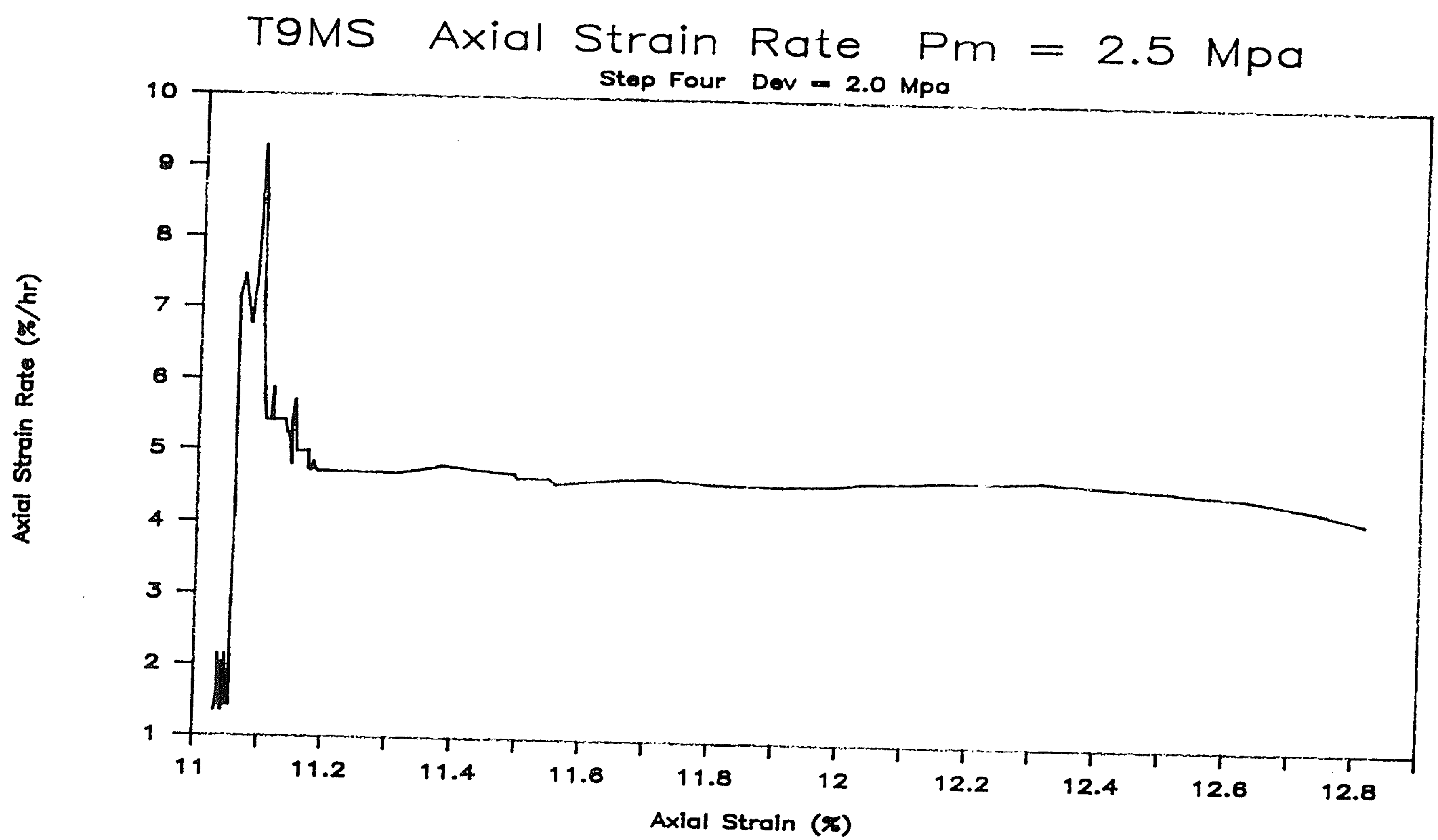

Figure 4.58 T9MS Step Four Axial strain rate

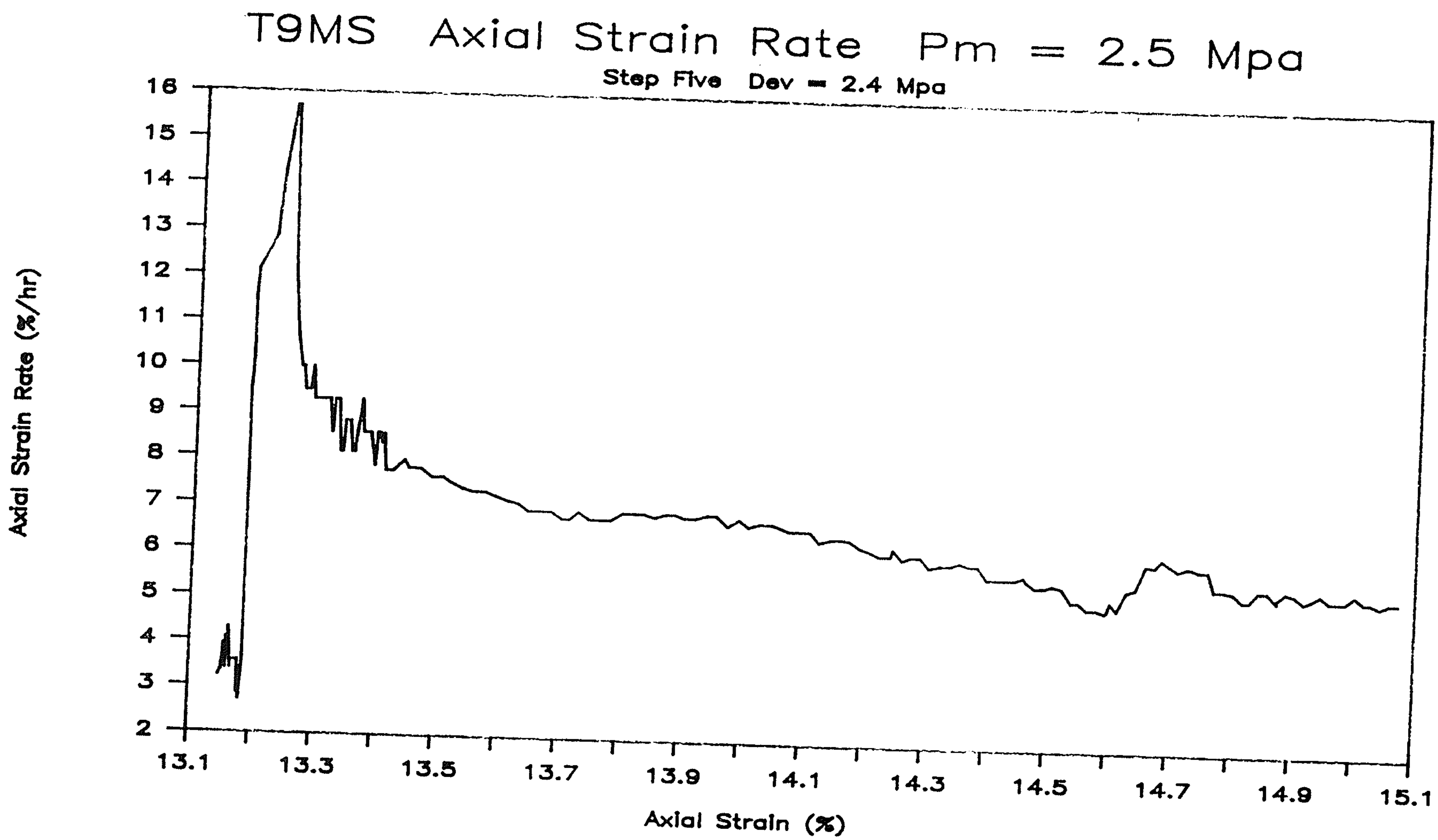

Figure 4.59 T9MS Step Five Axial strain rate

CHAPTER FIVE

Analysis of Test Resuluts

5.1 INTRODUCTION

The data obtained from the laboratory test program in the form of volumetric and axial deformation, temperature, and pressure were used to determine the bulk modulus, shear modulus, and Poisson's ratio of Kjartanson's ice. The theory of these moduli values is not complex and can be found in any introductory level text on the mechanics of materials. All theoretical considerations for the present study are reviewed in Chapter Two. This chapter presents the results of the analysis of the test data. The isotropic compression test results, used to determine bulk modulus, are presented separately from the constant mean normal stress shear test results, which were used to determine shear modulus and Poisson's ratio.

5.2 ANALYSIS OF ISOTROPIC COMPRESSION TEST RESULTS

Isotropic compression tests were performed on the ice specimens for two reasons. First and most important, the effective bulk modulus was determined from the volumetric strain of the specimen. Secondly, all volumetric deformation due to hydrostatic stress had to be complete before the constant mean stress shear test was begun. Single step isotropic compression tests were conducted at pressures of 1.0, 1.5, 2.0, and 2.5 Mpa. Quick-step isotropic compression tests were also performed in order to determine the elastic bulk modulus.

5.2.1 Elastic Bulk Modulus

Due to certain difficulties in determining the initial volume change in the single step tests, quick-step isotropic compression tests were performed to determine the elastic bulk modulus of the ice. Figure 4.23 summarizes the quick-step tests. As discussed in Section 4.2.3, the linear portion of the curves is thought to represent the true elastic behaviour of the ice. The slope of the linear portion of each curve was determined using regression analysis. The inverse of this slope is the elastic bulk modulus, and is summarized in Table 5.1. The average value of K was found to be 1.02 Gpa, with a standard deviation of 0.11 Gpa. Figure 5.1 illustrates the total volumetric strain of each test. The elastic bulk modulus was used to calculate the initial compression, and the creep strain was added, yielding the total volumetric strain.

5.2.2 Effective Bulk Modulus

The effective bulk modulus of each ice specimen was determined from its single step isotropic compression test. Plots of effective bulk modulus against time are shown in Figures 5.2 to 5.7. Effective bulk modulus, Ke, is calculated using equation 2.1. Note that εv in eqn. 2.1 refers to the total volumetric strain, so Ke is akin to the secant modulus, except that the stress does not change. Also note that the initial value of Ke is equivalent to the elastic bulk modulus. The elastic bulk modulus was determined from the quick-step tests and was used as the starting point for the Ke curves. That is, the initial elastic compression was calculated using a bulk modulus of 1.02 Gpa, and the creep volume strain for each test added to it to determine the total volumetric strain. The need for this approach arose from difficulties in determining initial elastic compression in the single stage tests. See Sections 4.2.3 and 5.2.1 for a further discussion of initial elastic compression. Table 5.2 is a summary of the effective bulk modulus data, including the asymptotic value of Ke. Figure 5.8 shows a summary of the plots of Ke for the purpose of comparison. Equations were fitted to the curves of Ke versus time in Figures 5.2 to 5.7, and are included for reference on the Figures themselves.

5.2.3 Density and Pressure Effects on Creep Volumetric Strain

One method of analyzing the effect of density on volumetric creep deformation is to examine the amount of time required to attain a certain volumetric strain level for different specimens. This approach is illustrated in Figures 5.9 to 5.11, for strains of 0.6%, 0.75%, and 0.85% respectively. The figures illustrate that in general the higher density specimens take a longer time to reach a given volumetric creep strain. The effect is more pronounced at higher strain levels. Figure 5.12 shows the time taken to reach a volumetric strain of 0.75% as a function of test pressure. The figure shows that the time required to reach $\varepsilon v = 0.75\%$ is not dependent on test pressure. T9IC is not included in this analysis because of it's unique stress history. See Section 6.2 for a further discussion of how specimen stress history affects test results.

5.3 ANALYSIS OF CONSTANT MEAN STRESS SHEAR TEST RESULTS

Constant mean normal stress triaxial tests were performed on the ice specimens after they had been isotropically compressed. Six shear tests were performed at mean stresses of 2.5, 2.5, 2.0, 1.5, and 1.0 Mpa, with one unconfined compression test. The deviator stress was kept constant at 0.8 Mpa for all tests. The multi-step test had five steps, with a mean normal stress of 2.5 Mpa, and deviator stresses of 0.80, 1.20, 1.60, 2.0, and 2.4 Mpa. Constant mean stress shear tests were performed in order to determine the effective shear modulus and the effective strain ratio of the ice.

5.3.1 Shear Modulus

As discussed in Section 2.3, some distinction must be made between elastic shear modulus, G, and effective shear modulus, Ge. The elastic shear modulus represents the behaviour of the ice at the instant of loading, while the effective shear modulus function represents the shear behaviour of the ice as it changes with time. These properties are discussed separately here.

5.3.1.1 Elastic Shear Modulus

The elastic shear modulus is a measure of the shear properties of a material and is determined at the instant of loading. The present analysis used equation 2.3 to determine G for the test specimens. Table 5.3 lists the values of G determined for each of the six shear tests performed. These values are the initial values for the Ge curves. The relationship between specimen density and elastic shear modulus is illustrated in Figure 5.21.

5.3.1.2 Effective Shear Modulus

Equation 2.3 was used to determine the effective shear modulus. The values of $\varepsilon 1$ and $\varepsilon 3$ used reflect the total strain, and not incremental values. The effective shear modulus is therefore akin to the secant modulus, except that the deviator stress does not change. Ge is plotted against axial strain for all shear tests in Figures 5.13 to 5.18. A summary of these figures is presented in Figure 5.19. Figure 5.20 shows effective shear modulus plotted against time for all six shear tests. Note the near perfect repetition of curves in Figures 5.19 and 5.20. Table 5.4 shows the value of Ge at 5% axial strain for each test. Note that Ge is equal to .005 Gpa for all tests at 5% axial strain. Equations for Ge against time and Ge against axial strain were calculated and are included on the summary Figures themselves (Figures 5.19 and 5.20). The fit is good for the Ge-time curves, and is very good for the Ge-axial strain curves.

5.3.2 Strain Ratio

As with shear modulus, strain ratio varies depending on whether the elastic or plastic deformation is being considered. Elastic strains are considered to dominate at the instant of loading, while plastic straining is the dominant mechanism under constant load as time progresses. The term Poisson's ratio is used to refer to the strain ratio (as determined by equation 2.5) for elastic behaviour and the term strain ratio is used for plastic behaviour.

5.3.2.1 Poisson's Ratio

Table 5.3 lists the values of Poisson's ratio calculated for each shear test in the present study. These values were calculated by taking the average of the first three readings, taken within approximately 10 seconds of the application of axial load. Note that in general Poisson's ratio decreases with increasing mean stress but the change is not large. Figure 5.22 shows the variation of μ with confining stress (i.e. cell pressure, as opposed to mean stress).

5.3.2.2 Strain Ratio

The effective strain ratio, μe, is plotted against axial strain in Figures 5.23 to 5.28 for each of the six shear tests. These curves are summarized in Figure 5.29 for comparison. Plotting μe against axial strain gives a better picture of specimen behaviour in the early stages of the test than when time is used as the independent variable. The asymptotic values of μe are listed in Table 5.4. The instantaneous strain ratio, μi, is plotted against axial strain in Figures 5.30 to 5.35 for each of the six shear tests (see section 2.4.1 for a description of the difference between μe and μi). The plots of μe and μi are quite similar, except that μi seems to vary in a systematic way before 1% axial strain is reached. Figures 5.30 to 5.35 show that μi dips slightly after the application of the deviator stress, and then rises again. In some cases, this pattern is repeated a second time. Note that the change in strain ratio is relatively small (±.04). Best-fit equations were calculated for μe versus time and μe versus axial strain. The average of the best-fit equations for μe versus axial strain and μe versus time are listed on Figure 5.29. The equations provide a poor fit. For the purposes of modelling ice behaviour, a more accurate approach would be to assume $\mu e = 0.5$ after 25 hours or 1 % axial strain. Before 25 hours or 1% axial strain, it would be best to use the experimental data from the present study as a basis for determining μe.

5.3.3 Multi-Step Test

A multi-step constant mean normal stress shear test was performed on specimen T9. The results of the test are shown in Figures 5.36 to 5.39. Figure 5.36 shows Ge against time, and 5.37 shows Ge against axial strain. μe is plotted against time and axial strain in Figures 5.38 and 5.39 respectively. Table 5.5 summarizes the elastic and effective values of shear modulus and Poisson's ratio. The deviator stress was applied instantaneously for the all five steps, as in all single step tests.

Figures 5.37 and 5.39, both plotted against axial strain are more comprehensible than the figures which are plotted against time because the specimen deformed very quickly at the higher deviator stresses. Figure 5.37 indicates that the shear modulus behaviour of the individual steps of the multi-step test is similar to that of the single-step shear tests. The main difference between the curves is that Ge tends to be larger in the beginning of each step than in the beginning of the single stage tests. Ge in the multi-step tests soon decreases in a similar manner to the single stage tests. The behaviour of the effective strain ratio in the multi-step tests is similar to that of the single step tests as well. Again, the most significant differences occur in the beginning of the individual steps of the multi-step test. As shown in Figure 5.39, μ (Poisson's ratio) is quite large (> 0.6) for steps two and three. The results of the multi-step test are discussed further in Section 6.5.

Table 5.1

Elastic Bulk Modulus

From Quick-Step Isotropic Compression Tests

Test	Elastic Bulk Modulus (Gpa)
QSIC1	1.18
QSIC2	0.95
QSIC3	0.89
QSIC4	1.02
QSIC5	1.06

Average = 1.02 Gpa

Sample Standard Deviation = 0.11 Gpa

Table 5.2

Effective Bulk Modulus

Test	Pressure (Mpa)	Final Ke (Gpa) (Gpa)	Final εv (%)
TIC1	2.5	0.25	0.98
TIC9	2.5	0.21	1.19
TIC2	2.0	0.18	1.09
TIC6	2.0	0.18	1.12
TIC5	1.5	0.14	1.01
TIC4	1.0	0.08	1.23

TABLE 5.3

Summary of Elastic Shear Properties

Test	Mean Stress (Mpa)	G (Gpa)	μ
T9S	2.5	0.08	.503
T7S	2.5	0.13	.483
T6S	2.0	0.18	.490
T5S	1.5	0.19	.532
T4S	1.0	0.22	.562
T8UC	0.3	0.12	.527

Table 5.4

Summary of Effective Shear Properties

At 5% Axial Strain

Test	Mean Stress (Mpa)	Ge (Gpa)	μ_e
T9S	2.5	0.005	.490
T7S	2.5	0.005	.489
T6S	2.0	0.005	.491
T5S	1.5	0.005	.481
T4S	1.0	0.005	.465
T8UC	-	0.005	.497

Table 5.5

Summary of Multi-Step Shear Test

Mechanical Properties

Test T9MS   Mean Stress = 2.5 Mpa

Deviator Stress (Mpa)	G	μ	@ 2% Axial Strain Ge (Mpa)	μe
0.8	0.08	.50	0.013	.49
1.2	0.22	.64	0.006	.50
1.6	0.41	.68	0.005	.50
2.0	0.38	.58	0.006	.50
2.4	0.08	.52	0.006	.50

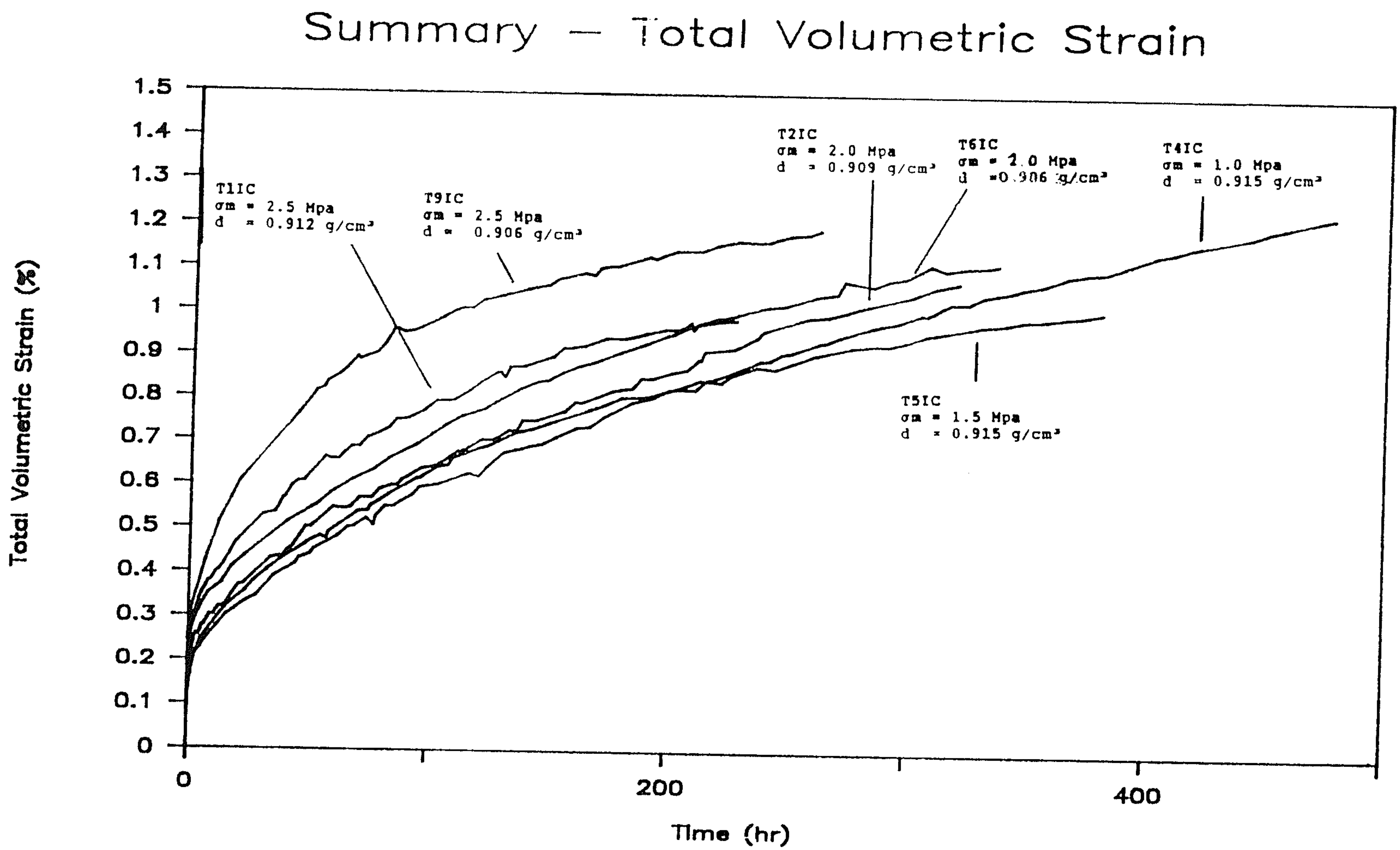

Figure 5.1 Summary of total volumetric strains of isotropic compression tests

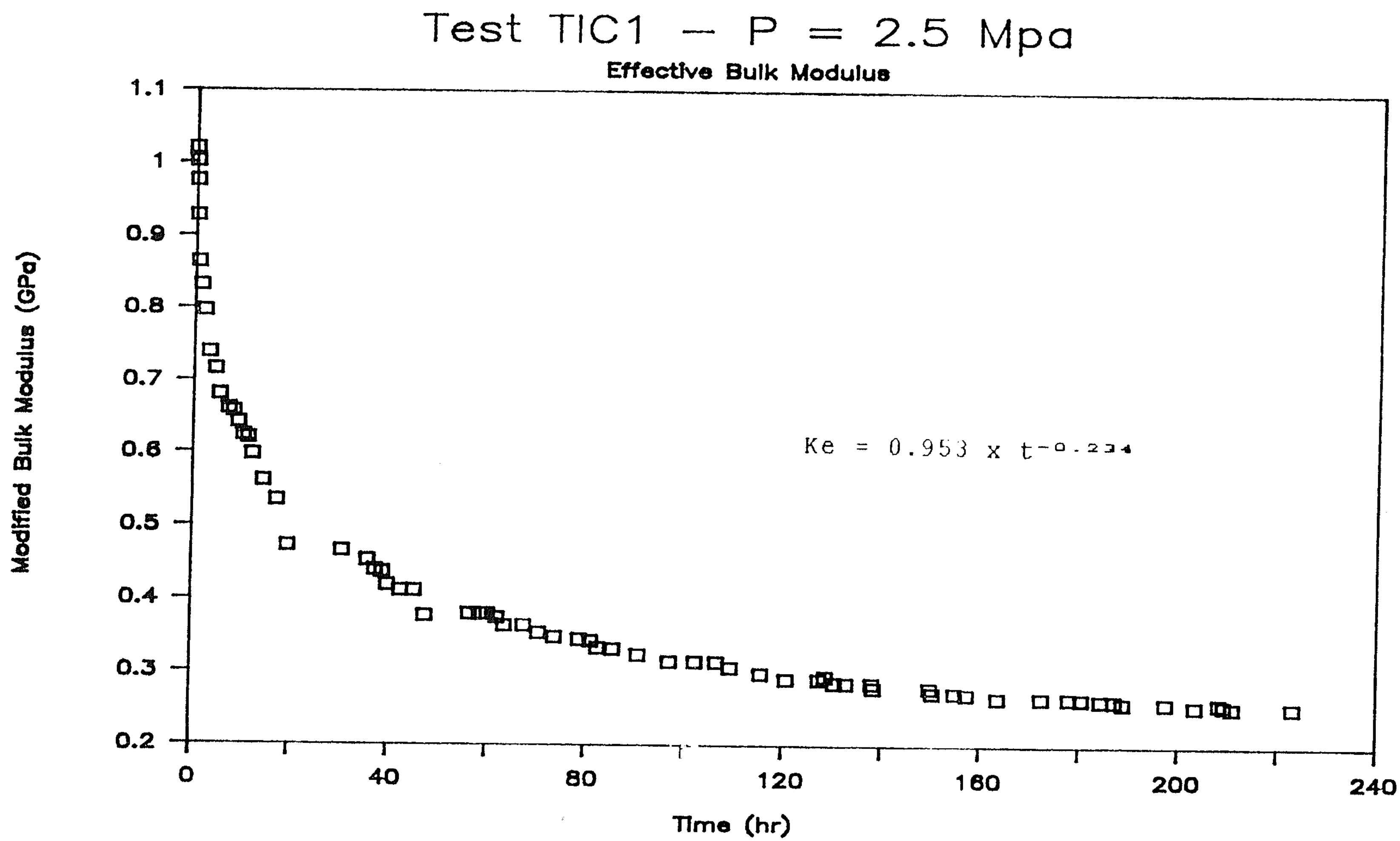

Figure 5.2 T1IC Effective bulk modulus

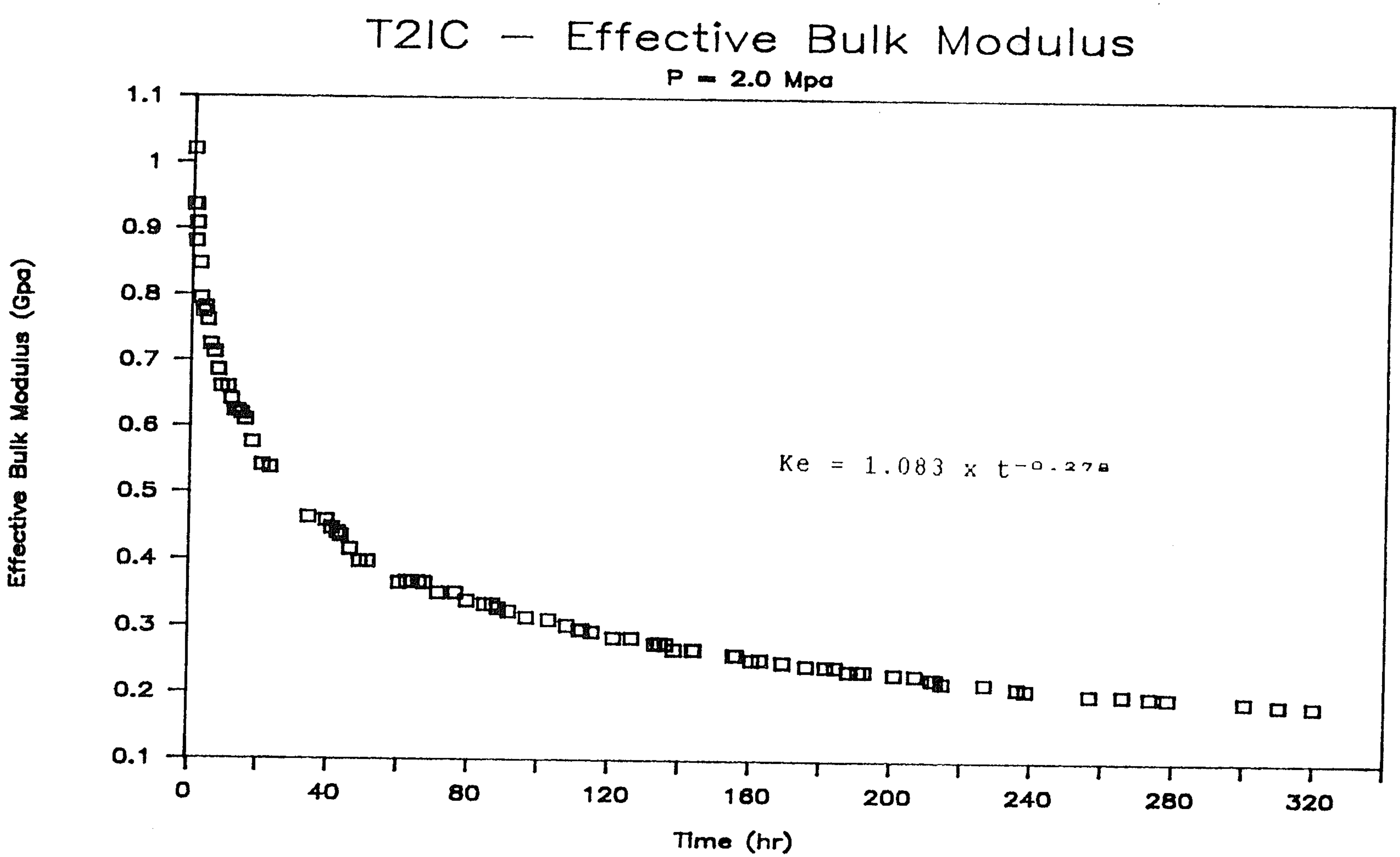

Figure 5.3 T2IC Effective bulk modulus

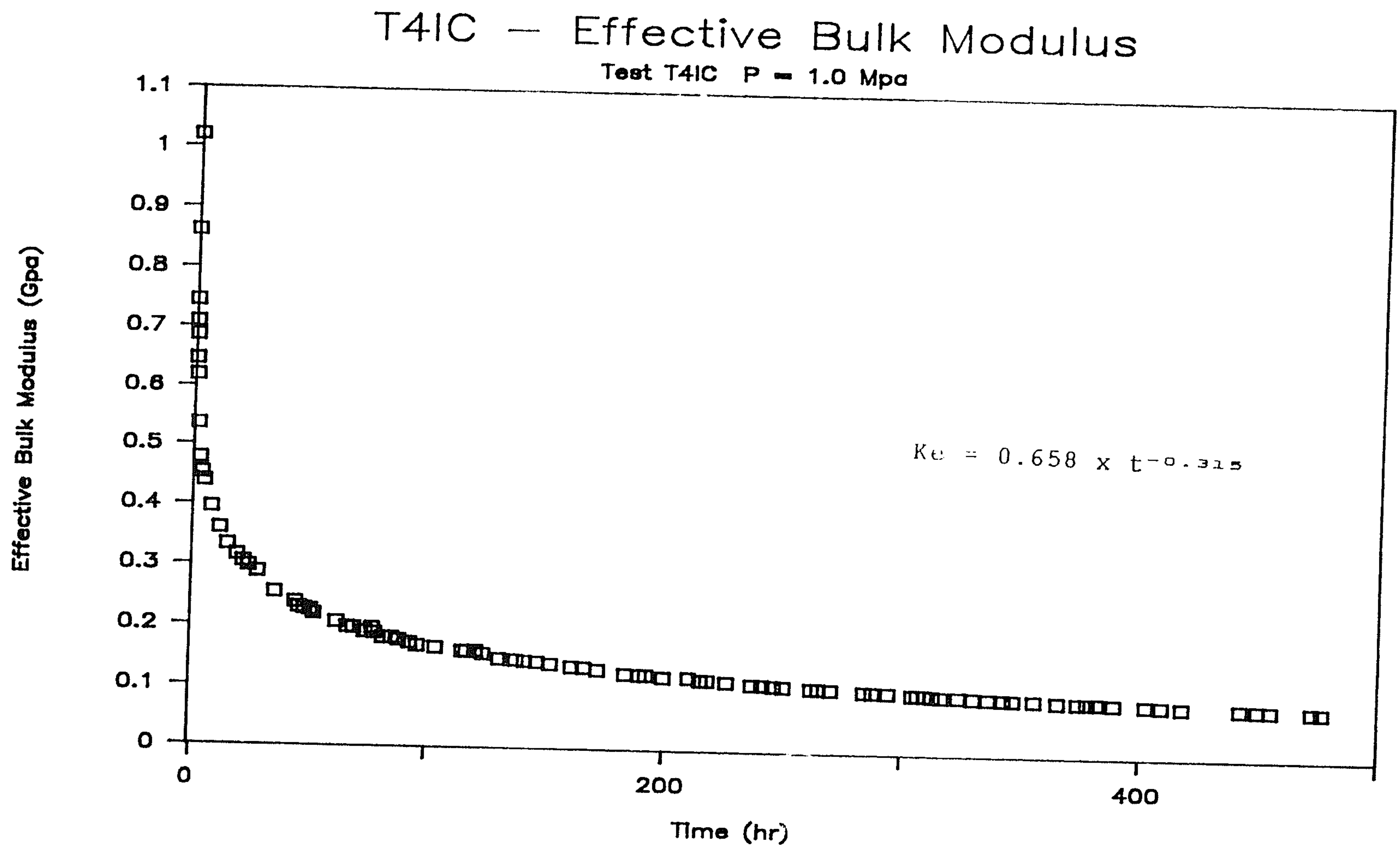

Figure 5.4 T4IC Effective bulk modulus

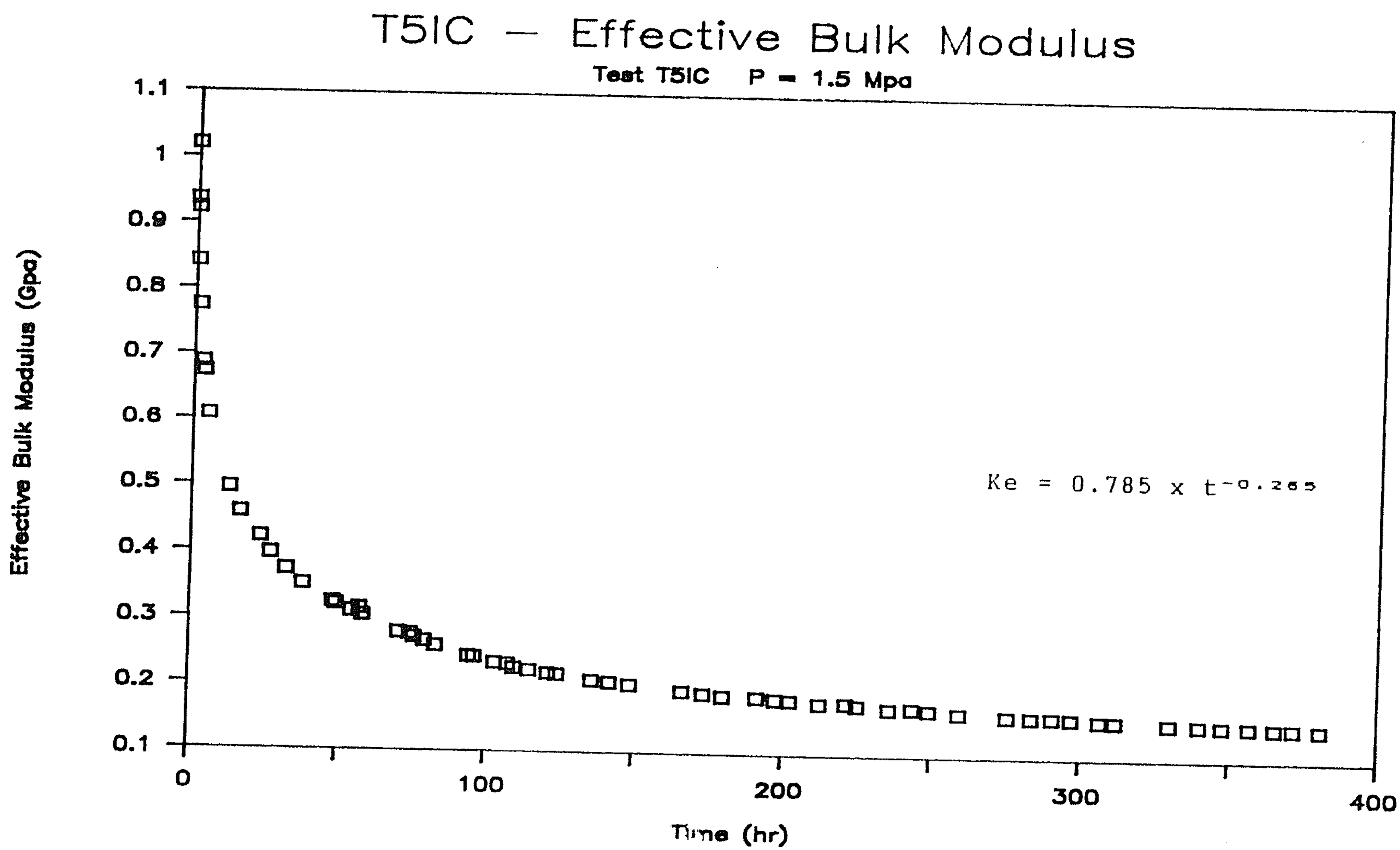

Figure 5.5 T5IC Effective bulk modulus

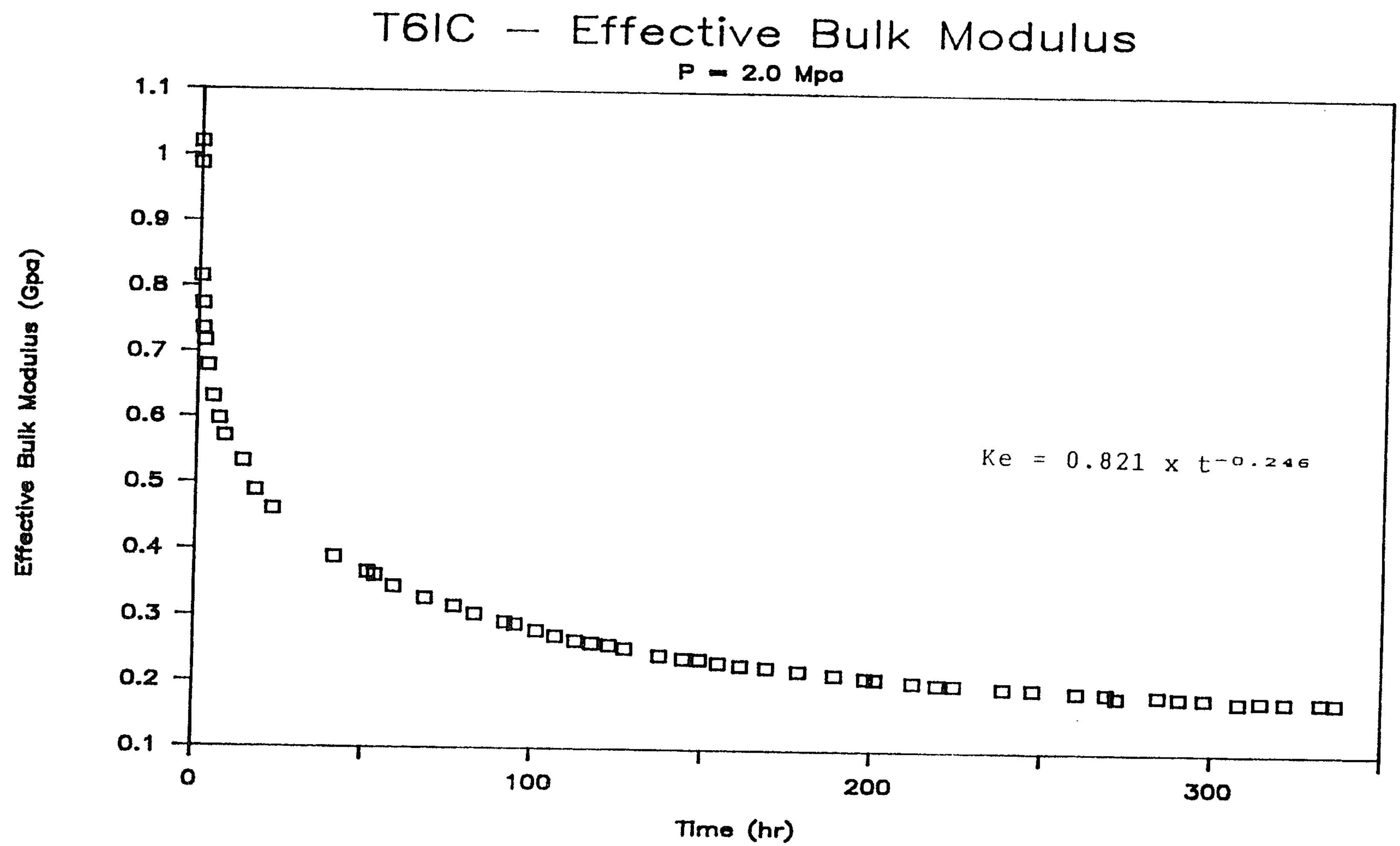

Figure 5.6 T6IC Effective bulk modulus

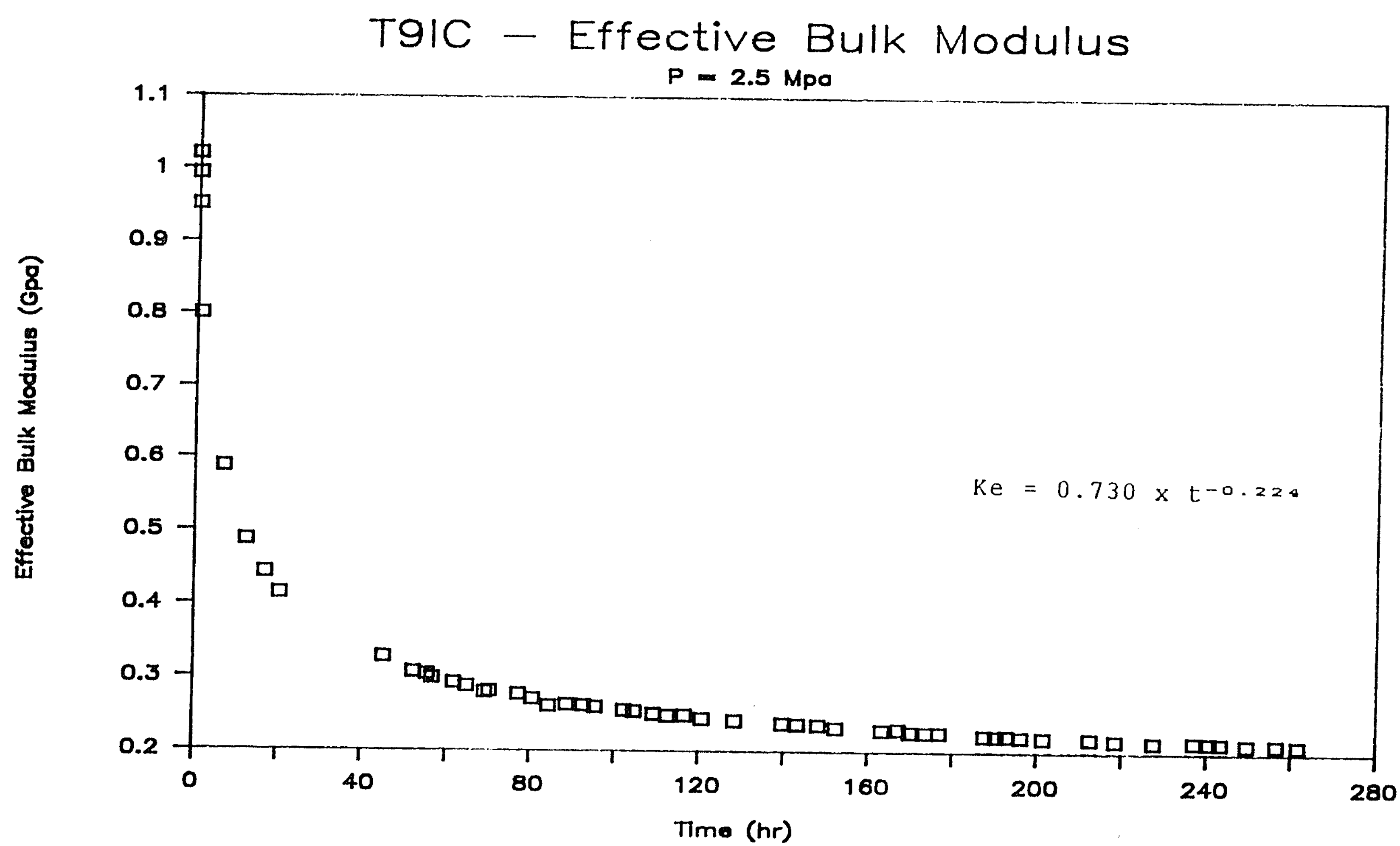

Figure 5.7 T9IC Effective bulk modulus

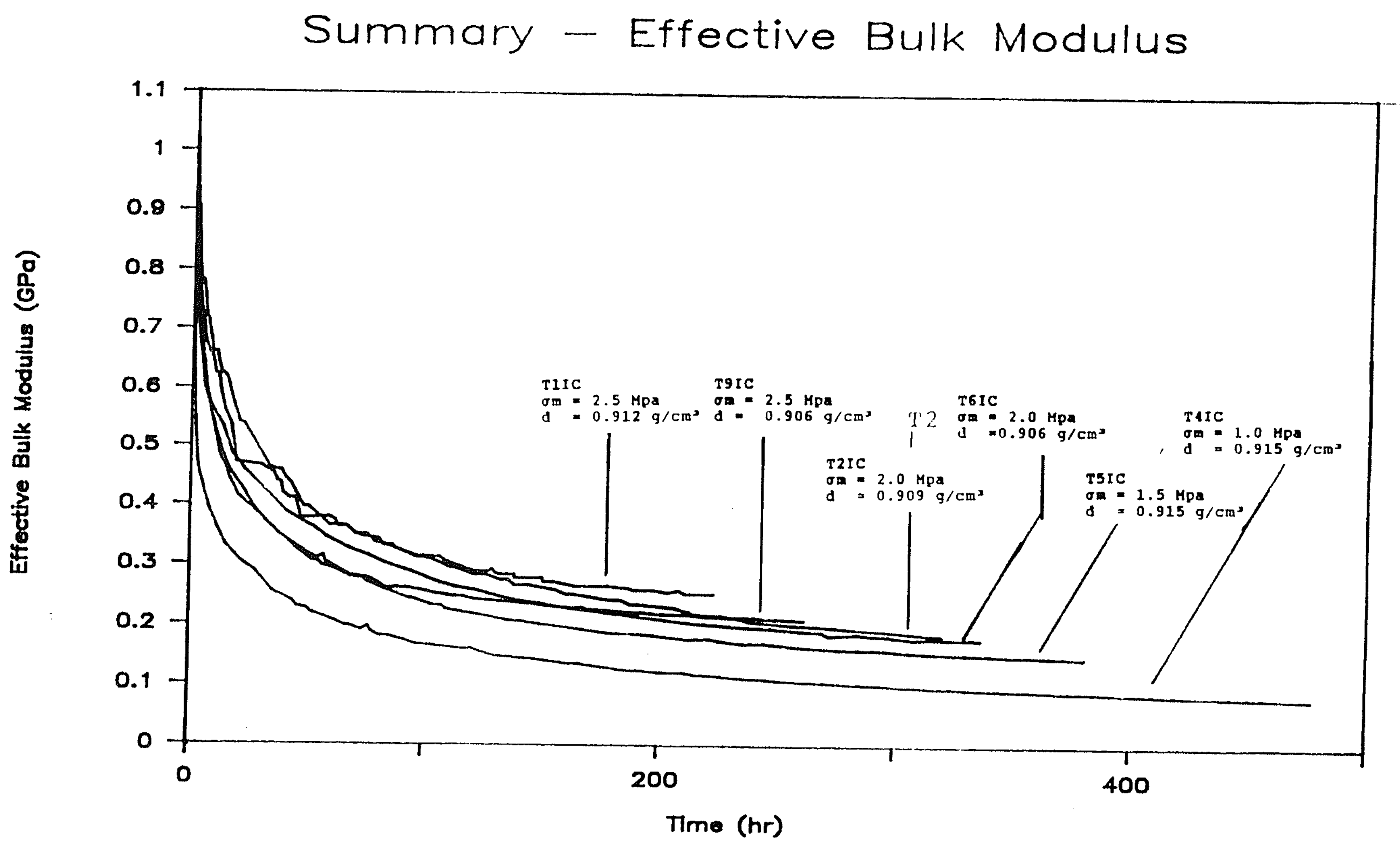

Figure 5.8 Summary of effective bulk modulus for isotropic compression tests

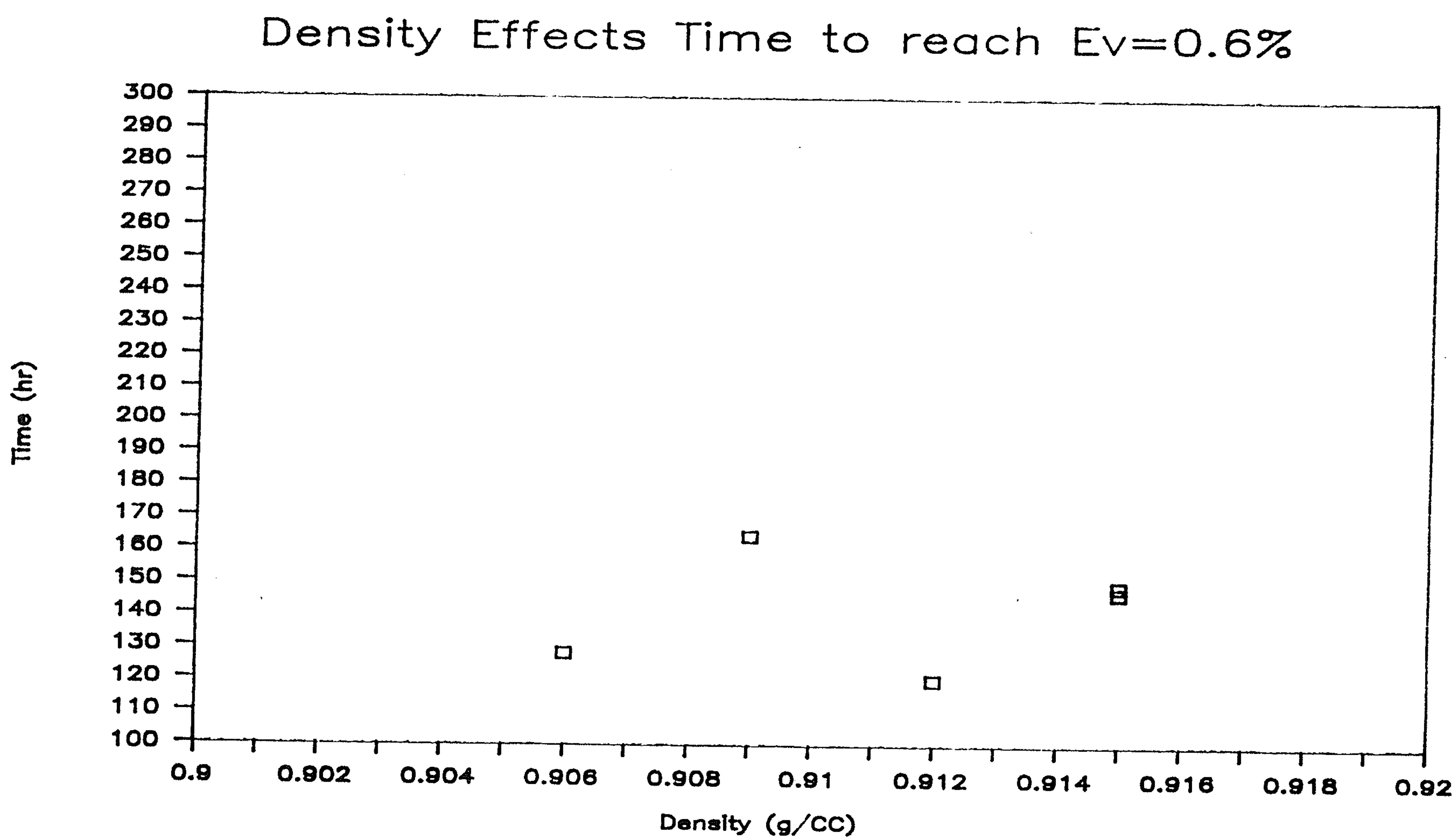

Figure 5.9 Time required to reach volumetric strain of 0.6% vs. density

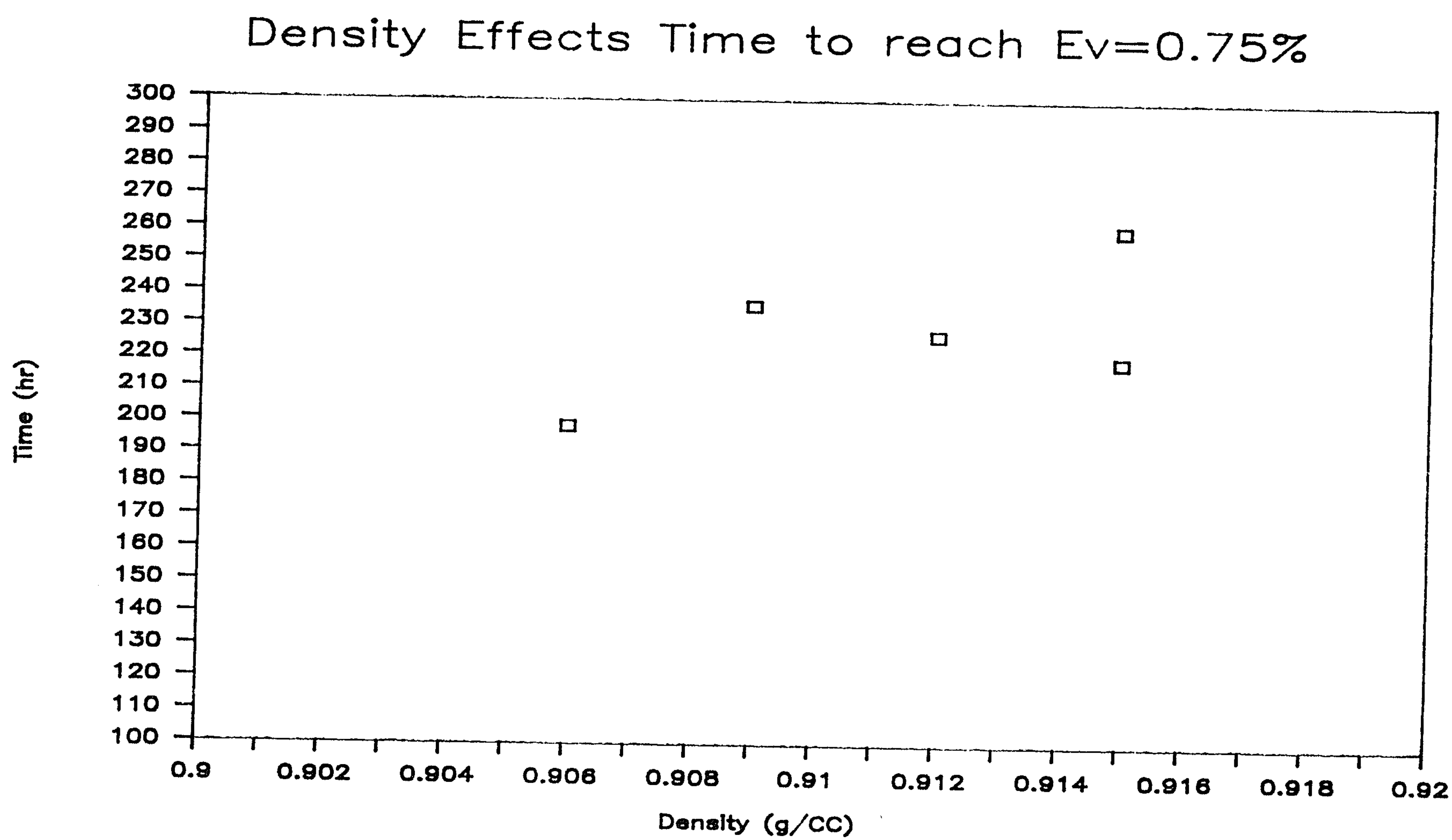

Figure 5.10 Time required to reach volumetric strain of 0.75% vs. density

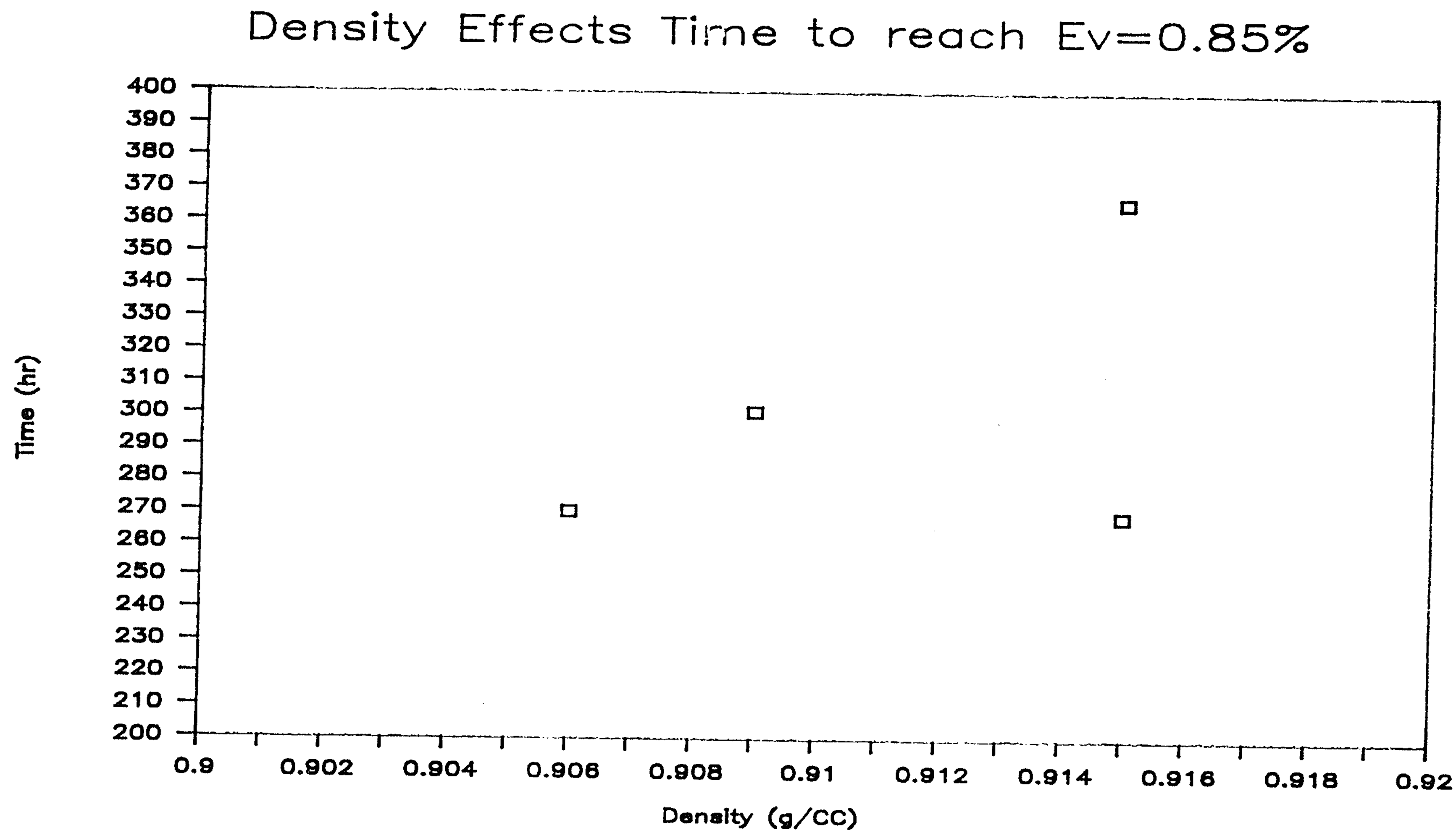

Figure 5.11 Time required to reach volumetric strain of 0.85% vs. density

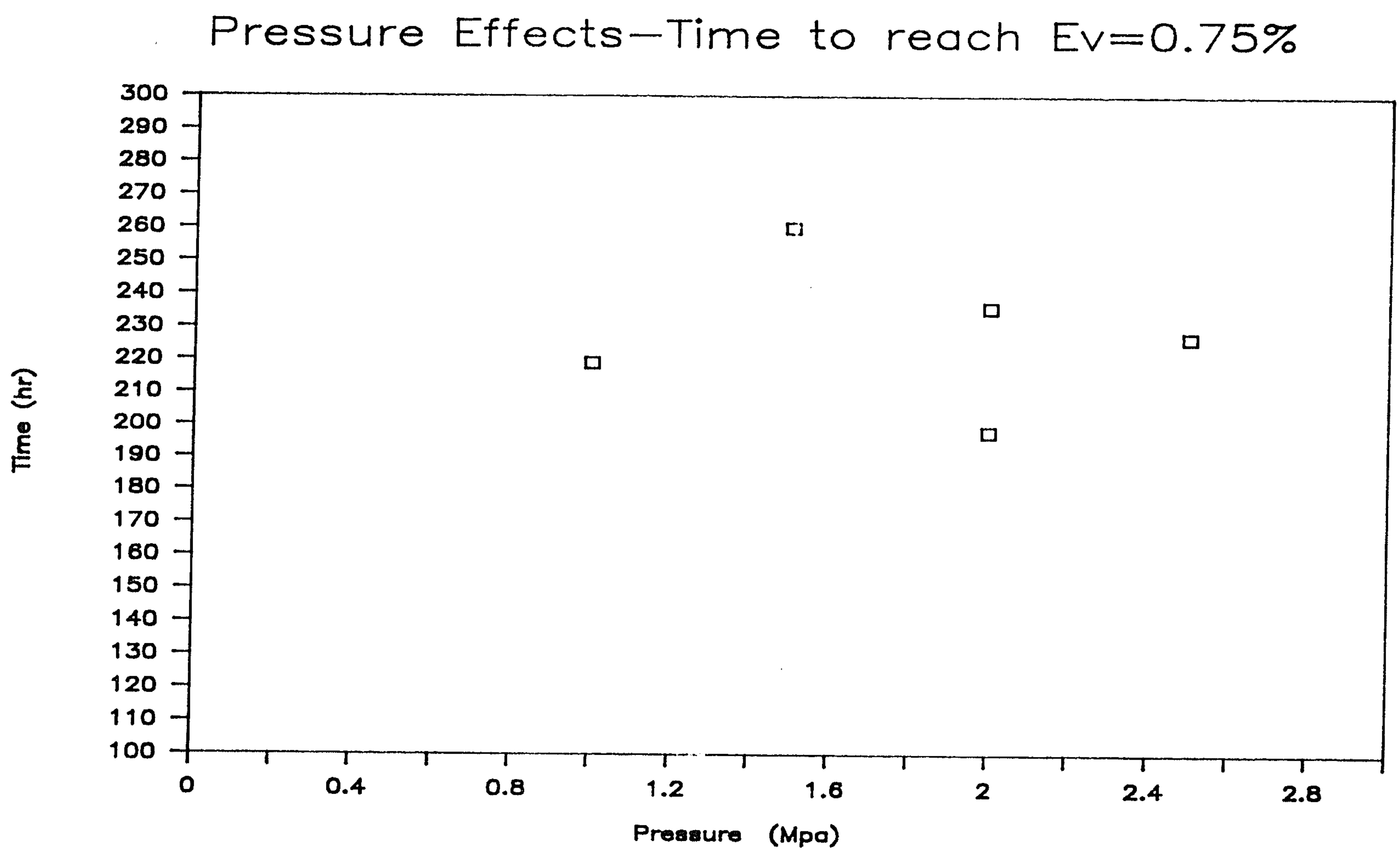

Figure 5.12 Time required to reach volumetric strain of 0.75% vs. test pressure

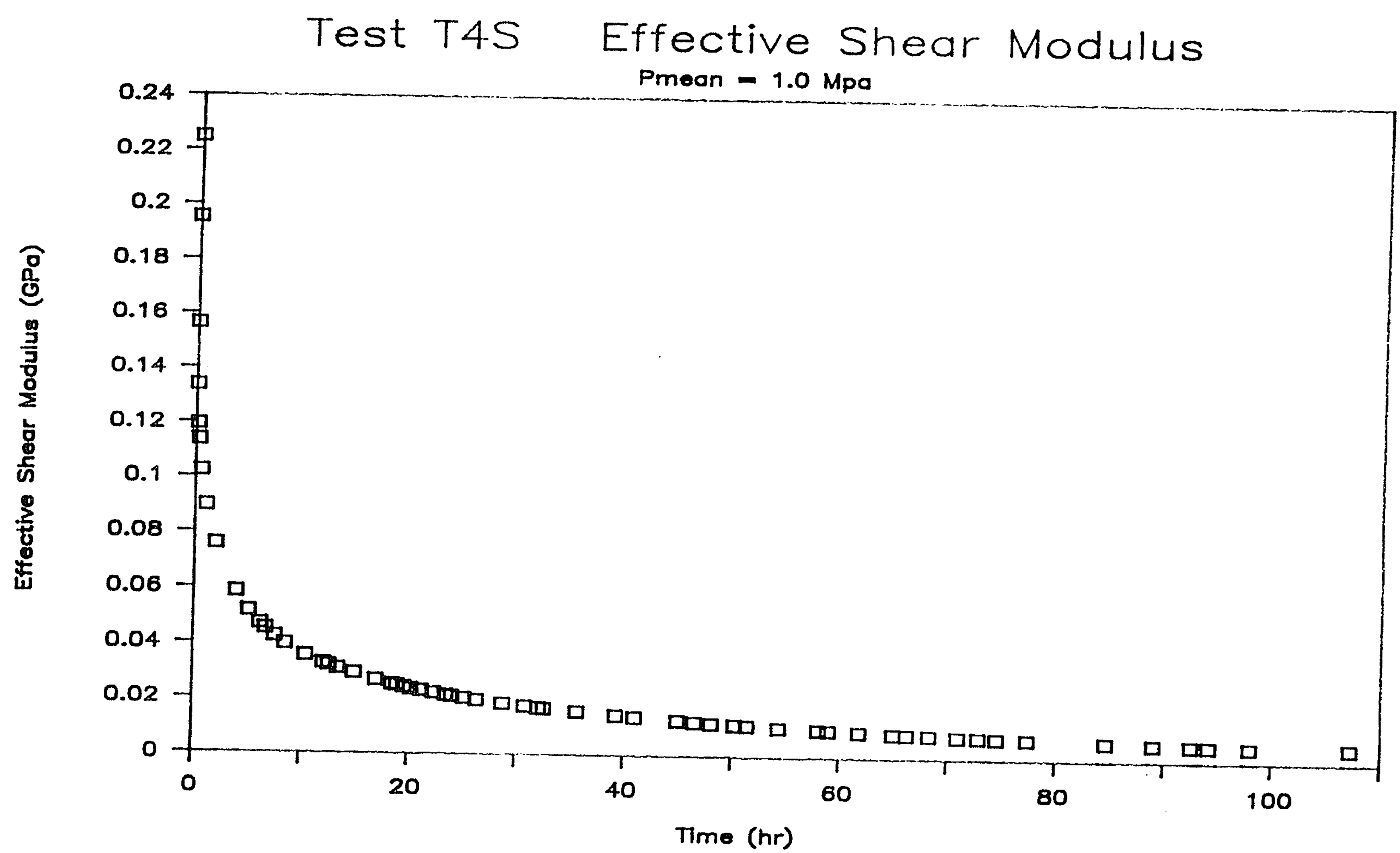

Figure 5.13 T4S Effective shear modulus

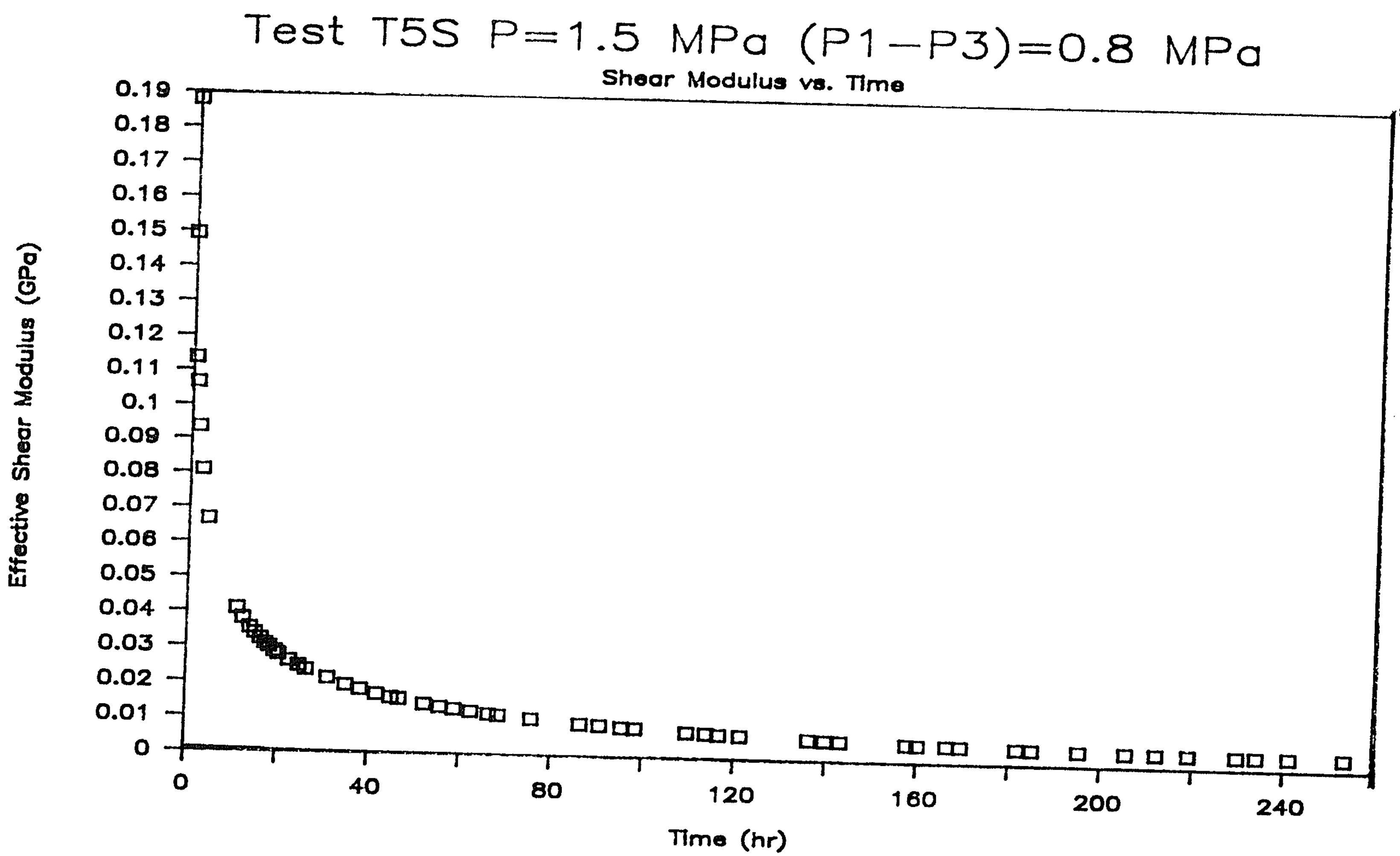

Figure 5.14 T5S Effective shear modulus

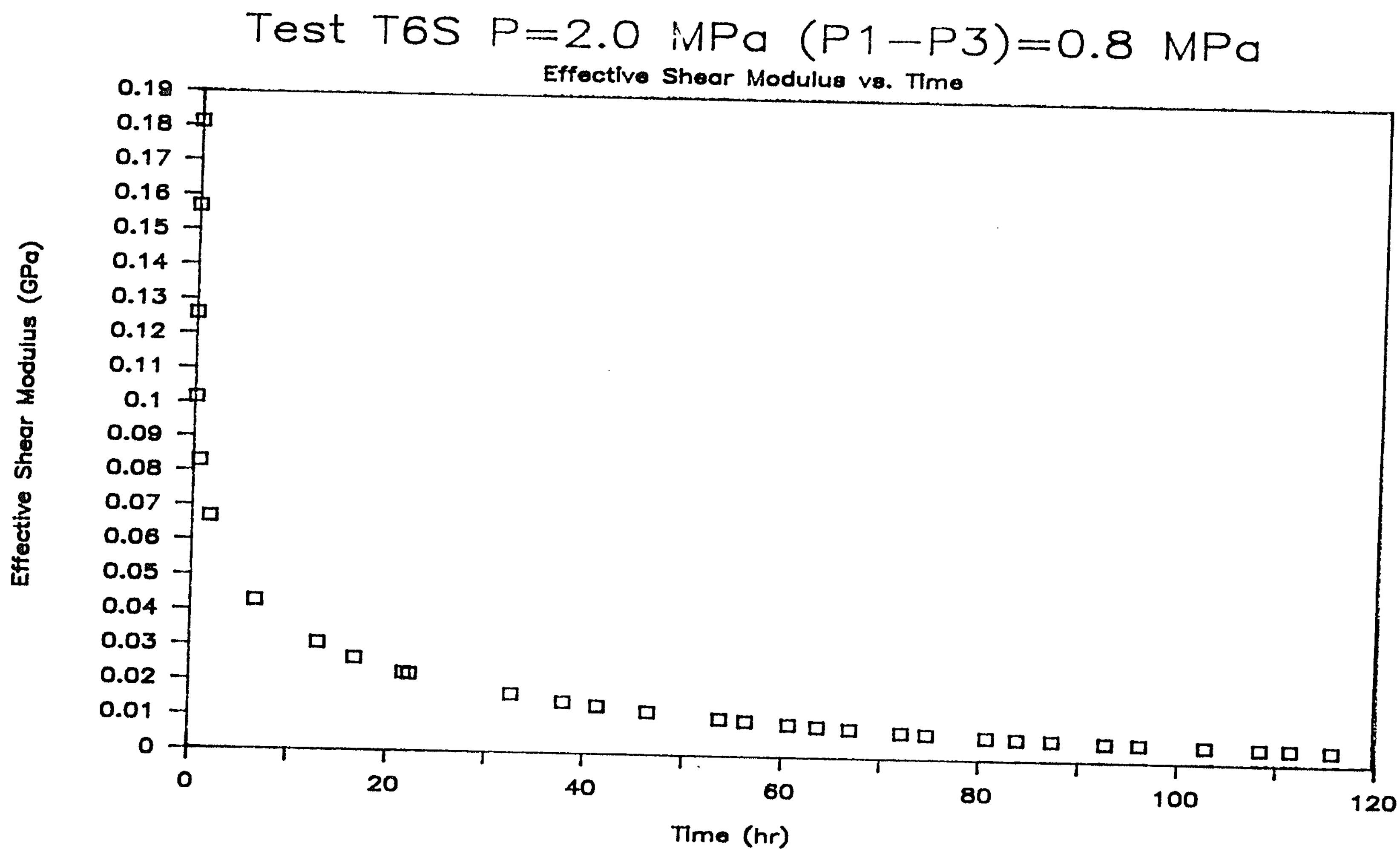

Figure 5.15 T6S Effective shear modulus

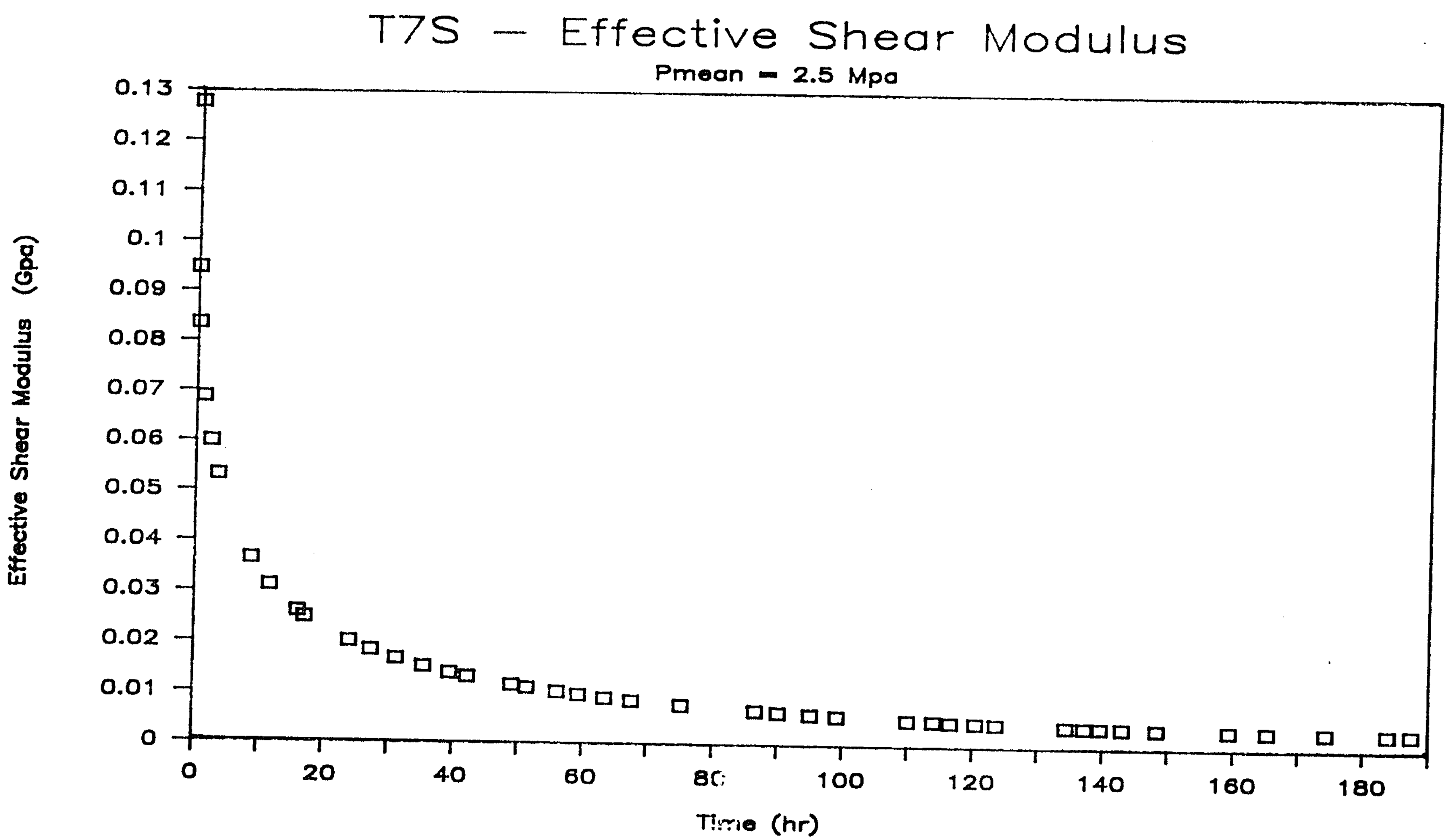

Figure 5.16 T7S Effective shear modulus

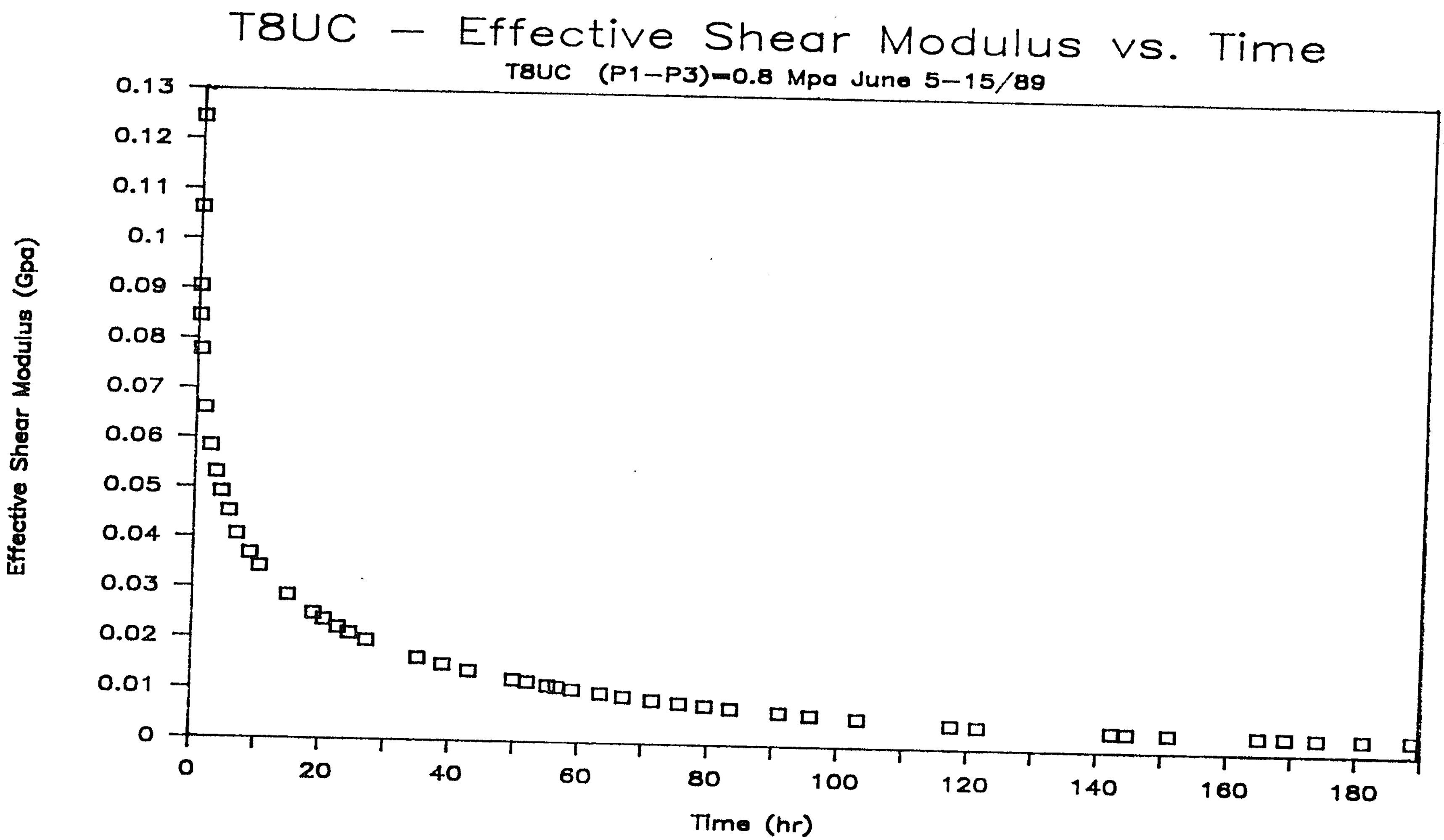

Figure 5.17 T8UC Effective shear modulus

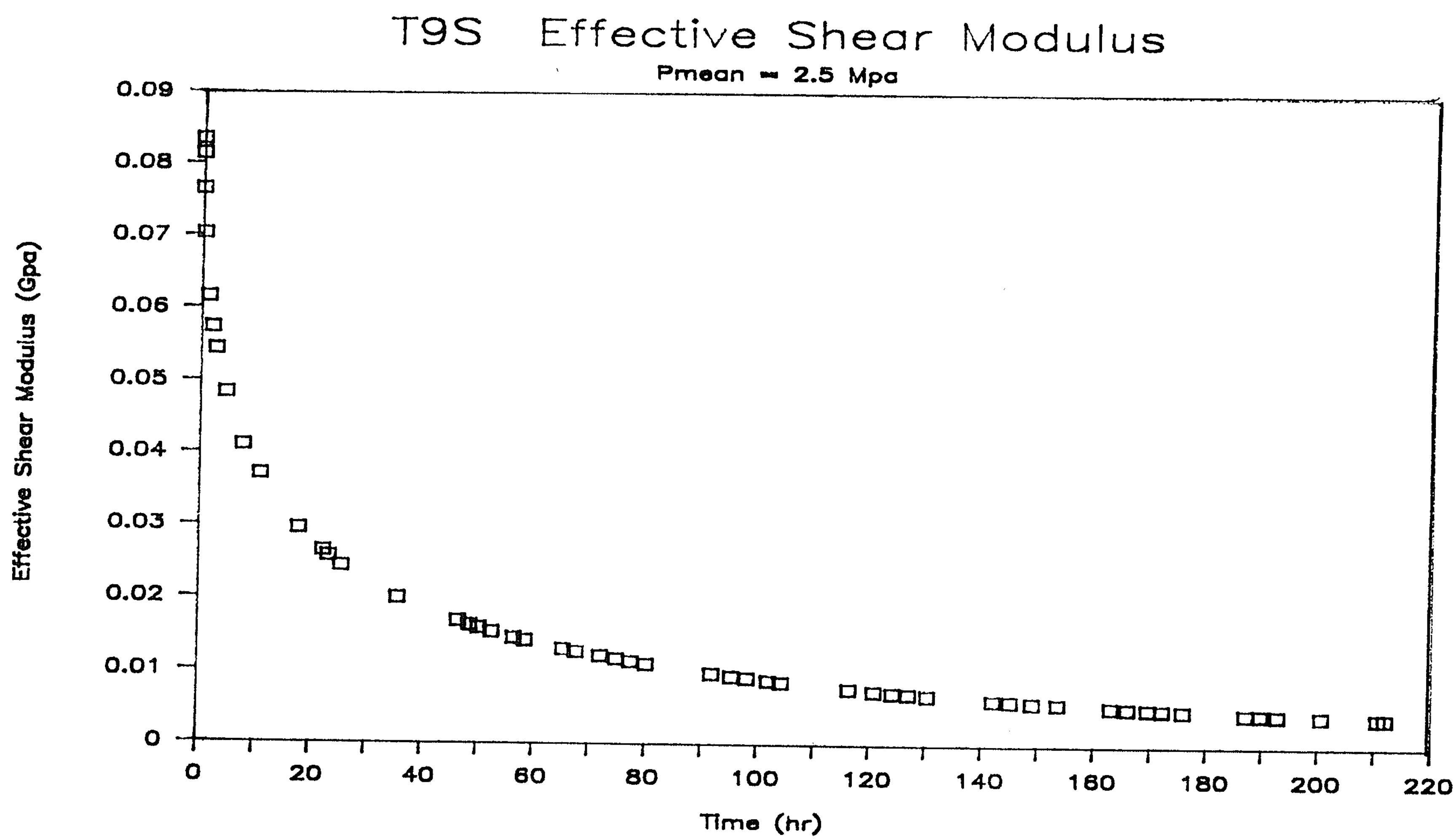

Figure 5.18 T9S Effective shear modulus

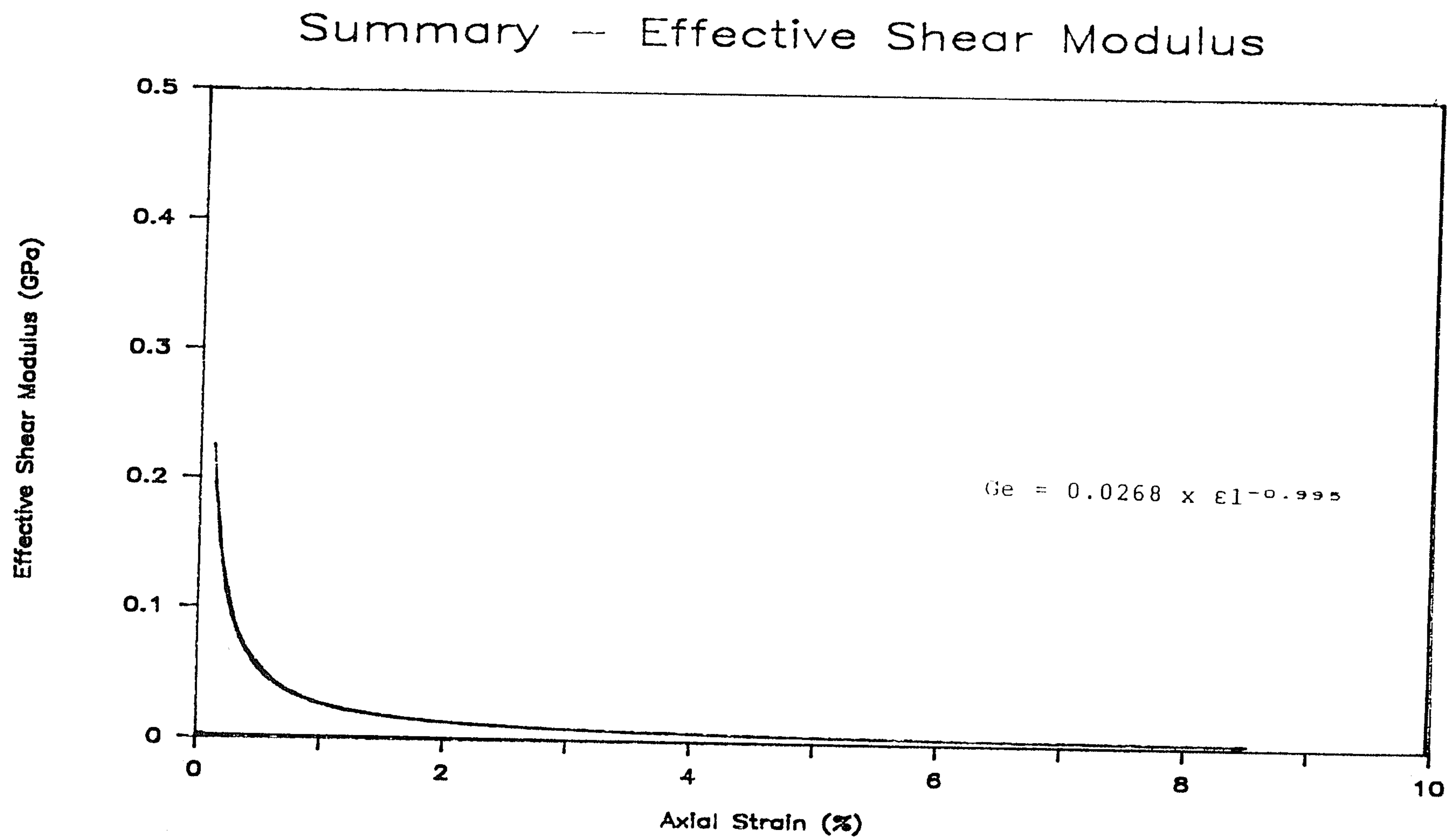

Figure 5.19 Summary of effective shear modulus data

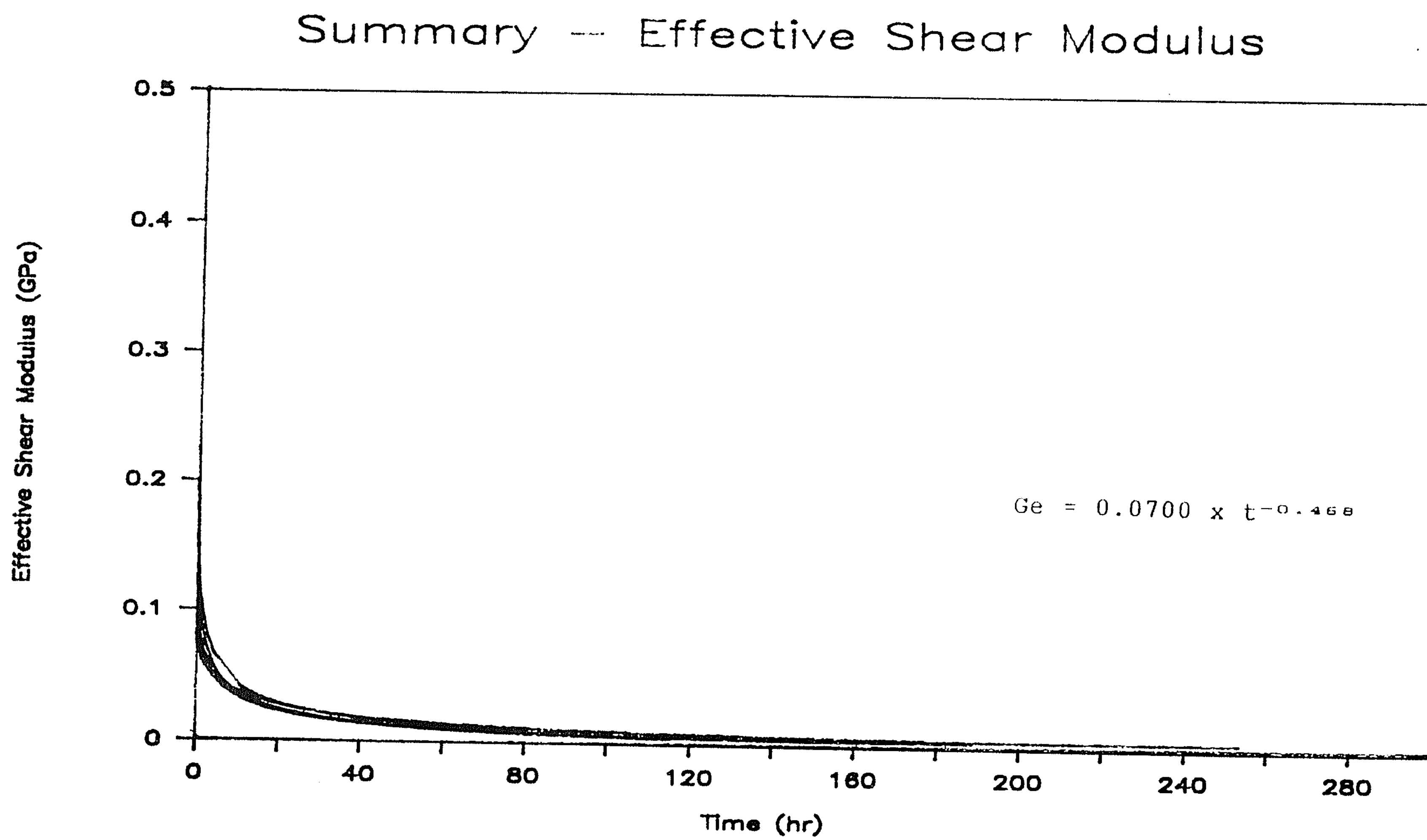

Figure 5.20 Summary of effective shear modulus data

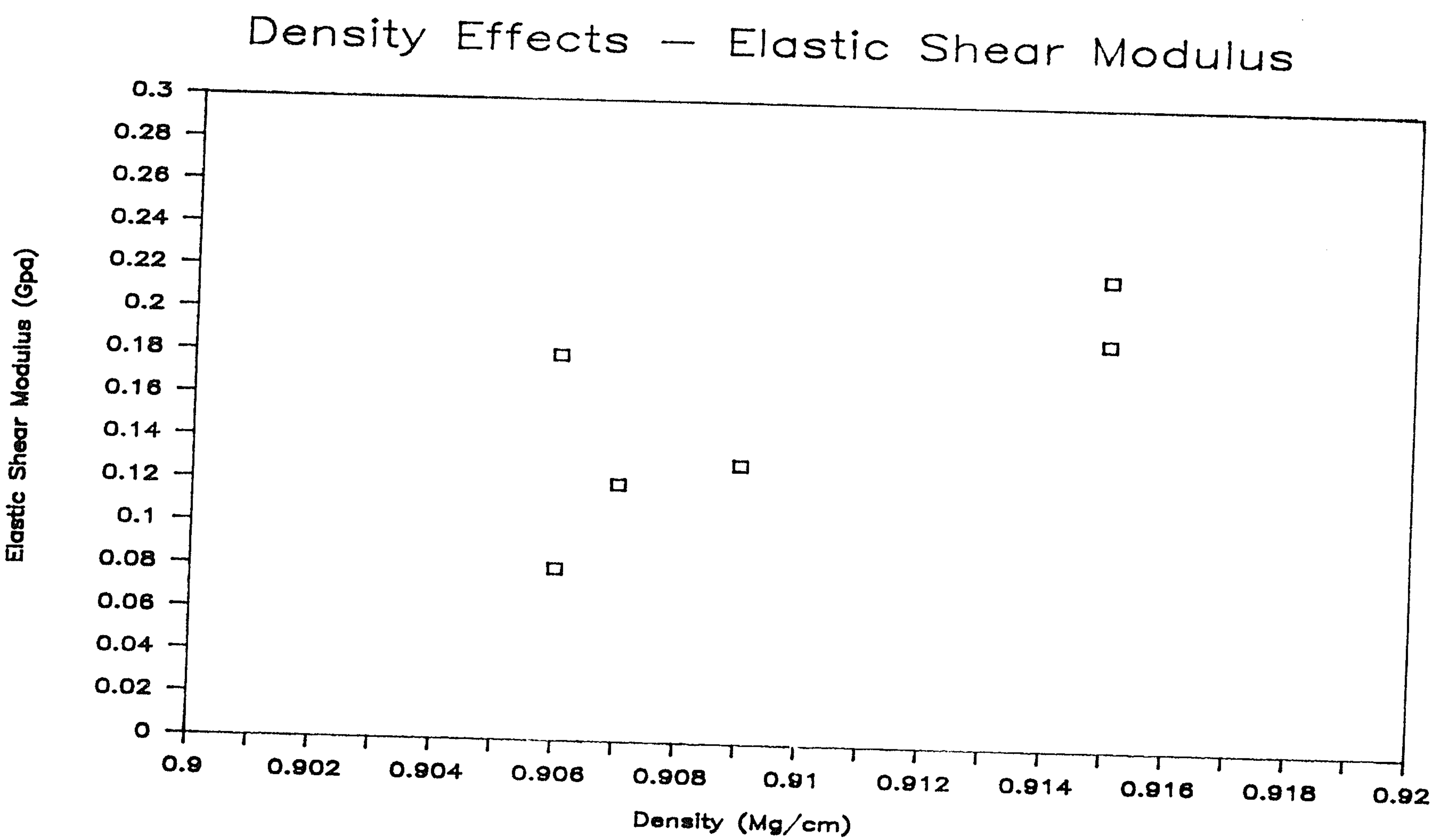

Figure 5.21 Elastic shear modulus versus density

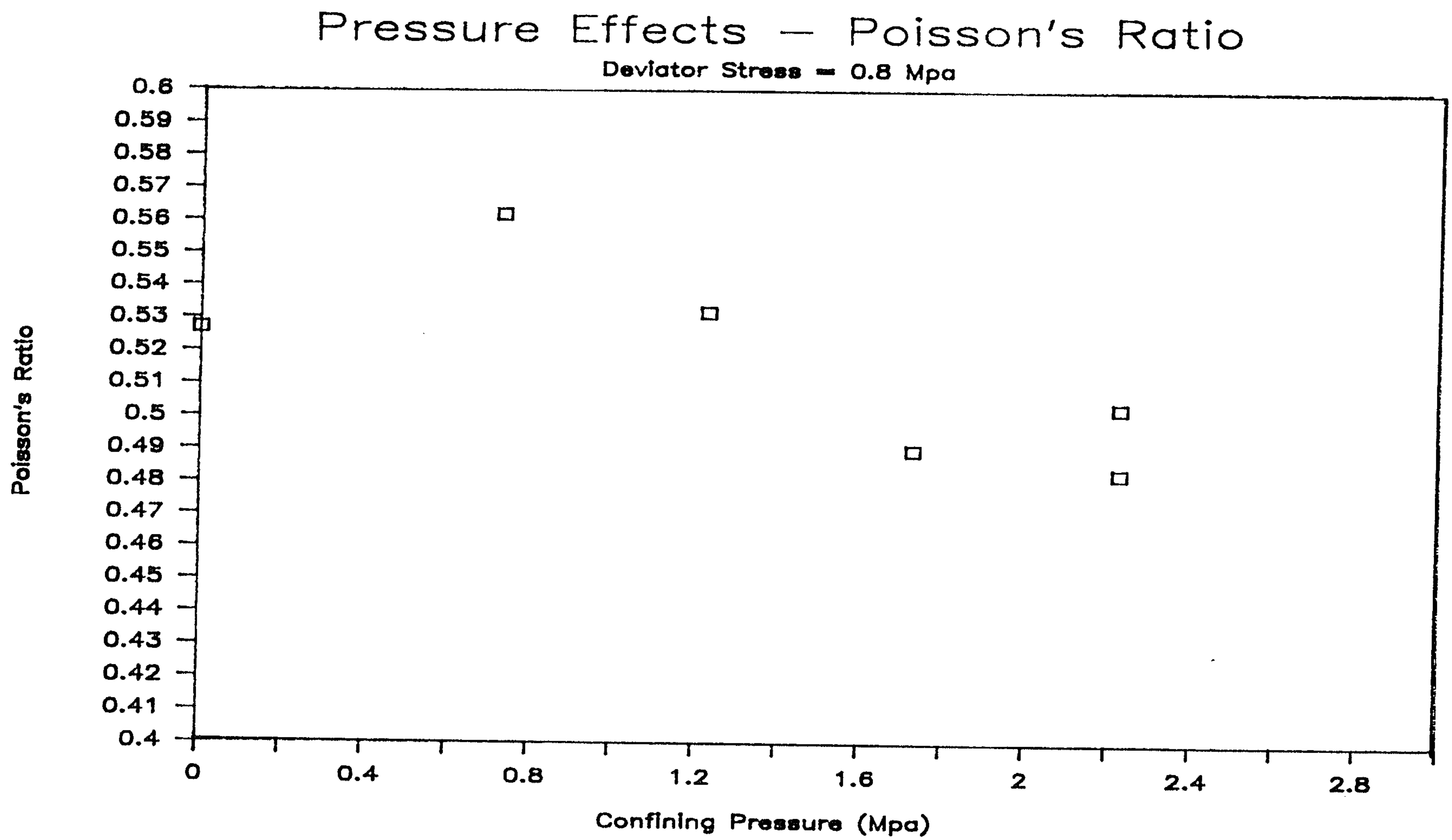

Figure 5.22 Poisson's ratio versus confining stress

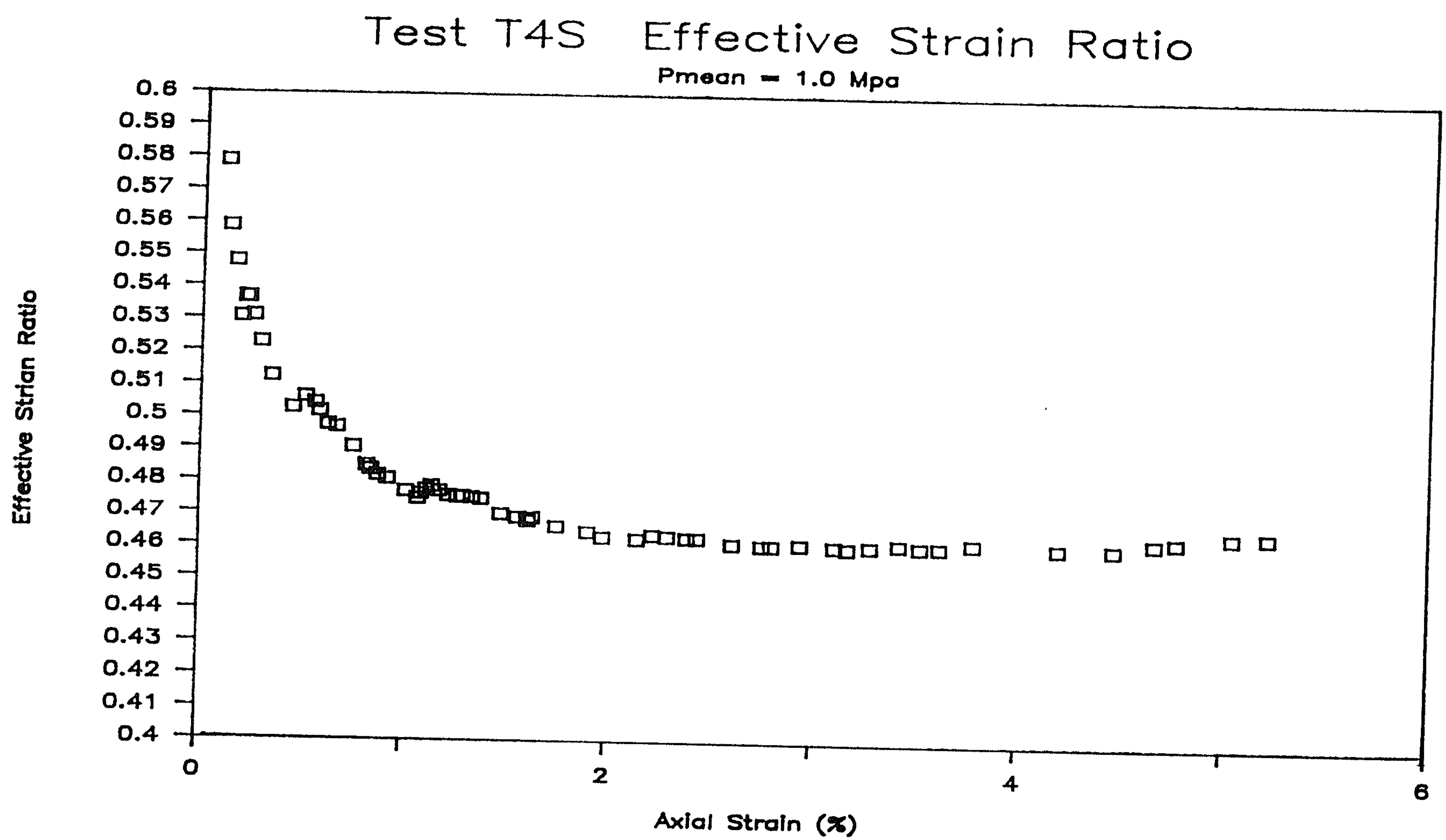

Figure 5.23 T4S Effective strain ratio

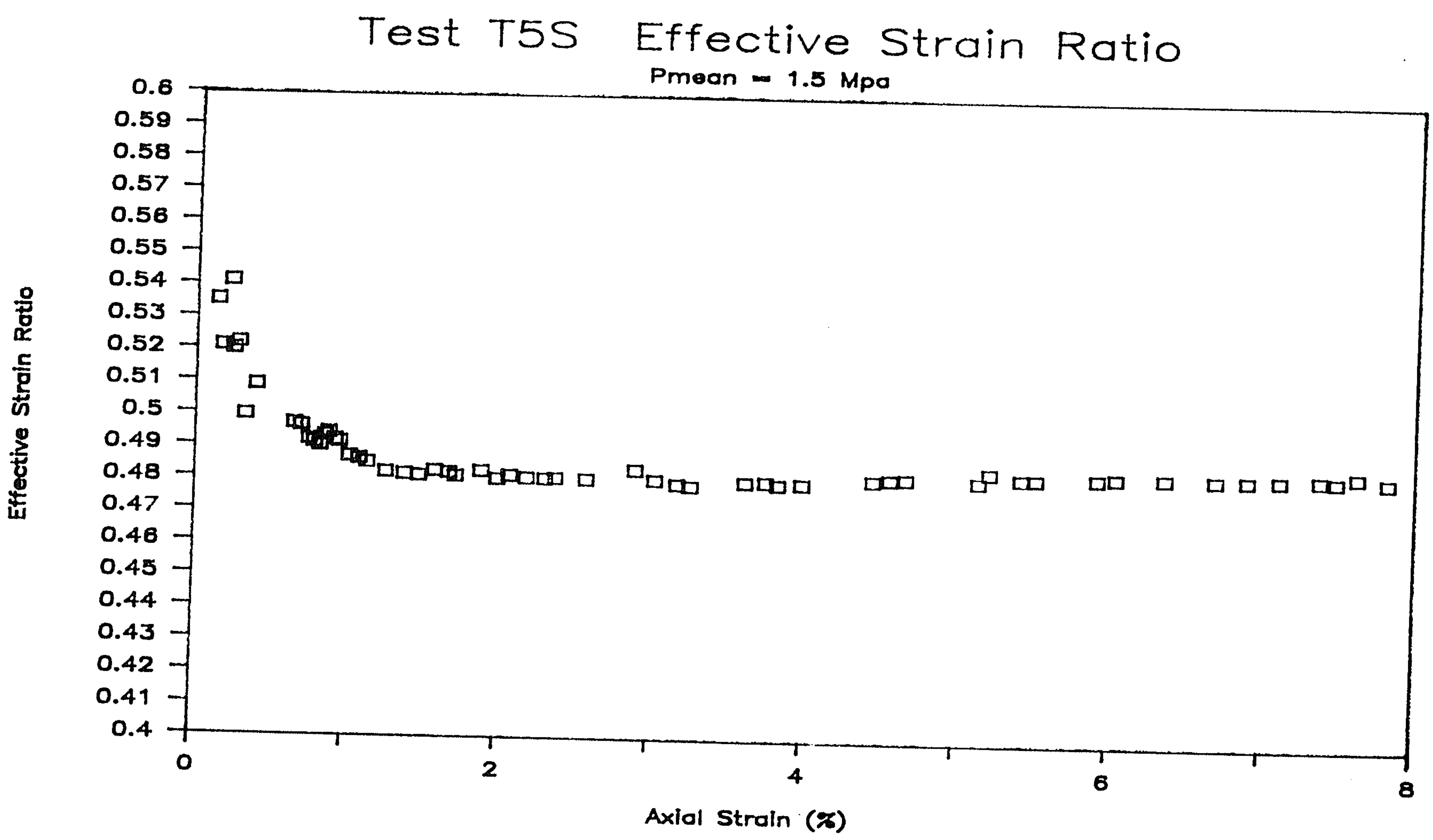

Figure 5.24 T5S Effective strain ratio

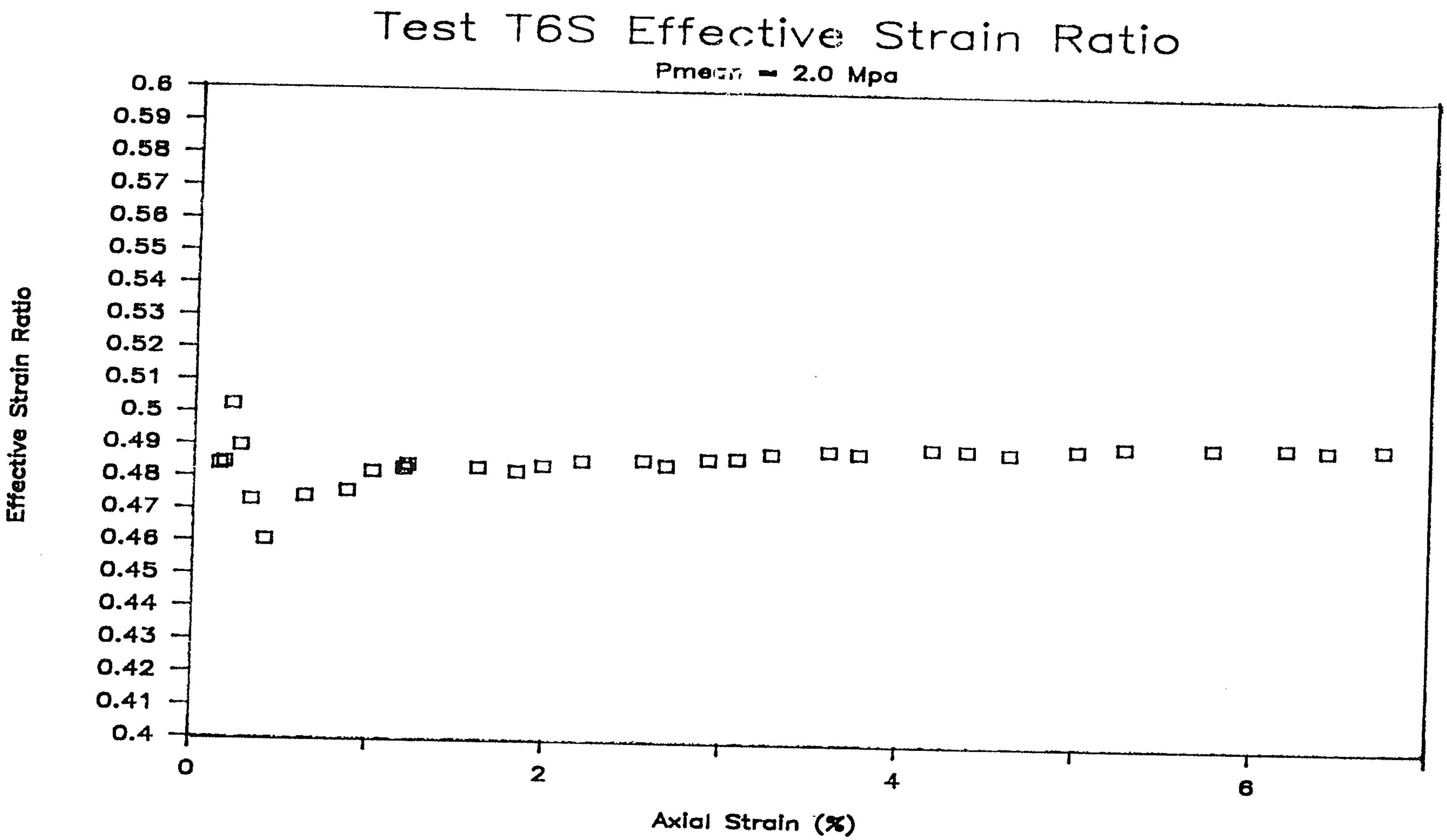

Figure 5.25 T6S Effective strain ratio

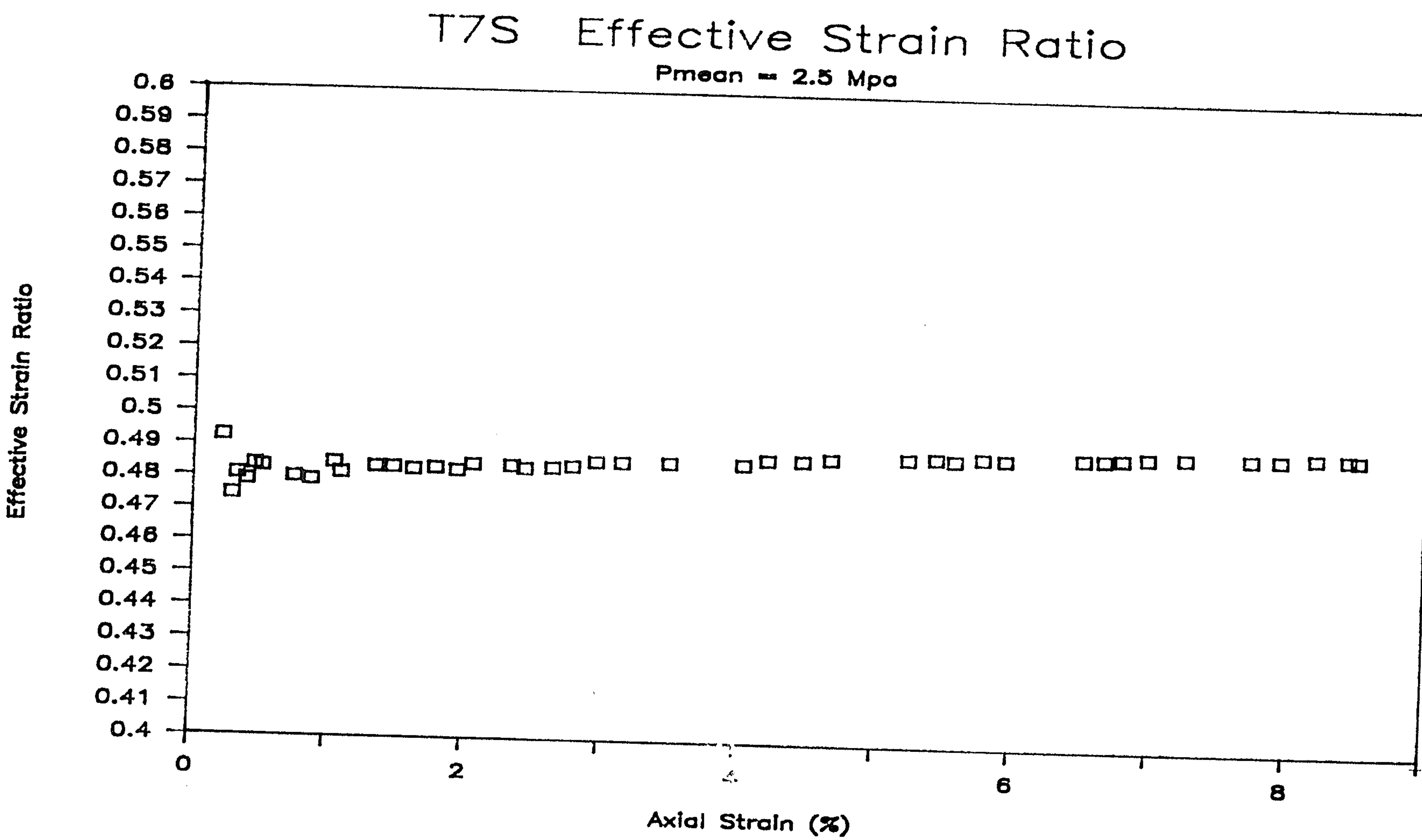

Figure 5.26 T7S Effective strain ratio

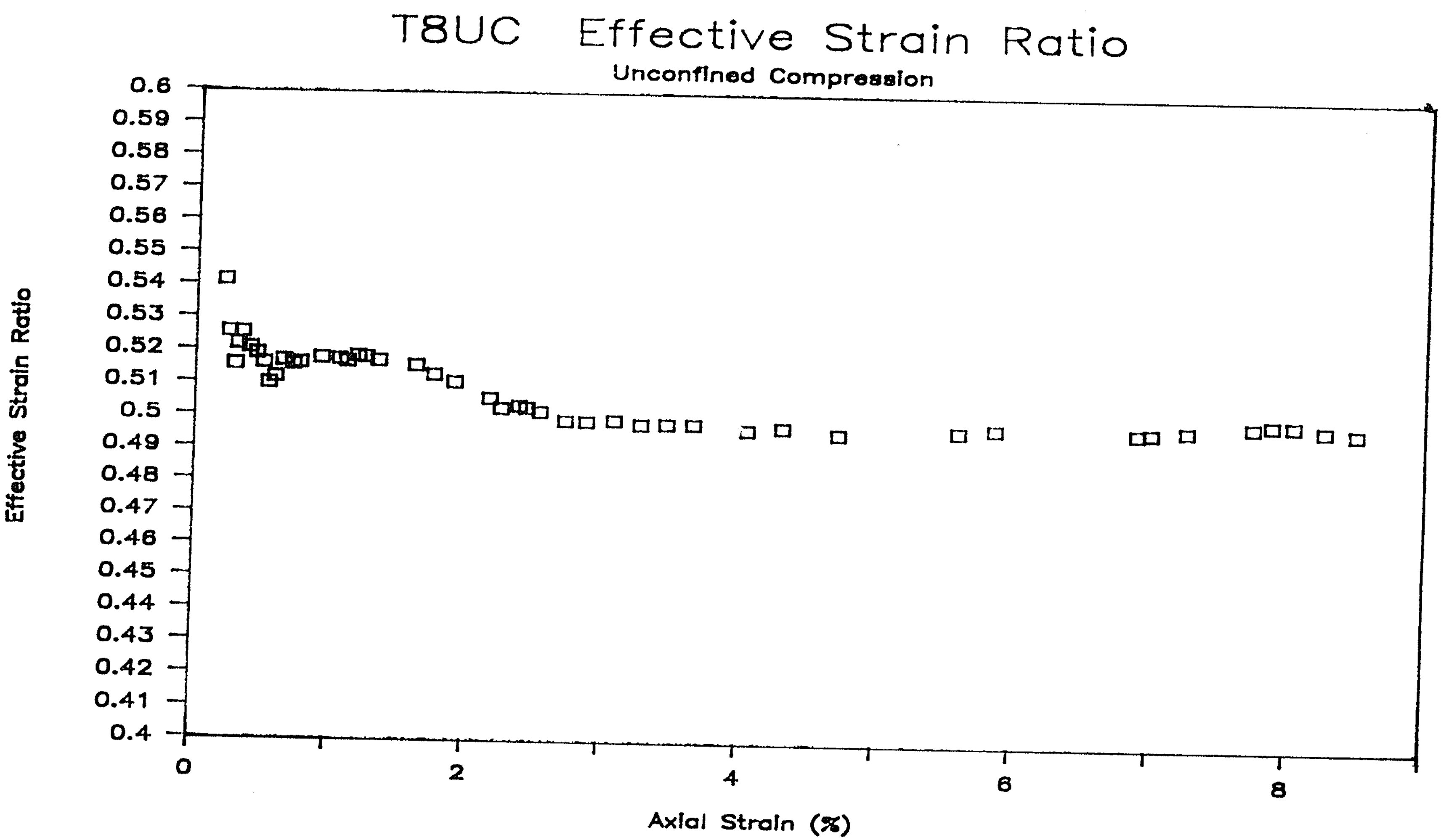

Figure 5.27 T8UC Effective strain ratio

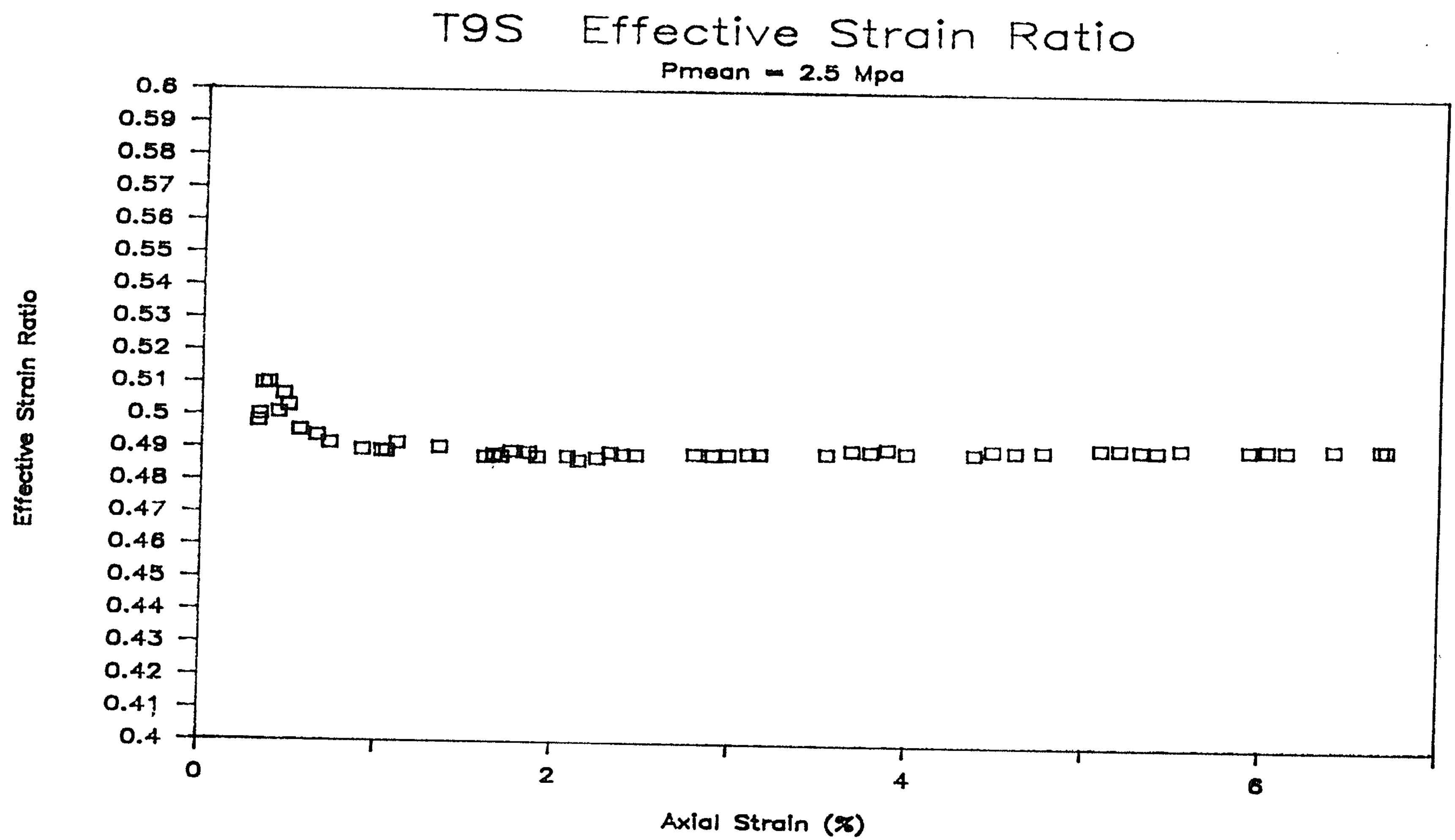

Figure 5.28 T9S Effective strain ratio

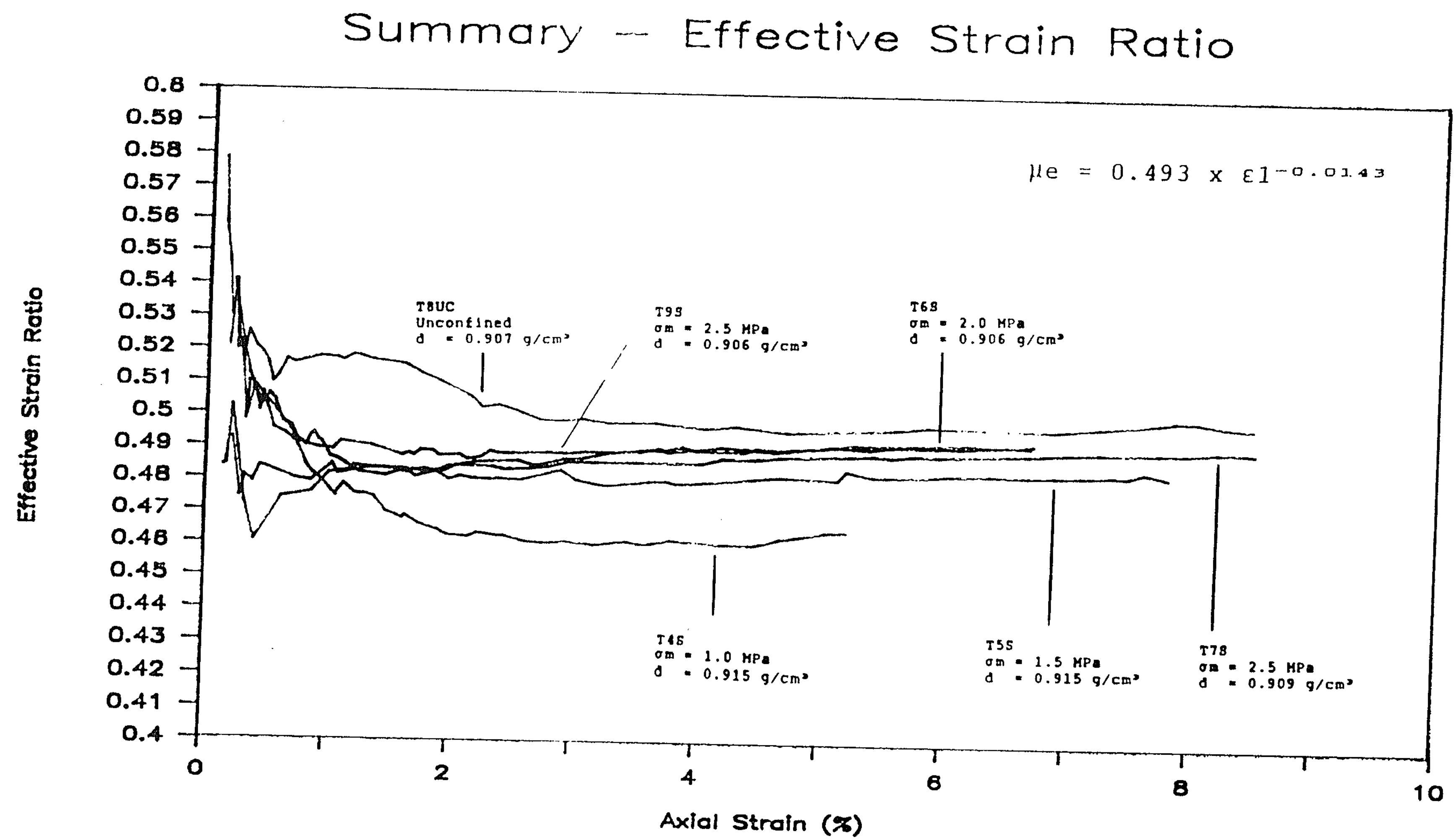

Figure 5.29 Summary of effective strain ratio data

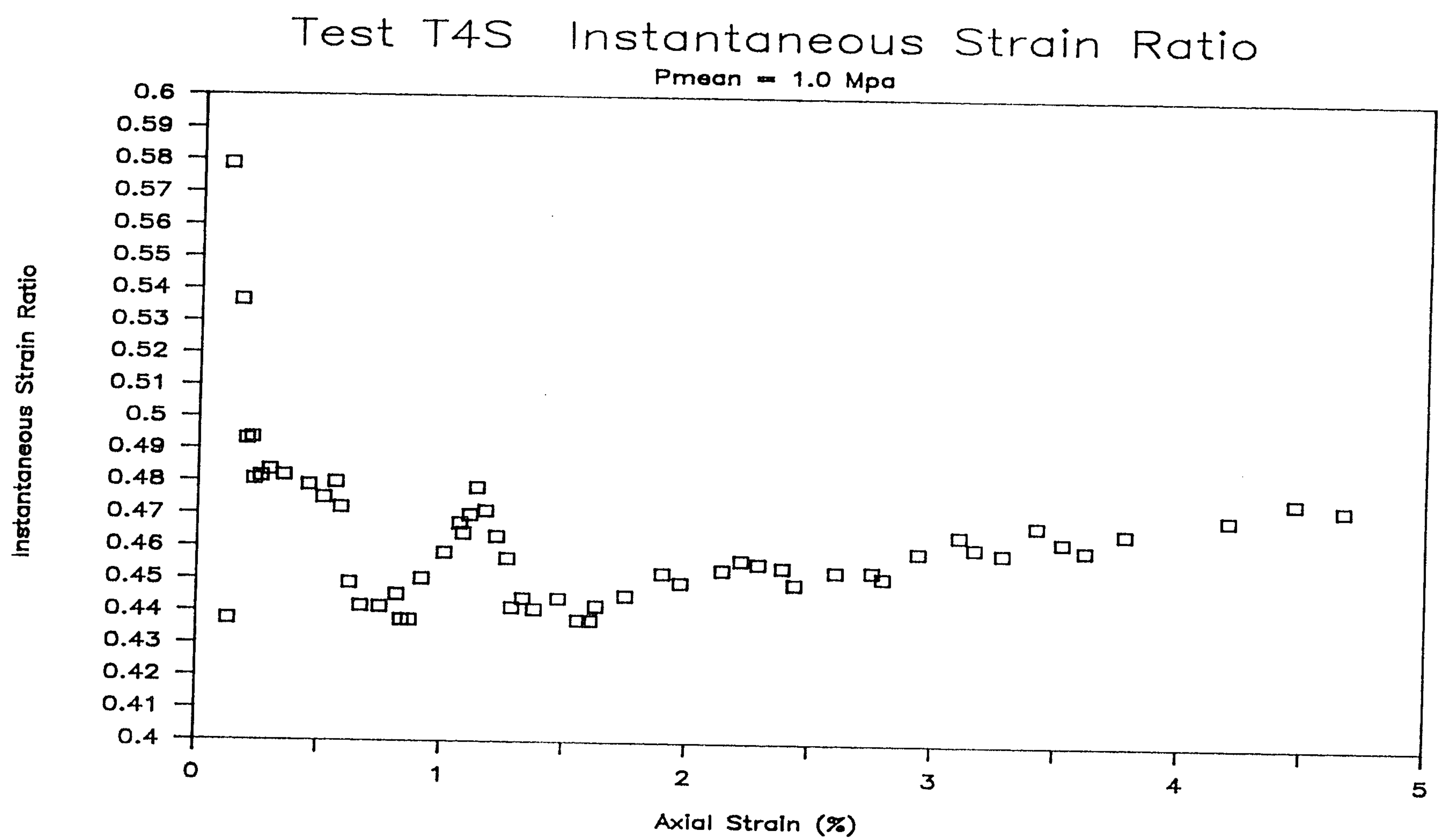

Figure 5.30 T4S Instantaneous strain ratio

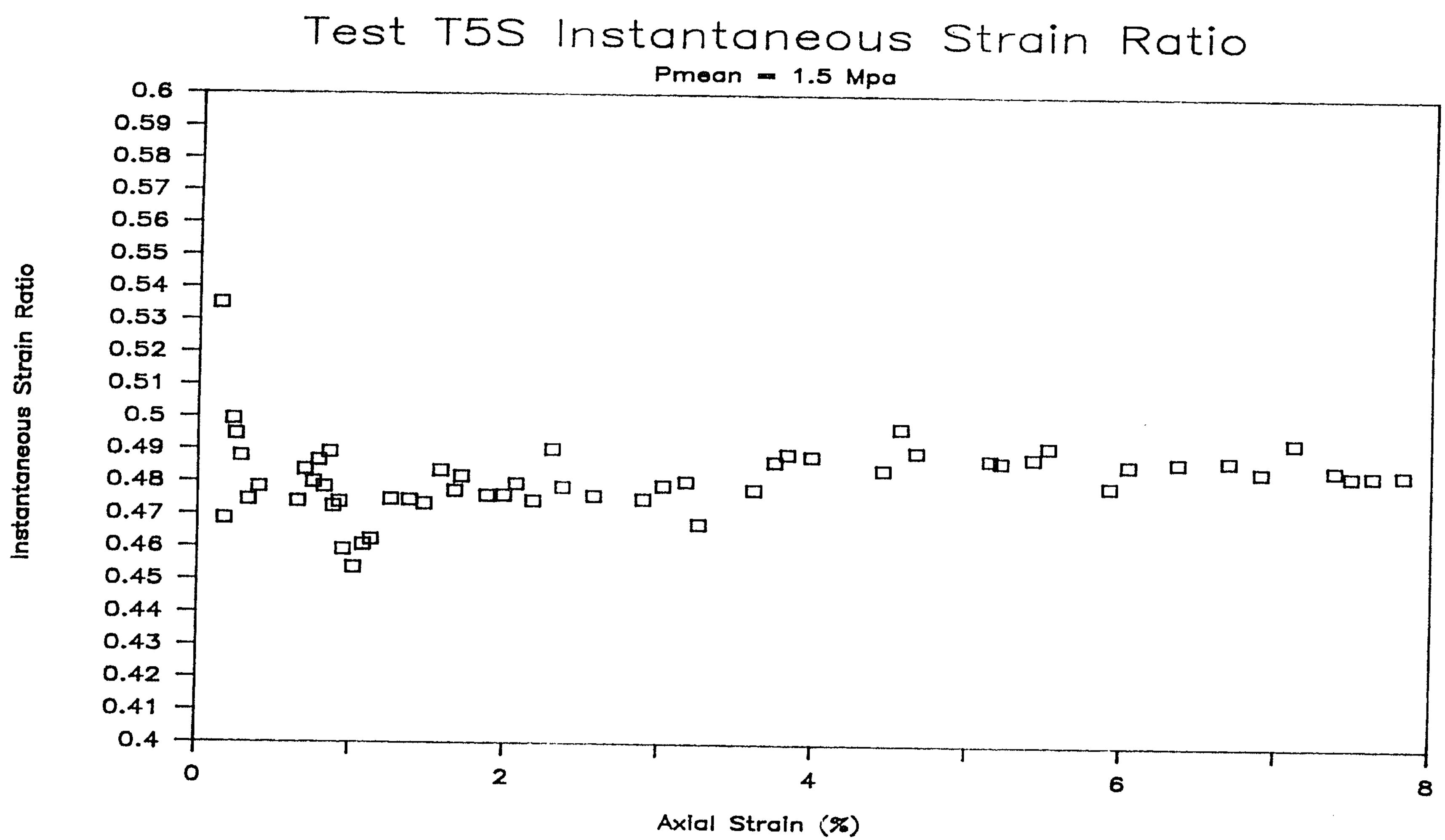

Figure 5.31 T5S Instantaneous strain ratio

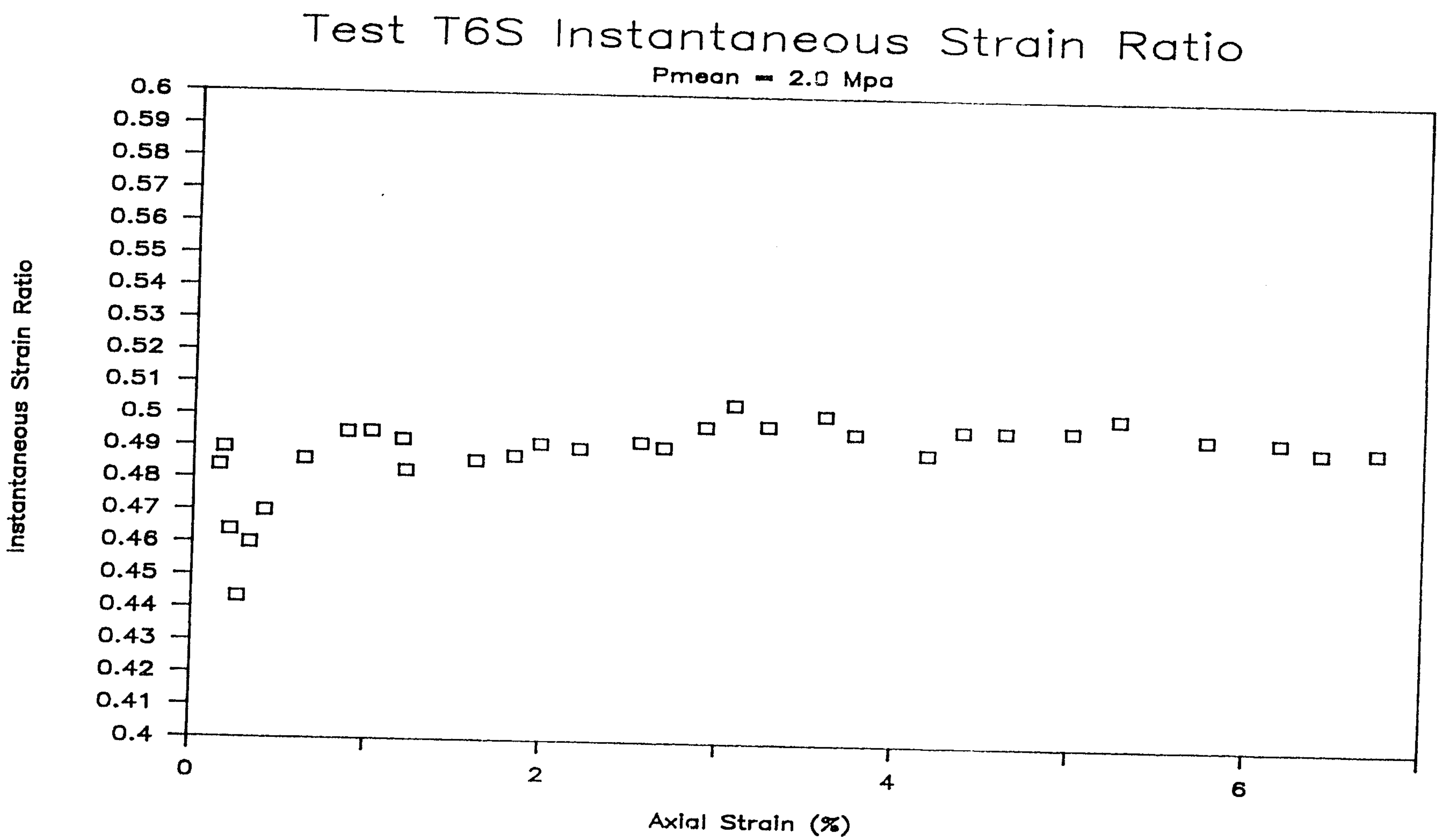

Figure 5.32 T6S Instantaneous strain ratio

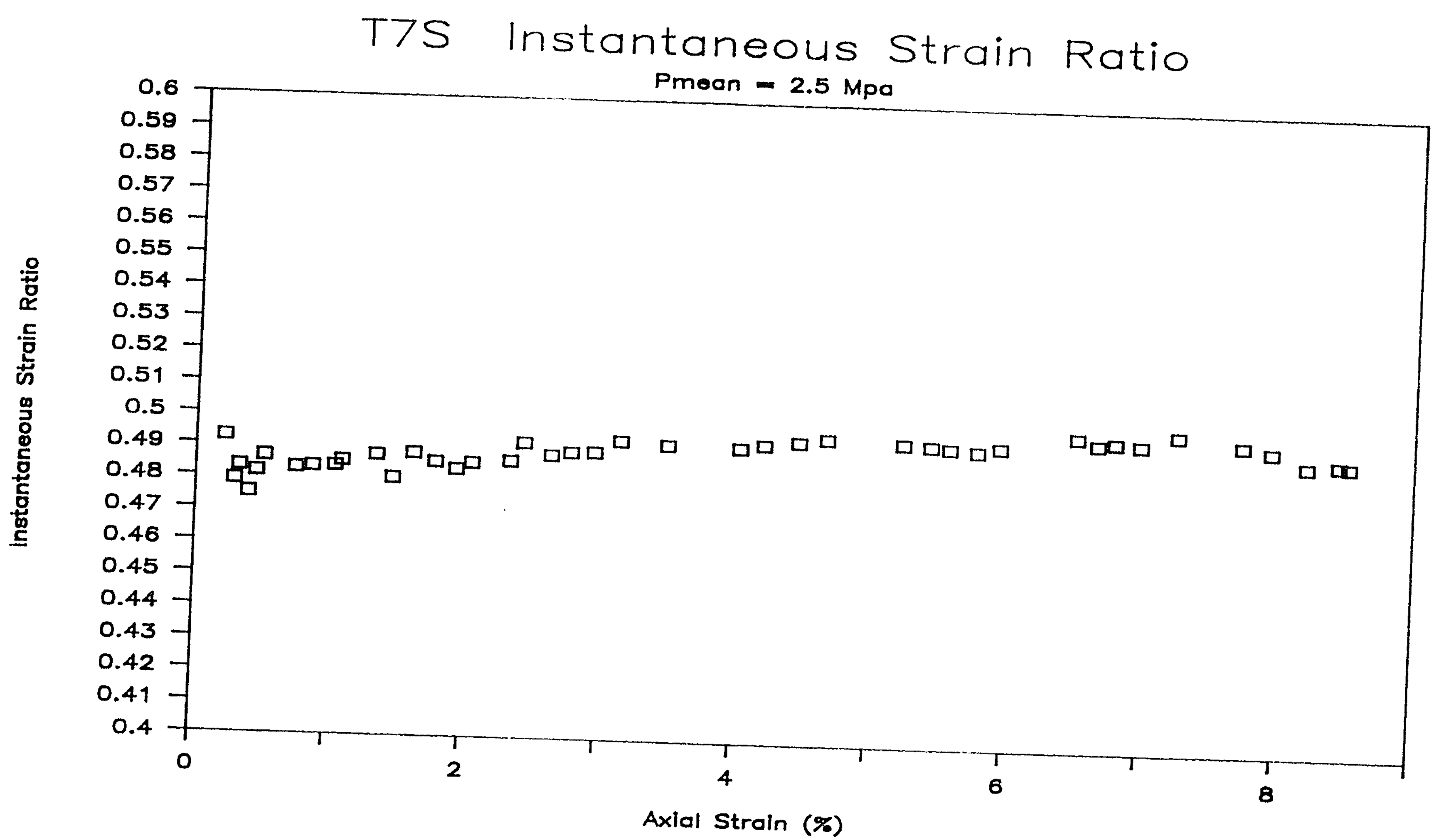

Figure 5.33 T7S Instantaneous strain ratio

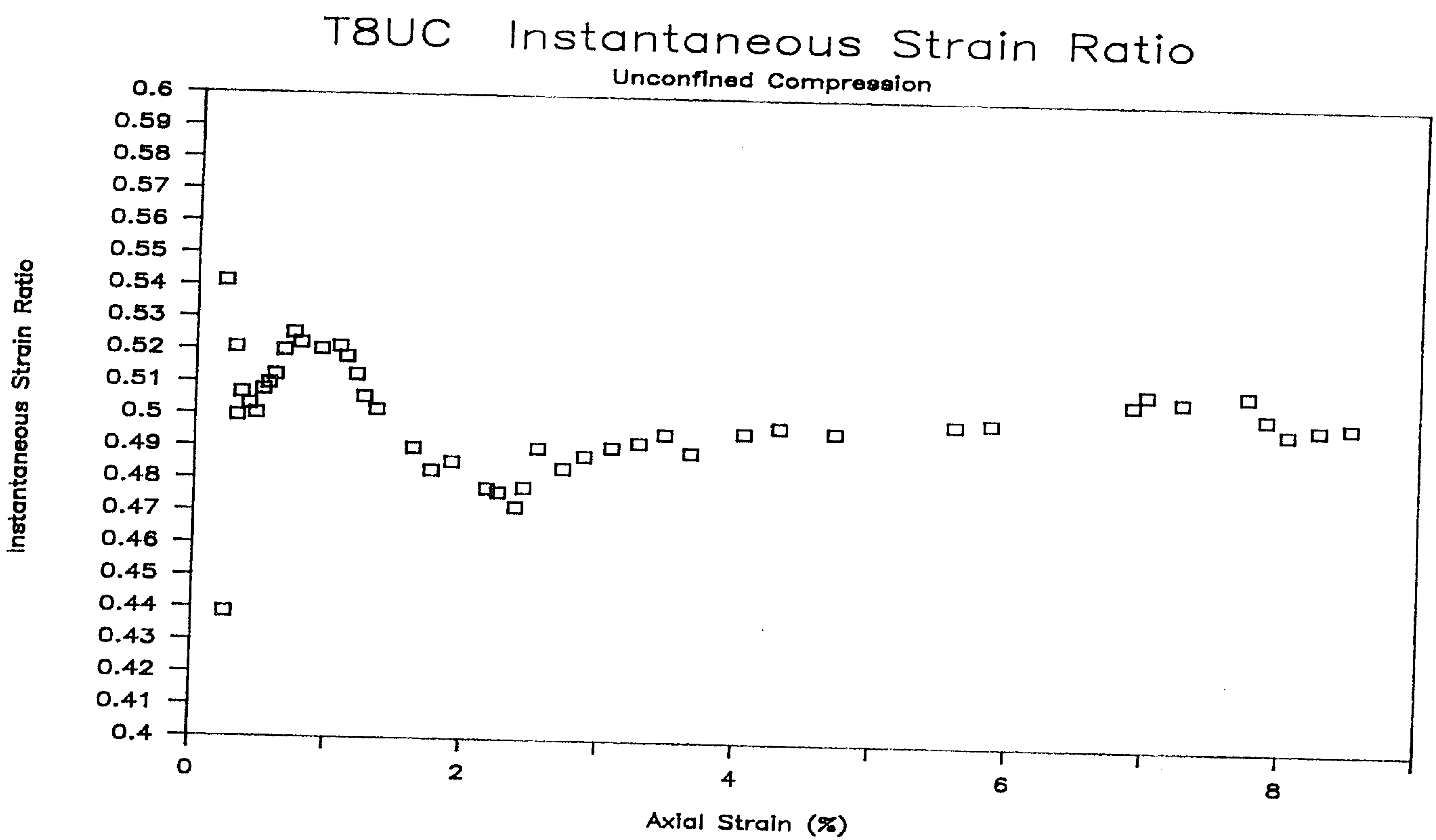

Figure 5.34 T8UC Instantaneous strain ratio

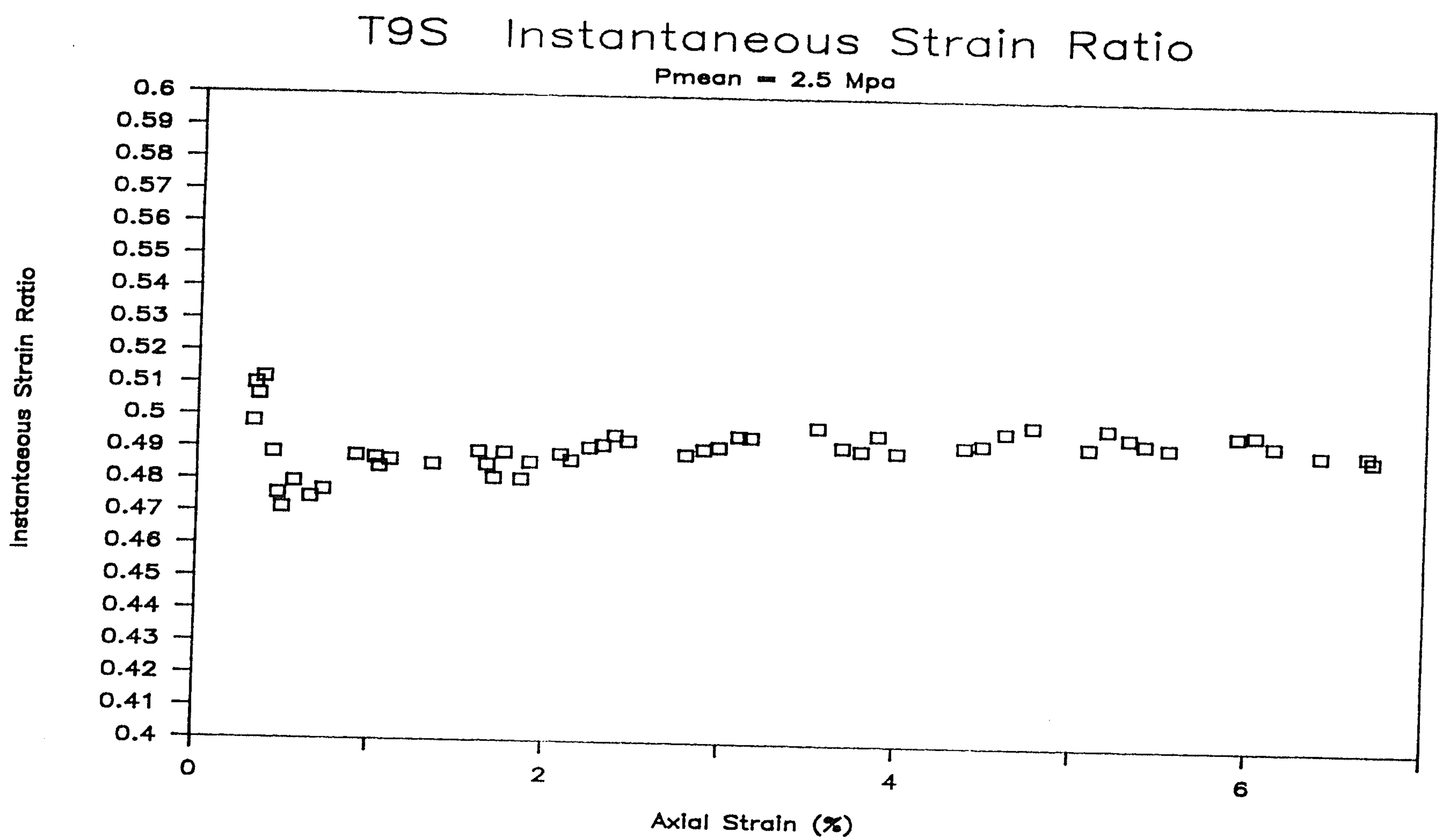

Figure 5.35 T9S Instantaneous strain ratio

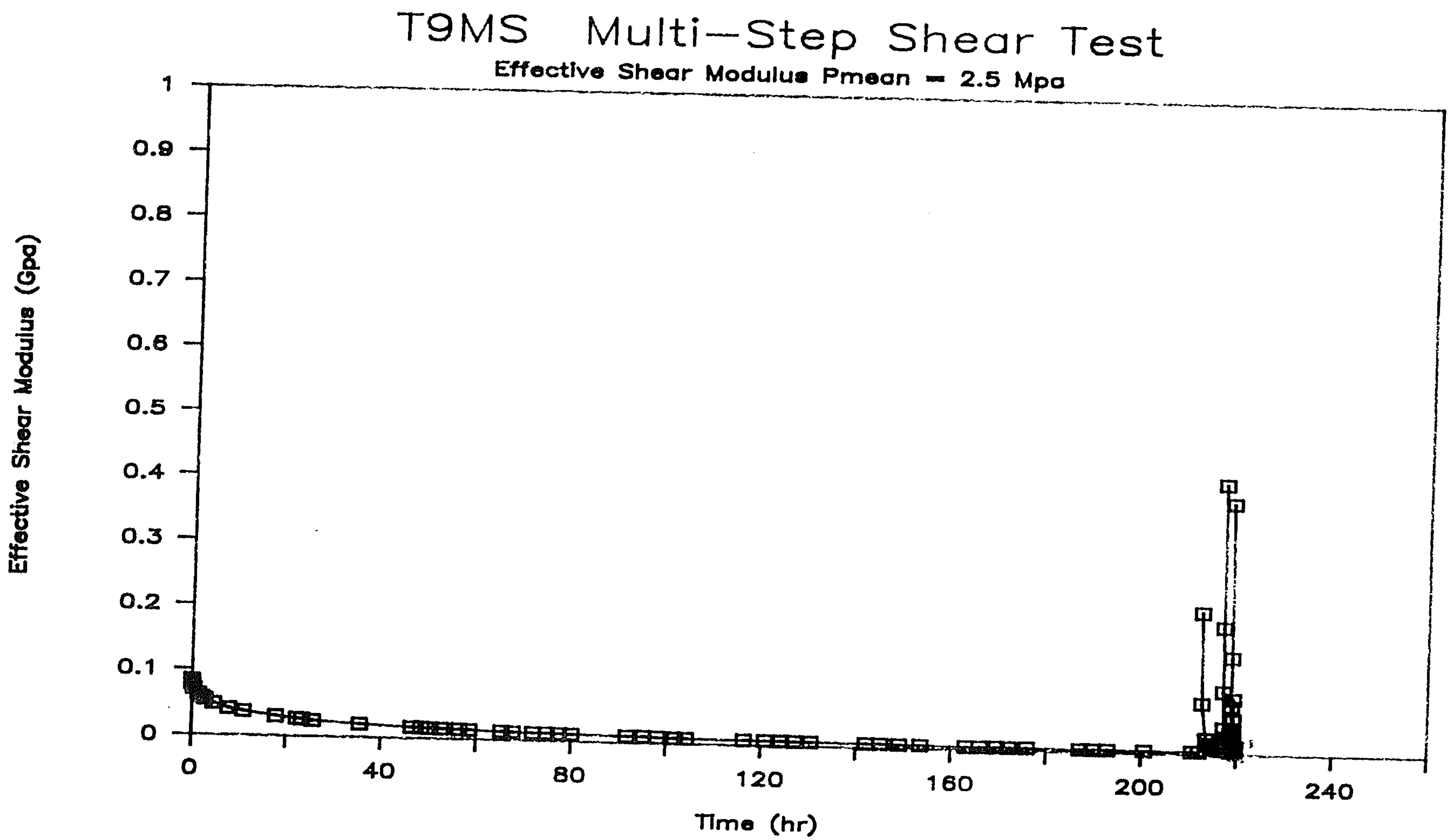

Figure 5.36 T9MS Effective shear modulus vs. time

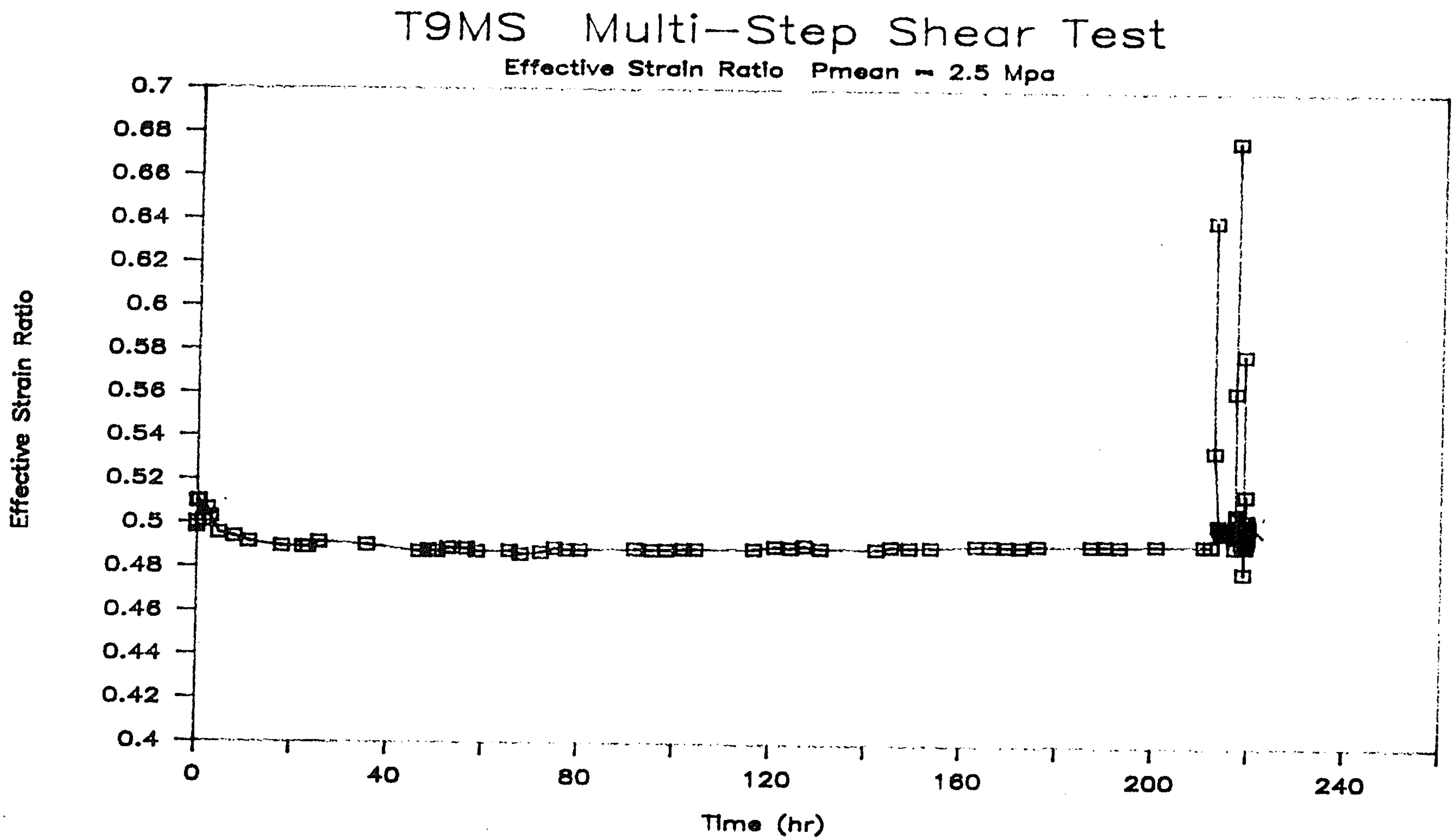

Figure 5.37 T9MS Effective strain ratio vs. time

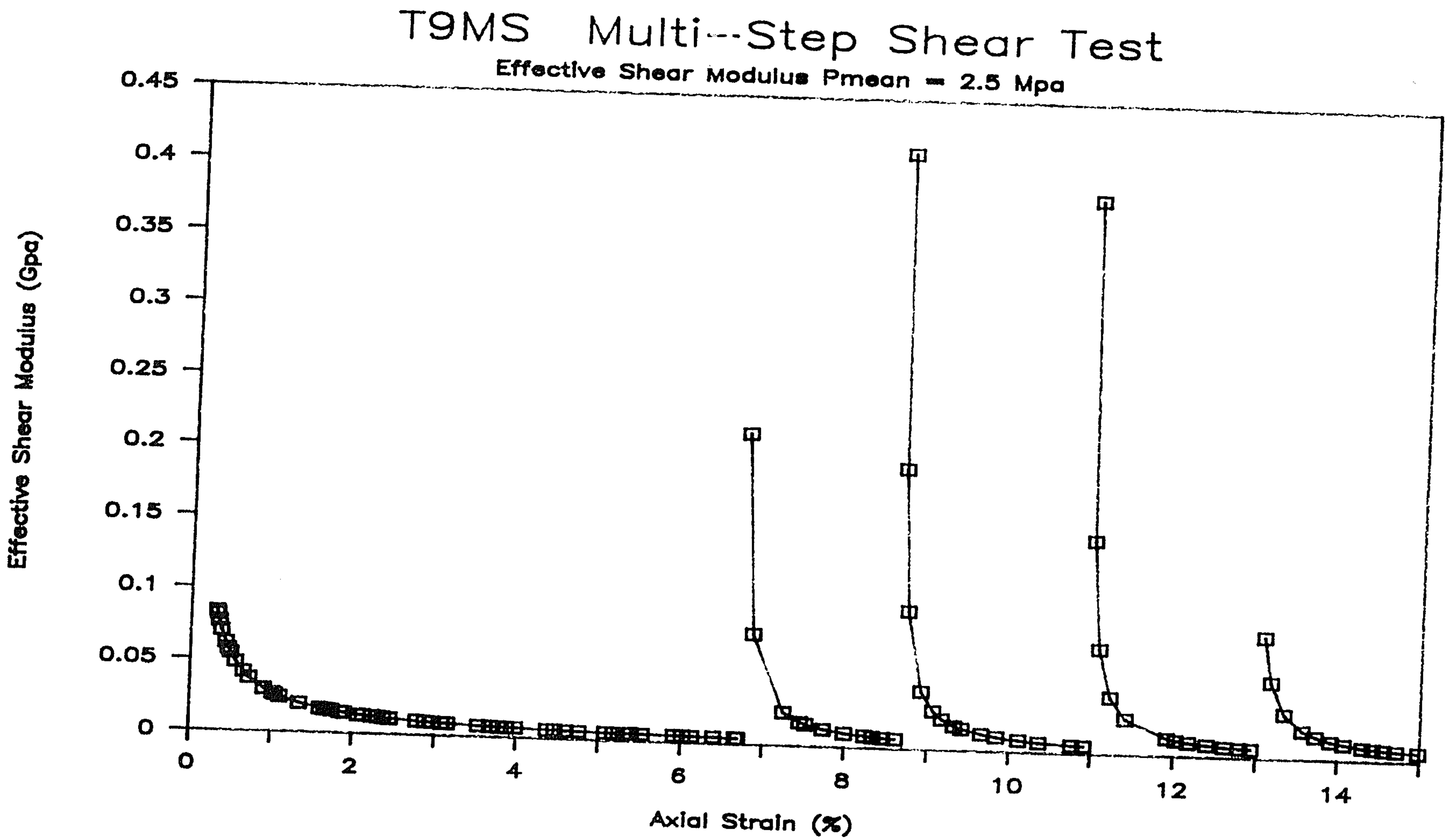

Figure 5.38 T9MS Effective shear modulus vs. axial strain

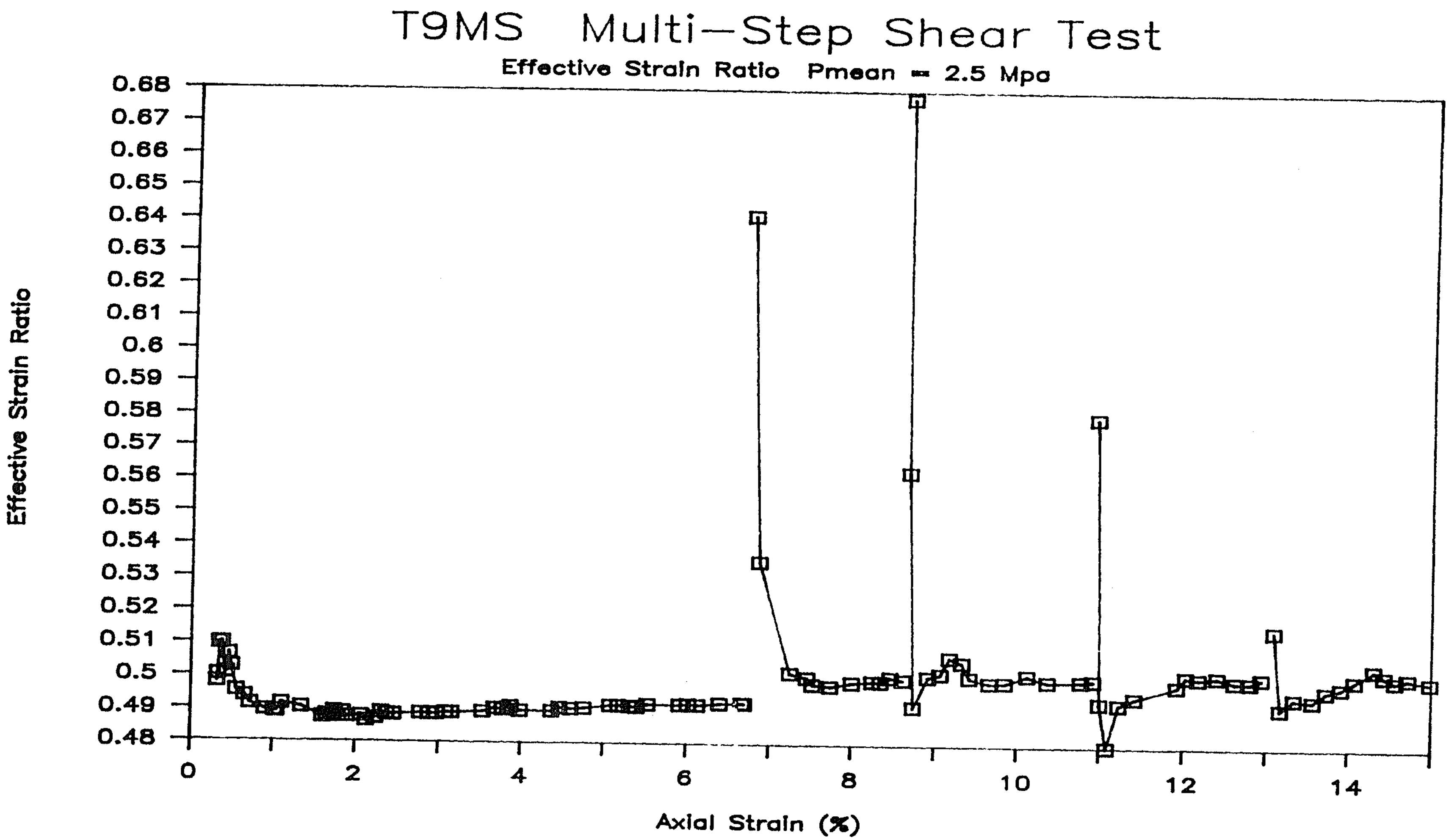

Figure 5.39 T9MS Effective strain ratio vs. axial strain

CHAPTER SIX

DISCUSSION OF TEST RESULTS

6.1 INTRODUCTION

In this chapter the results of the present study are discussed and compared to the work of previous authors on isotropic ice. Bulk modulus, shear modulus, and Poisson's ratio are discussed separately. The multi-step shear test, designed to investigate shear modulus and Poisson's ratio as the deviator stress changed, is discussed last.

6.2 BULK MODULUS

The elastic bulk modulus and effective bulk modulus of Kjartanson's ice are discussed separately here. The elastic bulk modulus K is a measure of the instantaneous bulk compressibility of the ice. K for Kjartanson's ice was found to be lower than that for pure ice with no air bubbles. The effective bulk modulus Ke is a functional measure of how the bulk compressibility of the ice changes with time. Ke was found to decrease by less than an order of magnitude from the initial elastic value as the tests progressed.

6.2.1 Elastic Bulk Modulus

The present study determined that the elastic bulk modulus of Kjartanson's ice at $-2^{o}C$ was 1.02 Gpa.

This is roughly an order of magnitude lower than the perfectly elastic bulk modulus of 10.3 Gpa for pure polycrystalline ice at -10°C discussed in Chapter 2 (see Section 2.2.1) and determined by static methods. There are two principal reasons for the discrepancy in values. The average density of Kjartanson's ice was 0.906 g/cm³, which is lower than the maximum density of ice (0.917 g/cm³). The average porosity of the ice was 1.2%. Some of the measured volume strain in the samples was due to the collapse or compression of the air bubbles in the ice. Most recent work on polycrystalline ice has been performed on pure ice with few if any bubbles. Direct comparisons are therefore difficult to make, especially considering the lack of volumetric data (see Section 2.2). Another reason for the low value of K obtained by this study may be the finite period of loading. Dynamic testing techniques have loading periods of less than one second. The quick-step tests performed here had loading periods of ≈60 seconds, the minimum time required to obtain four readings of the volume change burette. It is probable that some volumetric creep occured in this short time, both recoverable and non-recoverable. If creep did occur during the quick-step tests as postulated, then only part of the measured volumetric deformation would have been elastic, and the calculated bulk modulus would be too low. An automatic volume change measurement device would have aided in the determination of elastic bulk modulus as it would have allowed faster tests.

Three quick-step tests (QSIC3, QSIC4, QSIC5) were performed in succession on the same specimen, T9. Table 5.1 indicates that K increased slightly after the first and second tests on the specimen. This increase in stiffness may have been due to the presence of plastic volumetric strain, or viscous recoverable strain. The sample was allowed to sit for 10 minutes after each test, an amount of time deemed great enough to allow recovery of any purely elastic strain. This, however, may not have been enough time to recover all viscous recoverable strain (Sinha, 1988a). Therefore, based on the slight increase in bulk modulus with repeated testing on the same specimen, it seems evident that some permanent deformation occured in the ice even during the relatively short loading period of 60 seconds.

Figure 4.23 shows a slight stiffening of the ice specimens as hydrostatic pressure increases. This stiffening may have been due to creep during the loading period. The variation in the slope of the strain curve was not great in the study pressure range and therefore a single value of K, the average slope through the study pressure range, was used as a measure of elastic bulk modulus.

6.2.2 Effective Bulk Modulus

As stated in Section 2.2.1, the effective bulk modulus Ke for a single stage test is equal to the applied pressure divided by the total volume strain. Since it includes creep strain, Ke may be expected to be lower than the elastic bulk modulus and to decrease with time. These expectations are borne out in Figure 5.8. Note that the first value of Ke is equal to K.

While there is no published data to compare the effective bulk modulus results to, a number of observations can be made on the apparent effect of the controlling variables discussed in Section 2.2. As shown in Table 5.2, and in Figure 5.8, the effective bulk modulus increases with an increase in hydrostatic stress. In other words, volumetric creep strain does not increase in direct proportion to applied hydrostatic stress. Note that this observation is somewhat dependent on the synthetic nature of Figure 5.8. That is, the elastic bulk modulus was calculated from a separate series of tests and was used to calculate the initial elastic strain. Measured creep volumetric strains were then added to that initial value and the sum was used to calculate Ke. Figure 5.8 illustrates the dependency of effective bulk modulus on stress and on time. This is in agreement with the work of Rahman (1988) on frozen soil.

The test temperature for the present study was maintained at -2.0°C ±0.1°C. Therefore the effect of temperature on effective bulk modulus cannot be determined from this study. As mentioned in Section 2.2.3, pressure melting should not have an effect on effective bulk modulus. The appearance of water in the ice lattice due to pressure melting should not lead to an increase in compressibility since water has approximately the same bulk modulus as ice (Mellor, 1984). No pressure melting effect on bulk modulus was seen during the present study. If the effect was present, it may have been masked by density effects.

The dependency of volumetric creep strain on density has been illustrated in Figures 5.9 to 5.11. The asymptotic value of Ke, however, does not seem to be dependent on initial sample density, as outlined in Table 5.2. Instead, Table 5.2 shows that Ke is linearly dependent on bulk stress. Mellor (1979) shows that elastic bulk modulus is dependent on density. See Figure 2.3. It would be incorrect to compare his conclusion to that of the present study for two reasons. First, Mellor is discussing the elastic modulus, while the present study deals with effective modulus. Secondly, the present study deals with a much narrower range of density than does Mellor. While specimen density does have a noticeable effect on the volumetric creep strain (see Section 5.2.3), it does not appear to have a marked effect on Ke in the density range of this study.

In comparing the effective bulk modulus curve of specimen T9 to that of T1, several observations can be made. Both tests were carried out at 2.5 Mpa, but Figure 5.8 shows that the values of Ke for T9 are consistently lower than those of T1, indicating a more compressible sample. While the initial density of T9 (0.906 g/cm³) was lower than that of T1 (0.912 g/cm³), the author does not believe that density effects are solely responsible for the difference in the Ke curves. It is postulated that the particular stress history of T9 is the reason for it's low effective bulk modulus. Three successive quick-step isotropic compression tests were performed on T9 before the single stage test was started. Each quick-step test lasted for 60 seconds, and reached a maximum bulk stress of 2.2 Mpa. It would seem that cyclic bulk stress loadings of the ice cause a "softening" of the material. All single stage tests other than T9 had identical stress histories (except of course for the bulk stress level), with the isotropic load applied over approximately 30 seconds.

6.3 SHEAR MODULUS

The elastic shear modulus of Kjartanson's ice was found to be approximately one order of magnitude lower than that of pure ice as determined by dynamic methods. The effective shear modulus of the ice decreased by more than one order of magnitude from the elastic value during the shearing process. The shear modulus of the ice is discussed in this section, as well as the effect of controlling variables on the shear modulus.

6.3.1 Elastic Shear Modulus

As listed in Table 5.3, the values of G for Kjartanson's ice are from 10 to 20 times lower than the elastic shear modulus of 3.5 Gpa interpreted from dynamic and static test results. This value of 3.5 Gpa is obtained using equation 2.4, with a Young's modulus of 9.3 Gpa, and a Poisson's ratio of 0.35. Mellor (1983) states that for polycrystalline ice of low porosity (i.e. density very close to 0.917 Mg/m^3) in the temperature range -5°C to -10°C, Young's modulus has been found to be in the range 9.0 to 9.5 Gpa. However, Kjartanson's ice did have significant porosity (1.2%), and the test temperature for the present study was -2°C, therefore it may not be appropriate to directly compare the shear modulus data from the present study to that derived from Mellor. Note that Mellor also states that temperature does not have a large effect on Young's modulus.

Closer inspection of Table 5.3 indicates that the value of G increases as mean stress decreases. This seems unusual since it implies that shearing increases as confining stress increases for a constant axial stress. In other words, it implies that shear stiffness is reduced by confining pressure. This problem can be explained as follows. The values of elastic shear modulus are based on the first volumetric reading taken after the application of deviator stress. As mean stress increased from test to test, the corresponding axial strain at the time of the first reading increased. Thus the initial reading was further along the Ge-axial strain curve as mean stress increased (see Figure 5.19). But why was it further along the curve given that initial readings were all taken at approximately 3 seconds after load application? The answer is that the specimens tested at low mean stress had higher densities than those tested at high mean stress, as Tables 4.3 and 5.3 indicate. Because specimens T4 and T5 had high densities (0.915 Mg/m^3), they experienced less deformation upon application of load than did the other specimens. Mellor (1983) cites experimental data from a number of authors that show the stiffness of freshwater ice (as represented by Young's Modulus) to decrease with a decrease in density. It may be concluded that the elastic shear modulus is dependent on specimen density, as Figure 5.21 indicates. Note that for a density of 0.917 g/cm^3 Figure 5.21 indicates that G would be $\approx$ 0.3 Gpa.

6.3.2 Effective Shear Modulus

The effective shear modulus decreased from the elastic value by approximately thirty times when the specimen had reached 5% axial strain. Figure 5.19 illustrates this decrease for all six constant mean stress shear tests. Note that the curves are almost exactly alike. This is not surprising if the effective shear modulus is analyzed in the following manner:

$$Ge = \sigma / 3\, \varepsilon s \tag{6.1}$$

$$\varepsilon s = 2\, (\varepsilon 1 - \varepsilon r) / 3 \tag{6.2}$$

$\varepsilon v = \varepsilon 1 + 2\, \varepsilon r$ (strains positive in compression)

or ,

$$\varepsilon r = (\varepsilon v - \varepsilon 1) / 2 \tag{6.3}$$

Combining these yields,

$$Ge = \sigma / (3\varepsilon 1 - \varepsilon v) \tag{6.4}$$

During the shear test program, εv was on the average only 5% of $\varepsilon 1$. Therefore, it may be neglected from equation 6.4, yielding,

$$Ge = \sigma / 3\, \varepsilon 1 \tag{6.5}$$

Equation 6.5 is a good approximation to the effective shear modulus only if the sample is experiencing little volume change. This would be reflected by an effective strain ratio of ≈ 0.5, such as is shown in Figure 5.28 for the present study. For a deviator stress of 0.8 Mpa, and an axial strain of 5%, equation 6.5 yields an effective shear modulus of .005 Gpa, exactly equal to the values determined for the present study (see Table

5.4).

Mean stress did not seem to have an effect on effective shear modulus, as illustrated in Figures 5.19 and 5.20. As well, specimen density did not seem to have a significant effect on Ge. This is also shown in Figures 5.19 and 5.20. Note however that the ice tested in the present study had a fairly narrow range of density.

6.4 POISSON'S RATIO

As discussed in Section 2, the term Poisson's ratio, or μ, is used to refer the ratio of the lateral to axial strain for the case of elastic deformation. If plastic deformation is involved, then the term strain ratio is used. Poisson's ratio and strain ratio were determined from the constant mean stress shear tests. In the present study, Poisson's ratio was found to vary, depending on the mean stress. The strain ratio was found to approach 0.5 as each test progressed, indicating ductile flow with no volume change.

6.4.1 Poisson's Ratio (Elastic Case)

Table 5.3 shows the variation of μ with mean stress. This variation is illustrated in Figure 5.22. It may be seen that the specimens with a lower confining stress had a higher Poisson's ratio. It is postulated that specimens T4, T5, and T8 experienced dilation due to cracking, as indicated by a value of μ greater than 0.5. Sinha (1986b) notes that $\mu > 0.5$ is indicative of microcracking, or dilation. Sinha (1988a) also states,

> Microcracks, comparable in size to a grain facet, seem to occur under a constant-load creep condition where stress exceeds a critical value ($> 10^{-5}$ E, where E is Young's modulus)

For ice, $10^{-5}E$ = .095 Mpa. The stress for the present study was 0.8 Mpa. Note that Sinha does not address the effect of confining stress on microcracking. Poisson's ratio for specimens T6, T7, and T9 was not greater than 0.5, suggesting that any dilation was suppressed by the larger confining stresses which they were subject to.

As related in Section 2.4, the purely elastic value of μ is $\approx$ 0.35, as determined by dynamic testing techniques. Why then, did Kjartanson's ice not have μ=0.35? The deviator stress of 0.80 Mpa was applied almost instantaneously, so it may be assumed that no plastic deformation occurred during the loading process. However, this assumption cannot be made for even the earliest volumetric reading, which took place on the average 3 seconds after load application. Microcracking causing dilation may have occurred even in that short period of time. Sinha (1986a), in loading rectangular blocks of columnar sea ice at -10°C at a strain rate of $10^{-3}s^{-1}$ reports a value of μ of $\approx$1.0 after three seconds. The ice was loaded parallel to the direction of growth of the columnar grains. It is probable that in the extremely short loading times of dynamic tests, dilation does not occur, although the author is not familiar with dynamic testing techniques. It is also possible that cracking occurred in the specimens at higher mean stresses (T6, T7,and T9), and that the confining pressure reduced it to the extent that μ remained below 0.5. Post-test examination of single stage shear test specimens revealed no visible cracking, suggesting that the confining pressure healed any cracks formed during loading. This theory is partially confirmed by the behaviour of specimen T8, which was loaded with no confining pressure. Figure 5.27 shows that μe remained above 0.5 until the axial strain was ≈2%, when it gradually approached the condition of no volume change. It is postulated that μe remained above 0.5 for so long because there was no confining pressure to heal the cracks formed during the loading process.

6.4.2 Effective Strain Ratio

The effective strain ratio for all specimens tested in shear is shown in Figures 5.23 to 5.28. As axial strain increased, the ratio of total radial to total lateral strain remained constant at ≈ 0.5 in all cases. This indicates ductile flow with no volume change, and agrees with Sinha (1986a), who states,

> For conditions where cracking activity does not dominate the deformation processes and where final strain consists predominantly of viscous flow, μe

> in isotropic ice may be expected to increase with time during loading from an initial value (Poisson's ratio) to a final value of 0.5.

Mellor (1983) also states that,

> as material response becomes more ductile, the usual trend is for μe to increase up to a limit of 1/2, which represents incompressible flow

Note that in general, μ decreased from an initial value as a result of dilation. There is some slight variation in the final value of μe, as noted in Table 5.4.

6.4.3 Instantaneous Strain Ratio

Figures 5.29 to 5.35 illustrate the instantaneous strain ratio, μi, for all the shear tests. The curves of μi follow the same general pattern as those for μe. That is, μi is generally close to or equal to 0.50 for the greater proportion of each shear test. Note however that in the beginning of each test (before 1% axial strain is reached), μi often falls to ≈ 0.45 and then increases from that point to approach 0.50. This phenomenon may indicate the presence of some elastic behaviour, as indicated by Sinha and Mellor above. It is possible that micro-cracking occurring at the instant of loading caused dilation. It is possible that the micro-cracks were then healed (or at least stopped propagating) by the confining stress while the elasic behaviour of the ice was still evident. In effect, the cracking activity may have masked some of the elastic behaviour of the ice as represented by a strain ratio < 0.50.

6.5 MULTI-STEP CONSTANT MEAN NORMAL STRESS SHEAR TEST

The multi-step shear test was conducted to investigate how the shear modulus and strain ratio of Kjartanson's ice would change as the deviator stress was increased. Mean stress was held constant throughout the test. That is, the confining pressure was lowered in order to compensate for the increased axial stress. A mean normal stress of 2.5 Mpa was applied, and the deviator stress was increased in steps from 0.8 to 1.2 to 1.6 to 2.0 to 2.4 Mpa. In general, the specimen under multi-step loading exhibited similar behaviour to the specimens under single-step loading.

6.5.1 Shear Modulus of Multi-Step Test Ice

The effective shear modulus of specimen T9 is shown in Figure 5.35 for all five steps as a function of time, and in Figure 5.37 as a function of axial strain. The shear modulus in the individual steps of the multi-step test behave in much the same manner as the shear modulus in the single stage shear tests. Initial calculated values of G for the individual steps of the multi-step test are somewhat higher than those of the single step tests, especially the third and fourth steps.

In analyzing the results of the multi-step tests, it is important to consider the cumulative effect of the loading steps on the ice specimen. This cumulative effect makes it difficult to consider the separate steps of the multi-step test as individual tests equivalent to the single stage tests.

Table 5.5 and Figure 5.37 indicate that the elastic shear modulus, as represented by the first value for each step, increases as deviator stress increases. Since the axial strain rate also increased as the deviator stress increased (see Figure 4.54), it may be concluded that the shear stiffness increased with axial strain rate. Previous researchers (Hawkes and Mellor, 1972, Traetteberg et al, 1975) have established that axial stiffness (Young's modulus) increases with strain rate. It would seem reasonable to expect shear stiffness to increase with axial stiffness. Note that the initial value of Ge in the fifth step of T9MS (deviator stress was 2.4 Mpa) is low compared to steps two, three, and four. This loss of shear stiffness may be due to cumulative damage suffered by the specimen. Also note that the first reading for all steps of the multi-step test was taken at the same interval after load application ($\approx$ 3 seconds).

The effective shear modulus curves are quite similar for each step of the multi-step test. Table 5.5 indicates that Ge at 2% axial strain is the same for all but the first step. This is not unexpected in light of equation 6.5 since the first step had an incremental deviator stress twice that of the last four steps. Calculations performed by the author indicate that equation 6.5 is a very good approximation for the individual steps of the multi-step shear test.

6.5.2 Strain Ratio of Multi-Step Test Ice

The strain ratio of specimen T9 is shown in Figure 5.36 for all five steps as a function of time, and Figure 5.38 as a function of axial strain. Table 5.5 shows that Poisson's ratio tended to increase when the deviator stress was increased, and that the effective strain ratio decreased to ≈0.5 as each step proceeded.

The increase in Poisson's ratio exhibited by the specimen in the later steps of T9MS can be attributed to an increase in cracking activity causing dilation. Poisson's ratio shows some variation (μ for steps four and five is less than μ for steps two and three) as deviator stress increases however, and it is postulated that this is caused by cumulative damage to the specimen with successive loadings. Note that although the total deviator stress increased with each step of T9MS, the incremental change in deviator stress was the same (0.4 Mpa). That is, the ice specimen was responding to the same change in deviator stress with each step.

The ice specimen began to creep in a ductile manner with no volume change soon after the application of each deviator stress step. This is indicated by effective strain ratio values of ≈ 0.5 in Table 5.5. μ for the single stage shear tests exhibited the same behaviour. It may be concluded therefore that deviator stress level does not have an effect on effective strain ratio.

CHAPTER SEVEN

CONCLUSIONS

7.1 Summary of Test Program

Constant mean normal stress triaxial creep tests were carried out on isotropic ice to determine its bulk modulus, shear modulus, and Poisson's ratio. Each test was divided into two phases - the first phase was isotropic consolidation (from which bulk modulus was determined), and the second phase was constant mean normal stress shear (from which shear modulus and Poisson's ratio were determined). The temperature for all tests was -2.0 ^{o}C. Mean stresses ranged from 1.0 to 2.5 Mpa, and the deviator stress for all shear tests was 0.8 Mpa, except for the multi-step test, where the deviator stress was increased in steps. The following conclusions are based on the experimental data of the present study. There are two principal conclusions, one for the modulus values (bulk modulus and shear modulus) and one for Poisson's ratio (strain ratio) of Kjartanson's ice. Point form summaries of greater detail are also included for each of bulk modulus, shear modulus, and Poisson's ratio.

7.2 Principal Conclusions

The values of the elastic bulk modulus and elastic shear modulus of Kjartanson's ice are 1.02 Gpa and 0.18 Gpa respectively. This is approximately one order of magnitude lower than those values determined for freshwater ice by dynamic test methods. During constant stress creep testing, the time-dependent values of the bulk modulus and shear modulus of Kjartanson's ice decreased by another order of magnitude from the elastic values.

During constant mean stress creep testing Kjartanson's ice exhibited no significant volume change. This is indicated by an effective strain ratio of ≈ 0.5 for all specimens. Specimens tested at low mean stresses did exhibit cracking activity causing dilation in the initial phases of those tests as indicated by values of Poisson's ratio of > 0.5.

7.3 Bulk Modulus

1. The time required to reach an attenuated volumetric creep rate of 1.5×10^{-5} hr^{-1} was more dependent on initial specimen density than on hydrostatic stress.

2. The volumetric strain at the point of attenuated creep decreased as bulk stress increased.

3. There was evidence of "softening" of the ice in cyclic isotropic compression tests.

4. The elasic bulk modulus of Kjartanson's ice was determined to be 1.02 Gpa.

5. The asymptotic value of the effective bulk modulus increased as bulk stress increased.

7.4 Shear Modulus

1. The elastic shear modulus was determined to be dependent upon specimen density. For a specimen of average density the elastic shear modulus was 0.18 Gpa.

2. The elastic shear modulus was found to increase with deviator stress.

3. The effective shear modulus was found to decrease asymptotically with time. After initial elastic strain, the effective shear modulus for the single stage tests could be approximated very well by $Ge=(\sigma 1 - \sigma 3) \times (3\varepsilon 1)^{-1}$.

4. The effective shear modulus was independent of specimen density and mean stress.

5. The effective shear modulus was determined to be independent of deviator stress.

7.5 Poisson's Ratio and Strain Ratio

1. Poisson's ratio for Kjartanson's ice was determined to be dependent upon mean stress. For $\sigma m < 2.0$ Mpa, μ was > 0.5 because of cracking activity. For $\sigma m >= 2.0$ Mpa, the confining stress inhibited cracking activity, and μ was slightly less than 0.5.

2. Measurements of instantaneous strain ratio and effective strain ratio indicated that the specimens

experienced very little volume change during creep. μi and μe were ≈ 0.5 in all test cases.

3. As deviator stress was increased Poisson's ratio increased due to cracking acitivity. Care must be exercised in utilizing the multi-step test data because of the cumulative damage effect on the specimen.

7.6 Suggestions for Further Research

A number of recommendations can be made for further triaxial testing of ice. With regards to test equipment, it is recommended that an automatic volume change device be manufactured or purchased for use in the test program. This would allow greater accuracy and frequency of readings. It would be beneficial to use strain gauges mounted directly on the ice specimen in order to eliminate the possibility of erroneous LVDT readings due to frame compression or improperly aligned loading platens. These two changes to the equipment inventory (along with a load cell) would allow the use of constant strain rate tests. Constant strain rate tests have traditionally been used in the geotechnical field to determine elastic modulus values.

It would be of some benefit to eliminate the effects of density in the test results. Although most naturally occuring ice is porous, the use of non-porous ice in laboratory situations does lend more confidence to the test results. Finally, it would be advantageous to conduct triaxial tests over a range of temperatures. This would allow the determination of the effect of temperature on the bulk modulus, shear modulus, and Poisson's ratio of ice.

REFERENCES

Atkinson, J.H., and Bransby, P.L., 1978. "The Mechanics of Soils, An Introduction to Critical State Soil Mechanics". McGraw-Hill, London, 315 pp.

Barnes, P., Tabor, D., and Walker, J., 1971. "The Friction and Creep of Polycrystalline Ice". Proceedings of the Royal Society of London, Vol. A324, p. 127-155.

Chung, Ed. 1987. "Ice Mechanics Review". Applied Mechanics Reviews, Vol. 40, no. 9.

Clayton, C.R.I., and Katrush, S.A., 1986. "A New Device for Measuring Local Axial Strains on Triaxial Specimens". Geotechnique, Vol. 36, No. 4, p. 593-597.

Cole, D.M., 1983a. "The Relationship Between Creep and Strength Behaviour of Ice at Failure". Cold Regions Science and Technology, Vol. 8, p.189-197.

Cole, D.M., 1983b. "The Effect of Stress Application Rate of the Creep Behaviour of Polycrystalline Ice." Journal of Energy Resources Technology, Vol. 105, p. 454-459.

Cole, D.M., 1985a. "Grain Growth and the Creep Behaviour of Ice". Cold Regions Science and Technology, Vol. 10, p. 187-189.

Cole, D.M., 1985b. "The Influence of Grain Size on the Ductility of Ice". Proc. of the 10th Int. OMAE Symposium, Houston, Texas, p. 153-156.

Cole, D.M., Gould, L.D., and Burch, W.B., 1986. "A System for Mounting End Caps on Ice Specimens". Journal of Glaciology, Vol. 31. p.362-365.

Cole, D.M., 1987. "Strain Rate and Grain Size Effects in Ice". Journal of Glaciology, Vol. 33, No. 115, p. 274-280.

Cox, G., Richter-Menge, J.A., 1985. "Triaxial Compression Testing in Ice". Proceedings, ASCE Arctic '85 Conference, San Francisco, p.476-488.

Domaschuk, L., and Wade, N.H., 1969. "A Study of Bulk and Shear Moduli of a Sand". Journal of the Soil Mechanics and Foundations Division, Proceedings ASCE, Vol. 95, No. SM2, March, 1969, p. 561-581.

Duval, P., and Le Gac, H., 1980." Does the Permanent

Creep Rate of Polycrystalline Ice Increase with Crystal Size?". Journal of Glaciology, Vol. 8, p. 131-145.

Duval, P., 1981. "Creep and Fabrics of Polycrystalline Ice under Shear and Compression.", Journal of Glaciology, Vol. 27, No. 95, p. 129-140.

Duval, P., and Ashby, M.F., 1983. "Rate-Controlling Processes in the Creep of Polycrystalline Ice". Journal of Physical Chemistry, Vol. 87, p. 4066-4074.

Frank, R., 1987. "Creep and the Pressuremeter Test". Unpublished Internal Report, Dept. of Civil Engineering, The University of Manitoba, Winnipeg, Manitoba.

Glen, J.W., 1952. "Experiments on the Deformation of Ice". Journal of Glaciology, Vol. 2, No. 12, p.111-114.

Glen, J.W., 1955. "The Creep of Polycrystalline Ice". Proceedings, Royal Society of London. Ser. A Vol. 228, No. 1175, p.519-538.

Gold, L.W., 1958. "Some Observations on the Dependence of Strain on Stress for Ice". Canadian Journal of Physics, Vol. 36, p.1265-1275.

Gold, L.W., 1966. "Elastic and Strength Properties of Freshwater Ice". Symposium on Ice Pressures Against Structures, Laval University, Quebec City, p. 13-23, NRC Technical Memo #92.

Gold, L.W., 1969. "Crack Formation in Ice During Creep". Scripta Metallurgica, Vol. 3, no. 6, p.367-370.

Gold, L.W., 1970. "Process of Failure In Ice". Canadian Geotechnical Journal, Vol. 7, no. 4, p.405-413.

Gold, L.W., 1971. "Use of Ice Covers for Transportation". Canadian Geotechnical Journal, Vol. 8, p. 170-181.

Gold, L.W., and Traetteberg, A., 1974, "Young's Modulus of Ice and Ice Engineering Problems". 2nd Symposium on Application of Solid Mechanics, Proceedings, Hamilton, p.1-16.

Gold. L.W., 1977. "Engineering Properties of Freshwater Ice". Journal of Glaciology, Vol. 19, p. 197-212.

Gold, L.W., 1987. "Fifty Years of Progress in Ice Engineering". Journal of Glaciology, Special Issue, p. 78-85.

Hausler, F.U., 1981. "Multiaxial Compressive Strength Tests on Saline Ice with Brush-Type Loading Platens". IAHR 1981, Quebec City, Vol.2, p.526-539.

Hawkes, I.,and Mellor, M., 1972. "Deformation and Fracture of Ice Under Uniaxial Stress". Journal of Glaciology, Vol. 11, p. 103-131.

Head, K.H., 1986. "Manual of Soil Laboratory Testing Volume 3 - Effective Stress Tests". Pentech Press, London, 1986, 495 pp.

Hobbs, 1974. "Ice Physics". Clarendon Press, Oxford, 1974, 837 pp.

Hooke et al, 1980, "Mechanical Properties of Polycrystalline Ice". Cold Regions Science and Technology, Vol.3, p.263-276.

Jacka, T.H., 1984a. "Laboratory Studies on Relationship Between Ice Crystal Size and Flow Rate". Cold Regions Science and Technology, Vol.8, p.31-42.

Jacka, T.H., 1984b. "Time and Strain Required for Development of Minimum Strain Rates in Ice". Cold Regions Science and Technology, Vol.8, p.261-268.

Jacka, T.H., and Maccagnan, M., 1984. "Ice Crystallographic and Strain Rate Changes with Strain in Compression and Extension". Cold Regions Science and Technology, Vol. 8, p.269-286.

Jardine, R.J., Symes, N.J., and Burland, J.R., 1984. "The Measurement of Soil Stiffness in the Triaxial Apparatus". Geotechnique, Vol.34, no.3, p. 323-340.

Jones, S.J., 1978. "Triaxial Testing of Polycrystalline Ice". 3rd POAC, Edmonton, Vol.2, p.670-674.

Jones, S.J., 1982. "The Confined Compressive Strength of Polycrystalline Ice". Journal of Glaciology, Vol. 28, p.171-177.

Kivisild, H.R., 1975. "Ice Mechanics". Proceedings POAC '75 Anchorage, p.287-313.

Kjartanson, B.H., 1986. "Pressuremeter Creep Testing in Laboratory Ice". Unpublished Ph.D. Thesis, Civil Engineering Dept., University of Manitoba, Winnipeg, Manitoba.

Kjartanson et al, 1988. "The Creep of Ice Measured with the Pressuremeter". Canadian Geotechnical Journal, Vol.

25, p.250-261.

Mellor, M., and Testa, R., 1969. "Effect of Temperature on the Creep of Ice". Journal of Glaciology, Vol. 25, p. 151-157.

Mellor, M., 1979. "Mechanical Properties of Polycrystalline Ice". IUTAM Symposium, Copenhagen 1979, Edited by Per Tryde, p.217-245.

Mellor, M., and Cole, D.M., 1982. "Deformation and Failure of Ice Under Constant Stress or Constant Strain Rate". Vol. 5, No. 3, p. 201-220.

Mellor, M., 1983a. "Mechanical Behaviour of Sea Ice". CRREL Monograph 83-1.

Mellor, M., and Cole, D.M., 1983b. "Stress/Strain/Time Relations for Ice Under Uniaxial Compression". Cold Regions Science and Technology, Vol. 6, no.3, p. 207-230.

Michel, B., and Ramseier, R.O., 1971. "Classification of River and Lake Ice". Canadian Geotechnical Journal, Vol. 8, p. 36-45.

Murat, J.R., Lainey, L.M., 1982. "Some Experimental Observations on the Poisson's Ratio of Sea Ice". Cold Regions Science and Technology, Vol. 6, no. 2, p. 105-114.

Nadreau, J.P., and Michel, B., 1986. "Yield and Failure Envelope for Ice Under Multiaxial Compressive Stresses". Cold Regions Science and Technology, Vol.13, p. 75-82.

Nawwar, A.M., Nadreau, J.P., Wang, Y.S., "Triaxial Compressive Strength of Polycrystalline Ice". Proceedings POAC '83 Helsinki, p. 193-202.

O'Connor, M.J., and Mitchell, R.J., 1978. "Measuring Total Volumetric Strain During Triaxial Tests on Frozen Soils". Canadian Geotechnical Journal, Vol. 15, p.47-54.

Rahman, M.G., 1988. "The Creep of Frozen Sands". Unpublished Ph.D. Thesis, Civil Engineering Dept., University of Manitoba.

Richter-Menge, J.A., 1984. "Static Determination of Young's Modulus in Sea Ice". Cold Regions Science and Technology, Vol.9, p. 283-286.

Richter-Menge, J.A., et al, 1986. "Triaxial Testing of First-Year Sea Ice". CRREL Report 86-16.

Scwarz, J., and Weeks, W.F., 1977. "Engineering Properties of Sea Ice". Journal of Glaciology, Vol. 19, p. 499-530.

Sego, D.C., and Morgenstern, N.R., 1983. "Deformation of Ice Under Low Stresses". Canadian Geotechnical Journal, Vol. 20, p. 587-602.

Sego, D.C, 1980. "Deformation of Ice Under Low Stresses". Unpublished Ph.D. Thesis, University of Alberta, Edmonton, Alberta, 500 p.

Sinha, N.K., 1977. "Effective Elasticity of Ice". Workshop on the Mechanical Properties of Ice, January 24-25 1977, Calgary, Alta, p. 112-123.

Sinha, N.K., 1978. "Short-Term Rheology of Polycrystalline Ice". Journal of Glaciology, Vol. 21, No. 85, p.457-473.

Sinha, N.K., 1979. "Grain Boundary Sliding in Polycrystalline Materials". Philosophical Magazine, Vol. 40, No. 6, p. 825-842.

Sinha, N.K., 1981. "Constant Stress Rate Deformation Modulus of Ice". Proceedings POAC '81, Quebec City, p. 216-224.

Sinha, N.K., 1982. "Delayed Elastic Strain Criterion for First Cracks in Ice". IUTAM Conference of Deformation and Failure of Granular Materials, Delft, August 1982, p.323-330.

Sinha, N.K., and Frederking, R., 1986a. "Prelinimary Observations on Compressive Strength, Deformation and Poisson's Ratio of Iceberg Ice". Workshop on Extreme Ice Features, Banff Alberta. NRC Tech. Memo No. 41 NRCC 28003.

Sinha, N.K., 1986b. "Young Arctic Frazil Sea Ice: Field and Laboratory Strength Tests". Journal of Materials Science, Vol. 21, p. 1533-1546.

Sinha, N.K., 1987. "Effective Poisson's Ratio of Isotropic Ice". Proceedings, 6th OMAE Symposium, Houston, Vol. 4, p.189-195.

Sinha, N.K., 1988a. "Crack-Enhanced Creep in Polycrystalline Material: Strain-Rate Sensitive Strength and Deformation of Ice". Journal of Materials Science, Vol. 23, p. 4415-4428.

Sinha, N.K., 1988b. "Ice and Steel - A Comparison of Creep and Failure". Mechanics of Creep Brittle Materials (Euromech 239), Leicester, England.

Sinha, N.K., 1989. Personal Communication.

Thompson, D.B., 1986. "The Influence of Entrained Air on Crystallography, A Microscopic Study". Unpublished B.Sc. Thesis, Dept. of Geological Engineering, University of Manitoba, Winnipeg, Manitoba.

Timco, G.W., and Frederking, R.M.W., 1986. "Confined Compression Tests, Outlining the Failure Envelope of Columnar Sea Ice". Cold Regions Science and Technology, Vol. 12, p. 13-28.

Traetteberg, A., 1975. "The Strain Rate and Temperature Dependence of Young's Modulus of Ice". Proceedings, Third International Symposium on Ice Problems, Hanover, N.H., August 1975, p. 479-486.

Weeks, W., and Assur, A., 1967. "The Mechanical Properties of Sea Ice". U.S. Army Cold Regions Research and Engineering Lab., Monograph II-C3.

APPENDIX

Test T4S P=1.0 MPa (P1−P3)=0.8 MPa

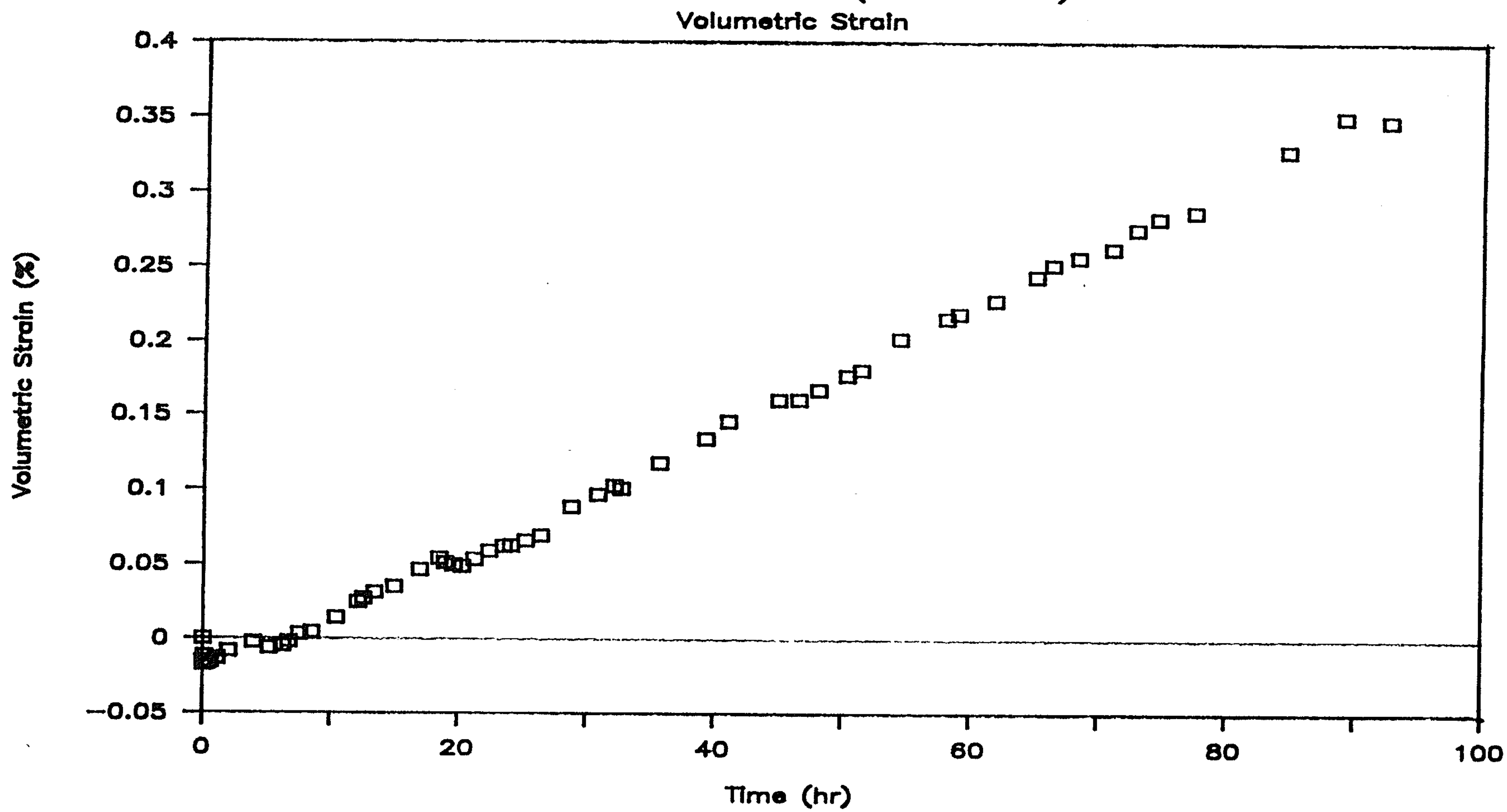

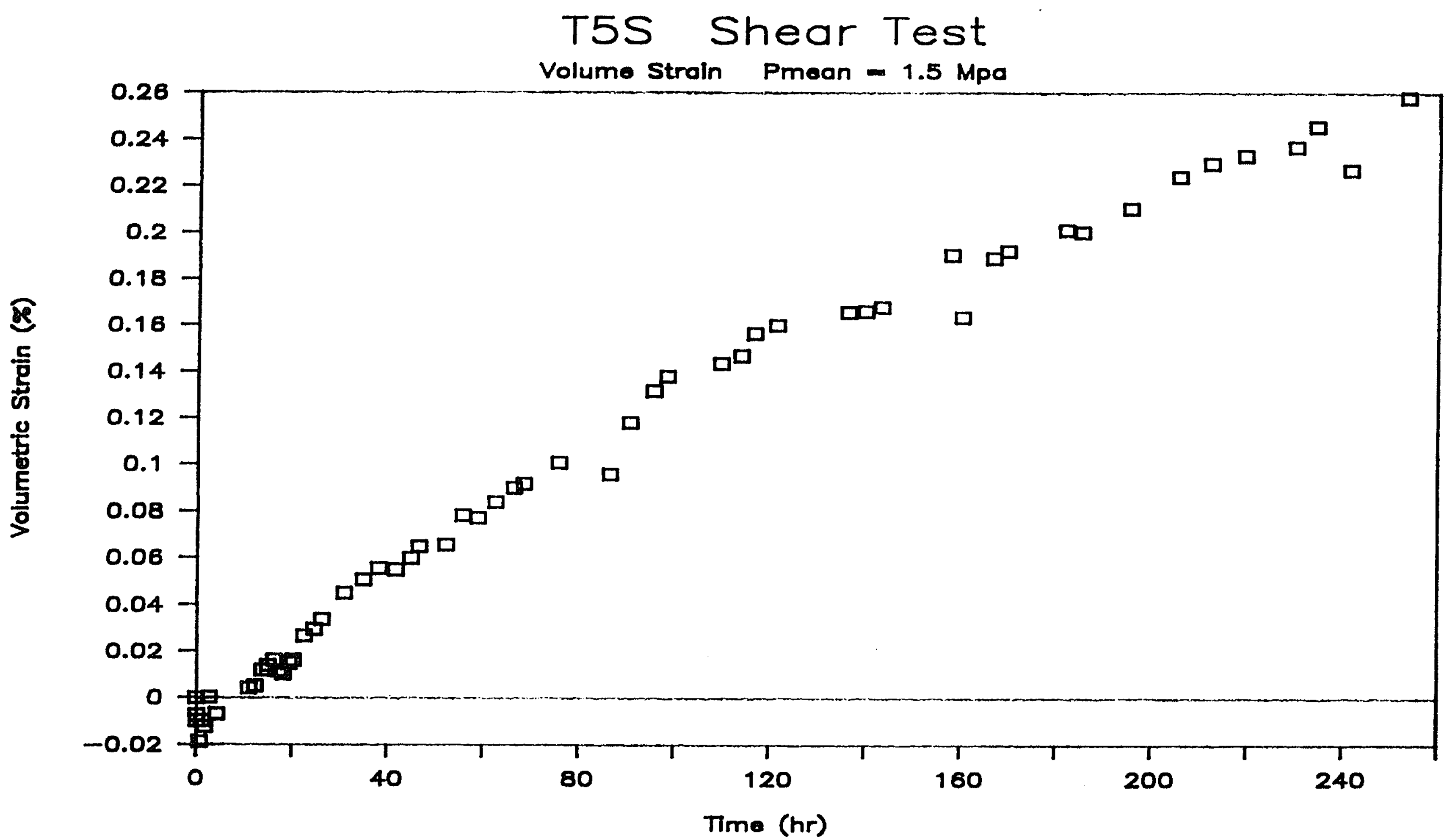

T5S Shear Test
Volume Strain Pmean = 1.5 Mpa
Volumetric Strain (%)
0.26
0.24
0.22
0.2
0.18
0.16
0.14
0.12
0.1
0.08
0.06
0.04
0.02
0
-0.02
0
40
80
120
160
200
240
Time (hr)

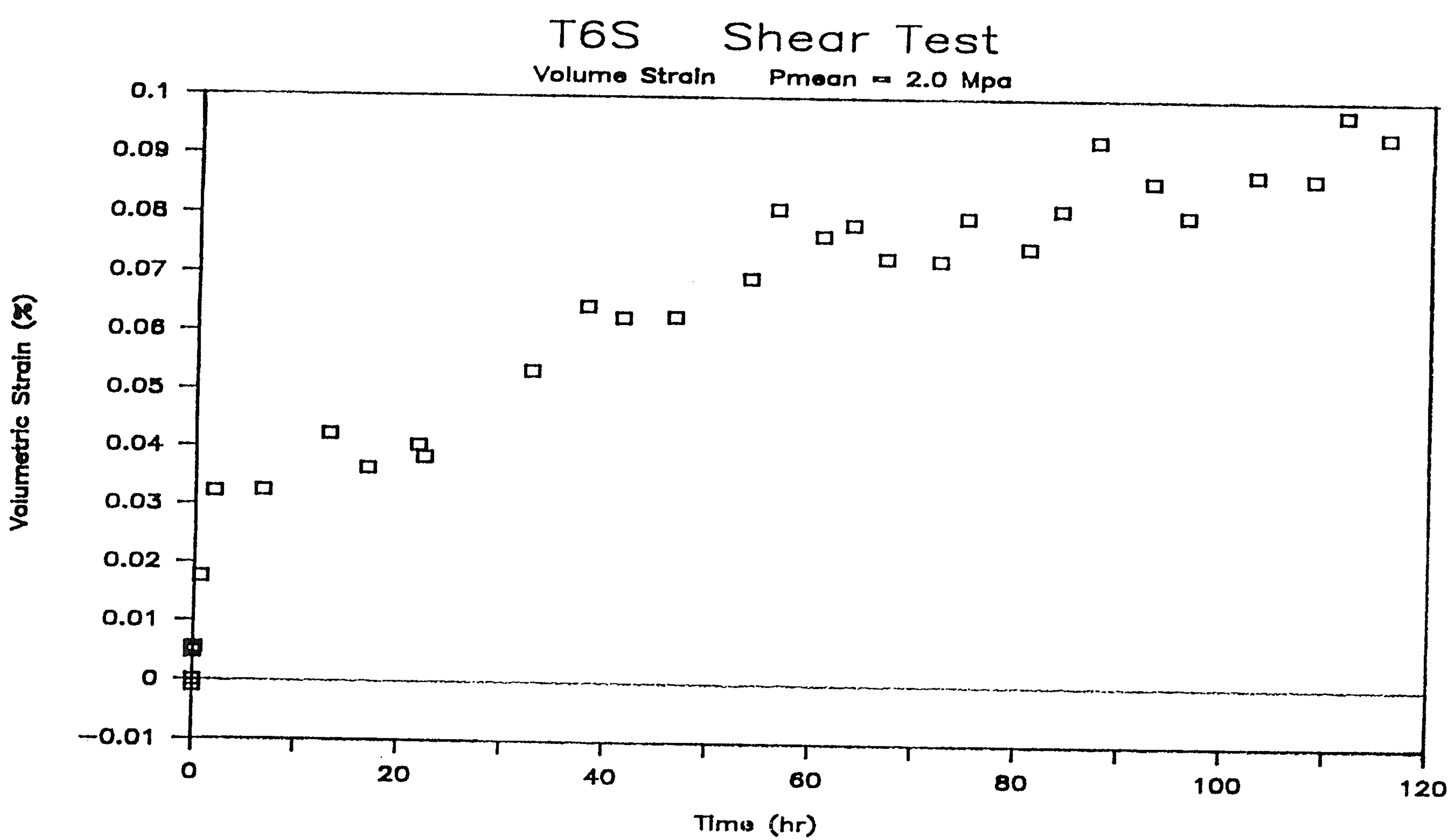
T6S Shear Test
Volume Strain Pmean = 2.0 Mpa
Volumetric Strain (%)
0.1
0.09
0.08
0.07
0.06
0.05
0.04
0.03
0.02
0.01
0
-0.01
0
20
40
60
80
100
120
Time (hr)

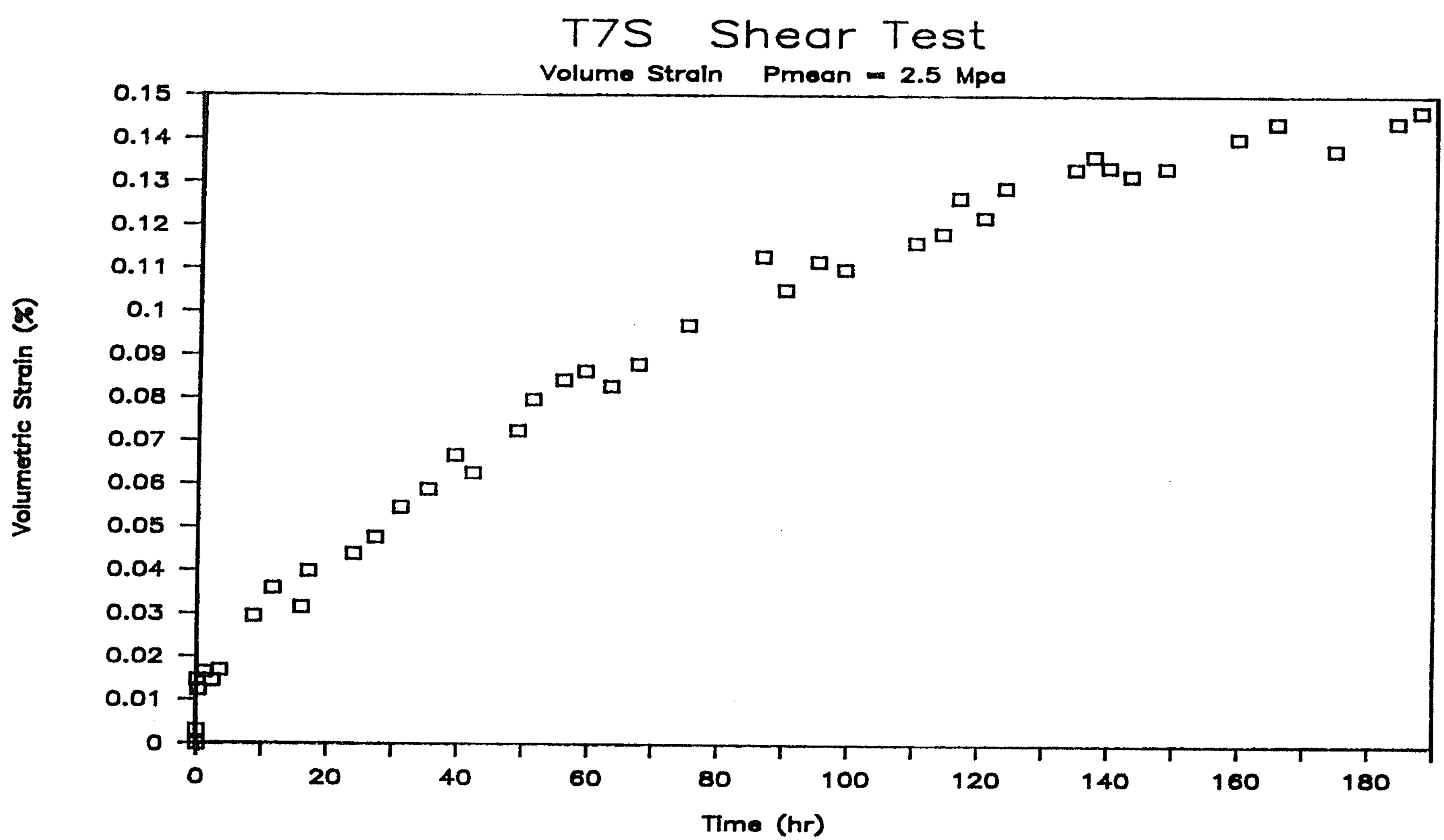
T7S Shear Test
Volume Strain Pmean = 2.5 Mpa
Volumetric Strain (%)
0.15
0.14
0.13
0.12
0.11
0.1
0.09
0.08
0.07
0.06
0.05
0.04
0.03
0.02
0.01
0
0
20
40
60
80
100
120
140
160
180
Time (hr)

T8UC Shear Test

Volume Strain Unconfined Compression

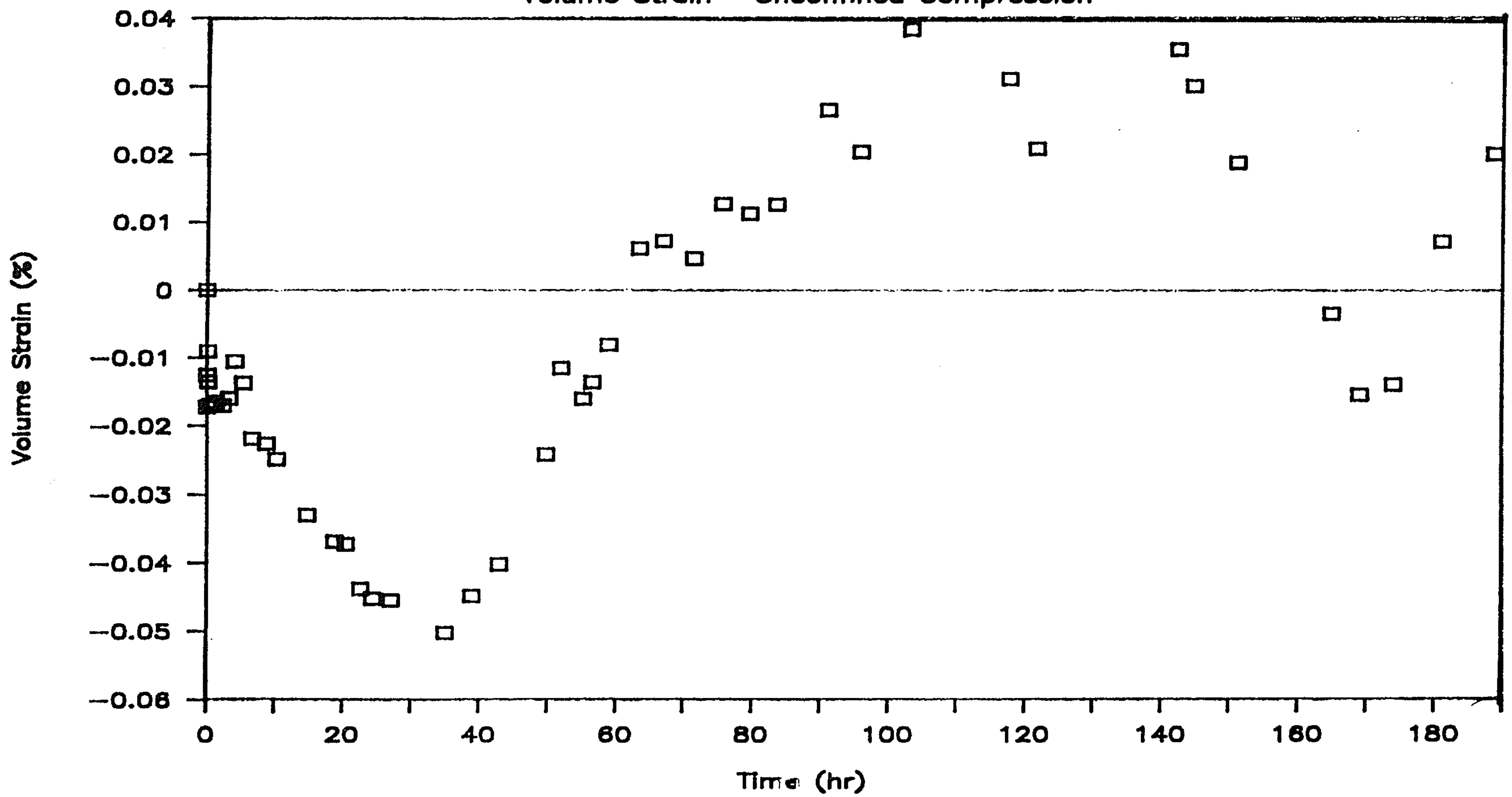

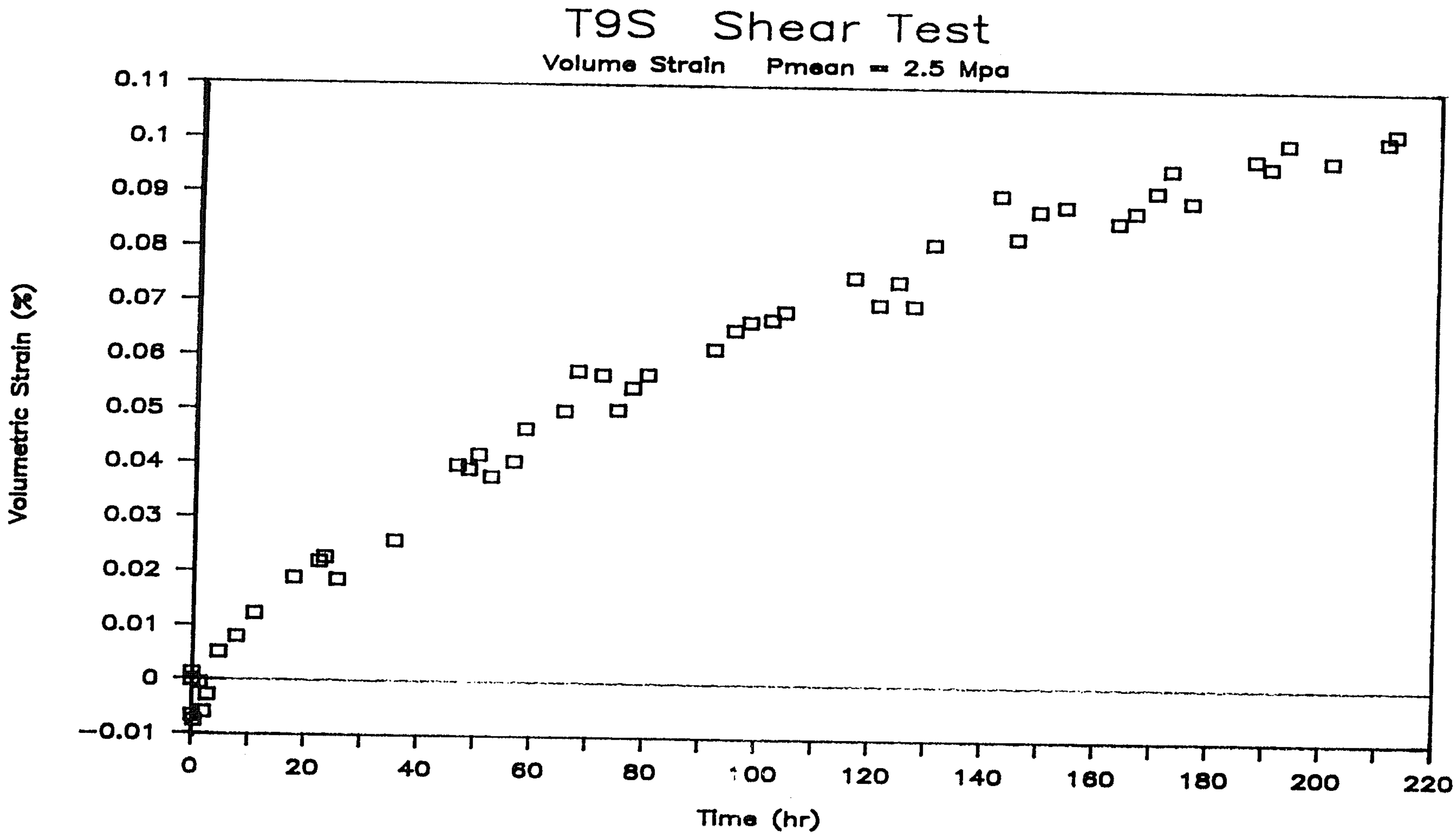
T9S Shear Test
Volume Strain Pmean = 2.5 Mpa
Volumetric Strain (%)
0.11
0.1
0.09
0.08
0.07
0.06
0.05
0.04
0.03
0.02
0.01
0
-0.01
0
20
40
60
80
100
120
140
160
180
200
220
Time (hr)

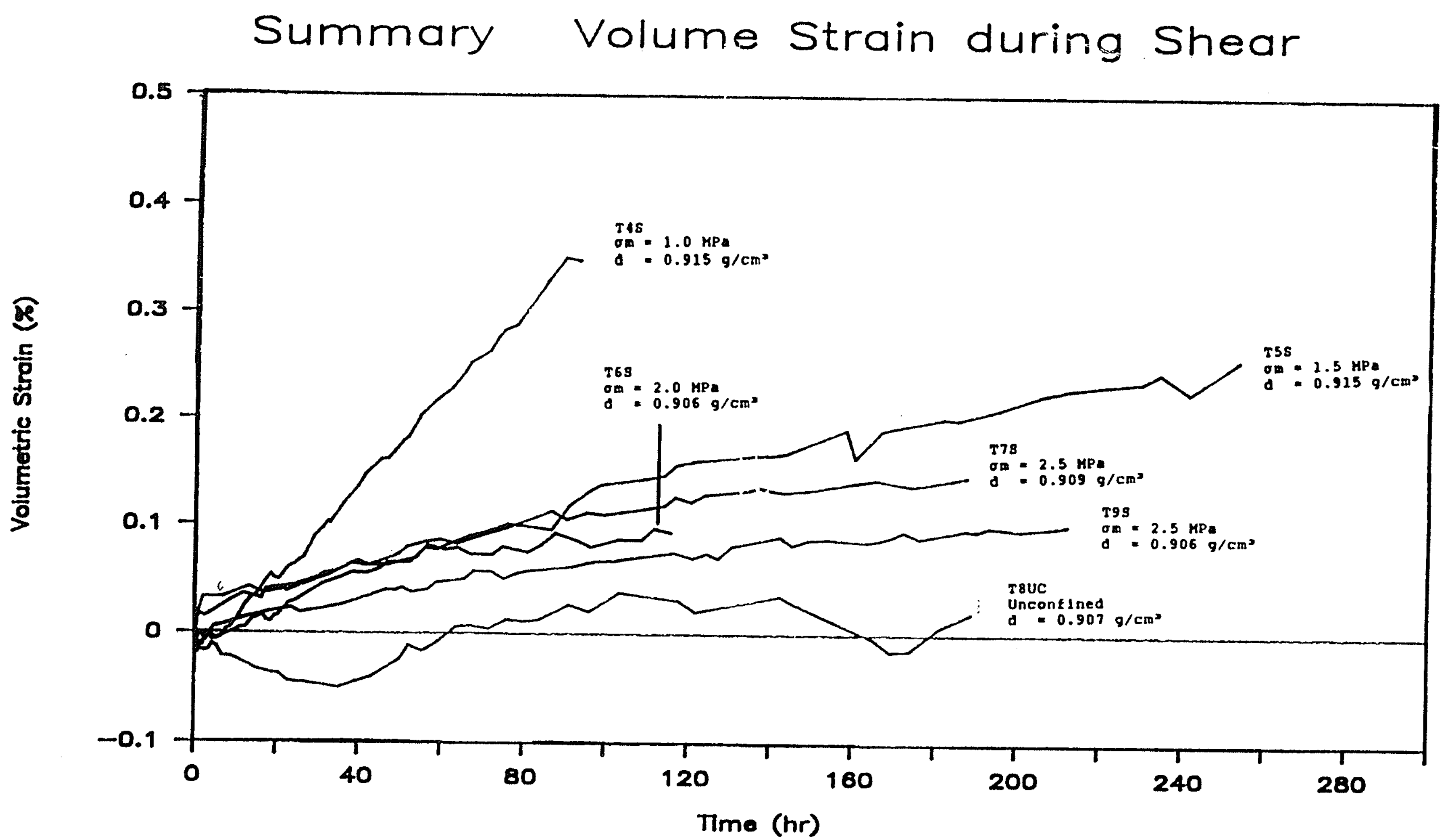
Summary Volume Strain during Shear
Volumetric Strain (%)
0.5
0.4
0.3
0.2
0.1
0
-0.1
0
40
80
120
160
200
240
280
Time (hr)
T4S
σm = 1.0 MPa
d = 0.915 g/cm³
T6S
σm = 2.0 MPa
d = 0.906 g/cm³
T5S
σm = 1.5 MPa
d = 0.915 g/cm³
T7S
σm = 2.5 MPa
d = 0.909 g/cm³
T9S
σm = 2.5 MPa
d = 0.906 g/cm³
T8UC
Unconfined
d = 0.907 g/cm³